Analyses transcriptomiques du dimorphisme levure-mycélium chez le champignon phytopathogène *Ophiostoma novo-ulmi*

Thèse

Martha Nigg

Doctorat en sciences forestières

Philosophiae doctor (Ph. D.)

Québec, Canada

Analyses transcriptomiques du dimorphisme levure-mycélium chez le champignon phytopathogène *Ophiostoma novo-ulmi*

Thèse

Martha Nigg

Sous la direction de :

Louis Bernier, directeur de recherche

RESUME

L'analyse de données de transcriptomique par le biais du séquençage d'ARN messagers (RNAseq) offre une perspective globale de la régulation de l'expression génique au cours d'un évènement biologique. Dans cette thèse, nous avons exploité cette technique dans le but de comprendre les mécanismes moléculaires qui régulent la transition morphologique réversible levure-mycélium qui est une caractéristique souvent liée au pouvoir pathogène chez les champignons. Dans un premier temps, par le biais de comparaisons de données de transcriptomique entre sept espèces fongiques dimorphiques, nous avons observé une certaine conservation des processus biologiques associés au changement de morphologie chez des champignons issus de branches très éloignées de l'arbre phylogénétique fongique. Dans un second temps, nous nous sommes concentrée sur notre modèle d'étude principal, *Ophiostoma novo-ulmi*, le champignon pathogène responsable de la maladie hollandaise de l'orme. Par l'analyse comparée des gènes exprimés en phases levure et mycélienne, nous avons défini les facteurs moléculaires qui sont spécifiques à chacune des phases chez *O. novo-ulmi* et établi une distinction claire entre les deux phases d'un point de vue du contenu en gènes exprimés. Par la suite, nous avons affiné notre étude en nous focalisant sur l'évènement de transition levure-mycélium afin déterminer les gènes dont l'expression était modulée au cours du temps dans le processus de changement morphologique. Nous avons mis en évidence plusieurs facteurs potentiellement impliqués dans la transition, notamment des gènes liés à la cascade de phosphorylation des MAPKs, connues pour jouer un rôle clé dans le dimorphisme chez plusieurs espèces fongiques. Finalement, dans le but d'évaluer plus précisément le niveau de conservation des processus biologiques liés au dimorphisme chez des espèces non modèles éloignées, nous avons comparé la régulation de l'expression génique au niveau des gènes orthologues entre *O. novo-ulmi* et l'espèce basidiomycète, *Pseudozyma flocculosa*. Nous nous sommes concentrée sur les gènes qui étaient différentiellement exprimés entre les phases de germination et de filamentation. Dans l'ensemble, les processus associés aux gènes pour lesquels la régulation de l'expression est conservée chez les deux espèces portent sur des fonctions essentielles du développement fongique. Ainsi, cette comparaison a permis de définir ce qui semble constituer la « base minimale » génique commune nécessaire à la transition asexuée levure-mycélium chez des espèces phylogénétiquement éloignées.

ABSTRACT

Large-scale transcriptomic analyses via messenger RNA sequencing (RNAseq) give access to the information on expression regulation of all the genes present in a sample at a given time and in a given experimental condition. In this thesis, we took advantage of this technology in order to investigate the molecular mechanisms that regulate the reversible yeast-to-hypha morphological switch which is a characteristic often linked to virulence in fungal pathogens. To begin with, we compared transcriptomic data among seven dimorphic fungi and found conserved biological processes associated with the morphological switch among species from very distant branches of the fungal phylogenetic tree. Later, we focused on our model species, *Ophiostoma novo-ulmi*, the causal agent of Dutch elm disease. We first compared the gene expression levels in yeast and mycelium growth phases. We defined the molecular factors that are specific to each growth phase and highlighted a clear molecular distinction between the two phases in terms of expressed gene contents. We further narrowed down our analysis by focusing on the yeast-to-hypha transition in a time course experiment. We determined the set of genes for which the expression was regulated during the morphological switch, thus potentially involved in the yeast-to-hypha transition. In particular, we identified genes that could be related to the MAPK cascade, known to play a crucial role in the dimorphic switch in many fungal species. Finally, in order to address the level of conservation in the biological processes linked to dimorphism in highly divergent non-model species, we compared the gene expression regulation of the orthologous genes between *O. novo-ulmi* and the basidiomycete *Pseudozyma flocculosa*. We focused on the genes that were differentially expressed between the germination and the filamentation phases. We identified several factors for which the regulation of expression seems conserved during the switch from germinating spore to filamentous growth. Overall, these genes are associated with biological processes that play essential roles in fungal development. Hence, our comparison here highlighted core components necessary for the yeast-to-hypha transition in phylogenetically distant species.

TABLE DES MATIERES

LISTE DES TABLEAUX

Annexes

LISTE DES FIGURES

Supplemental material

ABREVIATIONS

ADN/DNA	Acide désoxyribonucléique
AMPc/cAMP	Adenosine MonoPhosphate cyclique/cyclic Adenosine MonoPhosphate
ARN/RNA	Acide ribonucléique,
ARNt	Acide ribonucléique de transfert
mRNA	messenger Acide ribonucléique (acide ribonucléique messager)
BLAST	Basic Local Alignment Search Tool (algorythme d'alignement de sequences)
bp	Base pair (paires de bases)
CAZyme	Carbohydrate-Associated enZymes (enzymes du métabolisme des carbohydrates)
CRISPR	Clustered Regularly Interspaced Short Palindromic Repeat (technique de mutation)
DEG	Differentially Expressed Gene (gene différentiellement exprimé)
DEOG	Differentially Expressed Orthologous Gene (gene orthologue différentiellement exprimé)
EAN	Race Eurasienne
EST	Expressed Sequence Tag (marqueurs de séquences exprimées)
FDR	False Discovery Rate (taux de faux-positifs)
GO	Gene Ontology (ontologie génique)
GTP	Guanosine TriPhosphate
h	Heure/hour
L-M/Y-M	Levure-Mycélium/Yeast-Mycelium
MAPK	Mitogen-Activated Protein Kinase (protéine kinase activée par le mitogen)
MAPKK	Mitogen-Activated Protein Kinase Kinase
MAPKKK	Mitogen-Activated Protein Kinase Kinase Kinase
MDS	Multidimensional Scaling analysis (analyse multidimensionnelle)
MHO/DED	Maladie Hollandaise de l'Orme/ Dutch Elm Disease
M-to-Y	Mycelium-to-Yeast (mycélium vers levure)
NAN	Race Nord-américaine
OMM	*Ophiostoma* Minimum Medium (milieu minimum de croissance chez *Ophiostoma*)
OCM	*Ophiostoma* Complete Medium (milieu complet de croissance chez *Ophiostoma*)
PAL	pH signal transduction pathway (voie de perception du signal pH)
PCR	Polymerase Chain Reaction (reaction en chaîne par polymerase)
pH	puissance Hydrogène (mesure d'acidité ou basicité dans un milieu)
PKA	Protein Kinase A
qRT-PCR	quantitative Reverse Transcription PCR (PCR quantitative par transcription inverse)
RBH	Reciprocal Best Blast hit (alignement de sequences réciproque entre deux espèces)
RIM	Regulator of *IME2* (équivalent de la voie PAL)

RNAseq	Séquençage d'ARN/ RNA sequencing
RPKM	Reads per kilobase of transcript per million reads (lectures alignées par kilobase de transcrit par million de lectures alignées)
Y-to-M	Yeast-to-Mycelium (levure vers mycélium)
mg, µg	Milligramme, microgramme
mL, µL	Millilitre, microlitre
mm, µm	Millimètre, micromètre
mM, µM	Millimolaire, micromolaire
°C	Degré Celsius
%	Pourcentage

A ma grand-mère, Margrit,

dont le souvenir reste vif et dont l'amour m'accompagne dans chaque étape de ma vie.

REMERCIEMENTS

Il va de soi que la toute première personne à remercier sincèrement est mon directeur Louis Bernier qui m'a fait confiance pour la réalisation de ce projet de doctorat. Il m'a guidée tout au long du parcours en me laissant toute la liberté de suivre mes envies et en valorisant mes idées, ce qui m'a permis de grandir à travers ma thèse et de m'épanouir en tant que chercheure. Merci pour la patience et l'écoute aussi, qui ont été des éléments précieux durant ces 4 dernières années.

Merci aux membres de mon comité, Richard Bélanger et Danny Rioux, que j'ai rencontrés à plusieurs reprises lors de mon parcours et qui m'ont toujours appuyée et encouragée dans mes recherches. Merci aussi au professeur Christian Landry qui m'a guidée et assistée dans les premiers temps de mon doctorat. Merci au professeur Gregory Gauthier pour avoir accepté de réviser et d'évaluer ma thèse.

Merci au personnel de la plateforme de séquençage, en particulier Brian Boyle, pour leur patience et leur assistance.

Un merci tout spécial à Jérôme Laroche avec qui j'ai eu la chance de collaborer et sans qui mes analyses bioinformatiques auraient été très compliquées. Il m'a toujours accueillie dans son bureau avec calme et patience.

Je tiens à remercier également le professeur Uffe Hasbro Mortensen et Jakob Blaesbjerg Hoof ainsi que tous les membres de leur laboratoire à l'Université Technique du Danemark (DTU) qui m'ont accueillie à bras ouverts lors de mon stage en 2016 et qui m'ont guidée dans les expériences que j'ai menées chez eux.

Je remercie sincèrement toutes les personnes qui ont rendu mon quotidien à l'IBIS agréable et joyeux. Un merci en particulier aux collègues du laboratoire Bernier et tous ceux du deuxième étage pour les repas animés, les séances d'écoute amicales et l'assistance technique en tout temps. Je pense à André Gagné, Sébastien Gérardi, Julien Prunier, Julien Ponchart, Isabelle Giguère, Jean-Guy Catford, Sylvie Blais, Donna Mazerolle et tous les autres.

Merci aux membres du comité social de l'IBIS avec qui j'ai eu la chance d'organiser plusieurs évènements festifs qui m'ont permis de rencontrer plein de personnes à tous les étages de l'institut.

Parce que la vie à l'étranger est souvent un défi mais aussi une aventure enrichissante, je tiens à remercier sincèrement toutes les personnes qui ont fait de mon séjour à Québec une expérience inoubliable. J'ai eu la chance de rencontrer des gens formidables que je suis heureuse de compter parmi mes amis.

Merci aussi à mes amis de plus loin et de plus longue date, ceux qui sont toujours dans le cœur et ceux avec qui la distance n'a jamais été une limite à l'amitié profonde et sincère.

Enfin, *last but not least*, parce que sans eux, je ne serais pas là, je remercie du fond du cœur ma famille et mes parents qui ont toujours été là pour moi, pleins d'amour, sans condition et avec tout leur soutien. Merci de m'avoir toujours encouragée et aidée à être une meilleure personne.

AVANT-PROPOS

La thèse présentée ici est composée de publications mises en page conformément avec les règles de préparation de thèses de la Faculté des études supérieures et postdoctorales (FESP) de l'Université Laval. L'ouvrage inclut une introduction générale en français (Chapitre 1), une conclusion générale en français (Chapitre 6) ainsi que quatre articles rédigés en anglais présentés aux chapitres 2, 3, 4 et 5:

- Chapitre 2: Large-scale genomic analyses of dimorphism in human, insect and plant pathogenic fungi: from ESTs to RNAseq experiments. Revue publiée dans *Fungal Biology Reviews*.
- Chapitre 3: RNAseq analysis highlights specific transcriptome signatures of yeast and mycelial growth phases in the Dutch elm disease fungus *Ophiostoma novo-ulmi*. Article publié dans *G3 Gene/Genome/Genetics*.
- Chapitre 4: From yeast to hypha: defining transcriptomic signatures of the morphological switch in the dimorphic fungal pathogen *Ophiostoma novo-ulmi.* Article publié dans *BMC genomics*.
- Chapitre 5: Conserved components of the yeast-to-hypha transition revealed through comparative transcriptomic analyses of orthologous genes in the ascomycete *Ophiostoma novo-ulmi* and the basidiomycete *Pseudozyma flocculosa*. Article en préparation pour le journal *Fungal Biology*.

En annexe A sont présentés les résultats préliminaires d'une étude de la mutation génique chez *O. novo-ulmi* par CRISPR-Cas9 réalisée lors d'un stage de 4 mois au Danemark dans l'équipe du Prof. Uffe Hasbro Mortensen (DTU).

Les résultats obtenus lors de ce projet de doctorat ont été présentés lors des conférences et congrès suivants :

- 76^{e} colloque annuel de la division nord-est de l'American Phytopathology Society (NED-APS), à Ithaca NY, aux États-Unis le 20 octobre 2016. Les résultats du chapitre 4 ont été présentés à l'oral.

- 11e Journées Jean Chevaugeon, à Aussois, en France en janvier 2016. Les résultats du chapitre 4 ont été présentés à l'oral.
- Congrès annuel de la Société de Protection des Plantes du Québec (SPPQ) au Mont St-Anne en juin 2015. Les résultats du chapitre 1 ont été présentés à l'oral.
- 8^{e} et 9^{e} colloques annuels du Centre d'Étude de la Forêt (CEF) tenus à Montréal en avril 2014 et à Rimouski en avril 2015, respectivement. Les résultats du chapitre 3 ont été présentés sous forme d'affiche.
- 28th Fungal genetics conference (Genetics Society of America, GSA), tenu à Pacific Grove CA, aux États-Unis, du 17 au 22 mars 2015. Les résultats du chapitre 3 ont été présentés sous forme d'affiche.
- Gordon Research Conference (Fungal Cellular and Molecular Biology) à Holderness NH, aux Etats-Unis en juin 2014. Le plan de la thèse et les objectifs ont été présentés sous forme d'affiche.
- 74th meeting of the North Eastern Forest Pest Council (NEFPC) à Québec en mars 2014. Le plan de la thèse et les objectifs ont été présentés à l'oral.

J'ai planifié et organisé les activités de recherche des chapitre 2, 3 et 4. J'ai réalisé la revue de littérature ainsi que les essais au laboratoire, la prise et l'analyse des données et la rédaction des publications pour chacun des chapitres. Mon directeur de doctorat, le professeur Louis Bernier, m'a encadrée et guidée pendant toute la durée de mon doctorat. Il a assuré la relecture et révision des articles publiés ainsi que de la thèse dans son ensemble. Également, le professeur Christian Landry m'a conseillée lors de la mise en place des expériences du chapitre 3. Il a révisé et a corrigé le manuscrit de ce même chapitre. Jérôme Laroche, co-auteur du chapitre 3, a collaboré aux traitements de données de séquençage par analyses bioinformatiques et a révisé le manuscrit. Joan Laur a participé à la conception et à l'analyse des données du chapitre 5, ainsi qu'à la rédaction du chapitre. Le professeur Richard Bélanger a participé à la conception du chapitre.

CHAPITRE 1 Introduction

1.1 La maladie hollandaise de l'orme

1.1.1 Répartition, vecteurs, agents causals et dissémination

En Amérique du Nord, l'espèce végétale *Ulmus americana* L. (l'orme blanc d'Amérique) est largement utilisée comme arbre d'ornement et d'ombrage dans les villes. Elle est notamment très appréciée pour ses capacités à résister à des climats extrêmes et à la pollution urbaine. Cependant, depuis le début du 20^{e} siècle, les populations d'ormes sont ravagées par la maladie hollandaise de l'orme (MHO) à laquelle *U. americana* est particulièrement sensible. La MHO, aussi appelée graphiose de l'orme, a été décrite pour la première fois en Hollande en 1921 (Spierenburg 1921). Elle constitue l'une des maladies de plantes les plus dévastatrices connues dans l'hémisphère nord. La première épidémie de MHO date des années 1900. La maladie a d'abord été recensée au nord-ouest de l'Europe puis s'est rapidement répandue à l'est, au sud et dans le centre de l'Europe. L'épidémie a ensuite atteint l'Angleterre, le nord de l'Amérique en 1930 (Ohio, Indiana, état de New York et Virginie) (Campana 1978) et enfin, l'Asie centrale et du sud-ouest avant de décliner dans les années 1940 en Europe et en Asie. Une seconde épidémie fut détectée pour la première fois vers 1970 en Angleterre bien que probablement déjà présente en Europe de l'est avant cette période (Karnosky 1979; Brasier 1991). La dispersion globale de la maladie a entrainé la disparition d'une large proportion de la population mature des ormes d'Amérique du Nord, d'Europe et d'Asie centrale et du sud-ouest et des pertes économiques considérables pour les villes touchées.

Les deux épidémies furent engendrées par deux espèces de champignons ascomycètes nécrotrophes de la classe des Sordariomycètes et du genre *Ophiostoma* : *Ophiostoma ulmi* (Buism.) Nannf., responsable de la première pandémie et *Ophiostoma novo-ulmi* Brasier, le plus agressif[1] des deux, responsable de la seconde (Brasier 1991; Paoletti *et al.* 2006).

De nombreuses études ont tenté d'apporter des informations sur le développement de la MHO et la biologie des champignons pathogènes. Il a ainsi été démontré que la dispersion et la

[1] Ici, la notion d'agressivité était liée à la sévérité des symptômes observés sur des ormes modérément résistants à la maladie.

transmission fongique d'arbre en arbre s'effectuent par le biais d'insectes vecteurs (Middleton 1934) de type scolyte. L'insecte adulte transporte des spores couvertes de mucilage du champignon qui permet leur adhérence à l'exosquelette des insectes (Temple *et al.* 1997). Lorsque le scolyte se nourrit sur les arbres sains, les spores de champignon sont inoculées au niveau de la blessure causée par l'insecte et pénètrent rapidement dans le système vasculaire végétal. Les spores germent et le champignon envahit les vaisseaux du xylème. Les facteurs anatomiques déterminant la sensibilité d'un arbre à la MHO, et indirectement, la virulence du champignon, sont, entre autres, la longueur des vaisseaux du xylème (Elgersma 1970), leur diamètre (Elgersma 1970; Solla and Gil 2002; Martín *et al.* 2013) et la taille moyenne des groupes de vaisseaux (McNabb Jr *et al.* 1970; Martín *et al.* 2013). Selon l'espèce d'orme considérée, ces facteurs peuvent varier au cours de l'année. Ainsi, la période de l'année à laquelle les spores sont inoculées est un élément à prendre en compte lors de l'étude de la virulence (Solla *et al.* 2005).

Les ormes malades ou morts attirent les femelles scolytes et vont constituer les sites d'accouplement de l'insecte. Les arbres sont réinfectés lorsque les scolytes femelles, portant potentiellement des spores sur leur carapace, creusent leurs galeries de ponte dans l'écorce. Les larves d'insectes se développent donc dans ces galeries où le mycélium croit de manière saprophytique et forme des fructifications de reproduction asexuée (les synnemas), ou sexuée (les périthèces) (voir section 1.2.1). Ainsi, lorsque les jeunes insectes émergent de l'arbre, ils emportent des spores, assurant ainsi la continuité du cycle de maladie (Campana 1978). Au Québec, deux espèces de scolytes sont connues pour être impliquées dans la transmission d'*O. novo-ulmi* aux ormes : le scolyte indigène de l'orme (*Hylurgopinus rufipes* (Eichh.)) et le petit scolyte européen (*Scolytus multistriatus* (Marsh.)).

1.1.2 Symptômes de la MHO

Des études histopathologiques ont permis de mettre en évidence les différentes étapes de l'évolution de la maladie au sein des arbres. D'un point de vue macroscopique, l'infection des arbres par *O. novo-ulmi* induit la formation de stries dès trois jours après inoculation, observées sur des coupes de bois. Le nombre de stries et leur intensité augmentent avec la durée de l'infection et la virulence des souches fongiques. Elles se développent de manière tangentielle à partir du point d'inoculation (Et-Touil *et al.* 2005).

D’un point de vue microscopique, la pénétration des champignons dans les vaisseaux du xylème et les tissus végétaux induit rapidement (moins de 72h après inoculation) des torsions, des invaginations, des affaissements ou encore des ruptures des parois des cellules proches des vaisseaux infectés. Dans certains cas extrêmes, l’affaissement de cellule entière est observé. Les parois des gros vaisseaux infectés du xylème secondaire s’épaississent et les ponctuations sont souvent obstruées, notamment par des petits hyphes en croissance (Ouellette 1981). Un ajout de couches discontinues de paroi cellulaire est également observé dans des vaisseaux plus petits, comme les trachéides vasculaires. La structure des couches additionnelles est équivalente à celle des parois secondaires ou à du bois de tension, indiquant que la maladie semble avoir un impact sur la maturation des vaisseaux (Ouellette 1978; Ouellette *et al.* 1999).

Trois jours après inoculation, des réseaux de structures alvéolées (formes circulaires délimitées par une couche membranaire) sont visibles dans les gros vaisseaux du dernier cerne de croissance. Ces structures, dont le nombre est proportionnel à la virulence des souches fongiques, semblent essentiellement remplies de gaz et induisent une cavitation des vaisseaux (Ouellette *et al.* 2004a; Et-Touil *et al.* 2005). C’est au niveau de ces réseaux que sont également retrouvées de nombreuses cellules fongiques.

La croissance des hyphes semble restreinte à des cellules qui ne sont plus fonctionnelles (dégradées) ou à des zones de l’arbre infecté où les échanges gazeux sont différents de ceux observés dans des cellules vivantes (espaces intercellulaires ou structures alvéolées) (Ouellette 1978; Aoun *et al.* 2009).

Enfin, d’un point de vue externe, les symptômes de la maladie sont multiples : les premiers apparaissent au moment du débourrage des bourgeons lorsque les gros vaisseaux de xylème sont produits afin de permettre un apport accru de sève aux jeunes parties aériennes en croissance. On observe alors un flétrissement des feuilles, suivi de leur enroulement et dessèchement. Elles deviennent jaunâtres mais restent généralement sur l’arbre. Au stade le plus avancé de la maladie, l’obstruction des vaisseaux de xylème est observée induisant : l’accumulation de thylles dans les vaisseaux pour freiner les déplacements fongiques (Ouellette 1978; Et-Touil *et al.* 2005); des dépôts de subérine (subérisation) (Rioux and Ouellette 1991a), de lignine et de composés phénoliques au niveau des parois cellulaires

(Rioux and Ouellette 1991a,b); une accumulation de phytoalexines toxiques pour le champignon (Duchesne *et al.* 1985) ainsi que la présence de structures fongiques. Tous ces éléments empêchent la répartition de l'air présent dans les vaisseaux non fonctionnels mais causent aussi la diminution de l'approvisionnement en sève brute des parties aériennes, ce qui entraine la mort de l'arbre infecté.

1.2 *Ophiostoma novo-ulmi* et dimorphisme

1.2.1 *O. novo-ulmi*

Le premier isolement de l'agent pathogène *O. ulmi* (alors nommé *Graphium ulmi* avant d'être rebaptisé *Ceratocystis ulmi*) fut réalisé par M.B. Schwarz en 1919 (Schwarz 1922). Les recherches effectuées suite à la deuxième épidémie dans les années 1970 ont permis de mettre en évidence deux souches distinctes de champignons, définies alors comme deux sous-groupes de l'espèce *O. ulmi* présentant des niveaux d'agressivité contrastés envers les ormes (agressif et non-agressif) (Gibbs and Brasier 1973). Or, malgré quelques croisements occasionnels observés dans la nature (Brasier *et al.* 1998) et en laboratoire, une forte barrière reproductive existe entre ces deux souches, laissant suggérer que leurs génomes sont incompatibles, du moins partiellement, et que, plutôt que de deux sous-espèces, il s'agit de deux espèces différentes. Ainsi, en 1991, C.M. Brasier établit que la sous-espèce agressive d'*O. ulmi* est en fait une autre espèce et la nomme *O. novo-ulmi* Brasier (Brasier 1991). Cette dernière est ensuite subdivisée en deux races : la race Nord-américaine (NAN) et la race Eurasienne (EAN) (Brasier 1991). Finalement, le concept de « race » est modifié et transformé en sous-espèce : la race Eurasienne (EAN) devient la sous-espèce *novo-ulmi*, et la race Nord-Américaine (NAN) la sous-espèce *americana* (Brasier and Kirk 2001). Actuellement, *O. novo-ulmi* ssp. *americana* semble avoir remplacé *O. ulmi* dans la majeure partie de l'Amérique du Nord tandis que *O. novo-ulmi* ssp. *novo-ulmi* est largement répandue en Europe et en Asie centrale et du sud (Bernier *et al.* 2015).

Ophiostoma novo-ulmi présente deux modes de reproduction : un premier de manière sexuée et un second asexué. Dans le premier cas, les spores formées sont des ascospores, contenues dans des asques, eux-mêmes rassemblés dans des périthèces qui sont des fructifications en forme de poire. Ces fructifications sont notamment retrouvées sur le mycélium en croissance dans les galeries de pontes des scolytes. *Ophiostoma novo-ulmi* étant une espèce

hétérothallique (auto-stérilité), la reproduction sexuée n'est obtenue qu'en présence de partenaires compatibles sexuellement (*mating type* différent). La compatibilité sexuelle est contrôlée par un locus génétique, *MAT,* qui présente différents idiomorphes (MAT-A ou MAT-1 et MAT-B ou MAT-2) (Paoletti *et al.* 2006). La reproduction sexuée est essentiellement observée *in vivo* mais peut être provoquée *in vitro* entre deux partenaires compatibles en manipulant certains facteurs comme la présence d'acide linoléique et l'ajout de copeaux de bois d'orme dans le milieu de croissance solide (Hubbes 1975; Brasier and Gibbs 1976; Brasier 1981; Marshall *et al.* 1982; Bernier and Hubbes 1990a).

Dans le cas de la reproduction asexuée, ou végétative, le cycle de vie fongique comporte deux phases de croissance distinctes : une première de type levure et une seconde de type mycélienne. La croissance levuriforme, phase unicellulaire, est obtenue à partir de conidies primaires formées aux extrémités des hyphes produits dans la phase mycélienne (état monomateux). Ces conidies primaires se multiplient de manière non polarisée par des divisions mitotiques, également appelées bourgeonnement, et forment des colonies homogènes de conidies secondaires (=levures) (Crane and Schoknecht 1973). Dans le cas de la croissance mycélienne, des hyphes sont produites à partir de levures qui ne bourgeonnent pas. Ces dernières forment des tubes germinatifs qui croissent par division mitotique polarisée. Contrairement à la croissance par bourgeonnement, les cellules des hyphes en croissance restent attachées entre elles. Des septa sont formés entre les cellules, par invagination des parois cellulaires. Les septa séparent ces dernières mais assurent une connexion cytoplasmique entre les cellules des hyphes via des pores. Les hyphes sont donc de longs tubes continus qui croissent par extension au niveau des extrémités. Ce processus est commun aux champignons dits filamenteux (Odds 1988; Sánchez-Martínez and Pérez-Martín 2001). En présence d'acide linoléique, les hyphes peuvent former des structures enchevêtrées et dressées de reproduction végétative, les synnemas (également appelées corémies ou conidiophores synnemateux) qui, comme mentionné précédemment, sont retrouvées, de manière plus fréquente que les périthèces, dans les galeries de pontes des scolytes (Hubbes 1975; Naruzawa *et al.* 2016). Les synnemas forment des spores de types conidies qui assurent la dispersion fongique.

Les deux phases de croissance végétative, levuriforme et mycélienne, d'*O. novo-ulmi* peuvent être maintenues *in vitro*, selon des conditions expérimentales précises (Kulkarni and Nickerson 1981a; Naruzawa and Bernier 2014) et le champignon est capable de passer d'une phase à l'autre de manière réversible sans intervention de la reproduction sexuée (Harris and Taber 1970; Kulkarni and Nickerson 1981a). Cette particularité est connue sous le nom de dimorphisme fongique.

Les études portant sur la répartition physique du champignon dans les arbres infectés suggèrent qu'au cours du cycle de la maladie, les deux formes sont utilisées afin de permettre la propagation complète du champignon dans l'arbre. La phase levuriforme assure une dispersion verticale rapide du champignon et est essentielle pour le transport du champignon dans les vaisseaux du xylème et la translocation de l'infection dans l'arbre hôte (Campana 1978). Dans ce sens, les levures assurent une colonisation passive des vaisseaux du xylème. Cette phase de croissance semble jouer un rôle important dans la virulence puisque des mutants spontanés d'*O. novo-ulmi* non-sporulants inoculés à des ormes d'Amérique n'induisent aucun symptôme de maladie (Richards *et al.* 1982; Richards 1994). La phase mycélienne, en contrepartie, pénètre d'un vaisseau à l'autre, notamment par pression mécanique des hyphes sur les parois cellulaires végétales ou via les ponctuations (Campana 1978 cité par Kulkarni and Nickerson 1981a) mais aussi par pénétration directe dans les cellules suite à la sécrétion d'enzymes de dégradation des parois végétales (Ouellette *et al.* 2004b). Cette phase est définie comme la forme « invasive » du champignon. Bien que décrite comme essentielle pour la pathogénie, la transition levure-mycélium et le lien avec la virulence chez *O. novo-ulmi* n'ont été que peu étudiés, puisqu'aucune étude n'a prouvé le caractère essentiel de la phase mycélienne dans le développement de la MHO. En effet, un mutant ne produisant que des levures, mutant *col1* (Royer *et al.* 1991; Pereira *et al.* 2000), a été caractérisé mais aucun test de virulence n'a été effectué avec cette souche.

1.2.2 Dimorphisme dans le règne des champignons

La survie des micro-organismes dans des conditions souvent hostiles dépend de leur capacité à répondre rapidement aux changements environnementaux, tels que des variations de température, des chocs osmotiques ou oxydatifs, ainsi que des carences en nutriments. Parmi plusieurs stratégies adoptées par les champignons, la plasticité morphologique est largement

répandue dans le règne fongique et de nombreux champignons pathogènes ont été identifiés comme étant dimorphiques (cf. Chapitre 2) (Nadal *et al.* 2008; Gauthier 2015). Chez ces derniers, on retrouve plusieurs espèces pathogènes des humains/animaux : entre autres, *Candida albicans* (candidose), *Histoplasma capsulatum* (histoplasmose), *Sporothrix schenckii* (sporotrichose, « maladie des éleveurs de roses »), *Blastomyces dermatidis* (blastomycose, maladie de Gilchrist), *Malazessia furfur* (pityriasis versicolor) et *Paracoccidioides brasiliensis* (paracoccidioidose). De même, plusieurs agents phytopathogènes, en plus d'*O. novo-ulmi* et *O. ulmi*, présentent un dimorphisme : *Ustilago maydis* (charbon du maïs), *Taphrina deformans* (maladie de la cloque du pêcher), *Pichia fermentans* (pourriture du pêcher) et *Mycosphaerella graminicola* (septoriose du blé) en font partie.

Quelques espèces entomopathogènes (*Nomuraea rileyi* et *Metarhizium anisopliae*) possèdent également cette caractéristique morphologique. Enfin, *Pseudozyma flocculosa*, un basidiomycète antagoniste naturel des champignons agents du blanc (powdery mildew), est aussi dimorphique (Lefebvre *et al.* 2013). Ainsi, bien que la plupart des champignons étudiés soit des ascomycètes appartenant à des familles pouvant être très éloignées phylogénétiquement (cf, Chapitre 2, Figure 2.2), il est intéressant de noter que le dimorphisme est également présent chez les basidiomycètes et chez les Mucormycota.

Le dimorphisme fongique est également retrouvé chez *Saccharomyces cerevisiae*, l'espèce de levure modèle, dont certaines souches diploïdes montrent une transition de la forme levure en une forme de type « pseudohyphe ». Dans ce cas, les cellules de levures bourgeonnent et forment des chaines de cellules ellipsoïdales qui ne se détachent pas les unes des autres (Evans and Richardson 1989; Sánchez-Martínez and Pérez-Martín 2001). Les pseudohyphes, à la différence des vrais hyphes, ne possèdent pas de septa entre les cellules. Bien que la plasticité morphologique chez *S. cerevisiae* reste limitée (Gancedo 2001), cette espèce fongique fait l'objet de très nombreuses études et les connaissances accumulées offrent des perspectives intéressantes pour aborder le dimorphisme chez des espèces non-modèles.

1.2.2.1 Régulation du dimorphisme par contrôle nutritionnel

Les sources de nutriments dans les milieux de croissance jouent un rôle significatif dans l'induction de la transition d'une phase à l'autre chez de nombreuses espèces dimorphiques. Ainsi, le type de ressources et la quantité sont déterminants.

La transition levure-pseudohyphe chez *S. cerevisiae* s'observe en cas de carence en azote (taux faible d'ammonium dans le milieu croissance) ou présence de proline en tant qu'unique source azotée (Gimeno *et al.* 1992).

Chez *C. albicans*, la transition levure-pseudohyphe/hyphe est également activée par la carence en azote (Biswas *et al.* 2007). La présence d'arginine dans le milieu de croissance favorise la production de pseudohyphes (Ghosh *et al.* 2009). Le N-acetylglucosamine (GlcNAc) et la proline sont deux molécules connues pour induire la production d'hyphes (Ernst 2000).

Pour *P. fermentans*, la concentration dans le milieu de croissance en urée et diammonium phosphate définit la phase de croissance : des concentrations en millimolaires de ces deux sels induisent la production de cellules levuriformes alors que des concentrations en micromolaires favorisent la croissance de pseudohyphes (Sanna *et al.* 2012). Selon la source azotée (sulfate d'ammonium, acides aminés etc.), la concentration de la source et le pH du milieu vont influencer la transition.

De manière similaire, la transition levure-mycélium (L-M) chez *O. novo-ulmi* est influencée par de nombreux stimuli externes tels que la source d'azote présente dans le milieu de croissance. Plusieurs études portant sur la souche NRRL6404, auparavant désignée comme *O. ulmi* mais récemment identifiée comme étant *O. novo-ulmi* ssp. *americana* (Naruzawa and Bernier 2014) ont mis en évidence le rôle de différentes sources azotées dans le dimorphisme. Ainsi, la proline favorise la croissance levuriforme alors que l'arginine ou l'ammonium entraine la germination des spores et la formation d'hyphes septés (Kulkarni and Nickerson 1981a). La présence de calcium (Ca^{2+}) et son interaction avec la calmoduline jouent également un rôle sur le contrôle du dimorphisme. Il a notamment été démontré qu'en présence d'inhibiteur de la calmoduline, le potentiel dimorphique d'*O. novo-ulmi* était

modifié et que l'interaction Ca^{2+}- calmoduline était nécessaire à la croissance mycélienne (Muthukumar and Nickerson 1984; Muthukumar *et al.* 1985). Une étude portant sur des mutants d'*O. ulmi* non-sporulants a révélé que, contrairement au champignon sauvage qui, en présence d'arginine dans un milieu « glucose-sels » (GPR, Kulkarni and Nickerson, 1981a) complémenté avec 50µm de trifluopérazine (inhibiteur de calmoduline), produit 100% de spores levuriformes, les mutants eux, ne poussent pas. Ainsi, le processus moléculaire qui permet à *O. ulmi* de passer de la phase mycélienne à la phase levuriforme semble inactif chez ces mutants. Au cours de ce travail, il a été rapporté, par croisement, l'existence d'un gène impliqué dans le contrôle de la non-sporulation et qui pourrait être lié à la régulation de la transition L-M par l'interaction Ca^{2+}-calmoduline (Richards 1994). La fonction et la séquence de ce gène n'ont cependant pas encore été établies.

1.2.2.2 Régulation du dimorphisme par les acides gras et les alcools

La transition levure-mycélium (L-M) chez les champignons de la MHO semble en partie contrôlée par des enzymes, telles que les lipoxygénases et cyclooxygénases, qui oxydent les acides gras polyinsaturés pour produire des oxylipines (Jensen *et al.* 1992; Naruzawa and Bernier 2014). L'acide linoléique fait partie de ces acides gras. Chez les agents pathogènes de la MHO, l'ajout d'acide linoléique dans un milieu de croissance riche solide induit la formation de synnemas (Hubbes 1975) et ce même acide stimule la production de mycélium en milieu minimum liquide agité (Naruzawa *et al.* 2016).

Chez *C. albicans*, le mécanisme de régulation du dimorphisme par la densité cellulaire (*quorum sensing*) est contrôlé par la production de farnesol, également une oxylipine (Hornby *et al.* 2001).

Chez *P. fermentans*, les alcools suivants : methionol, butanal, isobutanol et isopropanol induisent la production de pseudohyphes. Ces molécules sont également associées au processus de « quorum sensing » (Sanna *et al.* 2012).

Ce mécanisme est également retrouvé chez *O. novo-ulmi* (Hornby *et al.* 2004) et *O. ulmi* où l'isoleucine 2-methyl-1-buthanol a été identifié comme responsable du maintien de la phase levuriforme lorsque la concentration de cellules était supérieure à $2x10^7$ spores/mL (Hornby

et al. 2004; Berrocal *et al.* 2012). Ainsi, la régulation de la transition dépendant de la taille de l'inoculum est un processus conservé entre différentes espèces.

1.2.2.3 Régulation du dimorphisme par des voies moléculaires conservées

Initialement mises en évidence chez *S. cerevisiae*, au moins trois voies de régulation de la transition L-M par des stimuli environnementaux sont retrouvées chez les champignons modèles dimorphiques comme *Ustilago maydis* ou *Candida albicans* : i) une cascade de phosphorylation, la cascade « Mitogen-Activated Protein kinase» (MAPK), ii) une voie de régulation via la protéine kinase A dépendante de l'AMP-cyclique (cAMP-PKA), et iii) une dernière voie contrôlée par le pH de l'environnement de croissance (un pH alcalin ou neutre stimule la transition L-M chez *C. albicans*) : la cascade de signalisation Pal/Rim (Sánchez-Martínez and Pérez-Martín 2001; Nadal *et al.* 2008; Selvig and Alspaugh 2011).

1.2.2.3.1 Cascade de phosphorylation MAPK

La cascade MAPK est une voie de transduction de signaux environnementaux, retrouvée chez la plupart des eucaryotes. L'information de la perception des signaux est transmise au sein des cellules par des cycles de phosphorylation/déphosphorylation de protéines. Elle est composée d'un minimum de trois protéines kinases : une protéine MAPK kinase kinase (MAP3K) qui phosphoryle une MAPK kinase (MAP2K) au niveau de résidus sérine ou thréonine, induisant son activation. Cette seconde kinase, à son tour, phosphoryle une dernière protéine MAPK et l'active également. Cette dernière transmet le signal de phosphorylation à des substrats protéiques en aval de la cascade et induit des réponses spécifiques au signal perçu en amont de la cascade. Chez *S. cerevisiae*, il existe cinq voies MAPKs connues qui régulent des processus essentiels comme la conjugaison des cellules, l'intégrité de la paroi cellulaire, les réponses à l'hyperosmolarité, la formation d'ascospores et la croissance filamenteuse (croissance invasive de cellules haploïdes ou développement de pseudohyphes diploïdes) (Gustin *et al.* 1998). Ces cascades sont largement décrites et la plupart des acteurs sont connus. La voie des MAPKs impliquée dans la régulation de la croissance filamenteuse est induite par des carences nutritionnelles, essentiellement azotées (Gimeno *et al.* 1992). Le signal initial est perçu par deux osmorecepteurs situés au niveau de la membrane plasmique, Sho1 et Msb2. Par l'intermédiaire d'une GTPase, Cdc42, et d'une

protéine se liant au GTP, Ras2, une première kinase est activée par phosphorylation. Il s'agit de Ste20 (p21-activated kinase, PAK). Cette étape est suivie des phosphorylations successives de Ste11 (MAP3K ou MAPK/ERK kinase kinase = MEKK), Ste7 (MAP2K ou MAPK/ERK kinase =MEK) et enfin Kss1 (MAPK) (Cook *et al.* 1997; Madhani and Fink 1997). Une alternative à cette voie consiste à l'activation par Ste11 d'une autre MAP2K, Pbs2 puis de Hog1, une MAPK qui répond à des conditions de fortes osmolarités (Ferrigno *et al.* 1998; Shively *et al.* 2013). Hog1 est connue pour induire la répression de la croissance des pseudohyphes en absence de stimuli entrainant la transition. Une fois activée, Hog1 est transférée dans le noyau où elle active des facteurs de transcription qui régulent l'expression de gènes impliqués dans la réponse à l'hyperosmoralité (Ferrigno *et al.* 1998; De Nadal *et al.* 2003; Shively *et al.* 2013). La translocation détermine l'inhibition ou l'activation de la croissance filamenteuse par Hog1 (Shively *et al.* 2013). Les principaux substrats en aval des cascades MAPKs sont des facteurs de transcription comme Ste12 et Tec1, séquestrés dans le noyau. Suite à la phosphorylation de Kss1, qui induit ici son inactivation, ces facteurs sont libérés (Sánchez-Martínez and Pérez-Martín 2001; Nadal *et al.* 2008; Hamel *et al.* 2012). Tec1 et Ste12 reconnaissent des séquences FREs (Filamentation and invasive Response Element) dans les régions promotrices et régulent l'expression de gènes impliqués dans le développement de pseudohyphes et la croissance invasive haploïde, comme *Flo11* et *Tec1* lui-même, ou l'insertion du transposon *Ty1* (Company *et al.* 1988; Madhani and Fink 1997; Oehlen and Cross 1998). La croissance filamenteuse est inhibée chez des mutants *ste12*, *tec1* et *ste12tec1* chez *S. cerevisiae*. Flo11 code pour une floculine ancrée à la surface des cellules, et est un effecteur essentiel à la croissance des pseudohyphes (Pan and Heitman 1999; Shively *et al.* 2013).

Les recherches sur les champignons pathogènes indiquent que cette voie est hautement conservée entre les espèces. La plupart des protéines présentées ici ont des homologues chez les champignons dimorphiques. Ainsi, pour *C. albicans*, les deux cascades MAPKs (via Ste7 ou Hog1) sont conservées et jouent un rôle dans le changement de morphologie (Alonso-Monge *et al.* 1999; Lengeler *et al.* 2000). La voie de régulation de la transition L-M par les MAPKs implique deux « p21-activated kinases » (PAKs) (Cst20 et Cla4), une MAP2K (Hst7) et une MAPK (Cek1). La cascade active Cph1 (Candida PseudoHyphal regulator), un facteur de transcription homologue de Ste12 (Liu *et al.* 1994). Des mutations inactivant

chacun de ces gènes provoquent un développement d'hyphes défectueux en milieu solide mais n'ont aucun effet lorsque le champignon pousse dans du sérum. Dans ce cas, d'autres voies doivent prendre le relais et assurer le bon développement des hyphes, comme par exemple la voie de signalisation dépendante du pH (Lengeler *et al.* 2000; Sánchez-Martínez and Pérez-Martín 2001). Chez le basidiomycète *Ustilago maydis*, la voie des MAPKs est également impliquée dans la transition levure-mycélium car elle régule le processus de conjugaison (*mating* en anglais), essentiel à la production de mycélium dicaryotique à partir de spores haploïdes (Banuett and Herskowitz 1994; Mayorga and Gold 1999; Sánchez-Martínez and Pérez-Martín 2001).

1.2.2.3.2 Voie dépendante de l'AMPc-PKA

Une voie dépendante de la PKA est également impliquée dans la régulation de la croissance filamenteuse (Sonneborn *et al.* 2000; Pan and Heitman 2002; Hu *et al.* 2014). Chez *S. cerevisiae*, cette voie est requise pour l'activation de Flo11. Comme chez la plupart des levures ou des mammifères, la PKA de *S. cerevisiae* est un tétramère qui contient un dimère composé de deux parmi trois sous-unités catalytiques (Tpk1-3) et un homodimère de sous-unités régulatrices (Bcy1) (Pan and Heitman 1999). Ce dernier inhibe l'activité protéique des sous-unités catalytiques lorsqu'elles sont liées. Une mutation knockout *bcy1* induit une stimulation de la filamentation et permet de restaurer le développement des pseudohyphes chez *ste12*, *tec1* et *ste12tec1*, indiquant ainsi que la voie passant par la PKA est indépendante de la cascade des MAPKs. L'activation de la PKA est dépendante de l'AMP cyclique qui se lie à la sous-unité régulatrice et induit un changement de conformation, libérant ainsi les sous-unités catalytiques. En réponse à des signaux externes, la concentration intracellulaire d'AMPc augmente grâce à l'action d'un récepteur (Gpr1) couplé à la sous-unité α d'une protéine G (Gpa2). Sur les trois protéines Tpk1-3, seule Tpk2 a un effet positif sur le développement de pseudohyphes. Une fois libérée, la protéine interagit avec Flo8 et Sfl1 et induit leur phosphorylation (Pan and Heitman 1999). Ces dernières régulent l'activité de Flo11. Flo8 est un activateur transcriptionnel qui régule positivement Flo11, favorisant ainsi la croissance filamenteuse. *A contrario,* Sfl1 est connu pour être un régulateur négatif de la floculation des levures et donc un inhibiteur de Flo11. La phosphorylation de Flo8 et Sfl1 par Tpk2 induit l'activation de l'une et l'inhibition de l'autre, respectivement (Pan and

Heitman 1999, 2002; Lengeler *et al.* 2000; Nadal *et al.* 2008; Shively *et al.* 2013). L'AMPc est un messager secondaire impliqué dans de nombreux processus développementaux chez les eucaryotes. Chez *O. novo-ulmi*, une étude sur la souche NRRL6404 d'A. Brunton et G. Gadd en 1989 a montré une corrélation entre l'augmentation de la concentration en AMPc, une inhibition des phosphodiestérases qui hydrolysent l'AMPc en 5'-AMP, et la transition L-M (Brunton and Gadd 1989). De manière similaire, une augmentation de la concentration en AMPc intracellulaire induit la transition L-M et la production d'hyphes chez *C. albicans*. Ici, la voie de transduction du signal est très semblable à celle chez *S. cerevisiae*, malgré l'absence de Tpk3. Tpk1 joue un rôle important dans le développement des hyphes en milieu solide et Tpk2 est requis pour la croissance filamenteuse en milieu liquide (Sonneborn *et al.* 2000; Bockmühl *et al.* 2001). Tpk1 et Tpk2 entrainent l'activation d'Efg1, un facteur de transcription ayant un rôle prédominant dans la croissance filamenteuse chez *C. albicans* (Lo *et al.* 1997; Bockmühl and Ernst 2001). Chez *U. maydis*, par contre, l'activation de la PKA inhibe la production d'hyphes et favorise le bourgeonnement levuriforme. Cependant, le déroulement de la voie reste globalement équivalent à ceux présentés pour *S. cerevisiae* et *C. albicans* (Lengeler *et al.* 2000).

Les deux voies présentées ci-dessus agissent donc de manière spécifique en fonction de l'espèce de champignon étudiée, bien que de nombreux acteurs soient retrouvés chez toutes les espèces : chez *C. albicans*, tout comme chez *S. cerevisiae*, les deux premières voies « collaborent » et influencent positivement la croissance filamenteuse alors que chez *U. maydis*, ces deux mêmes voies agissent en antagonistes, puisque des niveaux élevés d'AMPc induisent la répression de la formation des hyphes (Gold *et al.* 1994; Krüger *et al.* 1998; Sánchez-Martínez and Pérez-Martín 2001). Malgré ces divergences, il semblerait que les stratégies pour relier un stimulus externe à une modification de différentiation cellulaire soient relativement conservées dans le règne fongique (Lengeler *et al.* 2000; Sánchez-Martínez and Pérez-Martín 2001; Nadal *et al.* 2008), ainsi ces voies doivent exister chez *O. novo-ulmi* également.

1.2.2.3.3 Cascade de réponse aux variations de pH Pal/RIM

La cascade de signalisation Pal/Rim (Pal pour les champignons filamenteux et dimorphiques comme *U. maydis* ou *C. albicans*, Rim pour les champignons levuriformes et *S. cerevisiae*) contrôle les réponses morphologiques et l'adaptation à des variations de pH dans l'environnement (revu par Cervantes-Chávez *et al.* 2010). Pour *C. albicans*, ce dernier point est fondamental puisque, comme introduit précédemment, il colonise l'appareil digestif, les voies urogénitales (pH très acide), ainsi que le conduit oropharyngal et les vaisseaux sanguins (pH légèrement alcalin) des mammifères (Bernardis *et al.* 1998; Davis 2003). Le champignon doit être capable de modifier les réponses cellulaires en fonction de l'environnement. Le passage d'un pH acide à des conditions neutres ou alcalines induit la transition L-M chez *C. albicans* et des champignons mutés au niveau des gènes impliqués dans la voie Pal/Rim sont incapables de former des filaments à pH alcalin (Davis *et al.* 2000). La voie Pal/Rim est relativement conservée entre les différentes espèces de champignons.

Le pH joue un rôle déterminant dans la transition L-M obtenue *in vitro* chez *U. maydis*. A l'inverse de *C. albicans*, à pH neutre, le champignon produit des sporidies (levures) alors qu'un pH acide induit le développement de mycélium (Ruiz-herrera *et al.* 1995).

La cascade Pal/Rim comprend au moins six protéines qui régulent l'activation protéolytique d'un facteur de transcription de type « doigt de zinc », nommé PacC chez les champignons filamenteux et Rim101 chez *S. cerevisiae* et *C. albicans* (revu par Cervantes-Chávez *et al.* 2010; Selvig and Alspaugh 2011). L'activation intervient à pH neutre ou alcalin et induit le clivage d'une région dans la partie C-terminale de la protéine (revu par Selvig and Alspaugh, 2011). Les six protéines sont réparties en deux complexes : un premier au niveau de la membrane plasmique comprenant PalH/Rim21, PalI/Rim9 et PalF/Rim8, et un second au niveau de la membrane endosomale incluant PalA/Rim20, PalB/Rim13 et Snf7/Vps32 (pour *U. maydis*, Vps20/Snf7 chez *A. nidulans*) (machinerie ESCRT-III). Le premier complexe est le senseur initial du pH. PalH et PalI sont des protéines transmembranaires et PalF interagit avec le domaine C-terminal de PalH. En réponse à un pH neutre ou alcalin, le complexe PalF/PalH est ubiquitiné et phosphorylé. Cela induit son endocytose et permet l'interaction avec le second complexe endosomal et le transfert du signal de pH. PalC/Rim23 permet le contact physique entre les deux complexes. Leur rapprochement induit le recrutement de

PacC et son activation protéolytique par l'action de PalB. En conditions alcalines, PacC activé réprime l'expression des gènes de réponse au pH acide et induit celles des gènes de réponse au pH alcalin. La plupart de ces gènes codent des enzymes telles que des protéases, perméases ou phosphatases. PacC induit également sa propre expression (boucle d'autorégulation positive) (revu par Penãlva and Arst, 2002; Selvig and Alspaugh, 2011). Chez *C. albicans*, deux gènes régulés en aval de la voie RIM ont été mis en évidence : *Phr1* et *PHR2* qui codent deux protéines homologues 1-3-β-glucanosyltransférases impliquées dans la synthèse de la paroi cellulaire fongique. Le mutant homozygote *Δphr1* montre une morphologie anormale et présente une croissance défectueuse à pH alcalin mais n'est pas affecté en condition acide. Le mutant *Δphr2* présente le phénotype inverse. Les mutants *Δrim101, Δrim8* et *Δrim20* présentent une expression élevée de *PHR2* et une absence d'expression de *PHR1* (Penãlva and Arst 2002).

1.3 Génétique chez les agents de la MHO

O. novo-ulmi est une espèce facilement manipulable pour des études de génétique. Comme mentionné précédemment, il est possible de contrôler aisément la transition L-M par différents facteurs, comme la source azotée, ainsi que d'obtenir des périthèces *in vitro* en croisant des espèces compatibles sexuellement sur milieu solide contenant de l'acide linoléique et des copeaux de bois d'orme (Hubbes 1975; Marshall *et al.* 1982). De plus, les hyphes et les spores sont uni-nucléés de manière prédominante et le noyau somatique est haploïde. Ainsi, la ségrégation d'un phénotype lié à un gène unique est attendue avec un ratio 1:1 lors de croisement.

L'analyse génétique des agents pathogènes de la MHO a été, jusqu'ici, principalement basée sur la production de mutants par mutagénèse chimique ou insertionnelle et sur des croisements en laboratoire entre souches dont le phénotype de pathogénie est différent (Bernier and Hubbes 1990b, 1994; Kile and Brasier 1990; Plourde *et al.* 2008).

En 2013, le séquençage du génome d'*O. novo-ulmi* a été achevé. La taille du génome nucléaire est de 31,8 Mb. Il contient 8640 gènes annotés distribués sur huit chromosomes (Comeau *et al.* 2015). Le génome mitochondrial, lui, mesure 66,4 Kb et contient 15 gènes et 26 ARN de transfert (ARNt) (Forgetta *et al.* 2013). En parallèle, le génome nucléaire d'*O. ulmi* a également été séquencé et les 8639 gènes qu'il contient ont été annotés (Khoshraftar

et al. 2013). Ces travaux d'envergure ouvrent le champ à de nombreuses opportunités en matière d'études génétiques, de mises en évidence de processus moléculaires et de ciblage de gènes impliqués dans la pathogénie et la fitness des agents pathogènes de la MHO.

Les données obtenues par croisement ont fortement suggéré que plusieurs gènes sont impliqués dans la pathogénie d'*O. novo-ulmi* (Brasier and Gibbs 1976). L'un des premiers à avoir été identifiés et localisés à l'aide de marqueurs RAPD fut *Pat1* (Et-Touil *et al.* 1999). Deux allèles *Pat1-h* et *Pat1-m* ont été identifiés et ils confèrent des degrés de virulence différents (haut et modéré, respectivement) chez des souches d'*O. novo-ulmi*. Cependant, la nature exacte du gène reste inconnue.

Par comparaison de séquences protéiques, des orthologues de la plupart des protéines connues chez *S. cerevisiae* dans les trois voies de régulation du dimorphisme ont été retrouvés chez *O. novo-ulmi*. Ainsi, les acteurs clés de la transition L-M chez ces espèces modèles sont présents chez *O. novo-ulmi*, laissant supposer que les trois voies opèrent dans notre système d'étude. Néanmoins, peu de données sont disponibles quant à la régulation moléculaire de la pathogénie chez *O. novo-ulmi*.

1.4 Transcriptomique à l'échelle du génome entier

Le terme « transcriptome » renvoie à l'ensemble des transcrits/gènes exprimés dans un échantillon à un instant *t* dans une condition donnée (stade développemental ou condition physiologique) (Wang *et al.* 2009).

Le développement des techniques de séquençage de troisième génération a permis de mettre au point des méthodes d'analyses transcriptomiques précises et spécifiques à l'échelle du génome entier. Le séquençage à partir d'ARNs messagers totaux (RNAseq) offre l'opportunité d'accéder à l'entièreté du transcriptome. Chaque transcrit présent dans une cellule étudiée est représenté dans l'ensemble des séquences produites par RNAseq. D'une part, le nombre de transcrits est proportionnel au niveau d'expression des transcrits/gènes, permettant des analyses comparatives entre différentes conditions d'intérêt. D'autre part, si le génome de l'espèce étudié est disponible, le séquençage à partir d'ARNs messagers donne accès aux gènes non annotés et aux transcrits alternatifs qui sont issus de l'épissage alternatif

lors de la transcription. Le RNAseq permet de réduire la complexité des génomes et de définir les délimitations des introns (Wang *et al.* 2009).

Plusieurs technologies sont disponibles, offertes par des compagnies telles qu'Illumina ou Ion Torrent, dont les principales différences sont la taille des lectures séquencées (30-400 pb) et la profondeur du séquençage.

Chez *O. novo-ulmi*, aucune étude de transcriptomique par RNAseq n'avait été réalisée avant le début de cette thèse. En 2011, une analyse de l'expression génique chez *O. novo-ulmi* en phase levure a été réalisée en utilisant la technique des « Expressed Sequence Tags » (ESTs) (Hintz *et al.* 2011) (pour plus de détails sur la technique, voir Chapitre 2). Cette étude a permis d'identifier 880 gènes exprimés, sur les 8640 connus maintenant grâce au séquençage ultérieur du génome (Forgetta *et al.* 2013; Comeau *et al.* 2015) et constitue le premier rapport de transcriptomique à large échelle chez cette espèce.

1.5 Hypothèses et objectifs

Il est admis que la transition L-M est essentielle à la pathogénie et la fitness chez *O. novo-ulmi* (Richards *et al.* 1982; Richards 1994), bien que peu de données expérimentales soient disponibles. Comme nous l'avons mentionné dans la section 1.3, trois voies de régulation de la transition L-M sont connues chez la levure *Saccharomyces cerevisiae* et plusieurs champignons dimorphiques modèles. Les nombreuses informations décrites concernant la régulation de la transition L-M chez ces différents organismes offrent des bases de connaissances moléculaires solides pour explorer le mode de fonctionnement d'*O. novo-ulmi*, en assumant un certain niveau de conservation des mécanismes discutés à la section 1.3. Cette hypothèse est appuyée entre autres par les études préliminaires sur l'influence de l'AMPc sur le dimorphisme réalisées par Brunton et Gadd (1989). De plus, les informations de comparaison de séquence ont permis l'identification de gènes homologues, entre autres *Flo11*, *Ste12*, *Efg1* ou encore *Phr1*, chez *O. novo-ulmi*.

Dans ce contexte, la thèse de doctorat que nous présentons ici se propose d'investiguer l'impact du dimorphisme sur le développement de la MHO en cherchant et identifiant des facteurs moléculaires qui permettent de contrôler la transition levure-mycélium chez *O. novo-ulmi* sp. *novo-ulmi* afin de déterminer les voies moléculaires conservées/uniques

présentes chez ce champignon. Nous choisissons de travailler sur la souche de référence très virulente H327 (MAT1-1) d'*O. novo-ulmi* ssp. *novo-ulmi.* Cette souche a été isolée en 1979 par H. Jannicky sur un orme infecté de la ville de Bratislava en Slovaquie. Elle a fait l'objet de nombreuses recherches au sein de l'équipe de L. Bernier (Et-Touil *et al.* 1999; Plourde *et al.* 2008; Aoun *et al.* 2010; Naruzawa and Bernier 2014; Naruzawa *et al.* 2016) et a donc été choisie comme souche de référence. Son séquençage a été effectué (Forgetta *et al.* 2013) et les gènes ont été annotés (Comeau *et al.* 2015).

La thèse de doctorat se divise en quatre parties :

i. Revue de littérature sur les études transcriptomiques à large échelle chez les champignons dimorphiques pathogènes des humains, plantes et insectes

ii. Étude transcriptomique à large échelle des phases levuroïdes et mycéliennes chez *O. novo-ulmi*

iii. Étude transcriptomique à large échelle de la transition levure-mycélium chez *O. novo-ulmi*

iv. Analyse comparative des portraits transcriptomiques de la transition levure-mycélium chez deux champignons pathogènes : l'ascomycète *O. novo-ulmi* et le basidiomycète *Pseudozyma flocculosa*.

i. Revue de littérature sur les études transcriptomiques à large échelle chez les champignons dimorphiques pathogènes des humains, plantes et insectes.

L'objectif de cette revue est de faire un bilan sur les données de transcriptomiques qui ont été produites dans le cadre des recherches sur le dimorphisme chez les champignons pathogènes. Nous avons répertorié toutes les études portant sur la régulation de l'expression génique au cours de la transition levure-mycélium, ou vice-versa, réalisées par analyses de « séquences exprimées » (Expressed Sequence Tags, ESTs), de puces à ADN (ADN microarray) et RNAseq chez les champignons dimorphiques au cours des 20 dernières années.

ii. Étude transcriptomique à large échelle des phases levuroïdes et mycéliennes chez *O. novo-ulmi*

Étant donné le peu d'information disponible sur les différences moléculaires entre les phases levure et mycélium chez *O. novo-ulmi*, nous avons réalisé une étude transcriptomique à large échelle sur chacune des deux phases de croissance chez *O. novo-ulmi* afin de dresser un portrait étendu de l'expression génique dans ces conditions. Nous utilisons le RNAseq afin de déterminer les patrons d'expression de tous les gènes transcrits dans les deux phases. Afin de déterminer le niveau de conservation des mécanismes régulant le dimorphisme chez les champignons pathogènes, nous avons comparé nos données à celles obtenues chez *C. albicans* et *H. capsulatum*.

iii. Étude transcriptomique à large échelle de la transition levure-mycélium chez *O. novo-ulmi*

Dans ce chapitre, nous présentons les résultats d'une deuxième expérience de RNAseq réalisée au cours de la transition levure-mycélium chez *O. novo-ulmi* dans le but d'identifier les facteurs moléculaires clés de ce changement morphologique. L'analyse en série temporelle nous permet d'accéder aux patrons d'expression spécifiques de différentes étapes de la transition levure-mycélium et de déterminer les variations transcriptomiques à des stades très précoces.

iv. Analyse comparative des portraits transcriptomiques de la transition levure-mycélium chez deux champignons pathogènes : l'ascomycète *O. novo-ulmi* et le basidiomycète *Pseudozyma flocculosa*.

Dans ce dernier chapitre, nous présentons une analyse comparative des transcriptomes des phases de germination et mycélienne obtenues chez deux espèces fongiques très éloignées phylogenétiquement, *O. novo-ulmi* et *Pseudozyma flocculosa*, un basidiomycète. Le but était de vérifier la conservation de l'expression génique dans le processus de filamentation. Pour *O. novo-ulmi*, nous avons utilisé les données de RNAseq récoltées pour le chapitre 3 et pour *P. flocculosa*, nous avons exploité des données de RNAseq produites dans le cadre du séquençage du génome dans le laboratoire du Pr. Richard Bélanger, à l'Université Laval.

1.6 Bibliographie

Alonso-Monge R, Navarro-García F, Molero G, Diez-Orejas R, Gustin M, Pla J, Sánchez M, Nombela C, 1999. Role of the mitogen-activated protein kinase Hog1p in

morphogenesis and virulence of *Candida albicans*. *Journal of Bacteriology* **181**: 3058–3068.

Aoun M, Jacobi V, Boyle B, Bernier L, 2010. Identification and monitoring of Ulmus americana transcripts during in vitro interactions with the Dutch elm disease pathogen *Ophiostoma novo-ulmi*. *Physiological and Molecular Plant Pathology* **74**: 254–266.

Aoun M, Rioux D, Simard M, Bernier L, 2009. Fungal colonization and host defense reactions in *Ulmus americana* callus cultures inoculated with *Ophiostoma novo-ulmi*. *Phytopathology* **99**: 642–650.

Banuett F, Herskowitz I, 1994. Identification of Fuz7, a *Ustilago maydis* MEK / MAPKK homolog required steps in the fungal life cycle. *Genes and Development* **8**: 1367–1378.

Bernardis FD, Mühlschlegel FA, Cassone A, Fonzi WA, 1998. The pH of the host niche controls gene expression in and virulence of *Candida albicans*. *Infection and Immunity* **66**: 3317–3325.

Bernier L, Aoun M, Bouvet G, Comeau A, Dufour J, Naruzawa E, Nigg M, Plourde K, 2015. Genomics of the Dutch elm disease pathosystem: are we there yet? *iForest - Biogeosciences and Forestry* **8**: 149–157.

Bernier L, Hubbes M, 1990a. Meiotic analysis of induced mutations in *Ophiostoma ulmi*. *Canadian Journal of Botany* **68**: 232–235.

Bernier L, Hubbes M, 1990b. Mutations in *Ophiostoma ulmi* induced by N-methyl-N ’-nitro-N-nitrosoguanidine. *Canadian Journal of Botany* **68**: 225–231.

Bernier L, Hubbes M, 1994. Induction and genetic characterization of ultraviolet-sensitive mutants in the elm tree pathogen (sensu lato). *Mycological Research* **98**: 943–953.

Berrocal A, Navarrete J, Oviedo C, Nickerson KW, 2012. Quorum sensing activity in *Ophiostoma ulmi*: effects of fusel oils and branched chain amino acids on yeast-mycelial dimorphism. *Journal of applied microbiology* **113**: 126–134.

Biswas S, Van Dijck P, Datta A, 2007. Environmental sensing and signal transduction pathways regulating morphopathogenic determinants of *Candida albicans*. *Microbiol. Mol. Biol. Rev.* **71**: 348–376.

Bockmühl DP, Ernst JF, 2001. A potential phosphorylation site for an A-Type kinase in the Efgl regulator protein contributes to hyphal morphogenesis of *Candida albicans*. *Genetics* **157**: 1523–1530.

Bockmühl DP, Krishnamurthy S, Gerads M, Sonneborn A, Ernst JF, 2001. Distinct and redundant roles of the two protein kinase A isoforms Tpk1p and Tpk2p in morphogenesis and growth of *Candida albicans*. *Molecular Microbiology* **42**: 1243–1257.

Brasier CM, 1981. Laboratory investigation of *Ceratocystis ulmi*. In: Stipes RJ,, Campana RJ, eds. *Compendium of elm diseases*. St Paul, Minnesota, pp. 76–79.

Brasier CM, 1991. *Ophiostoma novo-ulmi* sp . *nov*., causative agent of current Dutch elm disease pandemics. *Mycopathologia* **115**: 151–161.

Brasier CM, Gibbs JN, 1976. Inheritance of pathogenicity and cultural characters in *Ceratocystis ulmi* : hybridization of aggressive and non -aggressive strains. *Annals of applied Biology* **83**: 31–37.

Brasier CM, Kirk SA., 2001. Designation of the EAN and NAN races of *Ophiostoma novo-ulmi* as subspecies. *Mycological Research* **105**: 547–554.

Brasier CM, Kirk SA., Pipe ND, Buck KW, 1998. Rare interspecific hybrids in natural populations of the Dutch elm disease pathogens *Ophiostoma ulmi* and *O. novo-ulmi*. *Mycological Research* **102**: 45–57. https://doi.org/10.1017/S0953756297004541

Brunton AH, Gadd GM, 1989. The effect of exogenously-supplied nucleosides and nucleotides and the involvement of adenosine 3':5'-cyclic monophosphate (cyclic AMP) in the yeast mycelium transition of *Ceratocystis* (= *Ophiostoma*) *ulmi*. *FEMS microbiology letters* **60**: 49–53.

Campana RJ, 1978. Inoculation and fungal invasion of the tree. In: Sinclair WA,, Campana RJ, eds. *Dutch elm disease: perspectives after 60 years*. Ithaca, N.Y, pp. 17–20.

Cervantes-Chávez JA, Ortiz-Castellanos L, Tejeda-Sartorius M, Gold S, Ruiz-Herrera J, 2010. Functional analysis of the pH responsive pathway Pal/Rim in the phytopathogenic basidiomycete *Ustilago maydis*. *Fungal genetics and biology* **47**: 446–57.

Comeau AM, Dufour J, Bouvet GF, Jacobi V, Nigg M, Henrissat B, Laroche J, Levesque RC, Bernier L, 2015. Functional annotation of the *Ophiostoma novo-ulmi* genome: insights into the phytopathogenicity of the fungal agent of Dutch elm disease. *Genome biology and evolution* **7**: 410–430.

Company M, Adler C, Errede B, 1988. Identification of a Tyl regulatory sequence responsive to Ste7 and Ste12. *Molecular and cellular biology* **8**: 2545-2554

Cook JG, Bardwell L, Thorner J, 1997. Inhibitory and activating functions for MAPK Kss1 in the *S. cerevisiae* filamentous-growth signalling pathway. *Nature* **390**: 85–88.

Crane JL, Schoknecht JD, 1973. Conidiogenesis in *Ceratocystis ulmi*, *Ceratocystis piceae*, and *Graphium penicillioides*. *American journal of botany* **60**: 346–354.

Davis D, 2003. Adaptation to environmental pH in *Candida albicans* and its relation to pathogenesis. *Current genetics* **44**: 1–7.

Davis D, Edwars, John J, Mitchell AP, Ibrahim AS, 2000. *Candida albicans* RIM101 pH response pathway is required for host-pathogen interactions. *Infection and Immunity* **68**: 5953–5959.

Duchesne LC, Jeng RS, Hubbes M, 1985. Accumulation of phytoalexins in *Ulmus americana* in response to infection by a nonaggressive and an aggressive strain of *Ophiostoma ulmi*. *Canadian Journal of Botany* **63**: 678–80.

Elgersma DM, 1970. Length and diameter of xylem vessels as factors in resistance of elms to *Ceratocystis ulmi*. *Netherlands Journal of Plant Pathology* **76**: 179–182.

Ernst JF, 2000. Transcription factors in *Candida albicans* - environmental control of morphogenesis. *Microbiology* **146**: 1763–1774.

Et-Touil A, Brasier CM, Bernier L, 1999. Localization of a pathogenicity gene in *Ophiostoma novo-ulmi* and evidence that it may be introgressed from *O . ulmi*. *Molecular plant-microbe interactions : MPMI* **12**: 6–15.

Et-Touil A, Rioux D, Mathieu FM, Bernier L, 2005. External symptoms and histopathological changes following inoculation of elms putatively resistant to Dutch elm disease with genetically close strains of *Ophiostoma*. *Canadian Journal of Botany* **83**: 656–667.

Evans E, Richardson M, 1989. *Medical mycology: a practical approach*. Oxford.

Ferrigno P, Posas F, Koepp D, Saito H, Silver PA, 1998. Regulated nucleo/cytoplasmic exchange of HOG1 MAPK requires the importin beta homologs NMD5 and XPO1. *The EMBO journal* **17**: 5606–14.

Forgetta V, Leveque G, Dias J, Grove D, Lyons R, Genik S, Wright C, Singh S, Peterson N, Zianni M, Kieleczawa J, Steen R, Perera A, Bintzler D, Adams S, Hintz W, Jacobi V, Bernier L, Levesque R, Dewar K, 2013. Sequencing of the Dutch elm disease fungus genome using the Roche/454 GS-FLX Titanium System in a comparison of multiple genomics core facilities. *Journal of biomolecular techniques* **24**: 39–49.

Gancedo JM, 2001. Control of pseudohyphae formation in *Saccharomyces cerevisiae*. *FEMS Microbiology Reviews* **25**: 107–123.

Gauthier GM, 2015. Dimorphism in fungal pathogens of mammals, plants, and insects. *PLOS Pathogens* **11**: e1004608.

Ghosh S, Navarathna DHMLP, Roberts DD, Cooper JT, Atkin AL, Petro TM, Nickerson KW, 2009. Arginine-induced germ tube formation in *Candida albicans* is essential for escape from murine macrophage line RAW 264.7. *Infection and Immunity* **77**: 1596–1605.

Gibbs JN, Brasier CM, 1973. Correlation between cultural characters and pathogenicity in *Ceratocystis ulmi* from Britain, Europe and America. *Nature* **241**: 381–84.

Gimeno CJ, Ljungdahl PO, Styles C a., Fink GR, 1992. Unipolar cell divisions in the yeast *S. cerevisiae* lead to filamentous growth: Regulation by starvation and RAS. *Cell* **68**: 1077–1090.

Gold S, Duncan G, Barrett K, Kronstad J, 1994. cAMP regulates morphogenesis in the fungal pathogen *Ustilago maydis*. *Genes and Development* **8**: 2805–2816.

Gustin MC, Albertyn J, Alexander M, Davenport K, 1998. MAP kinase pathways in the yeast *Saccharomyces cerevisiae*. *Microbiology and molecular biology reviews : MMBR* **62**:

1264–1300.

Hamel L-P, Nicole M-C, Duplessis S, Ellis BE, 2012. Mitogen-activated protein kinase signaling in plant-interacting fungi: distinct messages from conserved messengers. *The Plant cell* **24**: 1327–51.

Harris JL, Taber WA, 1970. Influence of certain nutrients and light on growth and morphogenesis of the synnema of *Ceratocystis ulmi*. *Mycologia* **62**: 152–70.

Hintz W, Pinchback M, de la Bastide P, Burgess S, Jacobi V, Hamelin R, Breuil C, Bernier L, 2011. Functional categorization of unique expressed sequence tags obtained from the yeast-like growth phase of the elm pathogen *Ophiostoma novo-ulmi*. *BMC genomics* **12**: 431.

Hornby JM, Jacobitz-Kizzier SM, McNeel DJ, Jensen EC, Treves DS, Nickerson KW, 2004. Inoculum size effect in dimorphic fungi: extracellular control of yeast-mycelium dimorphism in *Ceratocystis ulmi*. *Applied and environmental microbiology* **70**: 1356–9.

Hornby JM, Jensen EC, Lisec AD, Tasto J, Jahnke B, Shoemaker R, Nickerson KW, Tasto JJ, Dussault P, 2001. Quorum sensing in the dimorphic fungus *Candida albicans* is mediated by farnesol. *Applied and environmental microbiology* **67**: 2982–2992.

Hu S, Zhou X, Gu X, Cao S, Wang C, Xu J-R, 2014. The cAMP-PKA pathway regulates growth, sexual and asexual differentiation, and pathogenesis in *Fusarium graminearum*. *Molecular plant-microbe interactions : MPMI* **27**: 557–66.

Hubbes M, 1975. Terpenes and Unsaturated Fatty-Acids Trigger Coremia Formation By *Ceratocystis-Ulmi*. *European Journal of Forest Pathology* **5**: 129–137.

Jensen EC, Ogg C, Nickerson KW, 1992. Lipoxygenase inhibitors shift the yeast mycelium dimorphism in *Ceratocystis ulmi*. *Applied and Environmental Microbiology* **58**: 2505–2508.

Karnosky DF, 1979. Dutch Elm Disease: A Review of the History, Environmental Implications, Control, and Research Needs. *Environmental Conservation* **6**: 311–22.

Khoshraftar S, Hung S, Khan S, Gong Y, Tyagi V, Parkinson J, Sain M, Moses AM, Christendat D, 2013. Sequencing and annotation of the *Ophiostoma ulmi* genome. *BMC genomics* **14**: 162.

Kile GA, Brasier CM, 1990. Inheritance and inter-relationship of fitness characters in progeny of an aggressive × non-aggressive cross of *Ophiostoma ulmi*. *Mycological Research* **94**: 514–522.

Krüger J, Loubradou G, Regenfelder E, Hartmann A, Kahmann R, 1998. Crosstalk between cAMP and phermone signalling pathways in *Ustilago maydis*. *Molecular and General Genetics* **260**: 193–198.

Kulkarni RK, Nickerson KW, 1981. Nutritional control of dimorphism in *Ceratocystis ulmi*.

Experimental Mycology **5**: 148–154.

Lefebvre F, Joly DL, Labbé C, Teichmann B, Linning R, Belzile F, Bakkeren G, Bélanger RR, 2013. The transition from a phytopathogenic smut ancestor to an anamorphic biocontrol agent deciphered by comparative whole-genome analysis. *The Plant cell* **25**: 1946–59.

Lengeler KB, Davidson RC, D'souza C, Harashima T, Shen WC, Wang P, Pan X, Waugh M, Heitman J, 2000. Signal transduction cascades regulating fungal development and virulence. *Microbiology and molecular biology reviews* **64**: 746–85.

Liu H, Köhler J, Fink GR, 1994. Suppression of hyphal formation in *Candida albicans* by mutation of a STE12 homolog. *Science* **266**: 1723–1726.

Lo HJ, Köhler JR, Didomenico B, Loebenberg D, Cacciapuoti A, Fink GR, 1997. Nonfilamentous *C. albicans* mutants are avirulent. *Cell* **90**: 939–949.

Madhani HD, Fink GR, 1997. Combinatorial control required for the specificity of yeast MAPK signaling. *Science* **275**: 1314–1317.

Marshall MR, Hindal DF, MacDonald WL, 1982. Production of perithecia in culture by *Ceratocystis ulmi*. *Mycological Society of America* **74**: 376–381.

Martín JA, Solla A, Ruiz-Villar M, Gil L, 2013. Vessel length and conductivity of *Ulmus* branches: ontogenetic changes and relation to resistance to Dutch elm disease. *Trees* **27**: 1239–1248.

Mayorga ME, Gold SE, 1999. A MAP kinase encoded by the ubc3 gene of *Ustilago maydis* is required for filamentous growth and full virulence. *Molecular Microbiology* **34**: 485–497.

McNabb Jr HS, Heybroek HM, Macdonald WL, 1970. Anatomical factors in resistance to Dutch elm disease 1. *Netherlands Journal of Plant Pathology* **76**: 196–204.

Middleton W, 1934. Engraver bark beetles attacking elm Trees and associated with the Dutch elm disease. *Mim. Pub. Brent. U. S. Dept. Agr.*: 1–4.

Muthukumar G, Kulkarni RK, Nickerson KW, 1985. Calmodulin levels in the yeast and mycelial phases of *Ceratocystis ulmi*. *Journal of bacteriology* **162**: 47–9.

Muthukumar G, Nickerson KW, 1984. Ca(II)-calmodulin regulation of fungal dimorphism in *Ceratocystis ulmi*. *Journal of bacteriology* **159**: 390–2.

De Nadal E, Casadome L, Posas F, 2003. Targeting the MEF2-Like transcription factor Smp1 by the stress-activated Hog1mitogen-activated protein kinase. *Molecular and cellular biology* **23**: 229–237.

Nadal M, García-Pedrajas MD, Gold SE, 2008. Dimorphism in fungal plant pathogens. *FEMS microbiology letters* **284**: 127–34.

Naruzawa ES, Bernier L, 2014. Control of yeast-mycelium dimorphism in vitro in Dutch elm

disease fungi by manipulation of specific external stimuli. *Fungal biology* **118**: 872–84.

Naruzawa ES, Malagnac F, Bernier L, 2016. Effect of linoleic acid on reproduction and yeast-mycelium dimorphism in the Dutch elm disease pathogens. *Botany* **96**: 31–39.

Nigg M, Bernier L, 2016. From yeast to hypha: defining transcriptomic signatures of the morphological switch in the dimorphic fungal pathogen *Ophiostoma novo-ulmi*. *BMC Genomics* **17**: 920.

Odds FC, 1988. *Candida and Candidosis* (Elsevier Science Health Science Division, Ed,).

Oehlen L, Cross FR, 1998. The mating factor response pathway regulates transcription of TEC1, a gene involved in pseudohyphal differentiation of *Saccharomyces cerevisiae*. *FEBS letters* **429**: 83–8.

Ouellette GB, 1978. Light and electron microscope studies on cell wall breakdown in American elm xylem tissues infected with Dutch elm disease. *Canadian Journal of Botany* **56**: 2666–93.

Ouellette GB, 1981. Ultrastructural cell wall modifications in secondary xylem of American elm surviving the acute stage of Dutch elm disease: vessel members. *Canadian Journal of Botany* **59**: 2411–2424.

Ouellette GB, Chamberland H, Goulet A, Lachapelle M, Lafontaine J-G, 1999. Fine structure of the extracellular sheath and cell walls in *Ophiostoma novo-ulmi* growing on various substrates. *Canadian Journal of Microbiology* **45**: 582–597.

Ouellette GB, Rioux D, Simard M, Chamberland H, Cherif M, Baayen RP, 2004a. Ultrastructure of the alveolar network and its relation to coating on vessel walls in elms infected by *Ophiostoma novo-ulmi* and in other plants affected with similar wilt diseases. *Investigacion Agraria: Sistemas y Recursos Forestales* **13**: 147–160.

Ouellette GB, Rioux D, Simard M, Cherif M, 2004b. Ultrastructural and cytochemical studies of host and pathogens in some fungal wilt diseases : retro- and introspection towards a better understanding of DED. *Investigacion Agraria: Sistemas y Recursos Forestales* **13**: 119–145.

Pan X, Heitman J, 1999. Cyclic AMP-dependent protein kinase regulates pseudohyphal differentiation in *Saccharomyces cerevisiae*. *Molecular and cellular biology* **19**: 4874–87.

Pan X, Heitman J, 2002. Protein Kinase A operates a molecular switch that governs yeast pseudohyphal differentiation. *Molecular and cellular biology* **22**: 3981–3993.

Paoletti M, Buck KW, Brasier CM, 2006. Selective acquisition of novel mating type and vegetative incompatibility genes via interspecies gene transfer in the globally invading eukaryote *Ophiostoma novo-ulmi*. *Molecular ecology* **15**: 249–62.

Penãlva MA, Arst HN, 2002. Regulation of gene expression by ambient pH in filamentous fungi and yeasts. *Microbiology and molecular biology reviews* **66**: 426–446.

Pereira V, Royer JC, Hintz WE, Field D, Bowden C, Kokurewicz K, Hubbes M, Horgen PA, 2000. A gene associated with filamentous growth in *Ophiostoma novo-ulmi* has RNA-binding motifs and is similar to a yeast gene involved in mRNA splicing. *Current genetics* **37**: 94–103.

Plourde KV, Jacobi V, Bernier L, 2008. NOTE / NOTE Use of insertional mutagenesis to tag putative parasitic fitness genes in the Dutch elm disease fungus *Ophiostoma novo-ulmi* subsp *novo-ulmi*. *Canadian Journal of Microbiology* **54**: 797–802.

Richards WC, 1994. Nonsporulation in the Dutch elm disease fungus *Ophiostoma ulmi* : evidence for control by a single nuclear gene. *Revue canadienne de botanique* **72**: 461–467.

Richards WC, Takai S, Lin D, Hiratsuka Y, Asina S, 1982. An abnormal strain of C*eratocystis ulmi* incapable of producing external symptoms of Dutch elm disease. *European Journal of Forest Pathology* **12**: 193–202.

Rioux D, Ouellette GB, 1991a. Barrier zone formation in host and nonhost trees inoculated with *Ophiostoma ulmi*. I . Anatomy and histochemistry. *Canadian Journal of Botany* **69**: 2055–2073.

Rioux D, Ouellette GB, 1991b. Barrier zone formation in host and nonhost trees inoculated with *Ophiostoma ulmi*. II. Ultrastructure. *Canadian Journal of Botany* **69**: 2074–2083.

Royer JC, Dewar K, Hubbes M, Horgen PA, 1991. Analysis of a high frequency transformation system for *Ophiostoma ulmi*, the causal agent of Dutch elm disease. *Molecular and general genetics : MGG* **225**: 168–76.

Ruiz-herrera J, Leon CG, Guevara-Olvera L, Carabez-trejo A, 1995. Yeast-mycelial dimorphism of haploid and diploid strains of *Ustiago maydis*. *Microbiology* **141**: 695–703.

Sánchez-Martínez C, Pérez-Martín J, 2001. Dimorphism in fungal pathogens: *Candida albicans* and *Ustilago maydis*--similar inputs, different outputs. *Current opinion in microbiology* **4**: 214–21.

Sanna ML, Zara S, Zara G, Migheli Q, Budroni M, Mannazzu I, 2012. *Pichia fermentans* dimorphic changes depend on the nitrogen source. *Fungal Biology* **116**: 769–777.

Schwarz MB, 1922. Das Zweigsterben der Ulmen, Trauerweiden und Pfirsichbäume: eine vergleichend-pathologische Studie. *Mededelingen Phytopathologisch Laboratorium "Willie Commelin Scholten"* **5**: 1–74.

Selvig K, Alspaugh JA, 2011. pH response pathways in fungi: adapting to host-derived and environmental signals. *Mycobiology* **39**: 249–56.

Shively CA, Eckwahl MJ, Dobry CJ, Mellacheruvu D, Nesvizhskii A, Kumar A, 2013. Genetic networks inducing invasive growth in *Saccharomyces cerevisiae* identified through systematic genome-wide overexpression. *Genetics* **193**: 1297–310.

Solla A, Gil L, 2002. Xylem vessel diameter as a factor in resistance of *Ulmus minor* to *Ophiostoma novo-ulmi*. *Forest Pathology* **32**: 123–134.

Solla A, Martin JA, Corral P, Gil L, 2005. Seasonal changes in wood formation of *Ulmus pumila* and *U. minor* and its relation with Dutch elm disease. *New Phytologist* **166**: 1025–1034.

Sonneborn A, Bockmühl DP, Gerads M, Kurpanek K, Sanglard D, Ernst JF, 2000. Protein kinase A encoded by TPK2 regulates dimorphism of *Candida albicans*. *Molecular microbiology* **35**: 386–96.

Spierenburg D, 1921. Een Onbekende Ziekte In De Iepen. *Tijdschrift over plantenziekten*: 53–60.

Temple B, Horgen PA, Bernier L, Hintz WE, 1997. Cerato-ulmin, a hydrophobin secreted by the causal agents of Dutch elm disease, is a parasitic fitness factor. *Fungal genetics and biology* **22**: 39–53.

Wang Z, Gerstein M, Snyder M, 2009. RNA-Seq : a revolutionary tool for transcriptomics. *Nature Reviews Genetics* **10**: 57–63.

CHAPITRE 2 Large-scale genomic analyses of dimorphism in human, insect and plant pathogenic fungi: from ESTs to RNAseq experiments.

M. Nigg[a,b] and L. Bernier[a,b]

[a] Institut de Biologie Intégrative et des Systèmes (IBIS), Université Laval, Québec, G1V 0A6, Canada

[b] Centre d'Étude de la Forêt (CEF) and Département des sciences du bois et de la forêt, Université Laval, Québec, G1V 0A6, Canada

Corresponding author:

Martha Nigg
Centre d'Étude de la Forêt (CEF)
Département des sciences du bois et de la forêt
Institut de Biologie Intégrative et des Systèmes (IBIS)
Room 2255, Pavillon Charles-Eugène-Marchand
1030, Avenue de la Médecine
Université Laval
Québec (Québec) G1V 0A6
Canada

Email: martha.nigg.1@ulaval.ca

Ce chapitre a été accepté pour publication en avril 2017 dans la revue scientifique *Fungal Biology Reviews*. doi: 10.1016/j.fbr.2017.04.001

2.1 Résumé

Le dimorphisme levure-mycélium fait l'objet de nombreuses études, en particulier chez les champignons pathogènes pour qui le changement morphologique est souvent associé à la virulence. Cette caractéristique est retrouvée chez plusieurs espèces venant de classes taxonomiques très différentes. Ici, nous présentons 26 espèces de champignons dimorphiques qui sont pathogènes des mammifères, des insectes ou des plantes. Afin d'évaluer le lien entre pouvoir pathogène fongique et dimorphisme, il est nécessaire de bien comprendre les mécanismes moléculaires qui régulent la transition levure-mycélium. Au cours des deux dernières décennies, la découverte des gènes et réseaux géniques qui contrôlent les processus biologiques a été accélérée par le développement des techniques d'analyses de la transcriptomique à l'échelle des génomes telles que les marqueurs de séquences exprimées (ESTs), les puces à ADN et le séquençage d'ARN messagers. Dans cet article, nous discutons brièvement de ces trois techniques, de leurs avantages et inconvénients puis nous détaillons les études qui portent sur la régulation du dimorphisme réalisées par le biais de ces méthodes chez sept espèces fongiques. Nous avons considéré les principaux processus biologiques qui ressortent de ces études et avons trouvé des recoupements intéressants entre espèces qui suggèrent des mécanismes de régulation moléculaire potentiellement conservés. De par la baisse constante des prix associés aux expériences de séquençage de nouvelle génération, nous prévoyons d'assister à une expansion du nombre d'études portées sur le dimorphisme chez les champignons pathogènes, notamment chez des espèces non modèles moins étudiées.

2.2 Abstract

Yeast-mycelium fungal dimorphism is a complex trait studied for many years, particularly in pathogenic fungi for which the morphological switch is often associated with virulence. It is a characteristic shared by many species from very different taxonomic classes. In this review, we present 26 dimorphic fungal species which are pathogens of mammals, insects or plants. Understanding the molecular mechanisms that regulate the morphological switch from yeast to mycelium, or vice-versa, is necessary for the comprehension of virulence. In the last two decades, the development of genome-scale transcriptomic analysis techniques such as Expressed Sequence Tags, DNA microarrays and total messenger RNA sequencing has accelerated the discovery of genes and gene networks that control biological processes. We briefly discuss the three different large-scale transcriptomic techniques, their advantages and disadvantages, and we further detail the studies that used them on seven fungal species in order to understand dimorphism. We compiled the main processes highlighted in these studies and found interesting overlaps with potential conserved molecular regulatory mechanisms among species. With next generation sequencing technologies becoming increasingly affordable to investigators worldwide, we expect that more exhaustive transcriptomic studies of dimorphism will soon be conducted on a broader range of pathogens including many non-model species.

2.3 Introduction

Yeast-Mycelium (Y-M) dimorphism is a morphological characteristic often directly associated with virulence in fungal pathogens. Dimorphic fungi have the ability to switch from the unicellular yeast stage to the pluricellular mycelial stage in a reversible way and the transition involves major cell modifications such as alterations of the cell wall composition and cell reorganization. Yeast cells proliferate by unpolarised mitosis and cytokinesis proceeds, either by fission or budding, thus forming homogenous colonies (Madhani and Fink 1998; Nadal *et al.* 2008). Mycelium results from differentiation of a germ tube by unbudded yeast cells known as the mother cells. Germ tubes grow by cell division in a polarized way which is associated with rearrangement of the actin cytoskeleton (Sudbery *et al.* 2004). Cells stay attached, resulting in a filament, and compartments are formed when septa are deposited in-between cells. Thus, the term "hypha" refers to all filaments, unbranched and branched, that grow by tip extension and have septa with pores that allow cytoplasmic connection between compartments (Odds 1988). Pathogenic genera in the phylum Zygomycota are exceptions to this statement, as they grow essentially as aseptate hyphae or hyphae with only rudimentary septa (Emmons *et al.* 1977).

The description of dimorphism given here defines what we consider true dimorphic species. However, some species display dimorphic-like behaviour in the sense that they have the capability to alternate between polar and budding growth but the mechanisms involved in the proliferation of the yeast-like cells are unclear or unknown. In that perspective, species of *Fusarium* and *Verticillium* causing vascular wilt in plants are often considered dimorphic since they produce both yeast-like and mycelial forms within host tissue (Puhalla and Bell 1981). However, in order to proliferate, the mother yeast cell has to form conidiophore-like structures (phialides) that will further produce numerous secondary yeast cells (Buckley *et al.* 1969; Puhalla and Bell 1981). Therefore, such organisms will be considered dimorphic-like in this review.

In addition to yeast and mycelial phases, some species display a so-called "pseudohyphal growth" which requires unipolar budding from a single yeast cell that becomes thinner and longer, with an ellipsoidal shape. The reiteration of this unipolar cell division by pseudohyphal cells leads to the formation of pseudohyphae (Gimeno *et al.* 1992). Such

structures are formed in the well-known human pathogen *Candida albicans* (candidiasis) and result from incomplete wall separation. Septa of pseudohyphae contain no pores (Madhani and Fink 1998). Pseudohyphae are, in some conditions, an intermediate stage between yeast and mycelium. In that sense, *C. albicans* is often considered as pleomorphic.

In many species, only one of the two phases described previously is infectious. Most dimorphic fungi that are human pathogens grow as yeast in diseased tissues but exist as non-invasive mycelium in the external environment (Gow *et al.* 2002; Kadosh 2013). In fact, in strains of the human fungal pathogens *Histoplasma capsulatum* (histoplasmosis), *Blastomyces dermatidis* (North American blastomycosis or Gilchrist's disease) and *Paracoccidioides brasiliensis* (paracoccidioidomycosis or South American blastomycosis), only yeast-like cells trigger disease (San-Blas and Nino-Vega 2001). However, in the human pathogens *Malassezia furfur* (pityriasis/tinea versicolor) and *Hortaea werneckii* (tinea nigra) and the maize pathogen *Ustilago maydis* (corn smut), the infectious stage is the hyphal phase (Dorn and Roehnert 1977; Faergemann and Fredriksson 1981; Bölker 2001; Bonifaz *et al.* 2010). Finally, in some species, such as *C. albicans,* the wilt pathogen *Verticillium dahliae* and the two main causal agents of the Dutch elm disease, *Ophiostoma novo-ulmi* and *O. ulmi*, the yeast and mycelium phases are both involved in the infection process (Campana 1978; Puhalla and Bell 1981; Odds 1988; Kadosh 2013). So far, *O. novo-ulmi*, *O. ulmi* and *V. dahliae* are the only dimorphic plant pathogens known for having both phases produced within tree tissues.

Various physical and chemical stimuli trigger the switch between yeast and filamentous growth (Figure 2.1). For instance, in *C. albicans*, known stimuli include temperature, nitrogen source (proline, arginine, N-acetylglucosamine) (Ernst 2000; Biswas *et al.* 2007; Ghosh *et al.* 2009), pH (Davis 2003) and the quorum sensing molecule farnesol, produced at high cell density (Hornby *et al.* 2001). Morphological switch in response to temperature changes is a trait shared by pathogens of humans and mammals (Nemecek *et al.* 2006). In *U. maydis,* yeast-to-mycelium (Y-to-M) transition can be induced *in vitro* by acidic pH (Ruiz-Herrera *et al.* 1995) and *in planta* upon mating (Mills and Kotzé, 1981). In *O. novo-ulmi*, *O. ulmi* and *P. fermentans,* quorum sensing and modifications in nitrogen sources are both involved in the dimorphic change (Berrocal *et al.* 2012; Sanna *et al.* 2012; Naruzawa and

Bernier 2014; Kulkarni and Nickerson 1981). Nevertheless, in a recent review on dimorphism, Gauthier (2015) mentioned several dimorphic species for which the stimuli for the morphological switch are still unknown, such as for the plant pathogens *Taphrina deformans* (peach leaf curl) and *Holleya sinecauda* (mustard seed rot). This illustrates the need for additional work in order to understand the diversity of stimuli involved in the morphological switch throughout different species, families and orders. In fact, fungal pathogens in which Y-M dimorphism has been reported (Nadal *et al.* 2008; Gauthier 2015) are phylogenetically diverse (Figure 2.2). The list shown here is a representative sampling of all the fungal pathogens brought to our knowledge that are either truly dimorphic or display dimorphic-like growth. Internal Transcribed Spacer 1 (ITS1) sequence data are available in the GenBank database for all species included in it (for sequences, see Table S2.1). Although dimorphic species are found in all classes of fungi, they are more abundant in the Phylum Ascomycota. Classes Eurotiomycetes and Mucorales contain exclusively human pathogens. By contrast, the Sordariomycetes include pathogens of plants, insects, humans and animals.

Nowadays, the genomes of most of the known dimorphic fungal pathogens are sequenced, facilitating further "omics" studies. Thus, besides *Holleya sinecauda* and *Pichia fermentans* for which we found no mention of sequenced genome, the genomes of all the species included in this review are publicly available (Reyna-López *et al.* 1997; Dietrich *et al.* 2004; Jones *et al.* 2004; Felipe *et al.* 2005b; Kämper *et al.* 2006; Sharpton *et al.* 2009; Ma *et al.* 2010; Klosterman *et al.* 2011; Woo *et al.* 2011; Gao *et al.* 2011; Goodwin *et al.* 2011; Cissé *et al.* 2013; Lenassi *et al.* 2013; Khoshraftar *et al.* 2013; Forgetta *et al.* 2013; Pattemore *et al.* 2014; Cuomo *et al.* 2014; Muñoz *et al.* 2015; Tang *et al.* 2015; Wu *et al.* 2015; Chibucos *et al.* 2016). For *Nomuraea rileyi* and *Lacazia loboi*, draft genomes are available in the Genome OnLine Database (https://gold.jgi.doe.gov).

Genome-wide analyses of gene expression can help determine the factors regulating the morphological switch since the transcriptional levels of genes are a way to assess the gene activities in a particular cellular process. Genes that are differentially expressed during the Y-to-M or mycelium-to-yeast (M-to-Y) transition constitute key targets for functional analyses of the link between morphology and virulence. The objective of large-scale analyses made possible by technologies developed in the last 25 years is to produce a global

transcriptomic picture at a given time, in a given condition and to compare expression profiles among conditions. Transcriptomic analysis of dimorphism was recently reviewed for the genus *Paracoccidioides* (Tavares *et al.* 2015). Considering the phylogenetic diversity of known dimorphic fungi, here we discuss Expressed Sequenced Tag (EST)-, DNA microarray- and total messenger RNA sequencing (RNAseq)-based investigations of pathogenic dimorphic fungi from different classes. Our objective is to give an overview of the molecular variations between growth phases in highly divergent species. The main processes and molecular pathways highlighted by the transcriptomic experiments discussed in this review are summarized in Table 2.1.

2.4 Large-scale transcriptomic analysis

2.4.1 Expressed Sequence Tags (ESTs)

The analysis of ESTs, developed in the late 1990's, is one of the first genome-wide techniques allowing the exploration of the transcriptome. ESTs are single-read sequences produced by sequencing pools of complementary DNA (cDNA) (Figure 2.3). cDNAs are obtained by reverse transcription of total messenger RNAs (mRNA) extracted from a sample and further cloned into a vector library. Each clone is individually end-sequenced and the resulting data are tags of approximatively 400 bp of expressed genes. An EST dataset contain genes represented by varying number of tags, depending on their level of expression in the experimental condition chosen. This allows identification of the transcribed genes in a sample, especially those that are highly expressed. The analysis of ESTs does not require knowledge of the gene content nor a sequenced genome, thereby facilitating studies on non-model species and rapid discovery of unknown genes (Bouck and Vision 2007).

This technique has been widely used in *P. brasiliensis* for identifying genes that are differentially expressed during the M-to-Y transition (Goldman *et al.* 2003; Felipe *et al.* 2003, 2005a; Bastos *et al.* 2007). These studies, reviewed by Tavares and collaborators (2015), resulted in the first transcriptome maps for *P. brasiliensis* and allowed the identification of more than 1000 phase-regulated genes, including putative virulence factors. The first large-scale analysis of the transcriptome in *O. novo-ulmi* was conducted on ESTs from the yeast phase (Hintz *et al.* 2011). The authors categorized a collection of 880 unique transcripts and identified 5.3% of these as potentially associated with fitness and virulence.

However, the lack of biological repetitions and the absence of comparison with mycelium samples narrow the interpretation regarding the specificity in the regulation of gene expression.

Several limitations are associated with ESTs. First, they represent only a portion of the original transcripts and are usually of low quality with sequencing errors, thereby restricting the interpretation of gene expression and representation in a dataset. Second, transcripts with low abundance in the conditions tested may not be sequenced. Finally, the usage of ESTs does not provide information about genomic position, gene order, introns, or regulatory motifs (Bouck and Vision 2007).

2.4.2 DNA microarrays

Another genome-wide technology used for transcriptomic analysis is the DNA microarray. In this technology established in the early 2000's, sequences of nucleic acids (the probes) are bound at defined spots to a hydrophobic surface (the array), where each spot represents one gene (Figure 2.3). The total RNA of a sample is extracted, converted to a population of cDNAs (the target) which are labelled, usually with the incorporation of fluorescently labelled nucleotides. The labelled cDNAs are hybridized to the probes on the microarray and gene expression is measured by quantifying the level of fluorescence, i.e. the number of hybridized sequences (Bumgarner 2013). Microarrays are used to compare two or more given conditions. Building a microarray that fully represents a genome requires knowledge of all the gene sequences and, ideally, a sequenced genome.

DNA microarrays were used in 2002, 2005 and 2012 in order to describe the modifications in gene expression occurring during the Y-to-M transition in *C. albicans* (Nantel *et al.* 2002; Kadosh and Johnson 2005; Carlisle and Kadosh 2012). First, transcriptional profiles of cells switching from Y-to-M and their responses to changes in temperature and culture medium were assessed using glass DNA microarrays (Nantel *et al.* 2002). A total of 6333 predicted Open Reading Frames (ORFs) were tested in a time course experiment of the Y-to-M transition induced by addition of serum and high temperature (37°C). The abundance of a large number of transcripts changed even before the occurrence of cell elongation in *C. albicans*, suggesting early rewiring of gene expression. Then, Kadosh and Johnson (2005) used a whole-genome DNA microarray to study the activation of filament-specific genes by

investigating mutant strains that were highly attenuated for virulence and that produced hyphae under non–filament-inducing conditions. The authors identified 61 genes that were significantly induced (≥2-fold) during the Y-to-M transition that took place in response to exposure to serum and 37°C. Finally, DNA microarrays were used to explore the whole-genome transcriptional profile of morphological switch in *C. albicans* by using a strain in which the transition from yeast to pseudohyphae to hyphae could be controlled (Carlisle and Kadosh 2012). Here, the investigators demonstrated that genes associated with pseudohyphae represented a subset of those associated with hyphae and were generally expressed at lower levels, suggesting that pseudohyphae are intermediate stages towards true hyphal differentiation.

DNA microarrays have also been used for analysing gene expression in a context of morphological changes in *H. capsulatum* (Hwang *et al.* 2003), *P. brasiliensis* (Felipe *et al.* 2005a; Nunes *et al.* 2005), *B. dermatidis* (Marty *et al.* 2015) and *U. maydis* (Martínez-Soto and Ruiz-Herrera, 2013).

In *H. capsulatum*, Hwang and colleagues used a genomic shotgun microarray representing approximately one-third of the genome, and identified 500 phase-regulated genes (Hwang *et al.* 2003). Ten years later, a whole genome microarray-based study of *H. capsulatum* dimorphism looked at the differences in gene expression between two strains of *H. capsulatum* and three growth phases: conidia, yeast and mycelium (Inglis *et al.* 2013). For each strain, the authors identified more than 3000 genes differentially expressed in one of the three cell types with an overlap of gene expression regulation of 20-40% between the two strains.

In *P. brasiliensis*, experiments using cDNA microarrays confirmed that the genes previously identified by analyses of ESTs (Felipe, Andrade, *et al.* 2005; Nunes *et al.* 2005) were potentially associated to the M-to-Y transition. They also allowed the identification of additional genes (423 added to the 2160 originally highlighted by ESTs) that are differentially expressed between yeast and mycelial phases, therefore with expression patterns linked to the dimorphic switch (Nunes *et al.* 2005).

Upon exposure to acidic pH *in vitro*, yeast cells of *U. maydis* switch to non-infectious monokaryotic mycelium (Ruiz-Herrera *et al.* 1995). Regulation of gene expression during this dimorphic transition *in vitro* was assessed using full genome microarrays (6902 genes) (Martínez-Soto and Ruiz-Herrera 2013; Robledo-Briones and Ruiz-Herrera 2013). In both studies, the authors used yeast and mycelium monomorphic mutants as controls and compared them with a wild-type strain grown at pH 7 (yeast) and pH 3 (mycelium). In the first analysis, Robledo-Briones and Ruiz-Herrera used a DNA microarray representing the full genome but focused their investigations on the regulation of genes involved in cell wall synthesis and structure and genes coding for secreted proteins (639 genes in total) during the Y-to-M transition induced by acidic pH (Robledo-Briones and Ruiz-Herrera 2013). They found 66 genes whose expression is regulated during the dimorphic switch. In the second microarray experiment, two-by-two comparisons between each condition revealed large sets of differentially expressed genes and allowed the isolation of 154 genes which were specifically differentially regulated during the Y-to-M dimorphic transition (Martínez-Soto and Ruiz-Herrera 2013). Some of the latter had already been described by Robledo-Briones and Ruiz-Herrera (2013).

Finally, gene expression microarrays representing 9583 of the 9587 genes predicted in *B. dermatidis* strain SLH14081 were used to compare regulation of gene expression between a mutant isolate (ΔSREB) unable to switch from Y to M and a wild-type (*WT*) isolate of the same strain in the early phase of transition (four time points between 0–48 h) following a drop in temperature from 37°C to 22°C (Marty *et al.* 2015). A minimum of 1109 genes were found to be differentially expressed (≥ 1.5 fold) in at least one time-point between the *WT* and *ΔSREB* strains, allowing the identification of various molecular processes associated with the deletion of *SREB* and the dimorphic feature (Table 2.1).

As for the ESTs, the usage of microarrays presents limitations. First, the abundance of a gene is assessed indirectly by the signal level measured at a given position on a microarray. It is assumed to be proportional to the concentration of a single gene that can hybridize to that location. However, at high concentrations of labelled cDNAs, the array will become saturated and at low concentrations, detection will be difficult. Hence, the signal is linear only over a limited range of concentrations in solution. Second, in the case of multigenic families or

highly homologous genes, it is difficult to design probes that will be specific to only one gene. Third, microarrays do not allow the detection of alternative splicing. Finally, microarrays can only detect sequences that they are designed to hybridise with, thus relying on known genes or sequences. Hence, genes that have not yet been annotated in a genome or in EST datasets will not be represented on the array, causing bias towards known genes (Bumgarner 2013).

2.4.3 Whole-genome messenger RNA sequencing (RNAseq)

The development of next-generation sequencing approaches this past decade allowed the rise of a new technique for the analysis of transcriptomes: RNAseq, or whole-transcriptome shotgun sequencing. In this technique, the total set of mRNA in a sample is extracted, converted to cDNA and sequenced (Figure 2.3). The final products, called reads, are fragments of defined length. Gene expression levels can be then estimated as the number of reads per gene is assumed to be proportional with the number of transcripts present in a sample.

RNAseq facilitates the analysis of samples containing multiple species, such as a fungal pathogen and its host cells (Enguita *et al.* 2016), since sequenced read can be assigned to a species by alignment with sequenced genomes. Moreover, RNaseq experiments allow transcriptome profiling in species whose gene contents are unknown, since it is possible to do *de novo* transcriptome analysis, without requirement of a sequenced genome nor knowledge of gene sequences. Sequencing of the whole transcriptome guaranties the presence of all the transcripts expressed in a given condition and *de novo* assembling provides insights on the genomic location of the transcripts. In the context of identifying molecular regulators of the dimorphic transition in pathogenic fungi, RNAseq has been used in *C. albicans* (Bruno *et al.* 2010), *H. capsulatum* (Edwards *et al.* 2013), *P. marneffei* (Yang *et al.* 2014), and *O. novo-ulmi* (Nigg *et al.* 2015; Nigg and Bernier 2016).

In *C. albicans,* the RNAseq experiment reported by Bruno and colleagues (2010) comprised nine *in vitro* conditions in order to generate a high-resolution map of the transcriptome by sequencing. Two of the conditions represented yeast and mycelial forms. Although the goal was not to describe differences between yeast and mycelium growth phases, the RNAseq

data included the list of gene expression levels in every condition, thereby allowing further comparisons.

In order to provide insight into the transcriptional program that regulates morphological variation and the pathogenic lifestyle in *H. capsulatum*, Edwards and collaborators compared the gene expression profiles of the pathogenic yeast phase and non-pathogenic mycelial phase of two clinical isolates (Edwards *et al.* 2013). In each strain, between 500 and 700 genes were found to be differentially expressed between yeast and mycelial growth phases.

The RNAseq analysis of yeast and mycelial samples added to Y-to-M and M-to-Y time-course experiments in *Penicillium marneffei* revealed 2718 genes (28% of the total gene content) that are differentially expressed during the morphological change (Yang *et al.* 2014). Finally, in *O. novo-ulmi*, two recent RNAseq studies investigated the morphological switch, first by describing the transcriptomic differences between yeast and mycelium growth phases (Nigg *et al.* 2015), then by following the Y-to-M transition in a time-course experiment (Nigg and Bernier 2016). In both cases, around 20% of the total gene content were differentially expressed between the conditions tested, indicating that the morphological switch involves the modification of the expression of a very large set of genes implicated in diverse processes. In the first study, the authors compared their results with the RNAseq data reported for *C. albicans* (Bruno *et al.* 2010) and *H. capsulatum* (Edwards *et al.* 2013). They focused on the orthologous genes and found very few overlaps in gene expression regulation among the three species, which could be partly explained by differences in the experimental conditions used in the three works (Nigg *et al.* 2015). In the second study, the authors highlighted gene expression modulations at early stages of the Y-to-M switch, concomitant with the swelling of yeast cells but prior to elongation (Nigg and Bernier, 2016).

Despite the many advantages that RNAseq presents, a few limitations are associated with this technology: first, the identification of small transcripts can be difficult due the selected size of reads in a library. Second, as for microarray, genes belonging to the same family can have overlapping transcripts, which makes it difficult to assess the relative abundancy of each gene. Finally, in the case of polyploidy and complex genomes, local duplication or transposition events, the mapping of transcripts can be compromised (Hirsch *et al.* 2015).

2.5 Overlaps among findings and species

Three conserved Y-to-M regulating pathways involving Mitogen-activated Protein Kinases (MAPK), cyclic Adenosine MonoPhosphate (cAMP)-PKA and pH perception have been extensively studied in model species such as *C. albicans* and *U. maydis* (Banuett and Herskowitz 1994; Gold *et al.* 1994; Sánchez-Martínez and Pérez-Martín 2001; Martínez-Espinoza *et al.* 2004; Nadal *et al.* 2008; Hamel *et al.* 2012). Transcriptional analyses of the dimorphic switch generally identify the genes under the regulation of these signaling pathways, as the main downstream elements of the latter are transcription factors, which regulate the expression of genes whose changes in activity are involved in dimorphism. Despite the importance of these three pathways in the morphological switch, comparisons of results from large-scale transcriptomic analyses highlight many other processes that play a role in the Y-M dimorphism of different species belonging to different classes.

On one hand, Y-to-M transition is associated with the expression of genes encoding secreted proteins and the enrichment in gene involved in large signal transduction processes as well as large cell wall re-organization processes and cell divisions in *C. albicans* (Nantel *et al.* 2002; Kadosh and Johnson 2005; Carlisle and Kadosh 2012), *U. maydis* (Martínez-Soto and Ruiz-Herrera 2013; Robledo-Briones and Ruiz-Herrera 2013) and *O. novo-ulmi* (Nigg and Bernier 2016) (Table 2.1). Carbohydrate metabolism, which is closely linked with cell wall structure and synthesis, was also identified in *U. maydis* and *O. novo-ulmi* as being preferentially activated during the Y-to-M transition as well (Martínez-Soto and Ruiz-Herrera 2013; Nigg and Bernier 2016), whereas it is induced in the M-to-Y transition in *P. marneffei* (Yang *et al.* 2014) and *C. albicans* (Carlisle and Kadosh 2012). Cell wall composition in chitin and glucan differs between the two growth phases in many species. Thus, several studies report different levels of those compounds and differential expression regulation of genes such as chitin synthases, chitinases or genes involved in the synthesis of α-glucans or β-glucans in yeast and mycelium phases in *U. maydis* (Martínez-Soto and Ruiz-Herrera 2013; Robledo-Briones and Ruiz-Herrera 2013) as well as in *C. albicans, O. novo-ulmi, B. dermatidis, Coccidioides* sp., *H. capsulatum, Pichia fermentans* and *P. brasiliensis* (Domer *et al.* 1967; Chattaway *et al.* 1973; Hintz 1999; Andrade *et al.* 2006; Fiori *et al.* 2012; Whiston *et al.* 2012; Marty *et al.* 2015; Nigg *et al.* 2015).

Iron availability within host is a challenge for fungal pathogens and adaptation to iron deprivation is crucial for survival. Thus, fungi use high-affinity iron uptake systems based on reductive iron assimilation or secreted siderophores (Boyce and Andrianopoulos 2015). Interestingly, iron assimilation processes seem important during the Y-to-M transition for both *C. albicans* and *B. dermatidis* (Carlisle and Kadosh 2012; Marty *et al.* 2015). In fact, *B. dermatidis* shows a slower yeast growth in iron-depleted conditions. By contrast, iron acquisition is repressed in *U. maydis* during the Y-to-M transition (Martínez-Soto and Ruiz-Herrera 2013). Iron availability has been also shown to be essential for growth of mycelium and yeast of *P. brasiliensis*, with a greater impact on mycelium (Arango and Restrepo 1988). Siderophores were also found to be essential for the Y-to-H switch in *Nomuraea rileyi* (Li *et al.* 2016), where deletion of gene *SidA* encoding a L-ornithine-N5-monooxygenase which is essential for siderophore synthesis induces a delay in the Y-to-M transition.

On the other hand, M-to-Y induces a reduction in protein production correlated with ribosome biogenesis in *C. albicans* (Carlisle and Kadosh 2012) and *P. brasiliensis* (Nunes *et al.* 2005). In *O. novo-ulmi*, intracellular soluble protein content was found to be equivalent between yeast and mycelium cultures whereas, in *O. ulmi*, the content was higher in mycelium versus yeast (Bernier *et al.* 1983). Although the latter experiment was performed on 10 day-old cultures, the result is consistent with a reduction of protein production during the M-to-Y transition in *O. ulmi*. However, in the recent transcriptomic study of the Y-to-M transition over 27 h in *O. novo-ulmi*, ribosome biogenesis was found to be downregulated during the switch, suggesting a reduction of protein production in the mycelium phase compared to the yeast phase, at least in the early growth phase (Nigg and Bernier 2016). This suggests the occurrence of phenomena opposite of those observed in *O. ulmi*, *C. albicans* and *P. brasiliensis*. Further protein content measurements at specific time points are needed to confirm these results.

The biological process associated with the protection against oxidative stresses was found to be involved in the M-to-Y transition in *P. brasiliensis* (Nunes *et al.* 2005). This process was also highly represented in the set of genes overexpressed in the yeast phase of *O. novo-ulmi* (Nigg *et al.* 2015). Consistent with the enrichment of genes involved in this process, some genes encoding catalases were overexpressed in the yeast phase of *O. novo-ulmi* compared

to the mycelial phase (Nigg *et al.* 2015). Up-regulation of genes encoding catalases in the yeast phase had already been described in *P. marneffei, P. brasiliensis* and *H. capsulatum* (Chagas *et al.* 2008; Inglis *et al.* 2013; Pongpom *et al.* 2005; Xi *et al.* 2007). This finding suggests that yeasts are more exposed to oxidative stress than mycelium. For human pathogens, it is important to handle successfully the hydrolytic enzymes and toxic metabolites produced by phagocytes where the yeasts are internalized by the host in response to invasion (Boyce and Andrianopoulos 2015). In the case of *O. novo-ulmi* and plant pathogens, *in planta* investigations of the expression of catalases with follow up of the Y-to-M switch are needed in order to understand the link between growth phase and exposition to oxidative stress during the invasion of host tissue.

Finally, sulphur metabolism was found to be significantly induced in the M-to-Y switch in *P. brasiliensis* (Bastos *et al.* 2007). One hypothesis for this phenomenon is that *P. brasiliensis* yeasts synthesize cysteine from inorganic sulphate (Andrade *et al.* 2006). In this species, organic sulphate deprivation inhibits growth of the yeast phase and prevents the M-to-Y transition (Paris *et al.* 1985). Consistent with this observation it has been shown that genes involved in assimilation of sulphur-containing amino acids and *de novo* biosynthesis of cysteine are highly expressed in yeast cells (Marques *et al.* 2004; Andrade *et al.* 2006). Interestingly, sulphur metabolism is also important in the yeast phase of *H. capsulatum* (Hwang *et al.* 2003) since genes involved in sulphur processing were present in the set of yeast-specific genes. It was previously reported that pathogenic yeasts of *H. capsulatum* needed cysteine to grow (Boguslawski and Stetler 1979), suggesting a conserved role of cysteine in the Y-M dimorphism.

2.6 Conclusions and future perspectives

Although several pathogenic fungi exhibit a dimorphic lifestyle, studies on the molecular regulation of the morphological switch have been conducted on a few species only. In this review, we reported published works on seven of the 26 species displayed in the phylogenetic tree (Figure 2.2), including 24 species for which sequenced genomes are publicly available. Four species are part of the Eurotiomycetes (*B. dermatidis*, *H. capsulatum*, *P. brasiliensis* and *P. marneffei*), one from the Sordariomycetes (*O. novo-ulmi*), one from the Saccharomycetes (*C. albicans*) clades and one species (*U. maydis*) belongs to the

Basidiomycota. Despite the fact that little conservation in orthologous gene expression was reported earlier between *O. novo-ulmi*, *C. albicans* and *H. capsulatum* (Nigg *et al.* 2015), we showed the occurrence of many overlaps in the biological mechanisms involved in the Y-to-M and M-to-Y transitions within the small set of seven species studied, suggesting a potential conservation and evolutionary convergence of the molecular regulations of the dimorphism among fungal clades.

Overall, gene expression patterns associated to the Y-to-M and M-to-Y transitions in pathogenic fungi have been investigated through different technologies. We found that, when the latter are applied to the same species, the major processes involved in the dimorphic switch were highlighted regardless of the technique used.

The development of RNAseq technology opens up the field for analyses of gene expression regulation in non-annotated, even non-sequenced, species. In that perspective, we can expect that it will stimulate the conduct of large-scale transcriptomic studies of less known species and increase current knowledge of the genes, pathways and processes involved in the dimorphic switch. The few studies have been published up to now and that we discussed here present gene expression modulations during the morphological switch obtained in response to a subset among the conditions triggering Y-M dimorphism. Thus, considering the vast variety of stimuli known and the costs of sequencing which are decreasing every year, it would seem desirable that further investigations compare the morphological switch of one species in many different conditions. Also, data from a broader spectrum of species, especially in less studied classes, are needed in order to identify processes that may be unique to particular groups. For example, in the Sordariomycota class, where we find plant-, insect- and human pathogens which are phylogenetically close (*e.g., O. novo-ulmi* and *Sporothrix schenckii* are both from the Ophiostomataceae family), it would be of great interest to compare the regulation of gene expression during the Y-to-M and M-to-Y transition. Furthermore, studies investigating conditions *in vivo* or *in planta* are also needed to assess the involvement of Y-M dimorphism in pathogenicity. *Candida albicans, U. maydis* and *P. brasiliensis* are already the subject of *in vivo* investigations (Fradin *et al.* 2003; Lorenz *et al.* 2004; Thewes *et al.* 2007; Martínez-Soto *et al.* 2013; Tavares *et al.* 2015; Noble *et al.* 2017), but for most dimorphic fungal pathogens, very little is known about their transcriptional

program upon contact with their host. Ultimately, it is crucial to complement large-scale transcriptomic analyses with functional genetic studies in which knock-out mutants are produced and characterised in order to validate the presumed role of candidate genes in the Y-M dimorphism.

2.7 Acknowledgements

We kindly thank the anonymous reviewer who provided helpful comments and suggestions. Our research is funded by the Natural Sciences and Engineering Research Council of Canada (NSERC, Discovery Grant 105519 to L.B.).

2.8 Bibliography

Andrade RV, Paes HC, Nicola AM, de Carvalho MJ, Fachin AL, Cardoso RS, Silva SS, Fernandes L, Silva SP, Donadi EA, Sakamoto-Hojo ET, Passos GA, Soares CM, Brigido MM, Felipe MS, 2006. Cell organisation, sulphur metabolism and ion transport-related genes are differentially expressed in *Paracoccidioides brasiliensis* mycelium and yeast cells. *BMC Genomics* **7**: 208.

Arango R, Restrepo A, 1988. Growth and production of iron chelants by *Paracoccidioides brasiliensis* mycelial and yeast forms. *Journal of Medical and Veterinary Mycology* **26**: 113–8.

Banuett F, Herskowitz I, 1994. Identification of Fuz7, a *Ustilago maydis* MEK / MAPKK homolog required steps in the fungal life cycle. *Genes and Development* **8**: 1367–1378.

Bastos KP, Bailão AM, Borges CL, Faria FP, Felipe MSS, Silva MG, Martins WS, Fiúza RB, Pereira M, Soares CMA, 2007. The transcriptome analysis of early morphogenesis in *Paracoccidioides brasiliensis* mycelium reveals novel and induced genes potentially associated to the dimorphic process. *BMC microbiology* **7**: 29.

Bernier L, Jeng RS, Hubbes M, 1983. Differentiation of aggressive and non-aggressive strains of *Ceratocystis ulmi* by polyacrylamide gel electrophoresis of intramycelial proteins. *Mycotaxon* **17**: 456–72.

Berrocal A, Navarrete J, Oviedo C, Nickerson KW, 2012. Quorum sensing activity in *Ophiostoma ulmi*: effects of fusel oils and branched chain amino acids on yeast-mycelial dimorphism. *Journal of applied microbiology* **113**: 126–134.

Biswas S, Van Dijck P, Datta A, 2007. Environmental sensing and signal transduction pathways regulating morphopathogenic determinants of *Candida albicans*. *Microbiol. Mol. Biol. Rev.* **71**: 348–376.

Boguslawski G, Stetler DA, 1979. Aspect of the physiology of *Histoplasma capsulatum* (a review). *Mycopathologia* **67**: 17–24.

Bölker M, 2001. *Ustilago maydis* - A valuable model system for the study of fungal dimorphism and virulence. *Microbiology* **147**: 1395–1401.

Bonifaz A, Gómez-Daza F, Paredes V, Ponce RM, 2010. Tinea versicolor, tinea nigra, white piedra, and black piedra. *Clinics in Dermatology* **28**: 140–145.

Bouck A, Vision T, 2007. The molecular ecologist's guide to expressed sequence tags. *Molecular Ecology* **16**: 907–924.

Boyce KJ, Andrianopoulos A, 2015. Fungal dimorphism: The switch from hyphae to yeast is a specialized morphogenetic adaptation allowing colonization of a host. *FEMS Microbiology Reviews* **39**: 797–811.

Bruno VM, Wang Z, Marjani SL, Euskirchen GM, Martin J, Sherlock G, Snyder M, 2010. Comprehensive annotation of the transcriptome of the human fungal pathogen *Candida albicans* using RNA-seq. *Genome Research* **20**: 1451–1458.

Buckley PM, Wyllie TD, Devay JE, 1969. Fine structure of conidia and conidium formation in *Verticillium albo-atrum* and *V. nigrescens*. *Mycological Society of America* **61**: 240–250.

Bumgarner R, 2013. DNA microarrays: Types, Applications and their future. *Curr Protoc Mol Biol.* **6137**: 1–17.

Campana RJ, 1978. Inoculation and fungal invasion of the tree. In: Sinclair WA,, Campana RJ, eds. *Dutch elm disease: perspectives after 60 years*. Ithaca, N.Y, pp. 17–20.

Carlisle PL, Kadosh D, 2012. A genome-wide transcriptional analysis of morphology determination in *Candida albicans*. *Molecular biology of the cell* **24**: 246–60.

Chagas RF, Bailão AM, Pereira M, Winters MS, Smullian AG, Deepe GS, de Almeida Soares CM, 2008. The catalases of *Paracoccidioides brasiliensis* are differentially regulated: Protein activity and transcript analysis. *Fungal Genetics and Biology* **45**: 1470–1478.

Chattaway FW, Bishop R, Holmes MR, Odds FC, Barlow AJ, 1973. Enzyme activities associated with carbohydrate synthesis and breakdown in the yeast and mycelial forms of *Candida albicans*. *Journal of general microbiology* **75**: 97–109.

Chibucos MC, Soliman S, Gebremariam T, Lee H, Daugherty S, Orvis J, Shetty AC, Crabtree J, Hazen TH, Etienne KA, Kumari P, O/'Connor TD, Rasko DA, Filler SG, Fraser CM, Lockhart SR, Skory CD, Ibrahim AS, Bruno VM, 2016. An integrated genomic and transcriptomic survey of mucormycosis-causing fungi. *Nature Communications* **7**: 1–11.

Cissé OH, Almeida JMGCF, Fonseca A, Kumar AA, Salojarvi J, Overmyer K, Hauser PM, Pagni M, 2013. Genome sequencing of the plant pathogen *Taphrina deformans*, the causal agent of peach leaf curl. *mBio* **4**: 1–8.

Cuomo CA, Rodriguez-Del Valle N, Perez-Sanchez L, Abouelleil A, Goldberg J, Young S, Zeng Q, Birren BW, 2014. Genome Sequence of the Pathogenic Fungus *Sporothrix schenckii*. *Genome Announcement* **2**: e00446-14.

Davis D, 2003. Adaptation to environmental pH in *Candida albicans* and its relation to pathogenesis. *Current genetics* **44**: 1–7.

Dietrich FS, Voegeli S, Brachat S, Lerch A, Gates K, Steiner S, Mohr C, Pöhlmann R, Luedi P, Choi S, Wing R a, Flavier A, Gaffney TD, Philippsen P, 2004. The *Ashbya gossypii* genome as a tool for mapping the ancient *Saccharomyces cerevisiae* genome. *Science* **304**: 304–7.

Domer JE, Hamilton JG, Harkin JC, 1967. Comparative study of the cell walls of the yeastlike and mycelial phases of *Histoplasma capsulatum*. *Journal of Bacteriology* **94**: 466–474.

Dorn M, Roehnert K, 1977. Dimorphism of *Pityrosporum orbiculare* in a defined culture medium. *The Journal of investigative dermatology* **69**: 244–48.

Edwards JA, Chen C, Kemski MM, Hu J, Mitchell TK, Rappleye C a, 2013. *Histoplasma* yeast and mycelial transcriptomes reveal pathogenic-phase and lineage-specific gene expression profiles. *BMC genomics* **14**: 695.

Emmons C, Binford C, Utz J, Kwon-Chung K, 1977. *Medical mycology*. Lea and Febiger, Philadelphia.

Enguita FJ, Costa MC, Fusco-almeida AM, Mendes-Giannini MJ, Leitão AL, 2016. Transcriptomic crosstalk between fungal invasive pathogens and their host cells : opportunities and challenges for next-generation sequencing methods. *Journal of Fungi* **2**: 1–15.

Ernst JF, 2000. Transcription factors in *Candida albicans* - environmental control of morphogenesis. *Microbiology* **146**: 1763–1774.

Faergemann J, Fredriksson T, 1981. Experimental infections in rabbits and humans with *Pityrosporum orbiculare* and *P. ovale*. *The Journal of investigative dermatology* **77**: 314–318.

Felipe MSS, Andrade R V, Arraes FBM, Nicola AM, Maranhão AQ, Torres F a G, Silva-Pereira I, Poças-Fonseca MJ, Campos EG, Moraes LMP, Andrade PA, Tavares AHFP, Silva SS, Kyaw CM, Souza DP, Pereira M, Jesuíno RSA, Andrade E V, Parente JA, Oliveira GS, Barbosa MS, Martins NF, Fachin AL, Cardoso RS, Passos GAS, Almeida NF, Walter MEMT, Soares CMA, Carvalho MJA, Brígido MM, 2005a. Transcriptional profiles of the human pathogenic fungus *Paracoccidioides brasiliensis* in mycelium and yeast cells. *The Journal of biological chemistry* **280**: 24706–24714.

Felipe MSS, Andrade RV, Petrofeza SS, Maranhão AQ, Torres FAG, Albuquerque P, Arraes FBM, Arruda M, Azevedo MO, Baptista AJ, Bataus LAM, Borges CL, Campos EG,

Cruz MR, Daher BS, Dantas A, Ferreira MASV, Ghil GV, Jesuino RSA, Kyaw CM, Leitão L, Martins CR, Moraes LMP, Neves EO, Nicola AM, Alves ES, Parente JA, Pereira M, Poças-Fonseca MJ, Resende R, Ribeiro BM, Saldanha RR, Santos SC, Silva-Pereira I, Silva MAS, Silveira E, Simões IC, Soares RBA, Souza DP, De-Souza MT, Andrade EV, Xavier MAS, Veiga HP, Venancio EJ, Carvalho MJA, Oliveira AG, Inoue MK, Almeida NF, Walter MEMT, Soares CMA, Brígido MM, 2003. Transcriptome characterization of the dimorphic and pathogenic fungus *Paracoccidioides brasiliensis* by EST analysis. *Yeast (Chichester, England)* **20**: 263–71.

Felipe MSS, Torres FAG, Maranhao AQ, Silva-Pereira I, Poças-Fonseca MJ, Campos EG, Moraes LMP, Arraes FBM, Carvalho MJA, Andrade R V., Nicola AM, Teixeira MM, Jesuíno RSA, Pereira M, Soares CMA, Brígido MM, 2005b. Functional genome of the human pathogenic fungus *Paracoccidioides brasiliensis*. *FEMS Immunology and Medical Microbiology* **45**: 369–381.

Fiori S, Scherm B, Liu J, Farrell R, Mannazzu I, Budroni M, Maserti BE, Wisniewski ME, Migheli Q, 2012. Identification of differentially expressed genes associated with changes in the morphology of *Pichia fermentans* on apple and peach fruit. *FEMS Yeast Research* **12**: 785–795.

Forgetta V, Leveque G, Dias J, Grove D, Lyons R, Genik S, Wright C, Singh S, Peterson N, Zianni M, Kieleczawa J, Steen R, Perera A, Bintzler D, Adams S, Hintz W, Jacobi V, Bernier L, Levesque R, Dewar K, 2013. Sequencing of the Dutch elm disease fungus genome using the Roche/454 GS-FLX Titanium System in a comparison of multiple genomics core facilities. *Journal of biomolecular techniques* **24**: 39–49.

Fradin C, Kretschmar M, Nichtterlein T, Gaillardin C, d'Enfert C, Hube B, 2003. Stage-specific gene expresion of *Candida albicans* in human blood. *Molecular Microbiology* **47**: 1523–1543.

Gao Q, Jin K, Ying SH, Zhang Y, Xiao G, Shang Y, Duan Z, Hu X, Xie XQ, Zhou G, Peng G, Luo Z, Huang W, Wang B, Fang W, Wang S, Zhong Y, Ma LJ, St. Leger RJ, Zhao GP, Pei Y, Feng MG, Xia Y, Wang C, 2011. Genome sequencing and comparative transcriptomics of the model entomopathogenic fungi *Metarhizium anisopliae* and *M. acridum*. *PLoS Genetics* **7**: e1001264.

Gauthier GM, 2015. Dimorphism in fungal pathogens of mammals, plants, and insects. *PLOS Pathogens* **11**: e1004608.

Ghosh S, Navarathna DHMLP, Roberts DD, Cooper JT, Atkin AL, Petro TM, Nickerson KW, 2009. Arginine-induced germ tube formation in *Candida albicans* is essential for escape from murine macrophage line RAW 264.7. *Infection and Immunity* **77**: 1596–1605.

Gimeno CJ, Ljungdahl PO, Styles CA, Fink GR, 1992. Unipolar cell divisions in the yeast *S. cerevisiae* lead to filamentous growth: Regulation by starvation and RAS. *Cell* **68**: 1077–1090.

Gold S, Duncan G, Barrett K, Kronstad J, 1994. cAMP regulates morphogenesis in the fungal pathogen *Ustilago maydis*. *Genes and Development* **8**: 2805–2816.

Goldman GH, Savoldi M, Semighini CP, Oliveira RC De, Nunes LR, Travassos LR, Puccia R, Batista WL, Ferreira LE, Bogossian AP, Tekaia F, Nobrega MP, Nobrega FG, Goldman MHS, 2003. Expressed Sequence Tag analysis of the human pathogen *Paracoccidioides brasiliensis* yeast phase: identification of putative homologues of *Candida albicans* virulence and pathogenicity genes. *Eukaryotic Cell* **2**: 34–48.

Goodwin SB, M'Barek S Ben, Dhillon B, Wittenberg AHJ, Crane CF, Hane JK, Foster AJ, van der Lee TAJ, Grimwood J, Aerts A, Antoniw J, Bailey A, Bluhm B, Bowler J, Bristow J, van der Burgt A, Canto-Canché B, Churchill ACL, Conde-Ferràez L, Cools HJ, Coutinho PM, Csukai M, Dehal P, de Wit P, Donzelli B, van de Geest HC, van Ham RCHJ, Hammond-Kosack KE, Henrissat B, Kilian A, Kobayashi AK, Koopmann E, Kourmpetis Y, Kuzniar A, Lindquist E, Lombard V, Maliepaard C, Martins N, Mehrabi R, Nap JPH, Ponomarenko A, Rudd JJ, Salamov A, Schmutz J, Schouten HJ, Shapiro H, Stergiopoulos I, Torriani SFF, Tu H, de Vries RP, Waalwijk C, Ware SB, Wiebenga A, Zwiers LH, Oliver RP, Grigoriev I V., Kema GHJ, 2011. Finished genome of the fungal wheat pathogen *Mycosphaerella graminicola* reveals dispensome structure, chromosome plasticity, and stealth pathogenesis. *PLoS Genetics* **7**: e1002070.

Gow NAR, Brown AJP, Odds FC, 2002. Fungal morphogenesis and host invasion. *Current Opinion in Microbiology* **5**: 366–371.

Hamel LP, Nicole MC, Duplessis S, Ellis BE, 2012. Mitogen-activated protein kinase signaling in plant-interacting fungi: distinct messages from conserved messengers. *The Plant cell* **24**: 1327–51.

Hintz WE, 1999. Sequence analysis of the chitin synthase A gene of the Dutch elm pathogen *Ophiostoma novo-ulmi* indicates a close association with the human pathogen *Sporothrix schenckii*. *Gene* **237**: 215–221.

Hintz W, Pinchback M, de la Bastide P, Burgess S, Jacobi V, Hamelin R, Breuil C, Bernier L, 2011. Functional categorization of unique expressed sequence tags obtained from the yeast-like growth phase of the elm pathogen *Ophiostoma novo-ulmi*. *BMC genomics* **12**: 431.

Hirsch CD, Springer NM, Hirsch CN, 2015. Genomic limitations to RNAseq expression profiling. *The Plant Journal* **84**: 491–503.

Hornby JM, Jensen EC, Lisec AD, Tasto J, Jahnke B, Shoemaker R, Nickerson KW, Tasto JJ, Dussault P, 2001. Quorum sensing in the dimorphic fungus *Candida albicans* is mediated by farnesol. *Applied and environmental microbiology* **67**: 2982–2992.

Hwang L, Hocking-Murray D, Bahrami AK, Andersson M, Rine J, Sil A, 2003. Identifying phase-specific genes in the fungal pathogen *Histoplasma capsulatum* using a genomic shotgun microarray. *Molecular biology of the cell* **14**: 2314–2326.

Inglis DO, Voorhies M, Murray DRH, Sil A, 2013. Comparative Transcriptomics of infectious spores from the fungal pathogen *Histoplasma capsulatum* reveals a core set of transcripts that Specify infectious and pathogenic states. *Eukaryotic Cell* **12**: 828–852.

Jones T, Federspiel NA, Chibana H, Dungan J, Kalman S, Magee BB, Newport G, Thorstenson YR, Agabian N, Magee PT, Davis RW, Scherer S, 2004. The diploid genome sequence of *Candida albicans*. *Proceedings of the National Academy of Sciences of the United States of America* **101**: 7329–7334.

Kadosh D, 2013. Shaping up for battle: morphological control mechanisms in human fungal pathogens. *PLoS pathogens* **9**: e1003795.

Kadosh D, Johnson A, 2005. Induction of the *Candida albicans* filamentous growth program by relief of transcriptional repression: a genome-wide analysis. *Molecular biology of the cell* **16**: 2903–2912.

Kämper J, Kahmann R, Bölker M, Ma L-J, Brefort T, Saville BJ, Banuett F, Kronstad JW, Gold SE, Müller O, Perlin MH, Wösten H a B, de Vries R, Ruiz-Herrera J, Reynaga-Peña CG, Snetselaar K, McCann M, Pérez-Martín J, Feldbrügge M, Basse CW, Steinberg G, Ibeas JI, Holloman W, Guzman P, Farman M, Stajich JE, Sentandreu R, González-Prieto JM, Kennell JC, Molina L, Schirawski J, Mendoza-Mendoza A, Greilinger D, Münch K, Rössel N, Scherer M, Vranes M, Ladendorf O, Vincon V, Fuchs U, Sandrock B, Meng S, Ho ECH, Cahill MJ, Boyce KJ, Klose J, Klosterman SJ, Deelstra HJ, Ortiz-Castellanos L, Li W, Sanchez-Alonso P, Schreier PH, Häuser-Hahn I, Vaupel M, Koopmann E, Friedrich G, Voss H, Schlüter T, Margolis J, Platt D, Swimmer C, Gnirke A, Chen F, Vysotskaia V, Mannhaupt G, Güldener U, Münsterkötter M, Haase D, Oesterheld M, Mewes H-W, Mauceli EW, DeCaprio D, Wade CM, Butler J, Young S, Jaffe DB, Calvo S, Nusbaum C, Galagan J, Birren BW, 2006. Insights from the genome of the biotrophic fungal plant pathogen *Ustilago maydis*. *Nature* **444**: 97–101.

Khoshraftar S, Hung S, Khan S, Gong Y, Tyagi V, Parkinson J, Sain M, Moses AM, Christendat D, 2013. Sequencing and annotation of the *Ophiostoma ulmi* genome. *BMC genomics* **14**: 162.

Klosterman SJ, Subbarao K V., Kang S, Veronese P, Gold SE, Thomma BPHJ, Chen Z, Henrissat B, Lee YH, Park J, Garcia-Pedrajas MD, Barbara DJ, Anchieta A, de Jonge R, Santhanam P, Maruthachalam K, Atallah Z, Amyotte SG, Paz Z, Inderbitzin P, Hayes RJ, Heiman DI, Young S, Zeng Q, Engels R, Galagan J, Cuomo CA, Dobinson KF, Ma LJ, 2011. Comparative genomics yields insights into niche adaptation of plant vascular wilt pathogens. *PLoS Pathogens* **7**: e1002137.

Kulkarni RK, Nickerson KW, 1981. Nutritional control of dimorphism in *Ceratocystis ulmi*. *Experimental Mycology* **5**: 148–154.

Lenassi M, Gostinčar C, Jackman S, Turk M, Sadowski I, Nislow C, Jones S, Birol I, Cimerman NG, Plemenitaš A, 2013. Whole genome duplication and enrichment of

metal cation transporters revealed by de novo genome sequencing of extremely halotolerant black yeast *Hortaea werneckii*. *PLoS ONE* **8**.

Li Y, Wang Z, Liu X, Song Z, Li R, Shao C, 2016. Siderophore biosynthesis but not reductive iron assimilation is essential for the dimorphic fungus *Nomuraea rileyi* conidiation, dimorphism transition, resistance to oxidative stress, pigmented microsclerotium formation, and virulence. *Frontiers in microbiology* **7**: 1–19.

Lorenz MC, Bender JA, Fink GR, 2004. Transcriptional response of *Candida albicans* upon internalization by macrophages. *Eukaryotic Cell* **3**: 1076–1087.

Ma L-J, Van der Does HC, Borkovich KA, Coleman JJ, Daboussi M-J, Di Pietro A, Dufresne M, Freitag M, Grabherr M, Henrissat B, Houterman PM, Kang S, Shim W-B, Woloshuk C, Xie X, Xu J-R, Antoniw J, Baker SE, Bluhm BH, Breakspear A, Brown DW, Butchko RAE, Chapman S, Coulson R, Coutinho PM, Danchin EGJ, Diener A, Gale LR, Gardiner DM, Goff S, Hammond-Kosack KE, Hilburn K, Hua-Van A, Jonkers W, Kazan K, Kodira CD, Koehrsen M, Kumar L, Lee Y-H, Li L, Manners JM, Miranda-Saavedra D, Mukherjee M, Park G, Park J, Park S-Y, Proctor RH, Regev A, Ruiz-Roldan MC, Sain D, Sakthikumar S, Sykes S, Schwartz DC, Turgeon BG, Wapinski I, Yoder O, Young S, Zeng Q, Zhou S, Galagan J, Cuomo CA, Kistler HC, Rep M, 2010. Comparative genomics reveals mobile pathogenicity chromosomes in *Fusarium*. *Nature* **464**: 367–373.

Madhani HD, Fink GR, 1998. The control of filamentous differentiation and virulence in fungi. *Trends in Cell Biology* **8**: 348–353.

Marques ER, Ferreira MES, Drummond RD, Felix JM, Menossi M, Savoldi M, Travassos LR, Puccia R, Batista WL, Carvalho KC, Goldman MHS, Goldman GH, 2004. Identification of genes preferentially expressed in the pathogenic yeast phase of *Paracoccidioides brasiliensis*, using suppression subtraction hybridization and differential macroarray analysis. *Molecular genetics and genomics : MGG* **271**: 667–77.

Martínez-Espinoza AD, Ruiz-Herrera J, León-Ramírez CG, Gold SE, 2004. MAP kinase and cAMP signaling pathways modulate the pH-induced yeast-to-mycelium dimorphic transition in the corn smut fungus *Ustilago maydis*. *Current microbiology* **49**: 274–81.

Martínez-Soto D, Robledo-Briones AM, Estrada-Luna A a, Ruiz-Herrera J, 2013. Transcriptomic analysis of *Ustilago maydis* infecting *Arabidopsis* reveals important aspects of the fungus pathogenic mechanisms. *Plant signaling and behavior* **8**: 1–13.

Martínez-Soto D, Ruiz-Herrera J, 2013. Transcriptomic analysis of the dimorphic transition of U*stilago maydis* induced in vitro by a change in pH. *Fungal genetics and biology* **58**–**59**: 116–25.

Marty AJ, Broman AT, Zarnowski R, Dwyer TG, Bond LM, Lounes-Hadj Sahraoui A, Fontaine J, Ntambi JM, Kele?? S, Kendziorski C, Gauthier GM, 2015. Fungal morphology, iron homeostasis, and lipid metabolism regulated by a GATA transcription

factor in *Blastomyces dermatitidis*. *PLoS Pathogens* **11**: 1-40.

Muñoz JF, Gauthier GM, Desjardins CA, Gallo JE, Holder J, Sullivan TD, Marty AJ, Carmen JC, Chen Z, Ding L, Gujja S, Magrini V, Misas E, Mitreva M, Priest M, Saif S, Whiston EA, Young S, Zeng Q, Goldman WE, Mardis ER, Taylor JW, McEwen JG, Clay OK, Klein BS, Cuomo CA, 2015. The dynamic genome and transcriptome of the human fungal pathogen *Blastomyces* and close relative *Emmonsia*. PLoS Genetics **11**: 1-31

Nadal M, García-Pedrajas MD, Gold SE, 2008. Dimorphism in fungal plant pathogens. *FEMS microbiology letters* **284**: 127–34.

Nantel A, Dignard D, Bachewich C, Harcus D, Marcil A, Bouin A-P, Sensen CW, Hogues H, Hoog M van het, Gordon P, Rigby T, Benoit F, Tessier DC, Thomas DY, Whiteway M, 2002. Transcription profiling of *Candida albicans* cells undergoing the yeast-to-hyphal transition. *Molecular biology of the cell* **13**: 3452–3465.

Naruzawa ES, Bernier L, 2014. Control of yeast-mycelium dimorphism in vitro in Dutch elm disease fungi by manipulation of specific external stimuli. *Fungal biology* **118**: 872–84.

Naruzawa ES, Malagnac F, Bernier L, 2016. Effect of linoleic acid on reproduction and yeast-mycelium dimorphism in the Dutch elm disease pathogens. *Botany* **96**: 31–39.

Nemecek JC, Wüthrich M, Klein BS, 2006. Global control of dimorphism and virulence in fungi. *Science (New York, N.Y.)* **312**: 583–8.

Nigg M, Bernier L, 2016. From yeast to hypha: defining transcriptomic signatures of the morphological switch in the dimorphic fungal pathogen *Ophiostoma novo-ulmi*. *BMC Genomics* **17**: 920.

Nigg M, Laroche J, Landry CR, Bernier L, 2015. RNAseq analysis highlights specific transcriptome signatures of yeast and mycelial growth phases in the Dutch elm disease fungus *Ophiostoma novo-ulmi*. *G3 Genes|Genomes|Genetics* **5**: 2487–2495.

Noble SM, Gianetti BA, Witchley JN, 2017. *Candida albicans* cell-type switching and functional plasticity in the mammalian host. *Nature Reviews Microbiology* **15**: 96–108.

Nunes LR, Costa de Oliveira R, Batista Leite D, Schmidt da Silva V, dos Reis Marques E, da Silva Fereira ME, Duarte Ribeiro DC, de Souza Bernardes LA, Goldman HMS, Puccia R, Travassos LR, Batista WL, Nóbrega MP, Nobrega, FG, Yang D-Y, De Bragança Pereira CA, Goldman, GH 2005. Transcriptome analysis of *Paracoccidioides brasiliensis* cells undergoing mycelium-to-yeast. *Eukaryotic cell* **4**: 2115–2128.

Odds FC, 1988. *Candida and Candidosis* (Elsevier Science Health Science Division, Ed,).

Paris S, Durán-Gonzáles S, Mariat F, 1985. Nutritional studies on *Paracoccidioides brasiliensis*: the role of organic sulfur in dimorphism. *Sabouraudia* **23**: 85–92.

Pattemore J a, Hane JK, Williams AH, Wilson B Al, Stodart BJ, Ash GJ, 2014. The genome sequence of the biocontrol fungus *Metarhizium anisopliae* and comparative genomics of *Metarhizium* species. *BMC genomics* **15**: 660.

Pongpom P, Cooper CR, Vanittanakom N, 2005. Isolation and characterization of a catalase-peroxidase gene from the pathogenic fungus, *Penicillium marneffei*. *Medical mycology* **43**: 403–411.

Puhalla JE, Bell AA, 1981. Genetics and biochemistry of wilt pathogens. In: Mace M,, Bell A,, Beckman C, eds. *Fungal wilt disease of plants*. New York, pp. 146–184.

Reyna-López GE, Simpson J, Ruiz-Herrera J, 1997. Differences in DNA methylation patterns are detectable during the dimorphic transition of fungi by amplification of restriction polymorphisms. *Molecular and general genetics : MGG* **253**: 703–10.

Robledo-Briones M, Ruiz-Herrera J, 2013. Regulation of genes involved in cell wall synthesis and structure during *Ustilago maydis* dimorphism. *FEMS Yeast Research* **13**: 74–84.

Rodríguez-Kessler M, Baeza-Montañez L, García-Pedrajas MD, Tapia-Moreno A, Gold S, Jiménez-Bremont JF, Ruiz-Herrera J, 2012. Isolation of UmRrm75, a gene involved in dimorphism and virulence of *Ustilago maydis*. *Microbiological Research* **167**: 270–282.

Ruiz-Herrera J, Leon CG, Guevara-Olvera L, Carabez-Trejo A, 1995. Yeast-mycelial dimorphism of haploid and diploid strains of *Ustilago maydis*. *Microbiology* **141**: 695–703.

San-Blas G, Nino-Vega G, 2001. *Fungal pathogenesis: principles and clinical applications* (RA Calderone, RL Cihlar, Eds,). New York.

Sánchez-Martínez C, Pérez-Martín J, 2001. Dimorphism in fungal pathogens: *Candida albicans* and *Ustilago maydis*--similar inputs, different outputs. *Current opinion in microbiology* **4**: 214–21.

Sanna ML, Zara S, Zara G, Migheli Q, Budroni M, Mannazzu I, 2012. *Pichia fermentans* dimorphic changes depend on the nitrogen source. *Fungal Biology* **116**: 769–777.

Sharpton TJ, Stajich JE, Rounsley SD, Gardner MJ, Wortman JR, Jordar VS, Maiti R, Kodira CD, Neafsey DE, Zeng Q, Hung C-H, McMahan C, Muszewska A, Grynberg M, Mandel MA, Kellner EM, Barker BM, Galagiani JN, Orbach MJ, Kirkland TN, Cole GT, Henn MR, Birren BW, Taylor JW, 2009. Comparative genomic analyses of the human fungal pathogens *Coccidioides* and their relatives. *Genome research* **19**: 1722-1731

Steinberg G, Schuster M, 2011. The dynamic fungal cell. *Fungal Biology Reviews* **25**: 14–37.

Sudbery P, Gow N, Berman J, 2004. The distinct morphogenic states of *Candida albicans*.

Trends in Microbiology **12**: 317–324.

Tang X, Zhao L, Chen H, Chen YQ, Chen W, Song Y, Ratledge C, 2015. Complete genome sequence of a high lipid-producing strain of *Mucor circinelloides* WJ11 and comparative genome analysis with a low lipid-producing strain CBS 277.49. *PLoS ONE* **10**: 1–11.

Tavares AH, Fernandes L, Bocca AL, Silva-Pereira I, Felipe MS, 2015. Transcriptomic reprogramming of genus *Paracoccidioides* in dimorphism and host niches. *Fungal Genetics and Biology* **81**: 98–109.

Thewes S, Kretschmar M, Park H, Schaller M, Filler SG, Hube B, 2007. *In vivo* and *ex vivo* comparative transcriptional profiling of invasive and non-invasive *Candida albicans* isolates identifies genes associated with tissue invasion. *Molecular Microbiology* **63**: 1606–1628.

Whiston E, Zhang Wise H, Sharpton TJ, Jui G, Cole GT, Taylor JW, 2012. Comparative transcriptomics of the saprobic and parasitic growth phases in *Coccidioides* spp. *PloS one* **7**: e41034.

Woo PCY, Lau SKP, Liu B, Cai JJ, Chong KTK, Tse H, Kao RYT, Chan CM, Chow WN, Yuen KY, 2011. Draft genome sequence of *Penicillium marneffei* strain PM1. *Eukaryotic Cell* **10**: 1740–1741.

Wu G, Zhao H, Li C, Rajapakse MP, Wong WC, Xu J, Saunders CW, Reeder NL, Reilman RA, Scheynius A, Sun S, Billmyre BR, Li W, Averette AF, Mieczkowski P, Heitman J, Theelen B, Schröder MS, De Sessions PF, Butler G, Maurer-Stroh S, Boekhout T, Nagarajan N, Dawson TL, 2015. Genus-wide comparative genomics of *Malassezia* delineates its phylogeny, physiology, and niche adaptation on human skin. *PLoS Genetics* **11**: 1–26.

Xi L, Xu X, Liu W, Li X, Liu Y, Li M, Zhang J, Li M, 2007. Differentially expressed proteins of pathogenic *Penicillium marneffei* in yeast and mycelial phases. *Journal of Medical Microbiology* **56**: 298–304.

Yang E, Chow W, Wang G, Woo PCY, Lau SKP, Yuen K, Lin X, Cai JJ, 2014. Signature gene expression reveals novel clues to the molecular mechanisms of dimorphic transition in *Penicillium marneffei*. *PLoS genetics* **10**: e1004662.

Table 2.1 Summary of the major induced processes and molecular pathways highlighted in selected genomic studies in different species and different conditions

Species	Mycelium specific	Yeast specific	Yeast-to-mycelium induced	Mycelium-to-yeast induced	References
Blastomyces dermatidis			Iron assimilation, lipid metabolism, amino acid metabolism		Marty *et al.* 2015
Candida albicans			Secreted proteins, cell surface proteins, small GTPases, cytoskeletal modulators		Nantel *et al.* 2002
			Secreted proteins, cell wall components, cell motility, budding, cell division		Kadosh and Johnson, 2005
			Filamentous growth, adhesion, biofilm formation, carbohydrate metabolism, stress response, cell wall organization, signal transduction, cell cycle, microtubule-based movement, iron assimilation	Ribosome biogenesis, RNA metabolic process, response to chemical stimulus and response to drug, carbohydrate metabolism, amino acid metabolism	Carlisle and Kadosh, 2012
Histoplasma capsulatum	Conidiation involved genes, denitrification related genes, polar growth, melanin production	Sulphur metabolism, cell cycle, amino-acid metabolism			Hwang *et al.* 2003
	Asexual development, mating	Siderophore biosynthesis genes, secreted proteins, catalases			Inglis *et al.* 2013
		Coenzyme A (CoA) synthesis, membrane transporters, mitosis, cell cycle progression, siderophore biosynthesis			Edwards *et al.* 2013
Ophiostoma novo-ulmi	Protein phosphorylation, negative regulation of biological process, DNA replication initiation, aminoglycan metabolism,	Single-organism transport, regulation of transcription, oxidation-reduction process, catalases			Nigg *et al.* 2015

	cellular protein modification, MAPK				
			Cellular organization, cell division, vesicle transport, protein modifications, MAPK, CAZymes		Nigg and Bernier, 2016
Paracoccidioides brasiliensis, P. lutzii	Aerobic metabolism, citrate cycle	Ethanol production, anaerobic metabolism, chitin rich, higher number of chaperone and co-chaperone			Felipe *et al.* 2003, 2005
	Ion transport, Cell wall organization	Energy, metabolism of amino acids, α-glucan synthesis, sulphur metabolism			Andrade *et al.* 2006
				Energy generation, cell wall biogenesis, signal transduction, metabolism of amino acids, sulphur metabolism, alpha-glucan synthesis, putative virulence factors	Bastos *et al.* 2007
				Ribosome biogenesis, chitin synthesis, signal transduction, protection against oxidative stress, amino acid catabolism	Nunes *et al.* 2005
Penicillium marneffei	Carbohydrate metabolism, nucleosome assembly, inositol biosynthesis, protein transport, amino acid transport	tRNA processing, ribosome biogenesis, copper ion transmembrane transport, ATP synthesis coupled proton transport	Aromatic amino acid biosynthesis, plasma membrane fusion, cellular protein metabolism, ATP synthesis coupled proton transport, amino acid transport	Glycine catabolism, clathrin coat assembly, carbohydrate metabolism, protein transport, amino acid transport	Yang *et al.* 2014
Ustilago maydis	Chitin synthases, secretion, β-glucan synthesis, N-glycosylation	Chitin deacetylases			Robledo-Briones and Ruiz-Herrera, 2012
	Carbohydrate metabolism, amino acids metabolism, fatty acids metabolism and polyamines metabolism	Iron acquisition, siderophore biosynthesis	Cell cycle, DNA processing, transcription and protein fate, transport, cell differentiation, polarity, cell motility		Martinez-Soto and Ruiz-Herrera, 2013

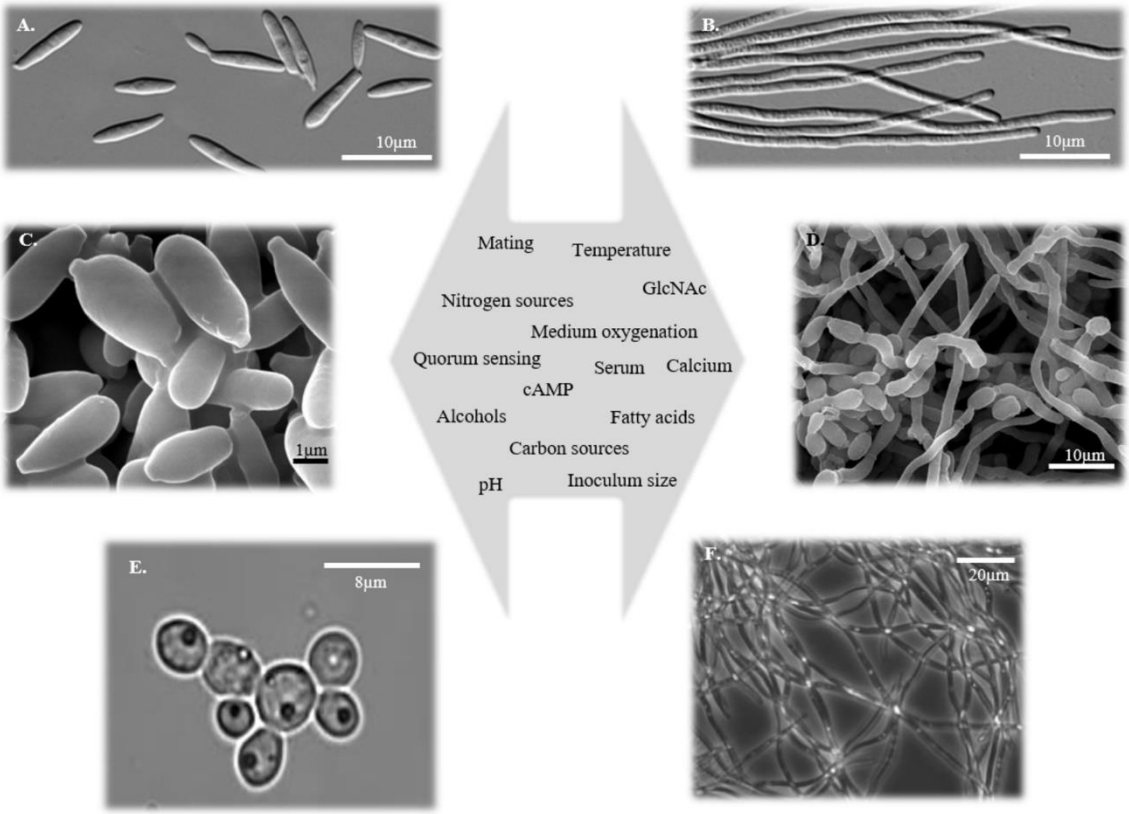

Figure 2.1 A variety of stimuli triggers the yeast-mycelium dimorphism in fungi. a.-f. Pictures illustrating the two growth phases in: a-b. *Ustilago maydis* (from Steinberg and Schuster 2011 with permission of the publisher), c-d. *Ophiostoma novo-ulmi* (from Nigg and Bernier, 2016) and e-f. *Candida albicans* (from Nantel *et al.* 2002). a., c., e.: yeast-like phase; b.,d.,f.: mycelium phase. cAMP: cyclic Adenosine MonoPhosphate; GlcNAc: N-acetylglucosamine. There is no link between the direction of the arrows and the position of the stimuli inside the arrows.

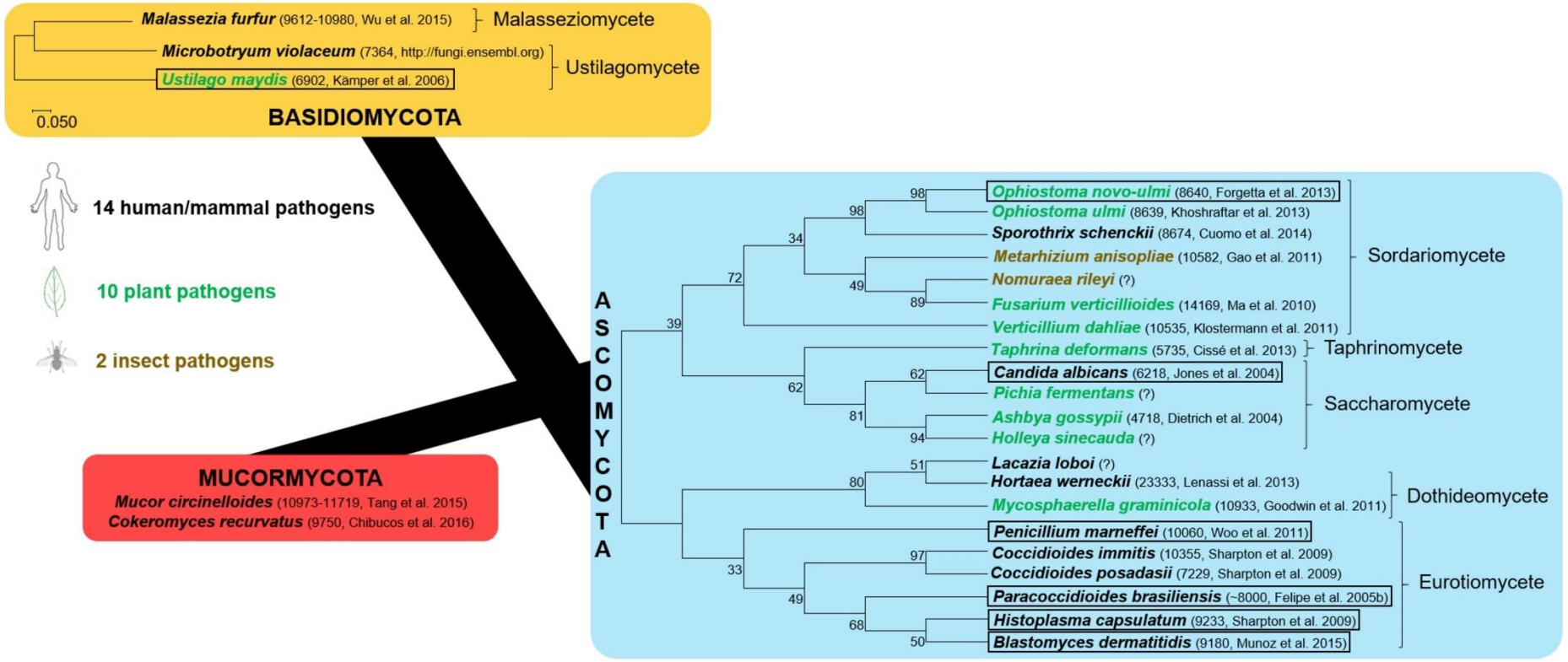

Figure 2.2 Phylogeny of Ascomycota, Basidiomycota and Mucormycotina dimorphic pathogenic fungi based on concatenated Internal Transcribed Spacer 1 (ITS1) sequences downloaded from the NCBI database. Each phylum was treated separately, thus links between phyla are fictitious. Sequences were aligned and concatenated with BioEdit 7.2.5 software (Hall 1999). For Ascomycota, a maximum-likelihood tree was constructed using Mega7 with 100 bootstraps (Tamura *et al.* 2013). Bootstrap support is shown on each node. For Basidiomycota, due to the small number of species, the tree was constructed based on maximum-likelihood distance without bootstraps. Lengths of branches reflect the number of substitutions per site. Sordariomycetes, Dothideomycetes, Eurotiomycetes, Saccharomycetes, Taphrinomycetes, Ustilagomycetes, Malasseziomycetes are classes. Species in green are phytopathogens (10), those in brown are entomopathogens (2) and species in black are pathogens of humans or other mammals (14). Numbers in brackets are the total gene content in sequenced species, with the reference associated with the number. Framed species (7) are those for which we found ESTs, microarray- or RNAseq experiments focused on the understanding of dimorphism.

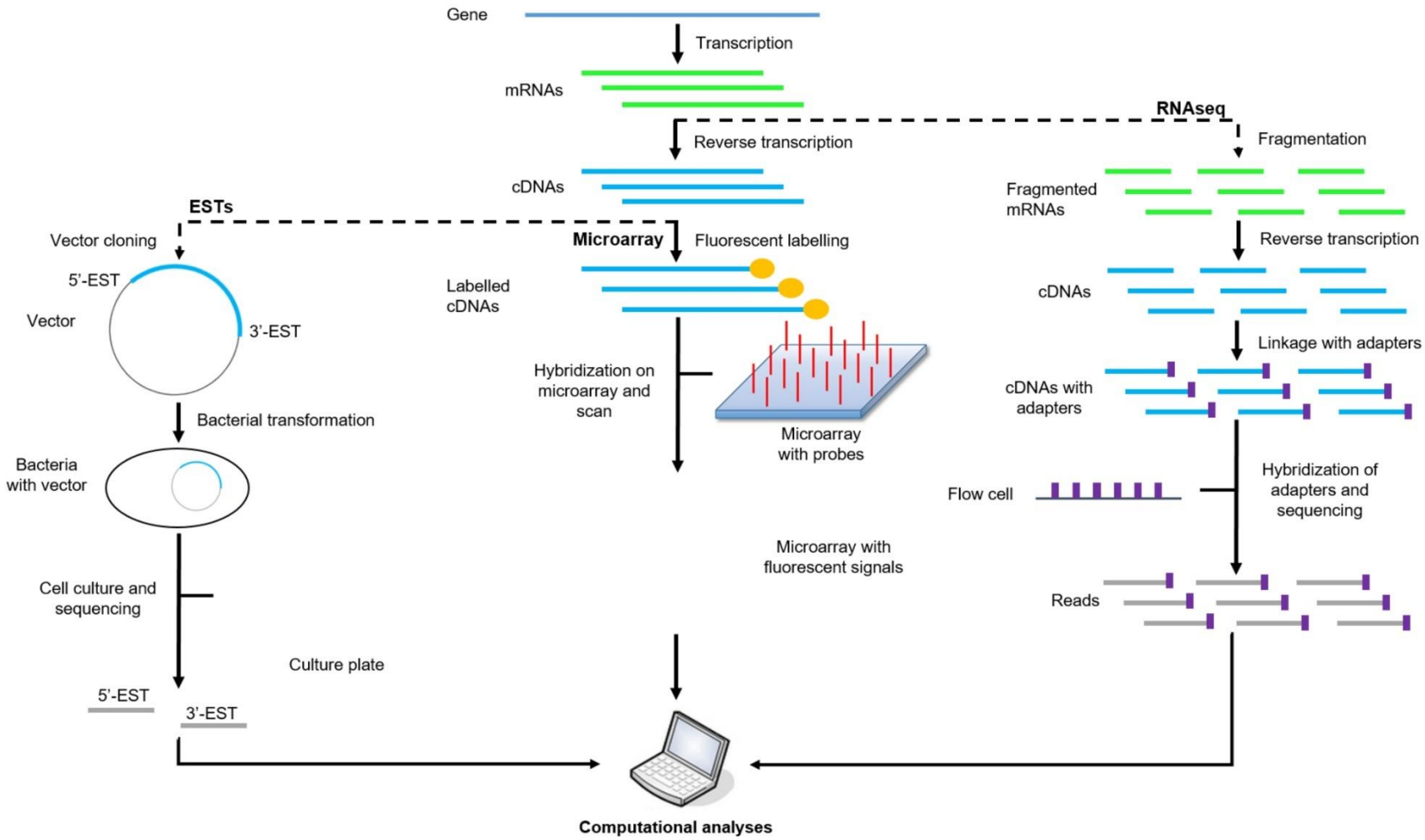

Figure 2.3 General and simplified workflows for EST-, microarray- and RNAseq experiments

Table S2.1 Species and strain/isolate names and GenBank ID of the sequences used to build the phylogenetic tree.

Species	Isolate/strain/clone	GenBank sequence ID	Genes
Anthracocystis flocculosa	isolate H	gi|10799048|gb|AF294695.1|	18S (partial), ITS1, 5.8S, ITS2 (complete), 28S (partial)
Ashbya gossypii	strain HA88	gi|493043|gb|U09322.1|AGU09322	ITS1, 5.8S, ITS2
Blastomyces dermatitidis	strain UAMH 10245	gi|156617155|gb|EF592163.1|	18S (partial), ITS1, 5.8S, ITS2 (complete), 28S (partial)
Candida albicans	strain SC5314	EF108226.1	ITS1 (partial), 5.8S (complete), ITS2 (partial)
Coccidioides immitis	strain Venezuela clone pVenezuela	gi|543888495|gb|KF539896.1|	18S (partial), ITS1, 5.8S, ITS2 (complete), 28S (partial)
Coccidioides posadasii	clone SS06UM-N2A.C3	gi|540367349|gb|KF386151.1|	18S (partial), ITS1, 5.8S (complete), ITS2 (partial)
Cokeromyces recurvatus	strain CBS 168.59	gi|409185647|gb|JN206245.1|	18S (partial), ITS1, 5.8S, ITS2 (complete), 28S (partial)
Fusarium verticillioides		X94166.1	18S (partial), 5.8S, 28S (partial), ITS1, ITS2 (complete)
Histoplasma capsulatum	strain VPCI 881/P/13	KM225289.1	ITS1, 5.8S, ITS2 (complete), 28S (partial)

Holleya sinecauda		gi|1262236|gb|U51435.1|HSU51435	ITS1, 5.8S, ITS2
Hortaea werneckii		gi|90812258|gb|DQ336709.1|	ITS1 (partial), 5.8S, ITS2 (complete), 28S (partial)
Lacazia loboi	strain GX2-5C	gi|199599779|gb|FJ037740.1|	18S (partial), ITS1, 5.8S, ITS2 (complete), 28S (partial)
Malassezia furfur		gi|7578951|gb|AF246896.1|	18S (partial), ITS1, 5.8S, ITS2 (complete), 28S (partial)
Metarhizium anisopliae	strain CP-Oax	gi|228204806|gb|FJ876298.1|	18S (partial), ITS1, 5.8S, ITS2 (complete), 28S (partial)
Microbotryum violaceum	strain H12	AY014242.1	ITS1 (partial), 5.8S(complete), ITS2 (partial)
Mucor circinelloides	strain TUM15	gi|165993422|emb|AM933555.1|	18S (partial), ITS1, 5.8S, ITS2 and 28S (partial)
Mycosphaerella graminicola		gi|1778760|gb|U77363.1|MGU77363	18S (partial), ITS1, 5.8S, ITS2 (complete), 28S (partial)
Nomuraea rileyi	isolate TNR0002	gi|648713990|gb|KJ728727.1|	18S (partial), ITS1, 5.8S (complete), ITS2 (partial)
Ophiostoma novo-ulmi	strain H327	KJ540050.1	ITS1, 5.8S (complete), ITS2 (partial)

Ophiostoma ulmi	strain W9	KJ540053.1	ITS1 (partial), 5.8S (complete), ITS2 (partial)
Paracoccidioides brasiliensis		AF322389.1	18S (partial), ITS1, 5.8S, ITS2 (complete), 28S (partial)
Penicillium marneffei	strain IFM47280	gi|10280988|dbj|AB049132.1|	ITS1, 5.8S, ITS2
Pichia fermentans	strain PMM09-907L isolate ISHAM-ITS_ID MITS781	gi|731445991|gb|KP132501.1|	18S (partial), ITS1, 5.8S, ITS2 (complete), 28S (partial)
Sporothrix schenckii	strain C9862	KJ999904.1	ITS1 (partial), 5.8S (complete), ITS2 (partial)
Taphrina deformans	strain NRRL T-470	AF492095.1	ITS1, 5.8S, ITS2
Ustilago maydis		gi|3811299|gb|AF038826.1|	ITS1, 5.8S, ITS2
Verticillium dahliae	isolate VP84 (Vd76)	JX104823.1	ITS1, 5.8S, ITS2

CHAPITRE 3 RNAseq analysis highlights specific transcriptome signatures of yeast and mycelial growth phases in the Dutch elm disease fungus *Ophiostoma novo-ulmi*.

Martha Nigg [*, ǂ], Jérôme Laroche [*, ǂ], Christian R. Landry [*, §] and Louis Bernier [*, ǂ]

[*] Institut de Biologie Intégrative et des Systèmes (IBIS), Université Laval, Québec, G1V 0A6, Canada

[ǂ] Centre d'Étude de la Forêt (CEF) and Département des sciences du bois et de la forêt, Université Laval, Québec, G1V 0A6, Canada

[ǂ] Plate-forme de bio-informatique, Institut de Biologie Intégrative et des Systèmes (IBIS), Université Laval, Québec, G1V 0A6, Canada

[§] Département de biologie, Université Laval, Québec, G1V 0A6, Canada

Ce chapitre a été publié en novembre 2015 dans le volume 5 du journal scientifique *G3 Genes/Genomes/Genetics*, pages 2487-2495. doi: 10.1534/g3.115.021022
L'article apparait dans la sélection annuelle 2015 de la Société Américaine de Génétique (GSA) disponible à l'adresse suivante : http://genestogenomes.org/gsa-journals-spotlights-2015/

3.1 Résumé

Le dimorphisme fongique est un trait morphologique complexe et notre compréhension de la capacité des champignons à croître selon différentes morphologies est limitée à un petit nombre d'espèces modèles. Dans ce chapitre, nous étudions un champignon dimorphique très agressif, l'ascomycète *Ophiostoma novo-ulmi,* qui est une espèce modèle en phytopathologie et l'agent causal de la maladie hollandaise de l'orme. Les deux phases de croissance retrouvées chez ce champignon, i.e., une phase levure et une phase mycélienne, semblent être impliquées dans les étapes clés du développement de la maladie. Nous avons utilisé la technique de RNAseq pour étudier, à l'échelle du génome entier, les profils d'expression génique qui sont associés aux phases de croissance levure et mycélienne obtenues *in vitro*. Nos résultats montrent une distinction moléculaire claire entre les profils de chacune de deux phases. Environ 12% du contenu génique total est exprimé de manière différentielle entre les deux phases, ce qui révèle des fonctions moléculaires spécifiques liées à chaque phase de croissance. Nous avons ensuite comparé les profils transcriptomiques obtenus chez *O. novo-ulmi* avec ceux de deux espèces modèles dimorphiques, *Candida albicans* et *Histoplasma capsulatum*. Peu de gènes orthologues montrent une régulation de l'expression similaire entre les deux phases de croissance, suggérant que, globalement, les gènes associés aux formes levures et mycélienne sont peu conservés. Cette faible conservation souligne l'importance de développer des outils spécifiques pour les espèces modèles émergeantes qui sont phylogénetiquement distantes des espèces étudiées traditionnellement. En conclusion, l'ensemble de nos résultats apporte des connaissances sur la régulation transcriptomique et la spécificité moléculaire chez *O. novo-ulmi* et ils offrent une nouvelle perspective de la compréhension du dimorphisme fongique.

3.2 Abstract

Fungal dimorphism is a complex trait and our understanding of the ability of fungi to display different growth morphologies is limited to a small number of model species. Here we study a highly aggressive dimorphic fungus, the ascomycete *Ophiostoma novo-ulmi,* which is a model in plant pathology and the causal agent of Dutch elm disease. The two growth phases that this fungus displays, i.e., a yeast and mycelial phase, are thought to be involved in key steps of disease development. We used RNAseq to investigate the genome-wide gene expression profiles that are associated with yeast and mycelial growth phases *in vitro*. Our results show a clear molecular distinction between yeast and mycelial phase gene expression profiles. Almost 12 % of the gene content is differentially expressed between the two phases, which reveals specific functions related to each growth phase. We compared *O. novo-ulmi* transcriptome profiles with those of two model dimorphic fungi, *Candida albicans* and *Histoplasma capsulatum*. Few orthologs showed similar expression regulation between the two growth phases, which suggests that globally, the genes associated with these two life forms are poorly conserved. This poor conservation underscores the importance of developing specific tools for emerging model species that are distantly related to the classical ones. Taken together, our results provide insights into transcriptome regulation and molecular specificity in *O. novo-ulmi* and offer a new perspective for understanding fungal dimorphism.

3.3 Introduction

Morphological dimorphism allows several human and plant pathogenic fungi to live either in a unicellular yeast phase or in a pluricellular mycelium stage. This characteristic provides an advantage to pathogenic fungi that colonize various environments during their lifecycle (Nemecek *et al.* 2006). Our understanding of the diversity of molecular processes that are involved in this morphological plasticity is rather limited due to the small number of species that have been studied, and which consist mostly of human pathogenic fungi for which dimorphism is thermally regulated. More investigations are needed to overcome this limitation and to cover a wider spectrum of the fungal kingdom. Here we develop an additional experimental system to study genes and pathways underlying dimorphism using the ascomycete *Ophiostoma novo-ulmi.*

This dimorphic fungus is a vascular plant pathogen that is responsible for the current pandemic of Dutch elm disease (DED), which has been killing elm tree (*Ulmus* sp.) populations in North America and Europe since the 1940s. *Ophiostoma novo-ulmi* is closely related to *O. ulmi*, which caused the first DED pandemic at the beginning of the 20th century (Brasier 1991). *O. novo-ulmi* is phylogenetically closely related to the dimorphic Ophiostomatoid human pathogen *Sporothrix schenckii* and to *Neurospora crassa,* a model fungus from the class Sordariomycetes (Berbee and Taylor 1992; Hintz 1999) (Figure 3.1).

The yeast-to-mycelium transition of *O. novo-ulmi* occurs at the haploid stage (Pereira *et al.* 2000) and is not dependent upon sexual reproduction or temperature. Both phases seem to be required to insure the complete infection of elm trees (Miller and Elgersma 1976). The nuclear genome of *O. novo-ulmi* was recently sequenced (Forgetta *et al.* 2013; Bernier *et al.* 2015) and contained approximately 8640 coding genes, of which about 25 % remain unannotated (Comeau *et al.* 2015). Knowing which of these genes are expressed specifically in the yeast and mycelium phases remains undetermined because data for *O. novo-ulmi* consist largely of expressed sequence tags (ESTs) that are associated with the yeast phase (Hintz *et al.* 2011) and the production of fruiting bodies (Jacobi *et al.* 2010). However, identifying the genes that are essential for maintaining yeast and mycelium growth phases is important to better understand diseases that are caused by dimorphic fungi and, eventually, to manipulate the switch between these two morphs.

Here we characterize and quantify the transcriptome of yeast and mycelial forms of *O. novo-ulmi* in stable (i.e., not in transition) growth stages using RNAseq. To assess the proportion of conserved expression patterns between *O. novo-ulmi* and well-established model species, we compare our data with those from two model species, *Candida albicans* and *Histoplasma capsulatum* (both dimorphic human pathogens) for which genomes and transcriptomes are available. Overall, our results provide new insights into the transcriptomic profiles that differentiate growth phases in *O. novo-ulmi* and establish a new model for the study of dimorphism in a phytopathogenic fungus.

3.4 Materials and methods

3.4.1 Strains and samples

Yeast- and mycelial-forms of *O. novo-ulmi* strain H327 (Centre d'Étude de la Forêt, fungal collection) were grown on *Ophiostoma* complete medium (OCM) with 1.15 g L^{-1} proline as the nitrogen source in incubators that were set at 22° (Bernier and Hubbes 1990). Three different life stages (treatments) were analyzed: 1) Yeast: five-day-old liquid cultures of yeast cells in agitated flasks on an orbital shaker (Infors HT Ecotron) at 150 rpm (initial concentration of spores: $1*10^5$ mL^{-1}); 2) Liquid mycelium: five-day-old liquid culture of mycelium without shaking (initial concentration of spores: $2.5*10^4$ mL^{-1}); and 3) solid mycelium: five-day-old solid culture (complete medium with 20 g L^{-1} agar in petri plates) of mycelium ($1.5*10^6$ spores spread on sterile cellophane membrane). In liquid medium, different spore concentrations were used for yeast and mycelial growth to prevent hyphal formation in the shaken medium by quorum sensing (Berrocal *et al.* 2012; Wedge and Bernier, unpublished results). Each treatment included three biological replicates (Figure S3.1).

3.4.2 RNA extraction, cDNA library production and RNA sequencing

Samples were harvested by centrifugation (5 min, 4700 g, 4°) for liquid cultures or by collecting mycelium directly on the membrane for solid cultures. Samples were then stored at -80°. Total RNA was extracted using the RNeasy Mini Kit (QIAGEN, yeast protocol) and quality control was assured using a spectrophotometer (NanoDrop ND-1000, Thermo Scientific) and a bioanalyzer (BioAnalyzer RNA 6000 Nano Kit, Agilent Technologies). Complementary DNA (cDNA) libraries were synthesized using the TruSeq RNA Sample Preparation Kit v2 (Illumina) with 1 µg of starting material per sample at the Plateforme d'Analyses Génomiques (IBIS/Université Laval). Libraries were sequenced on an Illumina HiSeq 2500 (v.1.9 single-end, 100bp) platform at McGill

University and the Genome Québec Innovation Centre. The nine bar-coded samples were multiplexed with three other samples (unpublished data) in the same sequencing lane. Two of the nine samples (one from yeast phase and one from mycelium phase grown on solid medium) were used by Comeau *et al.* (2015) to improve genome annotation. All nine RNAseq samples are available under the NCBI BioProject (PRJNA260920) on Genbank: the three replicates of yeast growth phase (accession numbers: SRR1574322, SRR2140671-2), the three replicates of mycelial phase grown on solid medium (accession numbers: SRR1574324, SRR2140674-5) and the three replicates of mycelial phase grown in liquid medium (accession numbers: SRR2140676-8).

3.4.3 Data pre-processing

Filtering and quality controls were applied following the procedure described by Comeau *et al.* (2015). Adaptors and poly-A/T tails (>10nt) were trimmed off with a combination of Trim Galore! (www.bioinformatics.babraham.ac.uk/projects/trim_galore/) and Prinseq v0.20.4 (Schmieder and Edwards 2011). Sequences containing more than 20 % Ns or shorter than 20 nt in length were removed. We also discarded duplicate reads from our data (duplicates can be removed if sequences are exactly the same, without allowing any mismatches, as they are considered as PCR duplicates). Because the percentage of reads that were eliminated was homogenous among conditions (Figure S3.2A, Table S3.2), we assumed that this would not bias the analysis. The remaining number of reads that were analyzed fell between 3.7 and 5.7 million per sample.

3.4.4 Data analysis

Filtered reads were mapped onto the *O. novo-ulmi* H327 genome (Forgetta *et al.* 2013) with TopHat2 (v.2.0.10) using default parameters (Kim *et al.* 2013). Reads were also mapped in parallel on exon sequences to assess the proportion that had mapped onto non-coding sequences. All further analyses were performed using R (v3.0.1; R Development Core Team 2011). Read counts for each of the nine samples were extracted and used for differential expression analyzes using the *EdgeR* package in *Bioconductor 3.0* (Robinson *et al.* 2009). For downstream analyses, we considered only the genes with 25 reads or greater in at least three samples. Library sizes (i.e., number of mapped reads) were corrected using a method based on Trimmed Mean of M-values (TMM) (Robinson and Oshlack 2010; Dillies *et al.* 2013). A multi-dimensional scaling (MDS) plot that was used for the visualization of the variability among samples (function implemented in *EdgeR*). In the MDS plot, distances correspond to the average of the largest absolute log-fold-

changes (logFC) between each pair of RNA samples (Robinson *et al.* 2009). The nine samples were clustered using the *k*-means method (Hartigan and Wong 1979) and the plot was produced using the R package *ggplot2* (Wickham 2009).

Differential expression levels (relative RNA counts) between yeast and each of the two mycelial conditions were considered as being significantly different with a False Discovery Rate (FDR, Benjamini and Hochberg, 1995) at a threshold of 1 %. Gene Ontology (GO) terms were attributed by BLAST2GO (www.blast2go.com; 3162 *O. novo-ulmi* H327 genes do not have a GO term) (Comeau *et al.* 2015). Enrichment was computed using *GOStats* and *Goseq* packages in *Bioconductor 3.0* (Young *et al.* 2010). Enriched GO terms with *P*-values (uncorrected) ≤ 1 % and a minimum of four genes per category were retained and trimmed off with GO Trimming to reduce term overlap (80 % soft trim threshold, Jantzen *et al.* 2011).

3.4.5 Gene orthology

Orthologous genes for species pairs (see species names below) were identified by reciprocal best blast hits (RBH) using *tblastx* (Altschul *et al.* 1990). Exon sequences of the two species were compared using local databases and the RBH was conducted using the following parameters: e-value = 1×10^{-3}, word size = 5. The parameters were validated by calculating the number of orthologous genes between *O. novo-ulmi* or *O. ulmi* (gene sequences downloaded on 2015/04/04, www.moseslab.csb.utoronto.ca/o.ulmi/, "nuc-seq-all-genes" named sequences) and *Neurospora crassa* (sequences retrieved on 2015/03/31, www.broadinstitute.org/annotation/genome/neurospora/, "or74a_12" named sequences). We also calculated the number of orthologous genes between *Ophiostoma* sp. and *Saccharomyces cerevisiae* strain S288C (www.yeastgenome.org/, "R63-1-120100105" named sequences) (Table S3.3). We compared our results with those obtained by Khoshraftar *et al.* (2013). Despite employing methods that differed from those of Khoshraftar *et al.* our estimates were similar to the values that these authors obtained. Thus, we assume that our workflow is successful in identifying orthologous genes. The limited variation that was seen between numbers of orthologs found can be explained by the different versions of the databases used. This RBH method was used to identify orthologous genes between *O. novo-ulmi* and the reference strains of *Histoplasma capsulatum* (strain G186) and *Candida albicans* (strain SC5314). For *H. capsulatum, de novo* transcriptome assembly data (Edwards *et al.* 2013) was kindly provided by Dr. C. Rappleye (Ohio State University, Columbus, OH, USA) and used for

constructing the local Blast database. For *Candida albicans*, exon sequences were downloaded on 2015/02/23 (www.candidagenome.org/). The RBH method was also used to assess the number of orthologous genes between *O. novo-ulmi* and *Sporothrix schenckii* strain ATCC58251 (transcript sequences downloaded on 2015/07/03) (Cuomo *et al.* 2014). The total number of genes present in each species that was tested was retrieved from databases on 2015/07/06 for *S. schenckii* and on 2015/05/08 for all of the other species.

3.4.6 Comparison with *Histoplasma capsulatum* and *Candida albicans* RNAseq data

Paired-end RNAseq data from H. capsulatum were downloaded from NCBI (www.ncbi.nlm.nih.gov/sra, accession numbers: SRX332751 [G186 mycelia, two files] and SRX332607 [G186 yeasts, two files]). SRA files were converted into fastq format with the SRA toolkit (www.ncbi.nlm.nih.gov/Traces/sra/). Fastq files with both ends concatenated were split into two files (one for each end, forward and reverse) with Fastq-splitter (www.kirill-kryukov.com/study/tools/fastq-splitter/). Split files were cleaned using Prinseq v0.20.4 (Schmieder and Edwards 2011) and 156 nt long reads were trimmed to the first 70nt (thereby avoiding the large proportion of "N" in the second half of reads). We analyzed differential gene expression following the method described above for *Ophiostoma* samples. The hypergeometric test was used to infer the probability of gene expression regulation conservation between two compared species. The same procedure was applied to *C. albicans* strain SC5314 data. Transcriptome data for *C. albicans* (Bruno *et al.* 2010) were downloaded from the NCBI SRA database (www.ncbi.nlm.nih.gov/sra, accession numbers: SRR064145-8). We selected samples corresponding to yeast form (accession numbers: SRR064145 and SRR064146) and hyphal growth (accession numbers: SRR064147 and SRR064148).

3.5 Results and discussion

O. novo-ulmi is a model species in terms of its interaction with the host tree, its epidemiology and its high virulence. This fungus has been studied for many years with respect to its involvement in Dutch elm disease (Bernier *et al.* 2015). As is the case with many other dimorphic fungi, this pathogen is capable of living either in a yeast or mycelial phase, depending upon environmental conditions. Even though the two growth phases can easily be obtained and controlled *in vitro* (Naruzawa and Bernier 2014), only a few studies have focused upon the molecular landscape of this dimorphism, and only on a

limited number of genes (Richards 1994; Pereira *et al.* 2000). Our study aimed at determining the gene expression profiles of different morphs of *O. novo-ulmi* to identify expression signatures that distinguish the yeast and mycelial phases. To do so, we sequenced the transcriptome of both phases of *O. novo-ulmi* in stable growth conditions (not in transition) and focused on the regulation of gene expression in yeast and mycelium.

3.5.1 RNAseq data statistics

All samples (three treatment conditions, each with three replicates) produced around 13-15 million raw reads each (Figure S3.2A). The cleaned and filtered data represent a depth of coverage of 28X for exons and 13X for the whole genome. A total of 1.75 % of reads is identified as mapping to non-coding regions, which represent non-coding RNA, introns or untranslated regions (UTRs) of protein-coding genes.

Under each condition, one or more reads is mapped to at least 95 % of the predicted genes in the *O. novo-ulmi* H327 genome. The distribution of the number of reads per gene is homogenous across conditions, suggesting that the transcriptomes of the two morphs have similar complexities (Figure S3.2B). Eight hundred and ninety-nine predicted genes (Comeau *et al.* 2015) were not detected or were discarded from our dataset after the EdgeR filtration steps. Of these, 470 are predicted to encode as yet uncharacterized proteins. Among the remaining 429 genes, some are clearly condition-specific, such as mating–type genes *MAT1-1-1, MAT1-1-2* and *MAT1-1-3,* and the pheromone mating α-factor receptor encoding genes *STE2* and *STE3*. These genes are related to mating conditions (Jacobi *et al.* 2010) that are distinct from the conditions that were examined here. Genes coding for salicylate hydroxylases (n = 7) and tannases (n = 4) were also absent. These enzymes are involved in plant metabolite degradation (Gaffney *et al.* 1993; García-Conesa *et al.* 2001) and, thus, may not be expressed in the set of conditions that we investigated. For further analyses, we consider the 7741 genes that are detected by EdgeR as being expressed (Table S3.4).

3.5.2 Expression data visualization and reproducibility

MDS analysis shows the variability and grouping among samples (Figure 3.2A). The three yeast biological replicates cluster together, as do the three replicates of mycelium grown in static liquid conditions. Mycelium samples that were grown on solid medium exhibit greater variability than other treatments. The MDS plot shows clear separation

between yeast samples and all mycelial samples along the 1st axis, which indicates the greatest variation measured in terms of gene expression is due to dimorphism. The second dimension discriminates the mycelium according to the medium that was used (liquid or solid), suggesting that the growth medium largely affects the transcriptome. Indeed, yeast samples are closer to the mycelium phase when grown in liquid medium than to mycelia that were grown in petri dishes. Thus, some genes are differentially regulated according to whether the fungus is in liquid or solid medium.

3.5.3 Phase-regulated gene expression

Gene expression levels of yeast samples were compared to each of the two mycelial conditions in pair-wise comparisons (Figure 3.2B). This test allows the identification of genes that are systematically differentially expressed between yeast and mycelium samples and that could explain the separation of the two life-cycle stages along the first dimension of the MDS plot. A set of 1040 genes was differentially expressed in both comparisons (yeast vs liquid mycelium; yeast vs solid mycelium) ($\log_2$ of fold change [logFC] from 0.75 to 8.5, FDR $\leq$ 1 %). For the majority (n = 1039), the pattern of over- or under-expression is consistent in both comparisons (Figure 3.2B). This number represents almost 12 % of the predicted nuclear gene content of *O. novo-ulmi*. Among these 1039 genes, 538 are overexpressed in yeast samples and 501 in mycelium samples (Tables S3.5 and S3.6). For both comparisons, the set of differentially expressed genes that do not overlap represents genes with expression profiles that depend upon the growth conditions (liquid versus solid medium). This could explain the differences seen in the second dimension of the MDS plot.

3.5.3.1 Single-cell lifestyle

In the list of the 538 genes that were overexpressed in the yeast condition, 141 are annotated as "putative uncharacterized protein."

Four biological processes stood out following GO terms enrichment analysis for the remaining 397 genes, (Figure 3.2C). There are less than 60 genes in each of the four terms (Table S3.5). Among the latter, the term *regulation of transcription, DNA-templated* contains nine of the 15 transcription factors overexpressed in the yeast condition (Table S3.5). There are 159 genes annotated as transcription factors in the genome (Comeau *et al.* 2015). In the set of overexpressed genes in the yeast growth phase, we found C6 zinc finger transcription factors (n = 4) and Bzip transcription factors (n = 4), two of which

are AP-1 like transcription factors (OphioH327g0401 and OphioH327g0658). In fungi, AP-1 like transcription factors are known to be involved in several processes such as the response to oxidative stress (Toone *et al.* 2001).

Another term, *single-organism catabolic process*, which represents less than 3 % of the whole genome, contains enzymes such as dehydrogenases (n = 14), oxidoreductases (n = 7), or oxidases (n = 5) (Table S3.5). The role of the enzymes in the yeast growth phase is not yet understood. However, in this term, we found several genes encoding catalases (OphioH327g1152, OphioH327g3052, and OphioH327g6217), which are enzymes involved in antioxidant defenses. These gene functions have already been associated with a yeast-specific expression in *H. capsulatum* (Inglis and Sherlock 2013). This suggests a conserved expression pattern for these genes. It has also been shown in *Paracoccidioides brasiliensis* and *Penicillium marneffei*, two dimorphic human pathogens, that gene expression and catalase activity are highly regulated with respect to the growth phase. For some of the catalases that have been described, both species show an increase in yeast phase (Pongpom *et al.* 2005; Xi *et al.* 2007; Chagas *et al.* 2008). Moreover, OphioH327g6217 is orthologous to *CAT1* of *Candida albicans* and *cat-4* of *Neurospora crassa*. In *C. albicans*, CAT1 is involved in hyphal differentiation in response to hydrogen peroxide and mutants of *CAT1* display abnormal hyphal growth (Nasution *et al.* 2008). Interestingly, *CAT1* expression is regulated by an AP1-like transcription factor, *CAP1* (Alarco and Raymond 1999). The function and regulation of the *O. novo-ulmi CAT1* ortholog, however, are not known but could be conserved and this gene could be involved in hyphal differentiation.

Although the OCM growth medium contained no urea, we found a gene encoding a urease, OphioH327g2055, which was overexpressed in the yeast phase (average logFC 1). In *P. brasiliensis*, a gene annotated as encoding the same enzyme is also preferentially expressed in the yeast phase (Felipe *et al.* 2005). An interesting aspect of urease is that these enzymes seem to have a conserved role across fungal and bacterial human infection as a general virulence factor for human pathogens (Rutherford 2014). Ureases particularly are required in one dimorphic and one saprophytic yeast fungi: *Cryptococcus neoformans* (Cox *et al.* 2000) and *Coccidioides posadasii* (Mirbod-Donovan *et al.* 2006), respectively. Our results may suggest that the role of this enzyme in fungal pathogenesis is conserved in *O. novo-ulmi*.

3.5.3.2 Filamentation signatures

Of the 501 genes that were overexpressed in the mycelium condition, 167 are genes coding for uncharacterized proteins.

For the remaining 334 genes, we found six enriched biological processes (Figure 3.2D, Table S3.6). Two processes are related to protein modification (*cellular protein modification process* and *protein phosphorylation*, which represent 8% and 12% of total gene content of these categories, respectively). They concern genes coding for serine/threonine kinases and mitogen-activated kinase (MAPK) (average logFC from 0.97 to 3.08; Table S3.6). MAPK cascades are involved in filamentation in the budding yeast *Saccharomyces cerevisiae* (production of pseudo-hyphae), in *Candida albicans* (Liu *et al.* 1993, 1994; Mitchell 1998), and in the phytopathogen *Ustilago maydis* (Mayorga and Gold 1999; Martínez-Espinoza *et al.* 2004). Given these results, we hypothesize that these molecular pathways are also involved in filamentation in *O. novo-ulmi*. The overexpression of these kinases may reflect their role in this cellular differentiation process. Also, the *aminoglycan metabolite process* is enriched in mycelium samples ($P < 0.01$). This category contains 0.2 % of the entire genome (17 genes in total and 4 overexpressed in mycelium). Interestingly, two chitin synthases (OphioH327g0970 and OphioH327g4365.1, logFC 1.08 and 1.34, respectively), one endochitinase (type 1, OphioH327g7070, logFC 1.7) and one anhydro-N-acetylmuramic acid kinase (OphioH327g4206, logFC 3.67) are present in this category (Table S3.6). Chitin synthases are well known in several fungi to be involved in filamentation, hyphal growth and conidiation (Borgia *et al.* 1996; Motoyama *et al.* 1996; Martín-Udíroz *et al.* 2004). These roles may be conserved in *O. novo-ulmi*.

In the set of overexpressed genes in mycelium growth phase, we found nine transcription factors, but none was part of an enriched GO term (Table S3.6).

3.5.3.3 Carbohydrate-active enzymes and pathogenicity genes

Using the annotation of CAZymes (Carbohydrate-Active Enzymes) that were described by Cantarel *et al.* (2009) and assigned to *O. novo-ulmi* genes by Comeau *et al.* (2015), we identified 11 genes encoding CAZymes that were overexpressed in the yeast phase and 16 in the mycelial phase (Table 3.1). Again, for each phase, the set of enzymes that is recruited is different, as yeast cells are enriched in glycoside hydroxylases (GH, $n = 8$) and mycelial growth in glycosyltransferases (GT, $n = 10$). GH are enzymes that are

involved in the breakdown of saccharides, whereas GT are responsible for the biosynthesis of glycosides. Looking at the differentially expressed genes between yeast and mycelial phases, there is very little overlap between the types of CAZymes that are recruited, depending upon the growth phase. Thus, yeast and mycelium seem to exert contrasting actions on the carbohydrate component, consistent with the fact that the cell wall of each growth phase is composed of different molecules, a phenomenon that has previously been described in *Candida albicans*, *Histoplasma capsulatum* and *P. brasiliensis* (Domer *et al.* 1967; Kanetsuna *et al.* 1969; Kanetsuna and Carbonell 1971; Chattaway *et al.* 1973).

In their study on *O. novo-ulmi* annotation, Comeau and colleagues identified 1731 genes as homologs of genes that are involved in pathogen/host interactions and as part of the PHI-base, a database that catalogs genes that are related to pathogenicity and virulence for fungal, oomycetes and bacterial pathogens (www.phi-base.org) (Winnenburg *et al.* 2008; Comeau *et al.* 2015). Here, we found that 217 of these genes are differentially expressed between yeast and mycelial phases (107 overexpressed in the yeast phase and 110 in the mycelial phase, Tables S3.5 and S3.6). Although cultures that were subjected to RNAseq analysis were grown under axenic conditions, these genes represent many opportunities to link each growth phase of *O. novo-ulmi* to pathogenicity.

3.5.4 Comparison of *Ophiostoma novo-ulmi* transcriptomes with those of other dimorphic pathogens

In order to systematically assess the molecular similarities between *O. novo-ulmi* and well-established model species for the study of dimorphism, we compared our transcriptomic data with previously published data for *Candida albicans* (Bruno *et al.* 2010) and *Histoplasma capsulatum* (Edwards *et al.* 2013), which are both ascomycete dimorphic human pathogens (Figure 3.1). Given that these three fungi are dimorphic, we expect many overlaps regarding regulation of phase-dependent gene expression.

In their study, Edwards and colleagues sequenced mRNA extracted from distinct yeast and mycelial growth phases of *H. capsulatum*. Yeast cells were grown to late exponential phase at 37 °C with agitation, whereas the mycelium was produced at 25 °C. As the values and gene names that are presented in this 2013 study corresponded to a *de novo* assembly from transcriptomes mapped onto the reference genome, we compared the complete set of O. *novo-ulmi* exons with the *de novo* assembly of G186 using *tblastx*. We found 5292

unique *de novo*-assembled *H. capsulatum* genes that matched *O. novo-ulmi* genes (Table S3.3, Figure 3.3A). The percentage of nucleotide sequence identity for the orthologous pairs ranged from 19.75 % to 100 % (average identity, 60.87 %; Figure S3.3).

We used the transcriptome dataset of *H. capsulatum* to compare gene expression levels between *H. capsulatum* and *O. novo-ulmi*. By re-analyzing RNAseq data from Edwards *et al.* (2013) with our workflow, we determined that 5240 orthologs of *O. novo-ulmi* are expressed in *H. capsulatum*. However, less than 1.5 % of orthologous genes are over-expressed in yeast or in mycelium in both species (Figure 3.3A, Tables S3.7 and S3.8). Thus, the overlap represents only a few orthologs and no more than 6.5 % of the differentially expressed genes between yeast and mycelium phases of *O. novo-ulmi*. The overlap is greater than expected by chance in the mycelium phase ($P = 0.015$, Table 3.2), suggesting that the expression profiles are conserved. Nevertheless, we still found some evidence of specific gene conservation in the yeast growth phase. Indeed, the gene encoding the aforementioned urease (OphioH327g2055) is orthologous to a *H. capsulatum* gene (HC186_00717.T1), which is also over-expressed in the yeast phase (Table S3.8). This supports our hypothesis of a conserved role for urease across fungal pathogens. In terms of biological processes, the small overlapping gene sets are not very representative of the diversity found in *Ophiostoma novo-ulmi* (Table 3.3). Only three biological processes for yeast were enriched (none for the mycelium). All of these processes are involved in the transport of ions (four genes) and cations (eight genes). It has been shown that genes involved in sulfur metabolism are overexpressed in the yeast phase of *H. capsulatum* (Hwang *et al.* 2003). Since this process is not enriched in *O. novo-ulmi,* it seems that this metabolic pathway is not as important in *O. novo-ulmi* as it is in *H. capsulatum*. Overall, these results highlight the occurrence of different molecular profiles for yeast and mycelial growth phases, depending upon the species. *Histoplasma capsulatum* is a thermally sensitive fungus that switches from avirulent mycelia to pathogenic yeasts at 37 °C (Maresca and Kobayashi 1989). Consequently, the growth conditions of yeast phases are distinct between *O. novo-ulmi* and *H. capsulatum*. The optimal growth temperature of *O. novo-ulmi* is 20-22 °C (Brasier 1991) and it grows well in both phases from 20 °C to 32 °C (data not shown). Thus, the ecological niches that are filled by these two fungi are distinct; both phylogenetic distance and the different ecological niches could explain most of the differences highlighted here.

We also compared *O. novo-ulmi* yeast-mycelium differential expression data with those obtained for the same phases in *Candida albicans*. As part of a large transcriptome analysis in *C. albicans*, two biological replicates for each of the yeast and mycelium growth phases were obtained using media incorporating serum at 37 °C (mycelium) or not incorporating serum at 30 °C (yeasts) (Bruno *et al.* 2010). We found 2774 *C. albicans* genes that had an ortholog in *O. novo-ulmi* genes (Figure 3.3B, Table S3.3). Here the range of nucleotide sequence identity percentages for each orthologous pair is between 16.54 % and 100 % (average identity: 53.27%; Figure S3.3). As *C. albicans* is from the class Saccharomycetes, we expected a number of orthologs that were close to the one associated with *Saccharomyces cerevisiae* (3179; Table S3.3). We determined that 2561 orthologs of *Ophiostoma* are expressed in *C. albicans* and only 21 genes are over-expressed in yeast and 16 genes are over-expressed in mycelium in both species (respectively, 0.8 % and 0.6 % of the total number of expressed orthologs) (Table S3.9). Here, only yeast growth phase overlap is significant (P = 0.0023, Table 3.2). The few orthologous genes that show the same regulation pattern between the two species may be conserved, but the small number may be related to the phylogenetic distance and the different growth conditions that allow yeast or mycelium to develop. In fact, increased temperature coupled with other conditions (presence of serum, pH modification) triggers filamentation in *C. albicans* (Odds 1988).

Interestingly, over the 3391 orthologs that were shared between *H. capsulatum* and *C. albicans* (average sequence identity: 53.94 %; Table S3.3, Figure S3.3), only 53 are overexpressed in the yeast phase of both species and 54 in mycelium (data not shown). Again, the overlap is statistically significant (P = 0.018) for only one growth phase, i.e., the mycelium (Table 3.2). Thus, it would appear that even thermally regulated species may have established different strategies to grow either in yeast form or in mycelium phase. As previously mentioned, *H. capsulatum* and *C. albicans* have contrasting responses to temperature as incubation at 37 °C induces yeast growth in the former but triggers filamentation in the latter. Moreover, in *C. albicans*, both phases are found at 37 °C; it is the combination of multiple factors that determine which growth phase will be favored (Odds 1988; Mitchell 1998). In the study of Bruno and colleagues, filamentation was induced by adding serum to the medium at 37 °C (Bruno *et al.* 2010). Thus, sharing the same host is not sufficient to induce similar regulation of the expression of orthologs. In this case, the phylogenetic distance between *H. capsulatum* and *C. albicans* may also

account for the small degree of overlap between overexpressed orthologs in yeast and mycelial phases. With the development of current technologies, closer plant and human pathogen models may be developed in the future and allow us to better understand how filamentation evolved and its relationship with ecology, for instance in the phylogenetic group of *O. novo-ulmi*. For example, *Sporothrix schenckii* would be an excellent candidate for comparison with *O. novo-ulmi* as they share 7171 orthologs (Figure 3.1, Table S3.3), but infect different host and show distinct ecological niches.

3.6 Conclusions

Our study provides insights into the molecular functions and gene expression profiles that are involved in fungal growth processes. It also highlights strategies that are related to yeast or mycelium phases in *O. novo-ulmi*, a non-thermally regulated dimorphic fungus. We showed that these phases display different transcriptome signatures and that some biological processes, such as protein modification or amino-acid metabolism, are specific to one of the two phases. Further, carbohydrate-active enzymes seem to be differentially involved in distinct growth phases. Some of these functions are already described for a limited number of fungal species and seem to be conserved in *O. novo-ulmi,* including MAP Kinases, catalases, chitinases and ureases. By comparing transcriptomes of *C. albicans* and *H. capsulatum* with our data, we found very few overlap and no conserved biological processes. Overall, we show that *O. novo-ulmi* possesses specific gene regulation processes and that comparisons with well-studied species do not cover most of the transcriptomic variation that was observed between yeast and mycelium growth phases. Given that most of the model species used for studying dimorphism are human pathogens, expanding our knowledge of an ascomycete plant pathogen is greatly needed; *O. novo-ulmi* is a perfect candidate with the ability to manipulate dimorphism *in vitro* (Naruzawa and Bernier 2014), a genome that has already been sequenced and, now, where large-scale transcriptomic data are available.

3.7 Acknowledgments

We thank Dr. Brian Boyle and the staff from the *Plateforme d'Analyses Génomiques* of IBIS for technical assistance, Dr. Chad R. Rappleye (Ohio State University, Colombus, OH, USA) for sharing his data, Marie Filteau, François-Olivier Hébert-Gagnon, Chris Eberlein, Véronique Hamel, Ben Sutherland, Éleonore Durand (IBIS, Université Laval, QC, CA) and Olivier Martin (CEF, Université du Québec à Rimouski, QC, CA) provided useful comments on the methods and the manuscript. We also thank Mary Thaler (IBIS,

Université Laval, QC, CA) and Dr. William F.J. Parsons (CEF, Université de Sherbrooke, QC, CA) who edited the English. Our research was funded by the Natural Sciences and Engineering Research Council of Canada (NSERC).

3.8 Bibliography

Alarco AM, Raymond M, 1999. The bZip transcription factor Cap1p is involved in multidrug resistance and oxidative stress response in *Candida albicans*. *Journal of bacteriology* **181**: 700–708.

Altschul SF, Gish W, Miller W, Myers EW, Lipman DJ, 1990. Basic Local Alignment Search Tool. *Journal of Molecular Biology* **215**: 403–410.

Benjamini Y, Hochberg Y, 1995. Controlling the False Discovery Rate : a practical and powerful approach to multiple testing. *Journal of the Royal Stastistical Society* **57**: 289–300.

Berbee M, Taylor JW, 1992. 18s ribosomal RNA gene sequence characters place the pathogen *Sporothrix schenckii* in the genus *Ophiostoma*. *Experimental Mycology* **16**: 87–91.

Bernier L, Aoun M, Bouvet G, Comeau A, Dufour J, Naruzawa E, Nigg M, Plourde K, 2015. Genomics of the Dutch elm disease pathosystem: are we there yet? *iForest - Biogeosciences and Forestry* **8**: 149–157.

Berrocal A, Navarrete J, Oviedo C, Nickerson KW, 2012. Quorum sensing activity in *Ophiostoma ulmi*: effects of fusel oils and branched chain amino acids on yeast-mycelial dimorphism. *Journal of applied microbiology* **113**: 126–134.

Borgia PT, Mia Y, Dodge CL, 1996. The orlA form *Aspregillus nidulans* encodes a trehalose-6-phosphate phosphatase necessary for normal growth and chitin synthesis at elevated temperatures. *Molecular microbiology* **20**: 1287–1296.

Brasier CM, 1991. *Ophiostoma novo-ulmi* sp . *nov*., causative agent of current Dutch elm disease pandemics. *Mycopathologia* **115**: 151–161.

Bruno VM, Wang Z, Marjani SL, Euskirchen GM, Martin J, Sherlock G, Snyder M, 2010. Comprehensive annotation of the transcriptome of the human fungal pathogen *Candida albicans* using RNA-seq. *Genome Research* **20**: 1451–1458.

Cantarel BI, Coutinho PM, Rancurel C, Bernard T, Lombard V, Henrissat B, 2009. The Carbohydrate-Active EnZymes database (CAZy): An expert resource for glycogenomics. *Nucleic Acids Research* **37**: 233–238.

Chagas RF, Bailão AM, Pereira M, Winters MS, Smullian AG, Deepe GS, de Almeida Soares CM, 2008. The catalases of *Paracoccidioides brasiliensis* are differentially regulated: protein activity and transcript analysis. *Fungal Genetics and Biology* **45**: 1470–1478.

Chattaway FW, Bishop R, Holmes MR, Odds FC, Barlow AJ, 1973. Enzyme activities associated with carbohydrate synthesis and breakdown in the yeast and mycelial

forms of *Candida albicans*. *Journal of general microbiology* **75**: 97–109.

Comeau AM, Dufour J, Bouvet GF, Jacobi V, Nigg M, Henrissat B, Laroche J, Levesque RC, Bernier L, 2015. Functional annotation of the *Ophiostoma novo-ulmi* genome: insights into the phytopathogenicity of the fungal agent of Dutch elm disease. *Genome biology and evolution* **7**: 410–430.

Cox GM, Mukherjee J, Cole GT, Casadevall A, Perfect JR, 2000. Urease as a virulence factor in experimental cryptococcosis. *Infection and Immunity* **68**: 443–448.

Cuomo CA, Rodriguez-Del Valle N, Perez-Sanchez L, Abouelleil A, Goldberg J, Young S, Zeng Q, Birren BW, 2014. Genome Sequence of the Pathogenic Fungus *Sporothrix schenckii*. *Genome Announcement* **2**: e00446-14.

Dillies MA, Rau A, Aubert J, Hennequet-Antier C, Jeanmougin M, Servant N, Keime C, Marot NS, Castel D, Estelle J, Guernec G, Jagla B, Jouneau L, Laloë D, Le Gall C, Schaëffer B, Le Crom S, Guedj M, Jaffrézic F, 2013. A comprehensive evaluation of normalization methods for Illumina high-throughput RNA sequencing data analysis. *Briefings in Bioinformatics* **14**: 671–683.

Domer JE, Hamilton JG, Harkin JC, 1967. Comparative study of the cell walls of the yeastlike and mycelial phases of *Histoplasma capsulatum*. *Journal of Bacteriology* **94**: 466–474.

Edwards JA, Chen C, Kemski MM, Hu J, Mitchell TK, Rappleye CA, 2013. *Histoplasma* yeast and mycelial transcriptomes reveal pathogenic-phase and lineage-specific gene expression profiles. *BMC genomics* **14**: 695.

Felipe MSS, Andrade RV, Arraes FBM, Nicola AM, Maranhão AQ, Torres F a G, Silva-Pereira I, Poças-Fonseca MJ, Campos EG, Moraes LMP, Andrade P a, Tavares AHFP, Silva SS, Kyaw CM, Souza DP, Pereira M, Jesuíno RS a, Andrade E V, Parente J a, Oliveira GS, Barbosa MS, Martins NF, Fachin AL, Cardoso RS, Passos G a S, Almeida NF, Walter MEMT, Soares CM a, Carvalho MJ a, Brígido MM, 2005. Transcriptional profiles of the human pathogenic fungus *Paracoccidioides brasiliensis* in mycelium and yeast cells. *The Journal of biological chemistry* **280**: 24706–24714.

Forgetta V, Leveque G, Dias J, Grove D, Lyons R, Genik S, Wright C, Singh S, Peterson N, Zianni M, Kieleczawa J, Steen R, Perera A, Bintzler D, Adams S, Hintz W, Jacobi V, Bernier L, Levesque R, Dewar K, 2013. Sequencing of the Dutch elm disease fungus genome using the Roche/454 GS-FLX Titanium System in a comparison of multiple genomics core facilities. *Journal of biomolecular techniques* **24**: 39–49.

Gaffney T, Friedrich L, Vernooij B, Negrotto D, Nye G, Uknes S, Ward E, Kessmann H, Ryals J, 1993. Requirement of salicylic acid for the induction of systemic acquired resistance. *Science (New York, N.Y.)* **261**: 754–756.

García-Conesa MT, Østergaard P, Kauppinen S, Williamson G, 2001. Hydrolysis of diethyl diferulates by a tannase from *Aspergillus oryzae*. *Carbohydrate Polymers* **44**: 319–324.

Hartigan JA, Wong MA, 1979. Algorithm AS 136: A K-Means Clustering Algorithm.

Applied Statistics **28**: 100.

Hintz WE, 1999. Sequence analysis of the chitin synthase A gene of the Dutch elm pathogen *Ophiostoma novo-ulmi* indicates a close association with the human pathogen *Sporothrix schenckii*. *Gene* **237**: 215–221.

Hintz W, Pinchback M, de la Bastide P, Burgess S, Jacobi V, Hamelin R, Breuil C, Bernier L, 2011. Functional categorization of unique expressed sequence tags obtained from the yeast-like growth phase of the elm pathogen *Ophiostoma novo-ulm*i. *BMC genomics* **12**: 431.

Hwang L, Hocking-Murray D, Bahrami AK, Andersson M, Rine J, Sil A, 2003. Identifying phase-specific genes in the fungal pathogen *Histoplasma capsulatum* using a genomic shotgun microarray. *Molecular biology of the cell* **14**: 2314–2326.

Inglis DO, Sherlock G, 2013. Ras signaling gets fine-tuned: Regulation of multiple pathogenic traits of *Candida albicans*. *Eukaryotic Cell* **12**: 1316–1325.

Jacobi V, Dufour J, Bouvet GF, Aoun M, Bernier L, 2010. Identification of transcripts up-regulated in asexual and sexual fruiting bodies of the Dutch elm disease pathogen *Ophiostoma novo-ulmi*. *Canadian Journal of Microbiology* **56**: 697–705.

Jantzen SG, Sutherland BJ, Minkley DR, Koop BF, 2011. GO Trimming: Systematically reducing redundancy in large Gene Ontology datasets. *BMC research notes* **4**: 267.

Kanetsuna F, Carbonell LM, 1971. Cell wall composition of the yeastlike and mycelial forms of *Blastomyces dermatitidis*. *Journal of Bacteriology* **106**: 946–948.

Kanetsuna F, Carbonell LM, Moreno RE, Rodiguez J, 1969. Cell wall composition of the yeast and mycelial forms of *Paracoccidioides brasiliensis*. *Journal of bacteriology* **97**: 1036–1041.

Kim D, Pertea G, Trapnell C, Pimentel H, Kelley R, Salzberg SL, 2013. TopHat2: accurate alignment of transcriptomes in the presence of insertions, deletions and gene fusions. *Genome biology* **14**: R36.

Liu H, Köhler J, Fink GR, 1994. Suppression of hyphal formation in *Candida albicans* by mutation of a *STE12* homolog. *Science* **266**: 1723–1726.

Liu H, Styles CA, Fink GR, 1993. Elements of the yeast pheromone response pathway required for filamentous growth of diploids. *Science* **262**: 1741–1744.

Maresca B, Kobayashi GS, 1989. Dimorphism in *Histoplasma capsulatum*: a model for the study of cell differentiation in pathogenic fungi. *Microbiological reviews* **53**: 186–209.

Martín-Udíroz M, Madrid MP, Roncero MIG, 2004. Role of chitin synthase genes in *Fusarium oxysporum*. *Microbiology* **150**: 3175–3187.

Martínez-Espinoza AD, Ruiz-Herrera J, León-Ramírez CG, Gold SE, 2004. MAP kinase and cAMP signaling pathways modulate the pH-induced yeast-to-mycelium dimorphic transition in the corn smut fungus *Ustilago maydis*. *Current microbiology*

49: 274–81.

Mayorga ME, Gold SE, 1999. A MAP kinase encoded by the *ubc3* gene of *Ustilago maydis* is required for filamentous growth and full virulence. *Molecular Microbiology* **34**: 485–497.

Miller HJ, Elgersma DM, 1976. The growth of aggressive and non-aggressive strains of *Ophiostoma ulmi* in susceptible and resistant elms, a scanning electron microscopical study. *Netherlands Journal of Plant Pathology* **82**: 51–65.

Mirbod-Donovan F, Schaller R, Hung CY, Xue J, Reichard U, Cole GT, 2006. Urease produced by *Coccidioides posadasii* contributes to the virulence of this respiratory pathogen. *Infection and Immunity* **74**: 504–515.

Mitchell AP, 1998. Dimorphism and virulence in *Candida albicans*. *Current opinion in microbiology* **1**: 687–92.

Motoyama T, Fujiwara M, Kojima N, Horiuchi H, Ohta A, Takagi M, 1996. The *Aspergillus nidulans* genes *chsA* and *chsD* encode chitin synthases which have redundant functions in conidia formation. *Molecular and General Genetics* **251**: 442–450.

Naruzawa ES, Bernier L, 2014. Control of yeast-mycelium dimorphism in vitro in Dutch elm disease fungi by manipulation of specific external stimuli. *Fungal biology* **118**: 872–84.

Nasution O, Srinivasa K, Kim M, Kim YJ, Kim W, Jeong W, Choi W, 2008. Hydrogen peroxide induces hyphal differentiation in *Candida albicans*. *Eukaryotic Cell* **7**: 2008–2011.

Nemecek JC, Wüthrich M, Klein BS, 2006. Global control of dimorphism and virulence in fungi. *Science (New York, N.Y.)* **312**: 583–8.

Odds FC, 1988. *Candida and Candidosis* (Elsevier Science Health Science Division, Ed,).

Pereira V, Royer JC, Hintz WE, Field D, Bowden C, Kokurewicz K, Hubbes M, Horgen PA, 2000. A gene associated with filamentous growth in *Ophiostoma novo-ulmi* has RNA-binding motifs and is similar to a yeast gene involved in mRNA splicing. *Current genetics* **37**: 94–103.

Pongpom P, Cooper CR, Vanittanakom N, 2005. Isolation and characterization of a catalase-peroxidase gene from the pathogenic fungus, *Penicillium marneffei*. *Medical mycology* **43**: 403–411.

Richards WC, 1994. Nonsporulation in the Dutch elm disease fungus *Ophiostoma ulmi* : evidence for control by a single nuclear gene. *Revue canadienne de botanique* **72**: 461–467.

Robinson MD, McCarthy DJ, Smyth GK, 2009. edgeR: A Bioconductor package for differential expression analysis of digital gene expression data. *Bioinformatics* **26**: 139–140.

Robinson MD, Oshlack A, 2010. A scaling normalization method for differential expression analysis of RNA-seq data. *Genome Biology* **11**: R25.

Rutherford JC, 2014. The emerging role of urease as a general microbial virulence factor. *PLoS Pathogens* **10**: 1–3.

Schmieder R, Edwards R, 2011. Quality control and preprocessing of metagenomic datasets. *Bioinformatics* **27**: 863–864.

Tamura K, Stecher G, Peterson D, Filipski A, Kumar S, 2013. MEGA6: Molecular evolutionary genetics analysis version 6.0. *Molecular Biology and Evolution* **30**:2725-2729.

Toone WM, Morgan BA, Jones N, 2001. Redox control of AP-1-like factors in yeast and beyond. *Oncogene* **20**: 2336–2346.

Wickham H, 2009. *ggplot2: elegant graphics for data analysis.* New York.

Winnenburg R, Urban M, Beacham A, Baldwin TK, Holland S, Lindeberg M, Hansen H, Rawlings C, Hammond-Kosack KE, Köhler J, 2008. PHI-base update: Additions to the pathogen-host interaction database. *Nucleic Acids Research* **36**: 572–576.

Xi L, Xu X, Liu W, Li X, Liu Y, Li M, Zhang J, Li M, 2007. Differentially expressed proteins of pathogenic *Penicillium marneffei* in yeast and mycelial phases. *Journal of Medical Microbiology* **56**: 298–304.

Young MD, Wakefield MJ, Smyth GK, Oshlack A, 2010. Gene ontology analysis for RNA-seq: accounting for selection bias. *Genome biology* **11**: R14.

Table 3.1 Genes associated with carbohydrate-active enzyme (CAZy) activity in the set of overexpressed genes in yeast or mycelial phase in *Ophiostoma novo-ulmi*.

Growth phase	*O. novo-ulmi* genes	Overexpression (logFC[a] Y vs LM)	Overexpression (logFC Y vs SM)	Description	CAZy[b]
Yeast	OphioH327g3368	3.15	2.65	Mannan endo-1,6-alpha-mannosidase DCW1	GH76
	OphioH327g0928	2.65	2.94	Alpha-L-fucosidase	GH29
	OphioH327g0277	1.74	1.16	Glycoside hydrolase 15-related	GH15
	OphioH327g0547	2.41	4.42	1.4-beta-D-glucan cellobiohydrolase C	GH6
	OphioH327g1070	1.38	0.92	Protein phosphatase regulatory subunit	CBM21
	OphioH327g5673	1.28	0.98	Mannan endo-1.6-alpha-mannosidase DCW1	GH76
	OphioH327g4175	1.55	1.95	Endochitinase 2	GH18
	OphioH327g8225	1.55	1.59	Chitin synthase D (GT2 family)	GT2
	OphioH327g2068	1.78	3.19	Xylosidase/arabinosidase (Beta-xylosidase)	GH43
	OphioH327g0647	3.65	3.6	Exoglucanase 1	GH7
	OphioH327g6063	0.94	0.91	UDP-N-acetylglucosaminyltransferase	GT41
Mycelium	OphioH327g0635	2.89	3.18	GDSL-like Lipase/Acylhydrolase	CE12
	OphioH327g3383	1.88	1.20	Carbohydrate-binding module family 52 protein	CBM52
	OphioH327g7070	1.81	1.60	Endochitinase 1 (Complement-fixation antigen)	GH18
	OphioH327g6213	1.42	1.48	Glycosyltransferase family 22 protein	GT22
	OphioH327g7370	4.60	3.68	Endo-N-acetyl-beta-D-glucosaminidase	GH18
	OphioH327g4365.1	1.38	1.30	Chitin synthase 3	GT2
	OphioH327g3285	1.30	1.64	Protein mannosyltransferase 1	GT39
	OphioH327g6864	1.41	1.66	Beta-glucanosyltransferase gel2	GH72
	OphioH327g7251	3.66	3.85	Putative cellulose synthase 3 (Cyclic di-GMP-binding	GT2
	OphioH327g5590	4.86	5.79	Rhamnogalacturonase	GH28
	OphioH327g8280	1.24	1.42	UDP-glucose:glycoprotein glucosyltransferase	GT24
	OphioH327g5097	1.10	1.20	Dolichol-phosphate mannosyltransferase	GT2
	OphioH327g2358	0.90	1.39	Oligosaccharyl transferase subunit	GT66
	OphioH327g3447	1.73	1.99	EGF domain-specific O-linked N-acetylglucosamine	GT61
	OphioH327g4450	0.91	1.03	Mannosyltransferase pmti	GT39
	OphioH327g0970	0.93	1.24	Chitin synthase 1 (Class-III chitin synthase 3)	GT2

[a] LogFC: $\log_2$ of fold change between yeast and mycelium phases. Y: yeast phase, LM: mycelium grown in liquid medium, SM: mycelium grown in petri dishes. FDR≤ 1%.
[b] GH: glycoside hydrolases; GT: glycosyltransferases; CBM: carbohydrate-binding module. Numbers associated with CAZy types refer to the family number.

Table 3.2 Significance of the overlap of overexpressed orthologs in yeast and mycelium with respect to the species comparison for *Ophiostoma novo-ulmi*, *Histoplasma capsulatum* and *Candida albicans*

Growth phase	Species compared	Overlap	*P-values* [a]
Yeast	*H. capsulatum - O. novo-ulmi*	63	0.1406
	C. albicans - O. novo-ulmi	21	0.0023
	H. capsulatum - C. albicans	53	0.7543
Mycelium	*H. capsulatum - O. novo-ulmi*	68	0.0149
	C. albicans - O. novo-ulmi	16	0.3688
	H. capsulatum - C. albicans	54	0.0182

[a] *P-values* calculated with that hypergeometric test indicate the probability of having an overlap greater than the observed value.

Table 3.3 Enriched GO terms (biological processes) in yeast for orthologs that are over-expressed in both *Ophiostoma novo-ulmi* and *Histoplasma capsulatum.*

Growth phase	GO accession	Term representation in gene set (%) [a]	Term representation in genome (%) [b]	*P-value* [c]	Term
Yeast	GO:0015672	9.52	0.49	0.0006	monovalent inorganic cation transport
	GO:0030001	7.84	0.59	0.0016	metal ion transport
	GO:0006811	4.54	2.04	0.0003	ion transport

[a] Term representation in gene set: percentage of genes associated with a given term which are found in the set of yeast overexpressed genes.
[b] Term representation in genome: percentage of the whole genome that is associated with a given term.
[c] *P-values* obtained using GOseq package

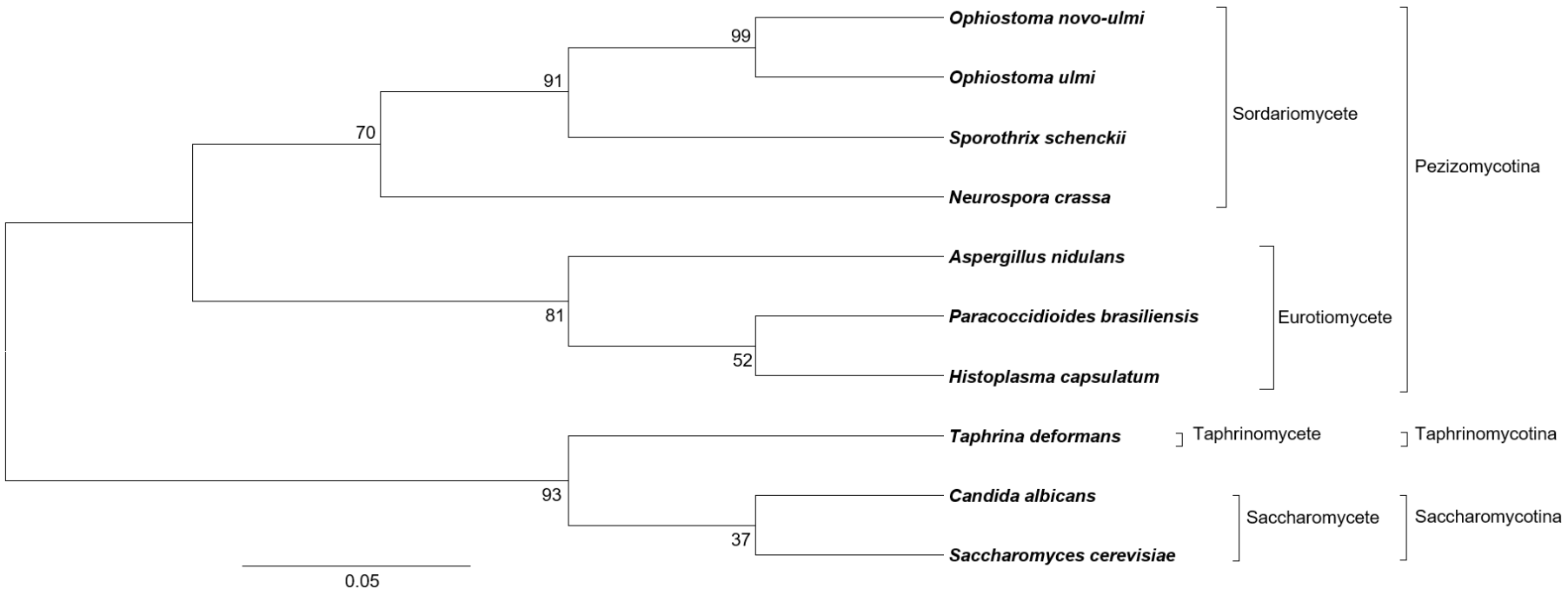

Figure 3.1 Phylogeny of ascomycete fungi based on concatenated Internal Transcribed Spacer 1 sequences (ITS1). Except for *Neurospora crassa*, all fungi are dimorphic. ITS sequences were downloaded from the NCBI database and exported to BioEdit 7.2.5 software (Hall, 1999) to align and concatenate the sequences (see strain or isolate names and references in Table S3.1). A maximum-likelihood tree was constructed using Mega6 with 1000 bootstrap (Tamura *et al.* 2013). Bootstrap support is shown on each node. Sordariomycete, Eurotiomycete, Taphrinomycete and Saccharomycete are classes; Pezizomycotina is a sub-division of the ascomycetes.

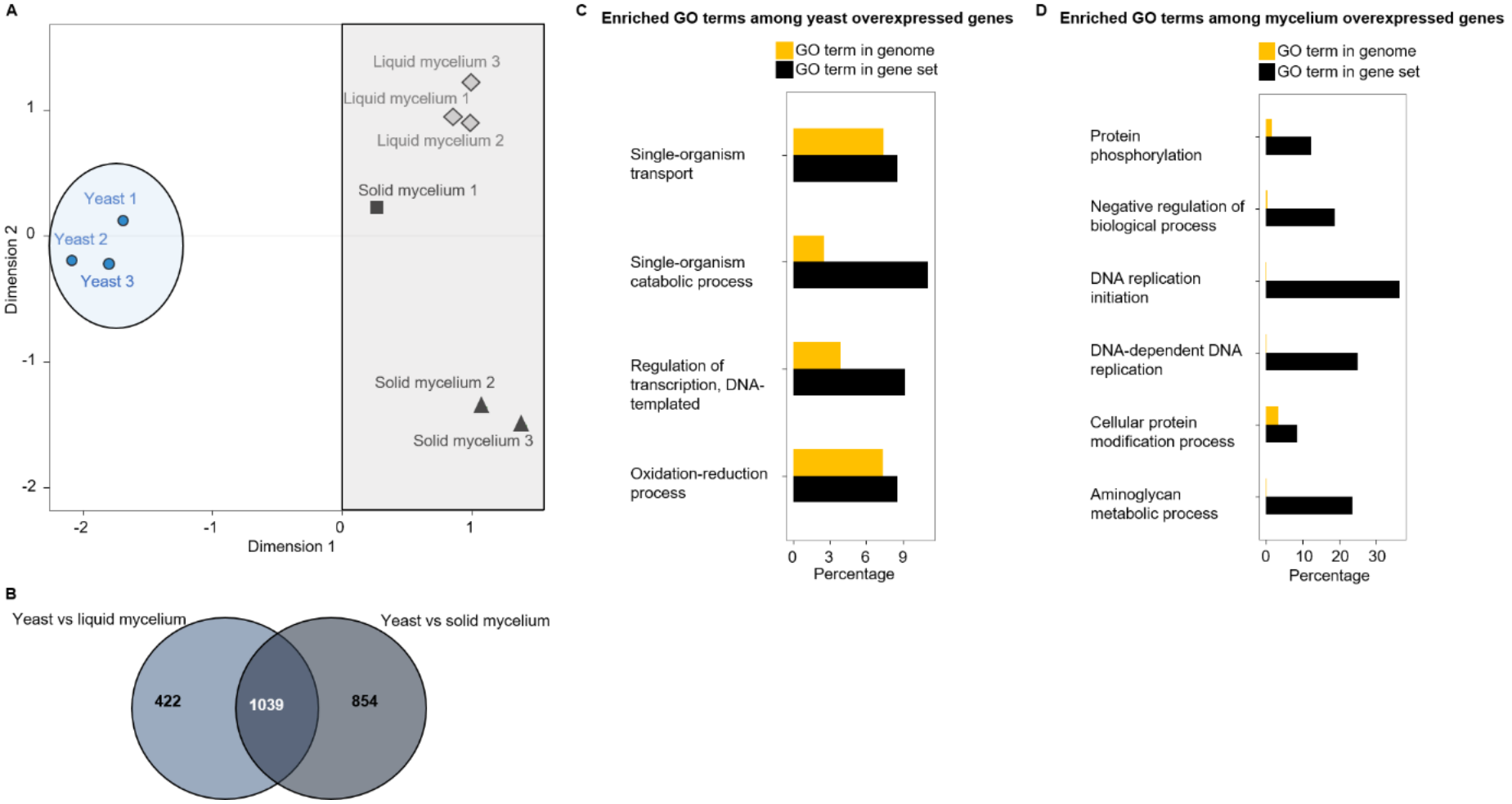

Figure 3.2 Sample variability, differential gene expression and enriched Gene Ontology (GO) analysis between yeast and mycelium samples of *Ophiostoma novo-ulmi*. (A) Multi-dimensional Scaling plot of the nine RNA samples sequenced from yeast phase, mycelium grown in liquid medium (liquid mycelium) and mycelium grown on petri plates (solid mycelium) inoculated with *Ophiostoma novo-ulmi.* Dot shapes: results of

cluster analysis by *k*-means test. Dot colors: growth conditions. Blue circle: yeast phase; Gray rectangle: all the mycelium samples. (B) Venn diagram of the number of differentially expressed genes (FDR ≤ 1 %), depending upon the comparison being made: yeast vs mycelium grown in liquid medium (1460 differentially expressed genes in total, light blue); yeast vs mycelium grown on petri dishes (1852 differentially expressed genes in total, grey). Number of differentially expressed genes that are shared between the comparisons: 1039. (C-D) Enriched GO terms (biological processes) in *Ophiostoma novo-ulmi* for (C) 397 annotated overexpressed genes in yeast; (D) 334 annotated overexpressed genes grown in the 2 mycelial conditions (liquid medium vs petri plates). Yellow bars: percentage of total genes present in a GO term in the genome, also present in the overexpressed set of genes. Black bars: percentage of the whole genome related to the category. $P \leq 0.01$ (Fisher's exact test implemented in GOseq).

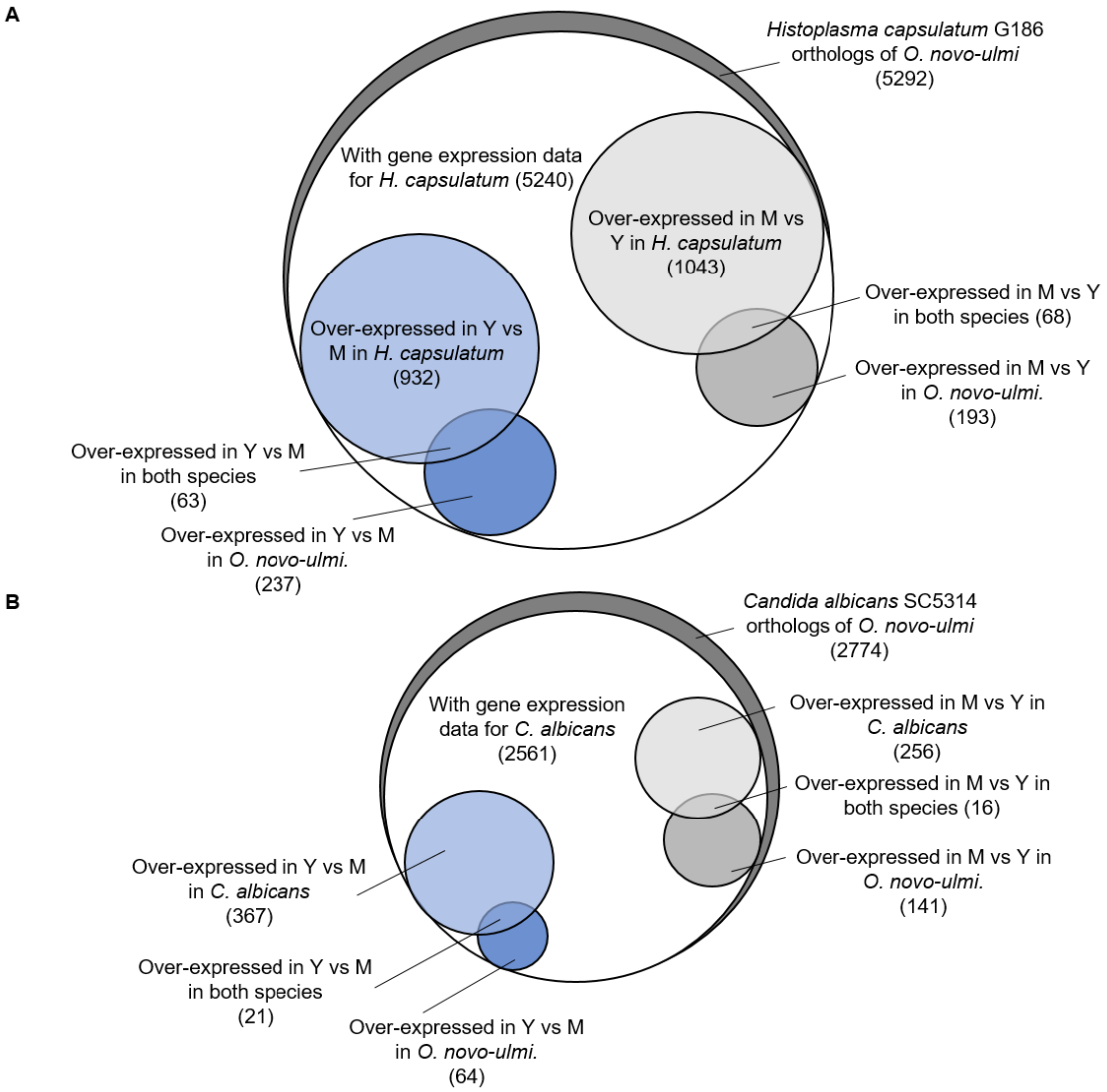

Figure 3.3 Comparison of gene expression using orthologous genes found between *Ophiostoma novo-ulmi* and (A) *Histoplasma capsulatum* or (B) *Candida albicans*. Y=yeast; M= mycelium.

Table S3.1 Species and strain/isolate names, references and sequence sizes for the species used to build the phylogenetic tree.

Species name	**Strain/isolate**	**Reference**	**Sequence size (nt)**
Neurospora crassa	WA0000019131	Palowska *et al.* 2014 The diversity of endophytic fungi in the above-ground tissue of two *Lycopodium* species in Poland. Symbiosis 63:(2)87-97	198
Aspergillus nidulans	YIMPH30005	Miao *et al.* 2015 Rhizospheric fungi of *Panax notoginseng*: diversity and antagonism to host phytopathogens. Journal of Ginseng Research, http://dx.doi.org/10.1016/j.jgr.2015.06.004	211
Candida albicans	SC5314	Diezmann and Dietrich (unpublished) Natural Variation in *Candida* and *Saccharomyces*	204
Saccharomyces cerevisiae	S288c	Diezmann and Dietrich (unpublished) Natural Variation in *Candida* and *Saccharomyces*	204
Paracoccidioides brasiliensis	-	Kasuga, White and Taylor (unpublished) *Ajellomyces* ITS	209
Sporothrix schenckii	C9862	Camacho *et al.* 2015 Molecular epidemiology of human sporotrichosis in Venezuela reveals high frequency of *Sporothrix globosa*. BMC Infect. Dis. 15:(1)839	209
Ophiostoma novo-ulmi	H327	Naruzawa and Bernier, 2014 Control of yeast-mycelium dimorphism in vitro in Dutch elm disease fungi by manipulation of specific external stimuli. Fungal Biol 118:(11)872-884	214

Ophiostoma ulmi	W9	Naruzawa and Bernier, 2014 Control of yeast-mycelium dimorphism in vitro in Dutch elm disease fungi by manipulation of specific external stimuli. Fungal Biol 118:(11)872-884	215
Histoplasma capsulatus	VPCI 881/P/13	Kathuria *et al.* (unpublished) *Histoplasma capsulatum* and histoplasmosis: A review	210
Taphrina deformans	NRRL T-470	Rodrigues and Fonseca, 2003 Molecular systematics of the dimorphic ascomycete genus *Taphrina*. Int. J. Syst. Evol. Microbiol. 53:(PT 2)607-616	216

Table S3.2 General characteristics for each RNAseq sample for *Ophiostoma novo-ulmi*.

Conditions	Yeast						Solid mycelium						Liquid mycelium					
Replicates	1		2		3		1		2		3		1		2		3	
Duplicates trimmed	No	Yes	No	Yes	No	Yes	No	Yes	No	Yes	No	Yes	No	Yes	No	Yes	No	Yes
#[a] Reads after trimming	1.52E+07	6.81E+06	1.14E+07	5.49E+06	1.21E+07	5.77E+06	1.24E+07	6.31E+06	1.30E+07	6.48E+06	1.71E+07	7.05E+06	1.72E+07	7.92E+06	1.44E+07	6.97E+06	1.36E+07	6.46E+06
# Mapped reads	1.01E+07	4.53E+06	7.59E+06	3.69E+06	7.67E+06	3.79E+06	7.37E+06	4.13E+06	7.92E+06	4.26E+06	9.46E+06	4.22E+06	1.08E+07	5.23E+06	8.92E+06	4.55E+06	8.70E+06	4.28E+06
# Mapped bases	9.87E+08	4.30E+08	7.42E+08	3.51E+08	7.51E+08	3.62E+08	7.21E+08	3.96E+08	7.75E+08	4.07E+08	9.25E+08	3.99E+08	1.06E+09	4.98E+08	8.72E+08	4.33E+08	8.51E+08	4.08E+08
Mean read length	97.87	94.98	97.81	95.21	97.81	95.32	97.82	95.80	97.81	95.63	97.77	94.52	97.82	95.20	97.75	95.30	97.83	95.31
Exons coverage depth	66.26	28.91	49.84	23.60	50.41	24.29	48.43	26.56	52.04	27.34	62.12	26.78	70.93	33.44	58.55	29.10	57.16	27.42
Genome coverage depth	30.04	13.10	22.59	10.70	22.85	11.01	21.96	12.04	23.59	12.40	28.16	12.14	32.16	15.16	26.54	13.19	25.91	12.43
EdgeR normalization factor	0.68	0.84	0.71	0.82	0.85	0.94	1.25	1.15	1.13	1.09	1.28	1.12	1.03	1.04	1.07	1.07	0.90	0.97
# Genes with at least 1 read	8175	8296	8144	8257	8143	8241	8194	8316	8199	8318	8200	8322	8200	8325	8189	8304	8175	8287

[a] #=number

Table S3.3 Number of orthologous genes found with the reciprocal best blast hits (RBH) method compared with the Inparanoid method of Khoshraftar *et al.* (2013). The number of genes in each species is indicated between parentheses.

Species compared (no of genes)	RBH method	Khoshraftar *et al.* 2013
Ophiostoma ulmi (8639)/ *Neurospora crassa* (9730)	6276	5517
O. ulmi/ *Saccharomyces cerevisiae* (6604)	3179	2483
O. ulmi/ *O. novo-ulmi* (8640)	8220	NA[a]
O. novo-ulmi/ *N. crassa*	6360	NA
O. novo-ulmi/ *S. cerevisiae*	3260	NA
O. novo-ulmi/ *Sporothrix schenckii* (8674)	7171	NA
O. novo-ulmi/ *Candida albicans* (6218)	2774	NA
O. novo-ulmi/ *Histoplasma capsulatum* (9233)	5292	NA
H. capsulatum / *C. albicans*	3391	NA

[a] NA: data Not Available

Tables S3.4-8: available at
http://www.g3journal.org/content/suppl/2015/09/17/g3.115.021022.DC1

Table S3.4 Read counts for each gene per sample in *Ophiostoma novo-ulmi*.

Table S3.5 Genes overexpressed in yeast phase of *Ophiostoma novo-ulmi*.

Table S3.6 Genes overexpressed in mycelium phase of *Ophiostoma novo-ulmi*.

Table S3.7 Description of the 63 orthologous genes overexpressed in yeast in both *Ophiostoma novo-ulmi* and *Histoplasma capsulatum*.

Table S3.8 Description of the 68 orthologous genes overexpressed in mycelium in both *Ophiostoma novo-ulmi* and *Histoplasma capsulatum.*

Table S3.9 Description of the 21 orthologous genes overexpressed in yeast in both *Ophiostoma novo-ulmi* and *Candida albicans*. LogFC: average log of fold change between yeast and mycelium phases. FDR ≤0.01

Growth phase	*O. novo-ulmi* genes	Over-expression (logFC)	Description	Candida orthologs	Over-expression (logFC *in C. albicans*)
Yeast	OphioH327g3645	2.76	Glutamate_dehydrogenase	C4_06120W_B	1.38
	OphioH327g4970	3.7	NOL1_NOP2_SUN_domain_containing_protein	CR_02030C_A	0.63
	OphioH327g3717	3.665	Aquaporin-1	CR_02920C_B	1.48
	OphioH327g2293	3.225	Denitrification_regulatory_protein_nirq	C4_00970C_B	0.68
	OphioH327g4808	2.845	Cytosine_deaminase	C6_00620W_B	0.78
	OphioH327g0568	1.93	ATP-dependent_RNA_helicase_ded1	C3_06100C_A	0.71
	OphioH327g2187	1.985	Flocculation_suppression_protein_(Protein_SFL1)	CR_05990C_B	1.15
	OphioH327g2220	2.175	RNA-binding_protein	C5_00790C_A	0.80
	OphioH327g8083	1.76	Low-temperature_viability_protein_ltv1	CR_10650W_A	0.71
	OphioH327g5596	1.71	U3_small_nucleolar_RNA-associated_protein_sof1	C3_00560C_A	0.60
	OphioH327g5986	2.04	Serine/threonine-protein_kinase_srk1_(Sty1-regulated_kinase_1)	C2_07130C_A	0.57
	OphioH327g5054	2.34	Hsp70/Hsp90_co-chaperone_CNS1_(Cyclophilin_seven_suppressor_1/STI1_stress-inducible_protein_homolog)	C1_00560W_A	0.66
	OphioH327g3374	2.28	Fluconazole_resistance_protein_1	C3_06850W_A	1.89
	OphioH327g5556	1.565	DNA-directed_RNA_polymerase,_mitochondrial	C1_00640C_B	0.64
	OphioH327g4855	2.365	U3_small_nucleolar_RNA-associated_protein_20_(U3_snoRNA-associated_protein_20)	C3_01200W_B	0.89
	OphioH327g7825	1.43	RNA_recognition_domain-containing_protein	C3_05150W_B	0.73
	OphioH327g0412	1.255	Fimbrin_(ABP67)	C6_02730W_A	0.50
	OphioH327g7377	2.235	Major_facilitator_superfamily_transporter_multidrug_resistance	C6_04610C_A	0.87
	OphioH327g8261	1.65	Integral_membrane_protein	C1_10360C_A	1.17
	OphioH327g1355	1.38	U3_small_nucleolar_ribonucleoprotein_protein_mpp10	C2_00070C_B	0.60
	OphioH327g5712	1.22	P-type_ATPase	C2_02490C_B	0.76

Mycelium	OphioH327g6748	3.285	N-acetyltransferase-like_protein	C6_00140C_A	0.94
	OphioH327g3302	2.48	IMP-specific_5'-nucleotidase_1	C1_01650W_B	0.72
	OphioH327g0724	2.25	Putative_uncharacterized_protein	CR_09930W_B	0.71
	OphioH327g3285	2.12	Protein_mannosyltransferase_1	C7_02890C_B	0.67
	OphioH327g8280	1.95	UDP-glucose:glycoprotein_glucosyltransferase	C3_02960C_B	0.85
	OphioH327g8395	1.785	Mitogen-activated_protein_kinase	C4_06480C_B	2.05
	OphioH327g4472	1.76	Aromatic_aminotransferase	C2_00340C_A	0.75
	OphioH327g5097	1.7	Dolichol-phosphate_mannosyltransferase	C1_08010W_B	0.75
	OphioH327g8526	1.655	Rho-GDP_dissociation_inhibitor	C3_05000W_A	1.00
	OphioH327g4520	1.75	Ornithine_carbamoyltransferase-like_protein	C6_03230W_B	1.17
	OphioH327g6717	1.58	Succinyl-3-ketoacid-coenzyme_a_transferase	C2_07240C_B	1.21
	OphioH327g6465	1.61	Fungal_specific_transcription_factor	CR_09210W_A	1.50
	OphioH327g2358	1.595	Oligosaccharyl_transferase_subunit	C2_01670C_B	0.74
	OphioH327g0333	1.3	Crotonase	C1_03320C_B	0.71
	OphioH327g2998	2.545	Aspartic-type_endopeptidase	CR_07800W_B	1.48
	OphioH327g4450	1.425	Mannosyltransferase_pmti	C2_06100W_B	0.98

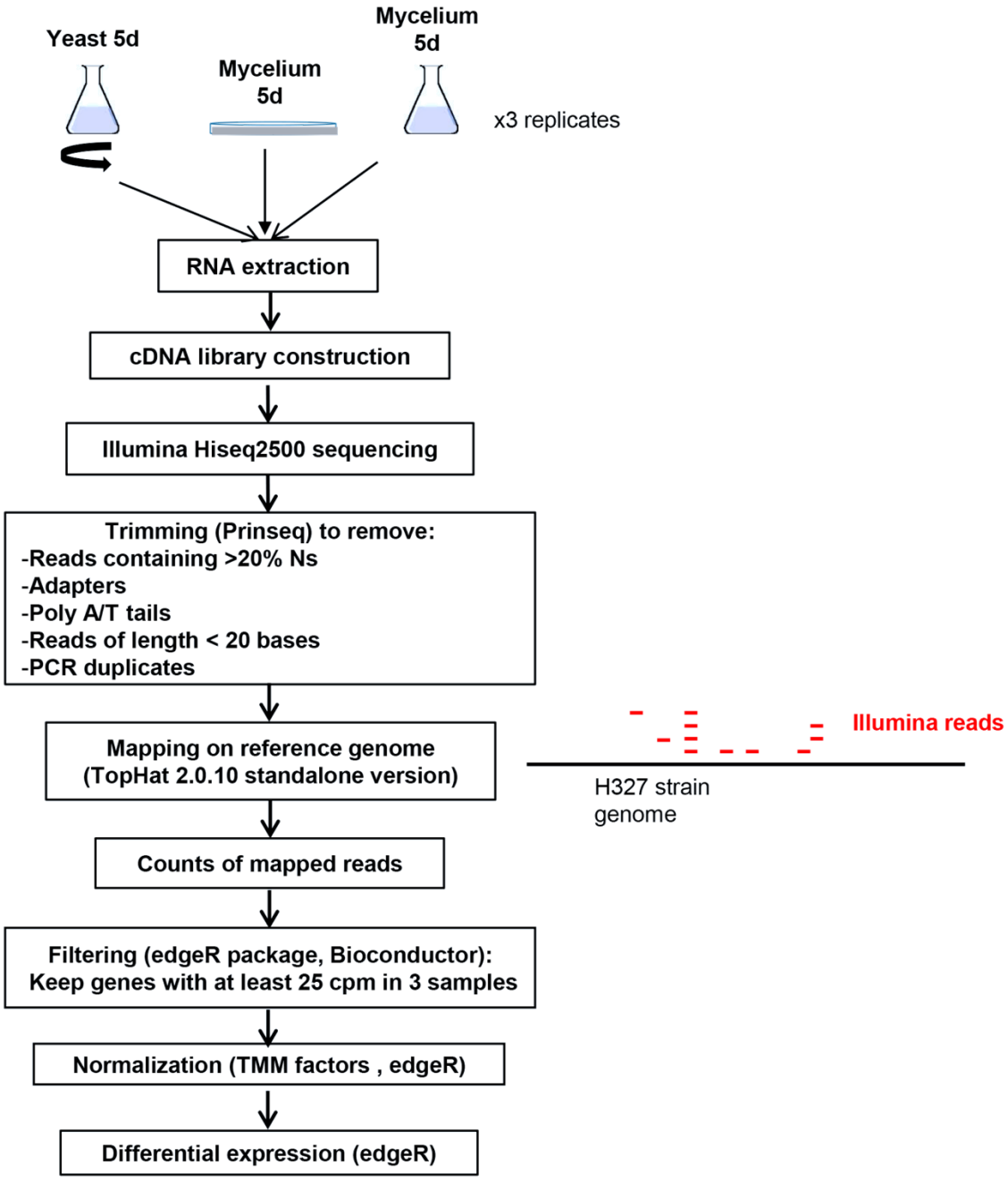

Figure S3.1 Workflow for RNAseq library preparation, cleaning and analysis for the 3 growth conditions (yeasts, mycelium on petri dishes and mycelium in flask, 3 replicates per condition) for *Ophiostoma novo-ulmi*.

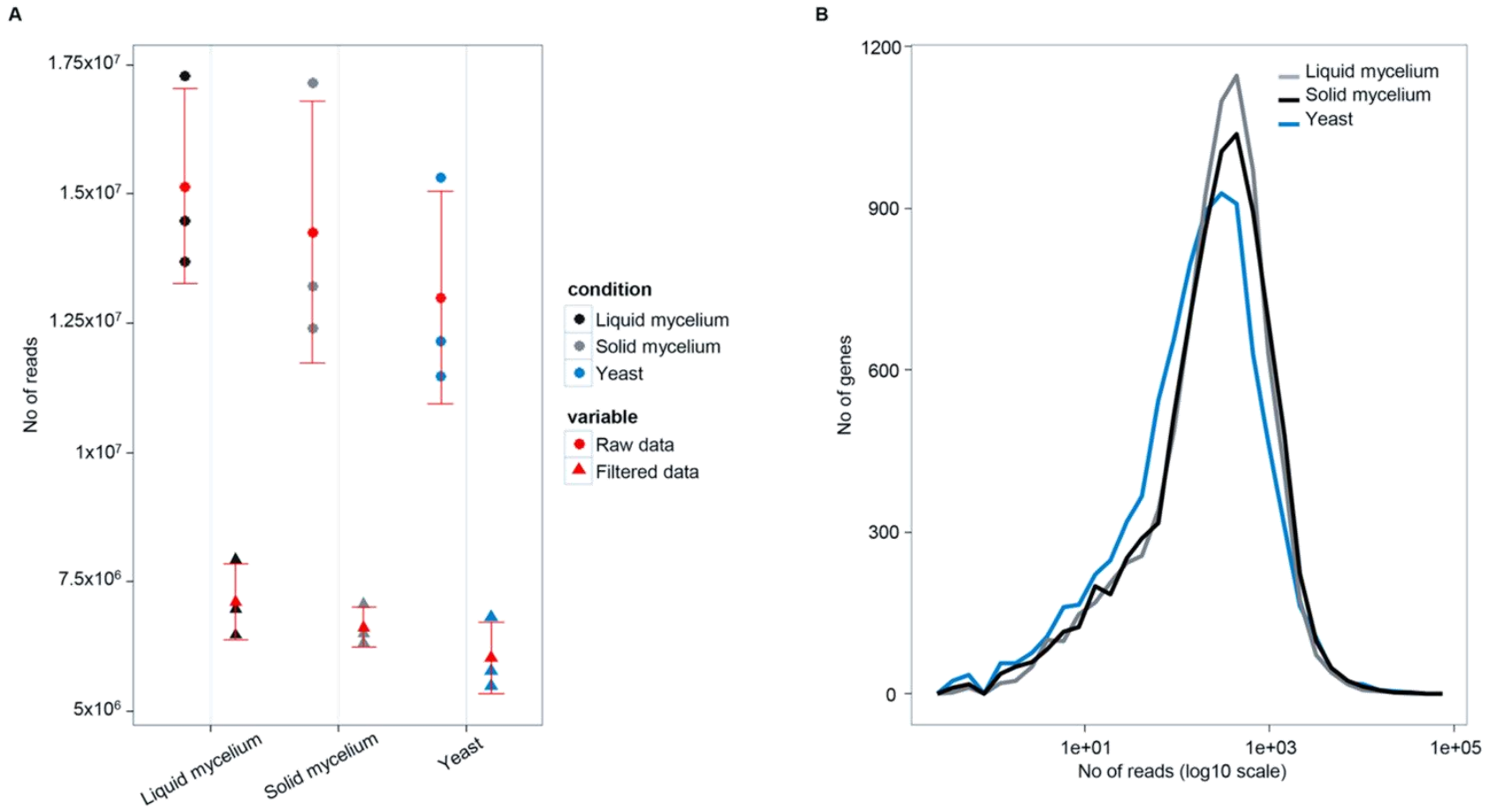

Figure S3.2 Number of *Ophiostoma novo-ulmi* RNAseq reads per sample and per gene: (A) Number of reads before (raw reads, dot) and after filtration/cleaning (filtered reads without duplicates, triangle) process present in each of the 3 conditions. Red dots: means of the 3 repetitions with standard deviation. No significant differences between conditions for each variable (Fisher's exact test). (B) Distribution of the number of reads ($\log_{10}$ scale) per genes, per conditions (mean of 3 replicates).

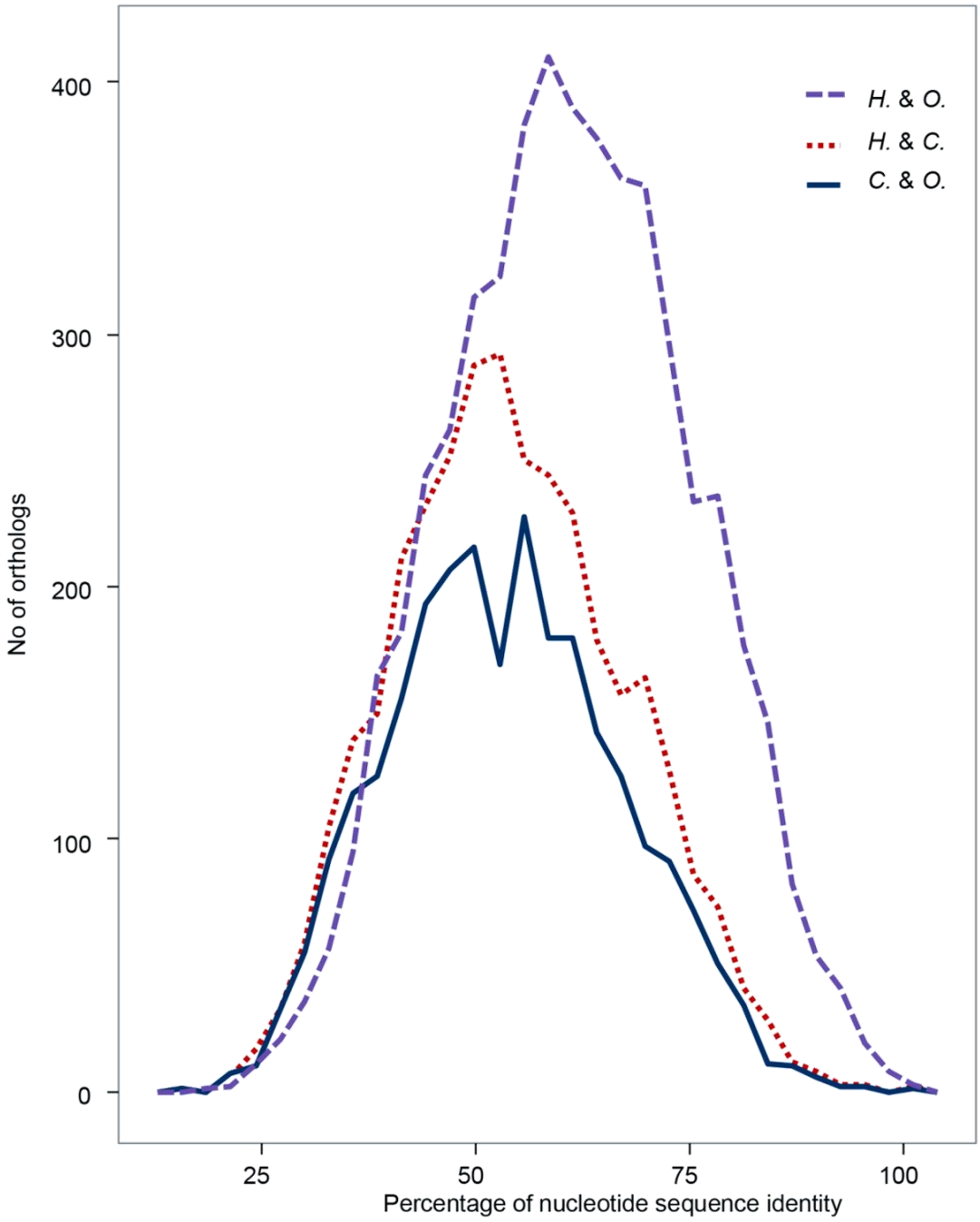

Figure S3.3 Distribution of the number of orthologs between two species per percentage of gene sequence identity. H.: *Histoplasma capsulatum*; C.: *Candida albicans*; O.: *Ophiostoma novo-ulmi*

CHAPITRE 4 From yeast to hypha: defining transcriptomic signatures of the morphological switch in the dimorphic fungal pathogen *Ophiostoma novo-ulmi*

M. Nigg [1,2] and L. Bernier[1,2]

[1] Institut de Biologie Intégrative et des Systèmes (IBIS), Université Laval, Québec, G1V 0A6, Canada

[2] Centre d'Étude de la Forêt (CEF) and Département des sciences du bois et de la forêt, Université Laval, Québec, G1V 0A6, Canada

Ce chapitre a été publié en novembre 2016 dans le volume 17 de *BMC Genomics*,
doi: 10.1186/s12864-016-3251-8

4.1 Résumé

Contexte : La transition levure-hyphe est un changement morphologique majeur chez les champignons. Les régulateurs et les voies moléculaires impliqués dans ce processus ont été largement étudiés chez les espèces modèles telles que *Saccharomyces cerevisiae*. Par exemple, la cascade de phosphorylation via les protéines kinases (Mitogen-Actived Protein Kinase, MAPK), est connue pour être impliquée dans la transition levure-pseudohyphe chez *S. cerevisiae*. Cependant, la conservation des mécanismes régulant les changements morphologiques reste encore peu comprise chez les espèces non modèles. Dans cette étude, nous investiguons le remodelage cellulaire et les modifications transcriptomiques qui ont lieu durant la transition morphologique chez le champignon ascomycète hautement agressif *Ophiostoma novo-ulmi*, l'agent causal de la maladie hollandaise de l'orme.

Résultats : Par le biais de la combinaison d'expériences de microscopie optique, à flux d'électrons ainsi que de cytométrie en flux, nous démontrons que la transition se déroule en moins de 27 h, avec des modifications phénotypiques au niveau des cellules visibles dès 4 h. Grâce au RNAseq, nous avons observé que 22% du génome d'*O. novo-ulmi* est différentiellement exprimé durant la transition. L'analyse de regroupement des données d'expression génique dans une série temporelle nous a permis d'identifier de nombreux groupes de gènes qui sont différentiellement exprimés selon des profils temporels distincts et représentatifs. De plus, nous avons trouvé plusieurs gènes homologues de gènes appartenant à la voie MAPK chez *S. cerevisiae* qui sont régulés durant la transition levure-hyphe chez *O. novo-ulmi*. La plupart sont surexprimés, ce qui suggère une convergence de la régulation de l'expression génique.

Conclusions : Nos résultats constituent le premier rapport d'une expérience en série temporelle suivant la transition morphologique chez une espèce non modèle de Sordariomycète. Ils révèlent de nombreux gènes d'intérêt pour de futures études fonctionnelles du dimorphisme fongique.

4.2 Abstract

Background: Yeast-to-hypha transition is a major morphological change in fungi. Molecular regulators and pathways that are involved in this process have been extensively studied in model species, including *Saccharomyces cerevisiae*. The Mitogen-Actived Protein Kinase (MAPK) cascade, for example, is known to be involved in the yeast-to-pseudohypha switch. Yet the conservation of mechanisms regulating such morphological changes in non-model fungi is still poorly understood. Here, we investigate cell remodeling and transcriptomic modifications that occur during this morphological switch in the highly aggressive ascomycete fungus *Ophiostoma novo-ulmi*, the causal agent of Dutch elm disease.

Results: Using a combination of light microscopy, scanning electron microscopy and flow cytometry, we demonstrate that the morphological switch occurs in less than 27 h, with phenotypic cell modifications being detected within the first 4 h. Using RNAseq, we found that over 22 % of the genome of *O. novo-ulmi* is differentially expressed during the transition. By performing clustering analyses of time series gene expression data, we identified several sets of genes that are differentially expressed according to distinct and representative temporal profiles. Further, we found that several genes that are homologous to *S. cerevisiae* MAPK genes are regulated during the yeast-to-hypha transition in *O. novo-ulmi* and mostly over-expressed, suggesting convergence in gene expression regulation.

Conclusions: Our results are the first report of a time-course experiment monitoring the morphological transition in a non-model Sordariomycota species and reveal many genes of interest for further functional investigations of fungal dimorphism.

4.3 Background

Ophiostoma novo-ulmi (Ascomycota, Sordariomycetes) is the highly aggressive dimorphic pathogen that is responsible for the ongoing pandemic of Dutch elm disease (DED) (Brasier 1991). This fungus is capable of assuming two distinct forms: a unicellular yeast stage and a multicellular hyphal form. In the context of DED, both forms are thought to be involved in pathogenesis. The yeast cells are considered to be responsible for the passive colonization of the xylem vessels as they are carried by the sap flow and found rapidly after invasion both in the shoots and in the roots (Campana 1978). The hyphal form (also known as the invasive phase) is suggested as being responsible for fungal dispersion between adjacent vessels by passing through the vessel pits. This pluricellular form is also very important during the saprophytic stage of *O. novo-ulmi* for the colonization of the principal egg galleries that are dug by female elm bark beetles on dead trees and further into secondary galleries that are excavated by the beetle larvae (Webber and Brasier 1984).

Many species within the genus *Ophiostoma* are known to be dimorphic, including the other two DED fungi, *O. ulmi* and *O. himal-ulmi* as well as the sapwood-staining fungi *O. piceae* (Krokene and Solheim 1998; Dogra and Breuil 2004) and *O. quercus* (Halmschlager *et al.* 1994). Few studies have been devoted to the identification of key factors that regulate the yeast-to-hypha (Y-to-H) transition within this genus. Nutritional factors, such as nitrogen sources (Kulkarni and Nickerson 1981; Naruzawa and Bernier 2014), pyridoxine (Dalpé 1983) or linoleic acid (Naruzawa *et al.* 2016), have been shown to be involved, together with other molecular factors, such as Ca^{2+}-calmodulin interaction (Muthukumar and Nickerson 1984; Muthukumar *et al.* 1985) or cyclic Adenosine MonoPhosphate (cAMP) (Brunton and Gadd 1991). Inoculum size is also implicated in the regulation of the Y-to-H transition in DED fungi and effects have been confirmed for *O. ulmi*, both subspecies of *O. novo-ulmi* (*americana* and *novo-ulmi*), and *O. himal-ulmi* (Kulkarni and Nickerson 1981; Hornby *et al.* 2004; Berrocal *et al.* 2012; Wedge *et al.* 2016). Moreover, quorum sensing has been shown in *O. ulmi, O. piceae and O. floccosum* (Berrocal *et al.* 2012, 2014; de Salas *et al.* 2015). Until now, only two genes have been identified as being involved in the dimorphism in *O. novo-ulmi*, namely *COL1* (Pereira *et al.* 2000) and an as yet uncharacterized gene that also affects asexual sporulation (synnematospores) and pathogenicity (Richards *et al.* 1982;

Richards 1994). The knockout *col1* mutant exhibits reduced mycelial growth, whereas yeast growth is barely affected by the mutation (Pereira *et al.* 2000). However, pathways and genes regulating the Y-to-H transition in *O. novo-ulmi* are still largely unknown.

Dimorphism in fungi is a morphological characteristic that has been studied for many years in model species, such as *Saccharomyces cerevisiae*, the human pathogens *Candida albicans* and *Histoplasma capsulatum*, and the plant pathogen *Ustilago maydis*. The hyphal state is very variable among species, and is represented by pseudo-hyphae in *S. cerevisiae* (not common in nature) or by true septate hyphae in filamentous fungi. In all of these species, several conserved pathways have been reported to be linked to the Y-to-H switch, including the Mitogen-Activated Protein Kinase (MAPK) cascade (Gancedo 2001; Sánchez-Martínez and Pérez-Martín 2001; Nadal *et al.* 2008), the Protein Kinase A (PKA) pathway (Sonneborn *et al.* 2000; Martínez-Espinoza *et al.* 2004; Agarwal *et al.* 2013), and the pH-dependent RIM pathway (Peñalva *et al.* 2008; Selvig and Alspaugh 2011).

In *S. cerevisiae*, the MAPK cascade that is involved in morphological changes is well described (for a simplified schematic, see Figure 4.1). The initial signal is perceived by the osmoreceptors Sho1 and Msb2, which are located on the plasma membrane. The signal is then transduced to a first kinase Ste20, and a cascade of phosphorylations is activated through Ste11 (MAPKKK), Ste7 (MAPKK), and Kss1 (MAPK). The unphosphorylated Kss1 acts as a repressor of the morphological switch since it sequestrates the transcription factors Tec1 and Ste12 in the nucleus. The phosphorylation of Kss1 by Ste7 induces the release of Tec1 and Ste12 (Madhani and Fink 1998; Sánchez-Martínez and Pérez-Martín 2001; Hamel *et al.* 2012). An alternative pathway involves the activation by Ste11 of another MAPKK, Pbs2, and then by Hog1, a MAPK that responds to hyperosmolar conditions (Ferrigno *et al.* 1998; Shively *et al.* 2013). Hog1 activates Msn4, which is a stress-response transcriptional factor that is linked to Ste12 (Shively *et al.* 2013). In *C. albicans*, both cascades (via Ste7 or Hog1) are conserved and involved in the control of morphogenesis (Alonso-Monge *et al.* 1999; Lengeler *et al.* 2000).

The PKA protein of *S. cerevisiae* is a tetramer composed of a homodimer of regulator sub-units (Bcy1) and a homo- or heterodimer of catalytic sub-units (two of the three possible Tpk1, Tpk2 or Tpk3 sub-units). The activation of the PKA pathway depends upon the presence of cAMP (Pan and Heitman 1999) (for a simplified schematic, see Figure 4.1). Of the three Tpk proteins, only Tpk2 exerts a positive effect on pseudohyphal growth in *S. cerevisiae*, since deletion of *Tpk2* represses filamentous growth. In contrast, *Tpk1* deletion has no effect, while knockout mutants of *Tpk3* exhibit hyperfilamentous growth (Robertson and Fink 1998; Pan and Heitman 1999). Both Tpk1 and Tpk2 regulate genes that are involved in the formation of pseudohyphae. Tpk1 regulates the activity of the dual-specificity tyrosine-regulated kinase Yak1, which controls the expression of *Flo11*. *Flo11* is a gene encoding a cell surface flocculin through the transcription factors Sok1 and Phd1 (Malcher *et al.* 2011). Through phosphorylation, Tpk2 activates the transcriptional factor Flo8 which, in turn, activates the expression of filamentation target genes, such as *Flo11* (Pan and Heitman 1999). Also through Tpk2, the PKA pathway induces the activation of the transcriptional factor Phd1. PKA is highly conserved in *C. albicans* and the Phd1 *S. cerevisiae* homolog, Efg1, is also activated through Tpk2 (Sonneborn *et al.* 2000). Both Phd1 and Efg1 are important regulators of dimorphism (Lo *et al.* 1997; Gancedo 2001).

Finally, the RIM pathway, which is also called the PAL cascade in filamentous fungi, is dependent on variation in pH within the environment. In *C. albicans* and *S. cerevisiae*, a change from acidic to neutral pH induces the Y-to-H switch (Y-to-pseudohyphae in *S. cerevisiae*) (Penãlva and Arst 2002; Davis 2003), whereas hyphal form in *U. maydis* is favoured by acidic pH. The PAL/RIM pathway involves at least six proteins which regulate the activation of a zinc-finger-like transcriptional factor called PacC or RIM101 (Selvig and Alspaugh 2011). RIM101 regulates, in turn, the expression of downstream genes, such as *PHR1* and *PHR2* in *C. albicans* (*GAS1* in *S. cerevisiae*) (Penãlva and Arst 2002).

A few large-scale transcriptomic analyses have been conducted to determine the molecular regulation of the Y-to-H transition in model species. RNAseq was recently used in *Penicillium marneffei* where 2718 genes (28% of the gene content) were differentially expressed during the morphological change (Yang *et al.* 2014). DNA microarrays in *Candida*

albicans were used under different conditions to identify sets of genes that are regulated during the transition (Nantel *et al.* 2002; Kadosh and Johnson 2005; Carlisle and Kadosh 2012). Yet genome-wide analyses of this major morphological change, which would describe the global cell response to Y-to-H transition-promoting stimuli, are still lacking. Indeed, most of the studies focus on a particular protein or pathway.

The *O. novo-ulmi* genome was recently sequenced (Forgetta *et al.* 2013) and almost 75 % of the 8640 predicted genes have since been annotated (Comeau *et al.* 2015), thereby facilitating further genomic studies. Comparative analyses of the transcriptomes of yeast and mycelial forms of *O. novo-ulmi* strain H327 (Nigg *et al.* 2015) show a clear difference in gene expression profiles between the two life stages and reveal processes that are specific to each form. Based on this study, we investigate the regulation of gene expression during the Y-to-H transition using a time-series approach, which allows the description of dynamic biological processes. We used RNAseq technology to characterize major molecular changes that are associated with the morphological switch. We also focused attention on the regulation of gene expression in *O. novo-ulmi* MAPK, PKA and RIM pathway homologs.

4.4 Results

4.4.1 Microscopy and flow cytometry

We first defined the Y-to-H transition in *O. novo-ulmi* by recording the modifications that were observed at the population and cell levels using light microscopy. During the Y-to-H transition that was induced by incubation in still-liquid culture in OCM (complemented with proline), the percentage of yeast cells decreases within the first 10 hours following transfer to the induction medium, while the percentage of mycelium increases (Figure 4.2A). Further, cell size increases with time (Figure 4.2B).

The Y-to-H transition was then followed using flow cytometry. We compared conditions that do not favor transition (shake-liquid OMM complemented with proline (Kulkarni and Nickerson 1981; Naruzawa and Bernier 2014), Figure 4.2C) with the condition that was selected in this study (Figure 4.2C). We observe that both cell size (FSC) and cell internal granularity (SSC) vary through time under conditions that induce the Y-to-H transition.

Within the first 10 hours, peaks of density shift towards higher FSC and SSC. Finally, scanning electron micrographs (SEM) that were taken at each time point confirm the Y-to-H transition and highlight cell shape modification within the first four hours, as cells may switch from an ovoid (OY, Figure 4.2D) to a spherical shape (SY)

4.4.2 Global view of transcriptomes of yeast-to-hypha transition

For each of the six time points that were previously defined by microscopy and flow cytometry (*i.e.*, 0, 2, 4, 6, 10 and 27 hours after transfer to the induction medium), samples were collected and total RNA was extracted to sequence the whole transcriptome. After filtering and trimming, RNAseq samples contained between 7 and 12 million reads (Table 4.1). By alignment on the complete set of exons of the *O. novo-ulmi* genome, we are able to achieve from 25.4 up to 63.6 X exon coverage depth.

We retained a total of 7605 genes expressed under our experimental conditions out of the 8640 genes that are predicted in *O. novo-ulmi* for downstream analyses. Each sample contains at least 7256 genes that are represented by more than one read (Table 4.1, Table S4.3). Multidimensional scaling (MDS) analysis shows that the samples cluster according to the time after transfer to OCM and, within-time points, the three biological replicates cluster together (Figure 4.3). The length of incubation of cells in non-agitated OCM (0-27 h) explains most of the variability in the data (first axis). Molecular variability is small between 10 h and 27 h. In the second dimension, there is a large difference between samples that were collected at the beginning of the experiment and those that were collected as early as two hours after transfer to non-agitated OCM.

4.4.3 Identification and analysis of differentially Expressed Genes (DEGs)

The *Next-maSigPro* package in R (v3.0.1) applies generalized linear models (GLM) to regression models in order to determine differentially expressed genes (DEGs) in RNAseq time-course analyses (Conesa *et al.* 2006; Nueda *et al.* 2014). Here, when the package was used on normalized read counts, a total of 1897 genes out of the 7605 expressed genes were identified as DEGs during the Y-to-H transition (0-27h), when a false rate discovery (FDR) threshold (Robinson *et al.* 2009) of 0.05 was employed. (Table S4.3). This set of DEGs was

then analyzed by clustering methods with STEM software (Ernst *et al.* 2005; Ernst and Bar-Joseph 2006). Here, we present results for the assignment of DEGs to 50 predefined gene expression model profiles (0-49) (Figure 4.4). A total of five profiles are identified as containing more genes than expected by chance (significant *P*-values that were corrected for FDR, ranging from 72 to 815 genes, colored profiles). Some genes are present in more than one profile (Table S4.4). The five profiles were then consolidated into four clusters that gather together similar model profiles, which were represented by different colors, with one cluster including two profiles (red, Figure 4.4). We performed a more in depth investigation of profiles 39 (815 genes, 9.4 % of the total gene content) and 8 (256 genes, 3 % of the total gene content), since they are the most significant (*P*-values of 0 and $1e^{-144}$, respectively) and exact opposites in terms of gene expression regulation (Figures 4.4, 4.5A and 4.5B).

4.4.3.1 Genes with increasing expression during Y-to-H transition (profile 39)

Profile 39 comprises genes that are increasingly expressed during the Y-to-H transition. The most notable gene in this profile is Onu3773, which is annotated as coding for an extracellular serine-threonine-rich protein, and also related to the Adhesin protein Mad1 (Table S4.4). This gene is over-expressed by 7819 times at 27 h compared to 0 h. Another notable gene is Onu6790.1, which is annotated as coding for the Woronin body major protein, and is homologous to Hex1 in *O. floccosum*. In *O. novo-ulmi*, this gene is barely expressed at the beginning of the switch, but its expression increases rapidly within the 27 first hours (959 times more strongly expressed at 27 h than at 0 h; Table S4.4). Genes coding for actin, tubulin and septin are also present in profile 39. Of the 67 genes encoding carbohydrate-active enzymes (CAZymes) that were found within the total set of DEGs, 31 genes are grouped in this profile. This set includes glycosyltransferases (GT, $n = 21$), glycoside hydroxylases (GH, $n = 8$) and carbohydrate binding modules (CBM, $n = 2$) (Table S4.4). Finally, 90 genes found in profile 39 have been already described as being over-expressed in the mycelium growth phase of *O. novo-ulmi* (Nigg *et al.* 2015) (Table S4.3). By gene ontology (GO) term-enrichment analysis, we determined that 112 biological processes (BPs) containing more than four genes are significantly enriched (*P*-value ≤ 0.01) in profile 39 (Table S4.5). After using REVIGO software (Supek *et al.* 2011) to reduce redundancy, 28 terms were retained (Figure S4.3). Among the enriched BPs, many are related to cellular organization, including

localization (GO:0051179, 127 genes), cellular component organization (GO:0016043, 67 genes) and microtubule-based movement (GO:0007018, 10 genes) (Table S4.5). Cell division, vesicle transport and protein modifications are also dominant processes.

4.4.3.2 Genes with decreasing expression during Y-to-H transition (profile 8)

Profile 8 comprises genes for which expression decreases during the Y-to-H transition (Table S4.6). Only four genes encoding CAZymes (three GHs and one GT) are found. Gene Onu5171 is one of the top genes in the profile (40 times more repressed at 27 h compared to 0 h), and encoding a siderophore iron transporter 1 (Ferrioxamine B permease). A total of 15 genes that were associated with yeast growth conditions by Nigg *et al.* (Nigg *et al.* 2015) are down-regulated during the Y-to-H transition and are present in profile 8 (Table S4.3). In this profile, we further found gene Onu8210, which was annotated as encoding a DNA-binding protein. This protein has a zinc-finger DNA binding domain, which is homologous to the domain of *S. cerevisiae* Mig1, Nrg1 and Msn4 proteins (data not shown). Gene Onu8210 is down-regulated during the Y-to-H transition (5.75 times less expressed at 27 h after transfer to OCM).

Finally, GO term enrichment analysis that was followed by the application of REVIGO highlighted 22 BPs and revealed over-representation of terms that were associated with non-coding RNA (ncRNA) metabolism and ribosome biogenesis (Figure S4.4, Table S4.7).

4.4.3.3 Other genes of interest

Gene Onu6217-*CAT1* homolog, which has already been described as being over-expressed in the yeast form compared to the mycelium phase (Nigg *et al.* 2015), is highly down-regulated along the Y-to-H transition (profile 0, 192 times less expressed after 2 h) (Table S4.3). Another gene, Onu7070, which codes for a type 1 endochitinase, was previously reported as being over-expressed in the mycelium phase (Nigg *et al.* 2015). This gene is also regulated during the Y-to-H switch and ends up being 14 times more strongly expressed at 27 h compared to 0 h (profile 27) (Table S4.3). Gene Onu4296 codes for Cerato-ulmin (CU), a hydrophobin that has been well studied in the context of DED. This gene is down-regulated through time and belongs to profiles 0 and 1 (Table S4.3).

4.4.4 Identification and expression analysis of *S. cerevisiae* MAPK, PKA, and RIM pathway homologs

4.4.4.1 *S. cerevisiae* MAPK protein homologs

We identified genes coding for potential proteins that were homologous to *S. cerevisiae* MAPK proteins. Of the 11 *S. cerevisiae* proteins with homologs in *O. novo-ulmi*, four have more than one potential homolog (Ste20, Kss1, Sho1 and Msn4; Table S4.2). Eight genes encoding these homologous proteins are actually orthologs: Onu0581-*Ste20*, Onu2999-*Ste11*, Onu4018-*Pbs2*, Onu1002-*Hog1*, Onu2279-*Cdc42*, Onu7491-*Ste12*, Onu1392-*Ste7*, and Onu5199-*Tec1* (Table S4.2). We found the following eight genes to be differentially expressed during the Y-to-H transition: Onu1002-*Hog1*, Onu2992-*Ste20*, Onu1392-*Ste7*, Onu7491-*Ste12*, Onu0070-*Msn4*, Onu8210-*Msn4*, Onu1780-*Kss1* and Onu8395-*Kss1* (Figure 4.6B). *Hog1*, *Ste20*, *Ste7*, *Kss1* and *Ste12* homologs are all over-expressed during the Y-to-H transition and are present in STEM profile 39 (Figure 4.6B).

4.4.4.2 *S. cerevisiae* cAMP-PKA protein homologs

We found homologous genes for the most important genes that were involved in the cAMP-PKA pathway of *S. cerevisiae* (*Bcy1*, *Tk1-3*, *Yak1*, *Phd1*, *Sok2*, *Flo8* or *Pde2*; Table S4.2). Only Onu6515-*Bcy1* and Onu7499-*Pde2* are orthologous genes. Phd1 and Sok2 are putative homologs of the same protein in *O. novo-ulmi*, Onu0977. Surprisingly, we did not find a homologous protein for Flo11. The gene encoding the best homologous match for *Yak1*, *i.e.*, Onu0836, is the only one that is differentially expressed under our set of experimental conditions. This gene is part of profile 39 and is already over-expressed almost 4-fold at 4 h following induction of the transition. For genes Onu0977-*Phd1/Sok2* and Onu7708-*Tpk*, large differences among biological replicates might explain why these genes do not pass the threshold set for DEG identification.

4.4.4.3 *S. cerevisiae* RIM protein homologs

All six well-described proteins that are involved in the RIM pathway have a homolog in *O. novo-ulmi* (Table S4.2) and five of them are actually encoded by orthologous genes. However, Onu0751-*RIM101* is the only gene that is differentially expressed during the Y-to-

H transition. Here, this gene is down-regulated (12-fold lower at 27 h compared to 0 h) and is present in profile 0 (Table S4.3).

4.4.5 Quantitative Reverse Transcription-PCR (qRT-PCR) analysis of selected genes

In order to confirm RNAseq data, we chose genes that were detected as being DE and tested their expression using qRT-PCR. We selected genes from the MAPK pathway (Onu1392-*Ste7*, Onu7491-*Ste12*, Onu8395-*Kss1*, Onu1002-*Hog1* and Onu8210-*Msn4*) and genes with contrasting expression profiles: over-expressed genes (Onu0980 and Onu6970.1-*Hex1*) and down-regulated genes (Onu0303 and Onu5171). For all nine genes, we confirmed a differential expression tendency seen in RNAseq by using qRT-PCR with three biological replicates (Figure S4.5 A-D). Indeed, all genes that were shown to be down-regulated in RNAseq are also found to be down-regulated in qRT-PCR (around a 2-fold decrease at 10 h compared to 0 h). In contrast, all genes that were shown to be upregulated in RNAseq have their expression increased through time in qRT-PCR with comparable fold changes between the two methods.

4.5 Discussion

Large-scale gene expression regulation during yeast-to-hypha (Y-to-H) transition in dimorphic fungi has been studied in model fungal species, such as *Saccharomyces cerevisiae* and *Candida albicans*, using RNAseq, DNA microarrays or phenotypic screening of mutants (Jin *et al.* 2008; Carlisle and Kadosh 2012; Shively *et al.* 2013; Desai *et al.* 2015). It also has been recently investigated in *Penicillium marneffei* (Yang *et al.* 2014). In *Ophiostoma novo-ulmi*, large-scale transcriptomic analyses have been performed to characterize molecular signatures of yeast and mycelial forms via Expressed Sequence Tags analyses (Hintz *et al.* 2011) or, more recently, by RNAseq (Nigg *et al.* 2015). Here, we present the first whole-transcriptome study of a time-course experiment in which we monitored the Y-to-H transition in *O. novo-ulmi* using Ion Torrent RNAseq technology.

4.5.1 Microscopy and flow cytometry

We first characterized the morphological switch process using various quantitative and qualitative techniques (light microscopy, scanning-electron microscopy, and flow cytometry) to assess the relevance of growth conditions that had been selected for the time-course experiment. Results show a greater degree of evidence for Y-to-H transition under the conditions that we have tested. We confirm the emergence of hyphae in culture by showing increasing cell size and the modification of single cell shapes in accordance with previous reports (Dalpé 1983). These changes are seen already within the first 4 hours after transfer in a medium that induces Y-to-H. These results could be explained by the phenomenon of cell swelling at 2 h after transfer to static liquid OCM, prior to germination, which has been described earlier (Dalpé 1983).

4.5.2 Global view of transcriptomes of yeast-to-hypha transition

Second, in order to characterize transcriptome modifications during this major morphological change, we used mRNA sequencing. Interestingly, we observed large changes in gene expression among samples that were taken at different times during the Y-to-H transition, with almost 22 % of *O. novo-ulmi* total gene content being differentially expressed. In particular, we found large transcriptomic variation between samples that were collected at the beginning of the experiment and those that were collected two hours after transfer to static liquid OCM. While this difference agrees with the cell swelling and reshaping observed through microscopy and flow cytometry, it may also be related to the perception of the signal triggering the Y-to-H switch and the regulation of many processes that are required to achieve the transition. In contrast, between 10 h and 27 h after transfer to static liquid OCM, molecular variability is relatively small, which could be explained by the fact that the percentage of hyphae that are produced is not increasing. Only the hyphae that were already present in the medium are growing between 10 and 27 hours.

By analyzing processes that were enriched in the set of up-regulated genes during the morphological switch, we highlight biological processes that were related to major cell modification and remodeling. For instance, the activation of the cell cycle has already been shown in *S. cerevisiae* and *C. albicans* as being critical during morphological changes (Lew

and Reed 1993; Moseley and Nurse 2009; Wang 2009). Furthermore, CAZyme genes are more likely to be actively transcribed than repressed, suggesting an active process of modifications in carbohydrate compounds, which is consistent with cell wall remodeling. By more in depth exploration of genes that are over-expressed during the morphological switch, we found genes that were related to specific hyphal structures, supporting the formation of hyphae. One of them is a gene that is predicted to encode a major protein (Hex1) that is associated with the formation of Woronin bodies. These organelles are associated with septal pores that are present in filamentous fungi (Woronin 1964; Reichle and Alexander 1965). The *Hex1* gene appears to be conserved across species and has been shown to be over-expressed in hyphae of *Coccidioides* spp. (Whiston *et al.* 2012). In *Neurospora crassa*, Woronin bodies have been reported as being responsible for protecting hyphae against cellular damage (Jedd and Chua 2000; Tenney *et al.* 2000). Even though their role has been clearly associated with stress response, Woronin bodies are found associated with septal pores but also in the cytoplasm of non-damaged hyphae in *A. fumigatus* (Beck and Ebel 2013). Finally, in *Magnaporthe grisea*, the Hex1 protein is apparently required for efficient pathogenesis and in responses to nitrogen starvation, since partial deletion induced a reduction of the virulence and made the fungus unable to survive nitrogen starvation (Soundararajan *et al.* 2004). The *Hex1* gene is included in the Pathogen-Host interaction database (PHI-Base, www.phi-base.org) (Winnenburg *et al.* 2008). The high expression of *Hex1* in *O. novo-ulmi* at 27 h after induction of the transition suggests that the expression of this gene is correlated with hyphal formation. Putative actin-, tubulin- and septin-coding genes are also over-expressed through time, consistent with major cellular reorganization due to the formation of pluricellular structures and septa. Septins, in particular, have been reported to play an important role in the filamentous growth of other dimorphic fungi such as *Aspergillus nidulans*, *C. albicans* and *U. maydis* (Warenda and Konopka 2003; Boyce *et al.* 2005; Gladfelter 2006; Lindsey *et al.* 2010).

Interestingly, the most highly over-expressed gene, Onu3773, is related to the gene coding for the adhesin protein Mad1. In *Metarhizium robertsii* (previously *M. anisopliae* (Bischoff *et al.* 2009)), which is a well-known insect pathogen that can also colonize plant roots, Mad1 is involved in the adhesion of blastospores to the insect cuticle (Wang and St. Leger 2007).

Also, the *Mad1* gene is highly expressed in the insect hemolymph (Wang *et al.* 2005). It is also responsible for cytoskeleton organization, cell division and actin polymerization. All of these processes are over-represented in putative functions of genes that are over-expressed during the Y-to-H transition in *O. novo-ulmi*. Deletion of *Mad1* (Δ*Mad1*) in *M. robertsii* induces a delay in conidial germination, a reduction in blastospore formation, and the production of large multicellular hyphal bodies. Moreover, whereas *Mad1* is not expressed in freshly collected conidia, its expression increases as soon as conidia start swelling prior to germination (Wang and St. Leger 2007). Accordingly, in *O. novo-ulmi*, Onu3773 is not expressed two hours after incubation under conditions promoting Y-to-H transition. However, after four hours of incubation in static OCM, its expression level increases rapidly. This response could be connected with the cell swelling that was observed earlier in this study. Finally, *M. robertsii* Δ*Mad1* mutants are less virulent towards insects than the wild-type strain (Wang and St. Leger 2007). If the functions of the *Mad1* homolog in *O. novo-ulmi* are conserved, this gene could be a candidate for the link between morphology and virulence, although *O. novo-ulmi* itself is not entomopathogenic.

In contrast, gene Onu4296, which encodes Cerato-ulmin (CU), is down-regulated under our experimental conditions. Cerato-ulmin is a hydrophobin (Stringer and Timberlake 1993) that has been studied extensively in the context of DED (Takai *et al.* 1983; Bowden *et al.* 1994; Temple *et al.* 1997; Sherif *et al.* 2014). Its role as a pathogenicity factor remains controversial, but it has been suggested that like Mad1 in *M. robertsii*, CU promotes the adherence of infectious spores to the cuticle of elm bark beetles (Temple *et al.* 1997). The *CU* expression level was previously reported to be 20-60 % higher in mycelium than in yeast cells that were grown *in vitro* (Tadesse *et al.* 2003). Yet the CU gene was equally expressed in RNAseq data of yeast and mycelial forms (Nigg *et al.* 2015). Taken together, these contrasting results may reflect medium-dependent regulation and show the lack of conservation of expression for the *CU* gene among different studies, which in turn explains the controversy regarding the specific role of CU in pathogenicity.

Even though growth conditions and sequencing technologies differ from those that we used to compare yeast and mycelium growth phases (Nigg *et al.* 2015), we found convincing

overlaps between the two studies. For instance, genes such as Onu4877, Onu5171, Onu6217 and Onu7070, which are already described as being over-expressed in yeast or mycelium growth phases, show the same expression pattern and are over- or down-regulated during the Y-to-H transition. In total, we found 105 genes for which the regulation of gene expression appears to be conserved under variable growth conditions.

4.5.3 Identification and expression analysis of *S. cerevisiae* MAPK, PKA, and RIM pathway homologs

We had previously shown that transcriptomes of yeast and mycelium phases of *O. novo-ulmi* are distinct from those of *H. capsulatum* and *C. albicans* (Nigg *et al.* 2015). However, we also found *O. novo-ulmi* homologs of genes encoding proteins involved in MAPK, PKA and RIM pathways. The role of the MAPK cascade in the Y-to-H transition has been studied extensively in model dimorphic fungal species such as *S. cerevisiae* (Cook *et al.* 1997; Madhani and Fink 1998) (Figure 4.1). We show that 11 key proteins have at least one homolog in *O. novo-ulmi,* of which four have two putative homologs (Ste20, Kss1, Sho1 and Msn4). More interestingly, the expression of eight genes encoding these proteins is differentially regulated during the Y-to-H transition in *O. novo-ulmi.* Homologs of *Ste12*, *Kss1*, *Ste7* and *Ste20* are all over-expressed through time, consistent with data that were collected for *S. cerevisiae* (Gancedo 2001). Ste12 is a transcriptional factor that regulates the expression of multiple genes that are related to the formation of pseudohyphae in *S. cerevisiae* (Liu *et al.* 1993). The *Ste12* homolog in *Candida albicans* is also involved in hyphal formation and its knockout mutation suppresses filamentation and virulence (Liu *et al.* 1994; Lo *et al.* 1997). During activation of pseudohyphal formation in *S. cerevisiae,* Ste12 acts as a heterodimer when combined together with Tec1 protein (Madhani and Fink 1997). Here, the *Tec1* homologous gene (Onu5199) is not differentially expressed during the Y-to-H transition. This result might suggest that Tec1 is not required in the filamentation process in *O. novo-ulmi*. In contrast, upregulation of the *Ste12* homolog in *O. novo-ulmi* is consistent with a conserved role in the activation of hypha formation.

Moreover, the *Hog1* homolog is also over-expressed during Y-to-H transition in *O. novo-ulmi*. The MAPK encoded by this gene is described as a key regulator of hyper-osmolarity

stress perception and is also related to morphological changes and virulence in *C. albicans* (Alonso-Monge *et al.* 1999). In *S. cerevisiae*, the Hog1 protein regulates invasive growth and contributes to the repression of pseudohyphal growth (O' Rourke and Herskowitz 1998; Shively *et al.* 2013). Protein Msn4 of *S. cerevisiae* is a stress-responsive transcriptional activator activated by Hog1. This protein has two putative homologs in *O. novo-ulmi* (Onu8210 and Onu0070). Interestingly, a paralog of *Msn4*, known as *Msn2*, is found in the genome of *S. cerevisiae* (Estruch and Carlson 1993). These two paralogs are largely functionally redundant and regulate stress response (Martínez-Pastor *et al.* 1996). In *S. cerevisiae*, *Msn4* expression is induced by stress, whereas *Msn2* expression is constitutive (Gasch *et al.* 2000). Under our experimental conditions, the two homologs of *Msn4* have contrasting gene expression regulation. Gene Onu8210 is downregulated, whereas Onu0070 is upregulated. The latter is consistent with the upregulation of *Hog1* and of the entire MAPK cascade.

Gene Onu8210 encodes a putative transcriptional factor containing a zinc-finger DNA binding domain. Interestingly, this domain is not only homologous with the Msn4 domain but also with those from *S. cerevisiae* Mig1 and Nrg1 proteins. Both Mig1 and Nrg1 are negative regulators of genes that are involved in multiple processes, including filamentous growth of *S. cerevisiae* under glucose-limiting conditions (Kuchin *et al.* 2002; Karunanithi and Cullen 2012). The downregulation of Onu8210 is consistent with the repression of a negative regulator of filamentatous growth, suggesting that this gene might encode a protein that acts more like Mig1 or Nig1 than Msn4.

Taken together, these results constitute the first report revealing potential involvement of the MAPK cascade in the process of morphological change in *O. novo-ulmi*. Further, they suggest a conserved mechanism across fungal families. Roles and activities for each of the proteins that are encoded by the identified genes must be further confirmed by functional analyses, such as gene knockout experiments, for which efficient protocols are still lacking in *O. novo-ulmi.*

Under the growth conditions that were selected for Y-to-H induction in *O. novo-ulmi*, gene Onu0836-*Yak1* is the only gene-encoding homolog of proteins involved in the PKA pathway in *S. cerevisiae* which is differentially expressed. Both genes encoding homologs of Phd1/Sok2 (Onu0977) and Tkp1-3 (Onu7708) showed variation in the number of reads between 0 h and 4 h. Phd1 and Sok2 are actually paralogous proteins in *S. cerevisiae*, which explains why the homologous protein in *O. novo-ulmi* is the same for both proteins. The fact that all three putative catalytic sub-units of the PKA (Tpk1-3) have a unique homolog in *O. novo-ulmi* suggests that there is only one catalytic sub-unit in this species. In previous studies (Brunton and Gadd 1991), cAMP was implicated in the dimorphism of *O. ulmi* NRRL6404. Over-expression of the gene encoding the downstream transcription factor of the PKA pathway, *Phd1* (*S. cerevisiae*) or *Efg1* (*C. albicans*), was sufficient to enhance filamentous growth in both species (Gimeno and Fink 1994; Lo *et al.* 1997; Gancedo 2001). The slight modification in the expression of *Phd1* and *Tpk* homologs in *O. novo-ulmi* could reveal either no obvious role for these genes in the Y-to-H transition or that a very small increase in gene expression is sufficient for activation of the positive functions of both genes in the process of Y-to-H transition. In the latter case, the modification of *Tpk* expression might induce *Yak1* expression, which then positively regulates *Phd1* expression. The absence of a *Flo11* homolog in *O. novo-ulmi* suggests that there likely is an as yet unknown gene that is targeted by Phd1. Further studies monitoring cAMP concentrations during the Y-to-H transition would aid in demonstrating whether there truly is a relationship between gene expression and cAMP levels.

Finally, analyses of the six putative candidates for the RIM pathway in *O. novo-ulmi* revealed overexpression of the gene encoding the homolog of RIM101, which is the downstream transcriptional factor regulated by the RIM pathway in *S. cerevisiae* and *C. albicans* (Davis 2003; Selvig and Alspaugh 2011). We did not monitor changes in pH of the growth medium over the entire experiment. However, we noted that the pH of the three-day-old pre-culture of yeast cells in OMM was 3.0, whereas fresh OCM that was used to induce transition to mycelium had a pH of 5.5 (data not shown). Therefore, modification in the expression of Onu0751-*RIM101* could be the result of the change in pH that was induced by the transfer to OCM, even though this modification is not as drastic as a switch from an acidic to a basic

pH. Nevertheless, this also suggests that this gene is involved in the switch and, thus, has a conserved role among dimorphic fungal species.

4.6 Conclusions

Our survey of morphological and transcriptomic changes during the yeast to hypha transition in *Ophiostoma novo-ulmi* highlights modifications in both the structure of cells and the regulation of gene expression within 10 hours after induction of the switch. Analyses of gene expression regulation in a time-course experiment provided the first insights into the processes that were activated and those that were repressed during the Y-to-H transition in *O. novo-ulmi*. These analyses further confirmed the occurrence of major rearrangement of the cell wall and cellular structures. We pointed out both genes and pathways that are either specific to *O. novo-ulmi* or not described in model dimorphic fungi, (*Hex1*, *Mad1* or *CU*), or which converge in gene expression regulation for genes encoding proteins that are homologous to *Saccharomyces cerevisiae* proteins involved in the MAPK cascade related to the yeast to pseudohypha switch. Our experimental conditions also suggest the involvement of PKA and RIM pathways, which should be confirmed in future studies. Taken together, our results indicate many genes of interest for further investigations of the Y-to-H transition in *O. novo-ulmi* and highlight the possible convergence of molecular regulation of dimorphism between very divergent fungal species.

4.7 Materials and methods

4.7.1 Fungal growth conditions and sample collection

4.7.1.1 Preparation of RNAseq samples

Yeast cells (1 x 10^6 spores mL^{-1}) of *Ophiostoma novo-ulmi* ssp. *novo-ulmi* strain H327 (Centre d'Etude de la Forêt, fungal collection, http://www.cef-cfr.ca/index.php?n=CEF.Collections ChampignonsPathogenes) were first grown in liquid minimum medium (OMM) (Bernier and Hubbes 1990) that was supplemented with 1.15 g L^{-1} proline as the sole nitrogen source on an orbital shaker (Infors HT Ecotron) at 150 rpm (22 °C). After three days, cultures were filtered through 16 layers of sterile cheesecloth and diluted to 1 x 10^6 spores mL^{-1} in flasks containing 100 mL of complete medium (OCM) with 1.15 g L^{-1} proline. Flasks were incubated under still conditions in darkness at room

temperature (22 °C). At each point during the time-course experiment (0, 2, 4, 6, 10 and 27 hours after transfer of cells to static liquid OCM), five photographs per flask were taken with a microscope (Olympus BX41, 400 X magnification) to measure the proportion of yeasts and hyphae. Cells were considered hyphal structures when they were at least twice as long as a typical yeast cell. About 60 structures were counted and measured at each time. One hundred mL of culture from each flask were transferred each time into two sterile Falcon 50 mL conical centrifuge tubes and centrifuged for 5 min at 4 °C and 3000 g. Pellets were resuspended in sterile water and transferred to 1.5 mL sterile microtubes. Samples were again centrifuged for 5 min at 4 °C and 3000 g, after which the pellets were flash-frozen in liquid N_2. Samples were stored at -80 °C until RNA extraction. Three time series replicates were collected (18 samples in total).

4.7.1.2 Flow cytometry

Time points for flow cytometry measurements were 0 h, 2 h, 4 h, 6 h and 10 h after transfer of cells to static liquid OCM. Samples that were incubated for 27 h in OCM were not analyzed since cell size and shape were no longer compatible with the flow cytometer. Cells were grown in OCM under the same conditions as for the RNAseq samples. At each time tested, cultures were diluted with sterile water in order to have 50-500 cells per µL in 300 µL of solution that was transferred to 96-well plates for analysis in a Guava® easyCyte HT Sampling flow cytometer (EMD Millipore Corp.). OMM that was supplemented with 1.15 g L^{-1} proline was used as negative control for the transition (Kulkarni and Nickerson 1981; Naruzawa and Bernier 2014).

4.7.1.3 Scanning electron microscopy (SEM)

Cells were grown and collected following the same procedure as for RNA extractions. Pellets of cells were resuspended in fixation buffer (2.5 % glutaraldehyde in 0.1 M sodium cacodylate buffer, pH 7.3). Samples were fixed for 20 min at room temperature and stored at 4 °C for at least 12 hours. Further processing of samples was performed at the Plateforme de Microscopie (IBIS/Université Laval) following the same procedure as described previously (Aoun *et al.* 2009). Samples were examined with a JEOL JSM6360LV microscope (JEOL Inc., Tokyo, Japan).

4.7.2 RNA extraction, cDNA library production and RNA sequencing

Total RNA from each of the 18 samples was extracted using the Ambion® Ribopure™ Yeast kit (Life Technologies). The quality was verified using a spectrophotometer (NanoDrop ND-1000, Thermo Scientific) and a bioanalyser (BioAnalyzer RNA 6000 Nano Kit, Agilent Technologies).

Complementary DNA (cDNA) libraries were constructed at the Plateforme d'Analyses Génomiques (IBIS/Université Laval) using the kapa stranded RNA-seq kit (Kapa Biosystems) with Y-adaptors that were custom made to be compatible with Ion Proton™ (Thermo Fisher Scientific) sequencing. Single-end RNA sequencing was performed following the manufacturer's recommendations.

4.7.3 RNAseq data preprocessing

RNAseq read quality was verified using FastQC software (http://www.bioinformatics.babraham. ac.uk/projects/fastqc/). Given the poor quality of 5' and 3' tails, 15 nt were removed in 5' and sequences were trimmed to a length of 150 nt using Prinseq v0.20.4 (Schmieder and Edwards 2011). Finally, sequences shorter than 25 nt were removed.

4.7.4 RNAseq data analysis

Filtered reads were mapped onto the exon sequences of the *O. novo-ulmi* H327 genome (Forgetta *et al.* 2013) with TopHat2 (v.2.0.10) using default parameters (Kim *et al.* 2013). For greater readability in the manuscript, genes of *O. novo-ulmi* are named "Onu" followed with the number of the gene. All further analyses were performed in the R statistical environment (v3.0.1; (R Development Core Team 2011)). Raw data were filtered and transformed with the *Bioconductor* package *EdgeR* (correction by the library size and filtering of genes for which the row sum was less than 3 counts per million [CPM]) (Robinson *et al.* 2009). A multidimensional scaling (MDS) plot was used for the visualization of the variability among samples (function implemented in *EdgeR*), following the procedure described previously (Nigg *et al.* 2015). The MDS plot was produced using the R package *ggplot2* (Wickham 2009). The updated version of *maSigPro* R package (Conesa *et al.* 2006),

Next-maSigPro (Nueda *et al.* 2014), was used for the detection of differentially expressed genes (DEGs) in R. *P*-values were corrected using the False Discovery Rate (FDR) (Benjamini and Hochberg 1995) with a threshold of 0.05.

Clustering analysis was performed using Short Time-series Expression Miner (STEM) software (Ernst and Bar-Joseph 2006) on the set of DEGs with our own annotation file. The software assigns genes to a set of model profiles predefined in order to capture all the potential distinct patterns that can be expected from the experiment (Ernst *et al.* 2005). We chose a maximum number of 50 for model profiles with a significance threshold of 0.01 and False Rate Discovery (FDR) correction. Determination of differentially expressed genes was based on 'Maximum−Minimum' that is the largest difference in the gene's value between any two time points, which are not necessarily consecutive (Ernst and Bar-Joseph 2006). A minimum fold change of 2 was required over time between normalized count values for a gene to be retained. Differential expression for each gene was calculated on the normalized count values, as:

Differential expression $=v(i)/v(0)$

where v(i) is the average number of normalized counts at a time point of interest, and v(0) is the average number of normalized counts at the beginning of the experiment. Values less than 0 were inverted to ease of interpretation; in this case, the equation was written as:

Differential expression $=-1/(v(i)/v(0))$

Gene ontology (GO) term enrichment analyses were performed as described in Nigg and collaborators (2015) using the *Goseq* package in *Bioconductor 3.0* (Young *et al.* 2010) and GO Trimming (Jantzen *et al.* 2011). REVIGO was used to reduce redundancy and produce treemaps (space-filling visualization of hierarchical structures) using the *treemap* package in R (Supek *et al.* 2011). Default parameters were used and the redundancy threshold (allowed similarity) was set at 0.4 (very small).

4.7.5 Protein homology and gene orthology assessment

Sequences of MAPK, PKA and RIM proteins from *S. cerevisiae* were downloaded from NCBI and the yeast genome database (www.yeastgenome.com). A standalone version of *BLASTp* (Altschul *et al.* 1990) was used (parameters: word-size = 3; e-value = 0.01) to assess homology with *O. novo-ulmi* proteins.

Orthologous genes among the identified homologs were highlighted by reciprocal best blast hits (RBH) using tblastx (Altschul *et al.* 1990). Exon sequences of the two species (*O. novo-ulmi* and *S. cerevisiae*) were compared using local databases and the RBH was conducted using the following parameters: e-value = 0.001 and word size = 5.

4.7.6 Reverse transcription, PCR and quantitative Reverse Transcription-PCR (qRT-PCR)

Samples for qRT-PCR were collected following the procedure that was described above. Total RNA was extracted and samples were conserved at -20 °C for a maximum of one month prior to complementary DNA (cDNA) synthesis.

The cDNAs for qRT-PCR were synthesized by reverse transcription using Superscript II enzyme (Invitrogen) and according to the following protocol: 500 ng of mRNA (final volume of 8 µL, completed with nuclease-free water) were mixed with 1 µL of dNTPs 10 mM and 1 µL of oligo-dT 0.5 µg/µL. The mixture was incubated at 65 °C for 5 min. Samples were then cooled on ice for 1 min and quickly centrifuged. A mixture of 10X Buffer RT (2 µL), MgCl2 (25 mM, 4 µL), DTT (0.1 M, 2 µL), RNase Out (1 µL, Invitrogen) and Superscript II (200 U, 0.25 µL) was added to each sample. Preparations were gently mixed, quickly centrifuged and incubated for 50 min at 42 °C. Reactions were completed by incubating samples for 15 min at 72 °C. Samples were finally cooled down on ice for 5 min and 80 µL of nuclease-free water were added. cDNA samples were stored at -20 °C.

For each gene that was tested in qRT-PCR, primers for fragments that were 120-200 base pairs in length were designed using Primer3plus (http://primer3plus.com/cgi-bin/dev/primer3plus.cgi) and properties were verified with Oligocalc

(http://www.basic.northwestern.edu/biotools/ oligocalc.html) (Table S4.1). Primers were then synthesized at the *Plateforme de séquençage et de génotypage des génomes* (Research Centre, Centre Hospitalier de l'Université Laval, Quebec QC, CA).

Prior to qRT-PCR, primers were tested on cDNA (9 ng μL^{-1}) in PCR. Reaction volume of each sample was 25 µL (12.2 µL Premix Ex Taq TaKaRa, 1.25 µL of each primer, 5 µL of sterile water and 5 µL of cDNA). PCR conditions for amplification were: 10 s at 98 °C followed by 30 cycles of 10 s at 98 °C, annealing for 30 s at Tm (usually 55 °C), amplification for 12 s at 72 °C and a final step of 5 min at 72 °C. PCR products were transferred to 2 % (m/v) agarose gel for electrophoresis (migration at 130 V) followed by staining in ethidium bromide bath for 15 min. DNA fragments were visualized under UV light.

Quantitative RT-PCR (qRT-PCR) reactions were performed with the PerfeCta™ SYBR® Green FastMix™, Low ROX kit (Quanta BioSciences) following the manufacturer's instructions, with 10 µL of PerfeCta™ SYBR® Green FastMix™, Low ROX mix, 2.5 µL of 5' and 3' 1 µM primers for each gene that was tested and 5 µL of 1 ng μL^{-1} cDNA (or water for negative control) for a final volume of 20 µL in MicroAmp® Fast Optical 96-well plates (Applied BiosystemsGene expression was quantified using the 7500 Fast Real-Time PCR system (Applied Biosystemss™). Genes Onu3626 (Ubiquitin conjugating enzyme), Onu1683 (Ubiquitin conjugating enzyme E2 6) and Onu0623 (RING finger ubiquitin ligase) were defined as reference genes using the R script of *NormFinder* software (Andersen *et al.* 2004). For each of the nine genes that were tested (Onu1392, Onu7491, Onu8395, Onu1002, Onu8210, Onu0980, Onu6970.1, Onu0303 and Onu5171), three biological replicates with three technical replicates were used to quantify expression with a comparative method ($2^{-\Delta\Delta Ct}$). The three reference genes were used to calculate the level of transcripts at each time point (2 h, 4 h, 6 h and 10 h) relative to 0 h (beginning of the Y-to-H transition experiment).

4.8 Declarations

Availability of data and material: The data set supporting the results of this article is included within the article and its additional files. The raw data from the 18 RNAseq samples

have been submitted to the National Center for Biotechnology Information (NCBI) in the BioProject PRJNA325932, study accession SRP078831

Acknowledgments: We thank Brian Boyle and staff from the *Plateforme d'Analyses Génomiques* (IBIS, Université Laval, Quebec, QC, CA) for the production of RNAseq samples and Richard Janvier from the *Plateforme de Microscopie* (IBIS, Université Laval, Quebec, QC, CA) for the SEM samples and pictures. We are indebted to Pr. Christian R. Landry and members of his group (IBIS, Université Laval, Quebec, QC, CA) for help with the design of the experiment and technical support during flow cytometry experiments. We also thank Jean-Guy Catford (CEF/IBIS, Université Laval, Quebec, QC, CA) for assistance with RT-qPCR experiments and Isabelle Giguère (CEF/IBIS, Université Laval, Quebec, QC, CA) for technical support in molecular biology. We thank François-Olivier Hébert Gagnon (IBIS, Université Laval, Quebec, QC, CA) and Jean-Baptiste Leducq (Université de Montréal, Montreal, QC, CA) for their useful comments on the manuscript. Finally, we acknowledge Dr. William F. J. Parsons (CEF, Université de Sherbrooke, Sherbrooke, QC, CA) who edited the English.

4.9 Bibliography

Agarwal C, Aulakh KB, Edelen K, Cooper M, Wallen RM, Adams S, Schultz DJ, Perlin MH, 2013. *Ustilago maydis* phosphodiesterases play a role in the dimorphic switch and in pathogenicity. *Microbiology* **159**: 857–68.

Alonso-Monge R, Navarro-García F, Molero G, Diez-Orejas R, Gustin M, Pla J, Sánchez M, Nombela C, 1999. Role of the mitogen-activated protein kinase hog1p in morphogenesis and virulence of *Candida albicans*. *Journal of Bacteriology* **181**: 3058–3068.

Altschul SF, Gish W, Miller W, Myers EW, Lipman DJ, 1990. Basic Local Alignment Search Tool. *Journal of Molecular Biology* **215**: 403–410.

Andersen CL, Jensen JL, Ørntoft TF, 2004. Normalization of real-time quantitative reverse transcription-PCR data: a model-based variance estimation approach to identify genes suited for normalization, applied to bladder and colon cancer data sets. *Cancer research* **64**: 5245–5250.

Aoun M, Rioux D, Simard M, Bernier L, 2009. Fungal colonization and host defense reactions in *Ulmus americana* callus cultures inoculated with *Ophiostoma novo-ulmi*. *Phytopathology* **99**: 642–650.

Beck J, Ebel F, 2013. Characterization of the major Woronin body protein HexA of the human pathogenic mold *Aspergillus fumigatus*. *International Journal of Medical Microbiology* **303**: 90–97.

Benjamini Y, Hochberg Y, 1995. Controlling the False Discovery Rate : a practical and powerful approach to multiple testing. *Journal of the Royal Stastistical Society* **57**: 289–300.

Bernier L, Hubbes M, 1990. Mutations in *Ophiostoma ulmi* induced by N-methyl-N ’-nitro-N-nitrosoguanidine. *Canadian Journal of Botany* **68**: 225–231.

Berrocal A, Navarrete J, Oviedo C, Nickerson KW, 2012. Quorum sensing activity in *Ophiostoma ulmi*: effects of fusel oils and branched chain amino acids on yeast-mycelial dimorphism. *Journal of applied microbiology* **113**: 126–134.

Berrocal A, Oviedo C, Nickerson KW, Navarrete J, 2014. Quorum sensing activity and control of yeast-mycelium dimorphism in *Ophiostoma floccosum*. *Biotechnology Letters* **36**: 1503–1513.

Bischoff JF, Rehner SA, Humber RA, 2009. A multilocus phylogeny of the *Metarhizium anisopliae* lineage. *Mycologia* **101**: 512–530.

Bowden CG, Hintz WE, Jeng R, Hubbes M, Horgen PA, 1994. Isolation and characterization of the cerato-ulmin toxin of the Dutch elm disease pathogen, *Ophiostoma ulmi*. *Current Genetics* **75**: 323–329.

Boyce KJ, Chang H, Souza CAD, Kronstad JW, 2005. An *Ustilago maydis* septin is required for filamentous growth in culture and for full symptom development on maize. *Eukaryotic cell* **4**: 2044–2056.

Brasier CM, 1991. *Ophiostoma novo-ulmi* sp . *nov*., causative agent of current Dutch elm disease pandemics. *Mycopathologia* **115**: 151–161.

Brunton AH, Gadd GM, 1991. Evidence for an inositol lipid signal pathway in the yeast-mycelium transition of *Ophiostoma ulmi*, the Dutch elm disease fungus. *Mycological Research* **95**: 484–491.

Campana RJ, 1978. Inoculation and fungal invasion of the tree. In: Sinclair WA,, Campana RJ, eds. *Dutch elm disease: perspectives after 60 years*. Ithaca, N.Y, pp. 17–20.

Carlisle PL, Kadosh D, 2012. A genome-wide transcriptional analysis of morphology determination in *Candida albicans*. *Molecular biology of the cell* **24**: 246–60. https://doi.org/10.1091/mbc.E12-01-0065

Comeau AM, Dufour J, Bouvet GF, Jacobi V, Nigg M, Henrissat B, Laroche J, Levesque RC, Bernier L, 2015. Functional annotation of the *Ophiostoma novo-ulmi* genome: insights into the phytopathogenicity of the fungal agent of Dutch elm disease. *Genome*

biology and evolution **7**: 410–430.

Conesa A, Nueda MJ, Ferrer A, Talon M, 2006. maSigPro: a method to identify significantly differential expression profiles in time-course microarray experiments. *Bioinformatics* **22**: 1096–1102.

Cook JG, Bardwell L, Thorner J, 1997. Inhibitory and activating functions for MAPK Kss1 in the *S. cerevisiae* filamentous-growth signalling pathway. *Nature* **390**: 85–88.

Dalpé Y, 1983. L'influence de la carence en pyridoxine sur la morphologie et l'ultrastructure cellulaire de *Ceratocystis ulmi*. *Canadian Journal of Botany* **61**: 2079–2084.

Davis D, 2003. Adaptation to environmental pH in *Candida albicans* and its relation to pathogenesis. *Current genetics* **44**: 1–7.

Desai PR, Van Wijlick L, Kurtz D, Juchimiuk M, Ernst JF, 2015. Hypoxia and temperature regulated morphogenesis in *Candida albicans*. *PLOS Genetics* **11**: e1005447.

Dogra N, Breuil C, 2004. Suppressive subtractive hybridization and differential screening identified genes differentially expressed in yeast and mycelial forms of *Ophiostoma piceae*. *FEMS Microbiology Letters* **238**: 175–181.

Ernst J, Bar-Joseph Z, 2006. STEM: a tool for the analysis of short time series gene expression data. *BMC bioinformatics* **7**: 191.

Ernst J, Nau GJ, Bar-Joseph Z, 2005. Clustering short time series gene expression data. *Bioinformatics* **21**: 159–168.

Estruch F, Carlson M, 1993. Two homologous zinc finger genes identified by multicopy suppression in a SNF1 protein kinase mutant of *Saccharomyces cerevisiae*. *Molecular and cellular biology* **13**: 3872–81.

Ferrigno P, Posas F, Koepp D, Saito H, Silver PA, 1998. Regulated nucleo/cytoplasmic exchange of HOG1 MAPK requires the importin beta homologs NMD5 and XPO1. *The EMBO journal* **17**: 5606–14.

Forgetta V, Leveque G, Dias J, Grove D, Lyons R, Genik S, Wright C, Singh S, Peterson N, Zianni M, Kieleczawa J, Steen R, Perera A, Bintzler D, Adams S, Hintz W, Jacobi V, Bernier L, Levesque R, Dewar K, 2013. Sequencing of the Dutch elm disease fungus genome using the Roche/454 GS-FLX Titanium System in a comparison of multiple genomics core facilities. *Journal of biomolecular techniques* **24**: 39–49.

Gancedo JM, 2001. Control of pseudohyphae formation in *Saccharomyces cerevisiae*. *FEMS Microbiology Reviews* **25**: 107–123.

Gasch AP, Spellman PT, Kao CM, Carmel-Harel O, Eisen MB, Storz G, Botstein D, Brown PO, 2000. Genomic expression programs in the response of yeast cells to environmental

changes. *Molecular biology of the cell* **11**: 4241–4257.

Gimeno CJ, Fink GR, 1994. Induction of pseudohyphal growth by overexpression of *PHD1*, a *Saccharomyces cerevisiae* gene related to transcriptional regulators of fungal development. *Molecular and cellular biology* **14**: 2100–2112.

Gladfelter AS, 2006. Control of filamentous fungal cell shape by septins and formins. *Nature reviews. Microbiology* **4**: 223–229.

Halmschlager E, Messner R, Kowalski T, Prillinger H, 1994. Differentiation of *Ophiostoma piceae* and *Ophiostoma quercus* by morphology and RAPD analysis. *Systematic and Applied Microbiology* **17**: 554–562.

Hamel LP, Nicole MC, Duplessis S, Ellis BE, 2012. Mitogen-activated protein kinase signaling in plant-interacting fungi: distinct messages from conserved messengers. *The Plant cell* **24**: 1327–51.

Hintz W, Pinchback M, de la Bastide P, Burgess S, Jacobi V, Hamelin R, Breuil C, Bernier L, 2011. Functional categorization of unique expressed sequence tags obtained from the yeast-like growth phase of the elm pathogen *Ophiostoma novo-ulmi*. *BMC genomics* **12**: 431.

Hornby JM, Jacobitz-Kizzier SM, McNeel DJ, Jensen EC, Treves DS, Nickerson KW, 2004. Inoculum size effect in dimorphic fungi: extracellular control of yeast-mycelium dimorphism in *Ceratocystis ulmi*. *Applied and environmental microbiology* **70**: 1356–9.

Jantzen SG, Sutherland BJ, Minkley DR, Koop BF, 2011. GO Trimming: Systematically reducing redundancy in large Gene Ontology datasets. *BMC research notes* **4**: 267.

Jedd G, Chua NH, 2000. A new self-assembled peroxisomal vesicle required for efficient resealing of the plasma membrane. *Nature cell biology* **2**: 226–231.

Kadosh D, Johnson A, 2005. Induction of the *Candida albicans* filamentous growth program by relief of transcriptional repression: a genome-wide analysis. *Molecular biology of the cell* **16**: 2903–2912.

Karunanithi S, Cullen PJ, 2012. The filamentous growth MAPK pathway responds to glucose starvation through the Mig1/2 transcriptional repressors in *Saccharomyces cerevisiae*. *Genetics* **192**: 869–887.

Kim D, Pertea G, Trapnell C, Pimentel H, Kelley R, Salzberg SL, 2013. TopHat2: accurate alignment of transcriptomes in the presence of insertions, deletions and gene fusions. *Genome biology* **14**: R36.

Krokene P, Solheim H, 1998. Pathogenicity of four blue-stain fungi associated with aggressive and nonaggressive bark beetles. *Phytopathology* **88**: 39–44.

Kuchin S, Vyas VK, Carlson M, 2002. Snf1 protein kinase and the repressors Nrg1 and Nrg2 regulate FLO11, haploid invasive growth, and diploid pseudohyphal differentiation. *Molecular and Cellular Biology* **22**: 3994–4000.

Kulkarni RK, Nickerson KW, 1981. Nutritional control of dimorphism in *Ceratocystis ulmi*. *Experimental Mycology* **5**: 148–154.

Lengeler KB, Davidson RC, D'Souza C, Harashima T, Shen WC, Wang P, Pan X, Waugh M, Heitman J, 2000. Signal transduction cascades regulating fungal development and virulence. *Microbiology and molecular biology reviews* **64**: 746–85.

Lew DJ, Reed SI, 1993. Morphogenesis in the yeast cell cycle: regulation by Cdc28 and cyclins. *Journal of Cell Biology* **120**: 1305–1320.

Lindsey R, Ha Y, Momany M, 2010. A septin from the filamentous fungus *A. nidulans* induces atypical pseudohyphae in the budding yeast *S. cerevisiae*. *PLoS ONE* **5**: 1–9.

Liu H, Köhler J, Fink GR, 1994. Suppression of hyphal formation in *Candida albicans* by mutation of a STE12 homolog. *Science* **266**: 1723–1726.

Liu H, Styles CA, Fink GR, 1993. Elements of the yeast pheromone response pathway required for filamentous growth of diploids. *Science* **262**: 1741–1744.

Lo HJ, Köhler JR, Didomenico B, Loebenberg D, Cacciapuoti A, Fink GR, 1997. Nonfilamentous *C. albicans* mutants are avirulent. *Cell* **90**: 939–949.

Madhani HD, Fink GR, 1997. Combinatorial control required for the specificity of yeast MAPK signaling. *Science* **275**: 1314–1317.

Madhani HD, Fink GR, 1998. The control of filamentous differentiation and virulence in fungi. *Trends in Cell Biology* **8**: 348–353.

Malcher M, Schladebeck S, Mösch HU, 2011. The Yak1 protein kinase lies at the center of a regulatory cascade affecting adhesive growth and stress resistance in *Saccharomyces cerevisiae*. *Genetics* **187**: 717–730.

Martínez-Espinoza AD, Ruiz-Herrera J, León-Ramírez CG, Gold SE, 2004. MAP kinase and cAMP signaling pathways modulate the pH-induced yeast-to-mycelium dimorphic transition in the corn smut fungus *Ustilago maydis*. *Current microbiology* **49**: 274–81.

Martínez-Pastor MT, Marchler G, Schüller C, Marchler-Bauer A, Ruis H, Estruch F, 1996. The *Saccharomyces cerevisiae* zinc finger proteins Msn2p and Msn4p are required for transcriptional induction through the stress response element (STRE). *The EMBO Journal* **15**: 2227–35.

Moseley JB, Nurse P, 2009. Cdk1 and cell morphology: connections and directions. *Current Opinion in Cell Biology* **21**: 82–88.

Muthukumar G, Kulkarni RK, Nickerson KW, 1985. Calmodulin levels in the yeast and mycelial phases of *Ceratocystis ulmi*. *Journal of bacteriology* **162**: 47–9.

Muthukumar G, Nickerson KW, 1984. Ca(II)-calmodulin regulation of fungal dimorphism in *Ceratocystis ulmi*. *Journal of bacteriology* **159**: 390–2.

Nadal M, García-Pedrajas MD, Gold SE, 2008. Dimorphism in fungal plant pathogens. *FEMS microbiology letters* **284**: 127–34.

Nantel A, Dignard D, Bachewich C, Harcus D, Marcil A, Bouin A-P, Sensen CW, Hogues H, Hoog M van het, Gordon P, Rigby T, Benoit F, Tessier DC, Thomas DY, Whiteway M, 2002. Transcription profiling of *Candida albicans* cells undergoing the yeast-to-hyphal transition. *Molecular biology of the cell* **13**: 3452–3465.

Naruzawa ES, Bernier L, 2014. Control of yeast-mycelium dimorphism in vitro in Dutch elm disease fungi by manipulation of specific external stimuli. *Fungal biology* **118**: 872–84.

Naruzawa ES, Malagnac F, Bernier L, 2016. Effect of linoleic acid on reproduction and yeast-mycelium dimorphism in the Dutch elm disease pathogens. *Botany* **96**: 31–39.

Nigg M, Laroche J, Landry CR, Bernier L, 2015. RNAseq analysis highlights specific transcriptome signatures of yeast and mycelial growth phases in the Dutch elm disease fungus *Ophiostoma novo-ulmi*. *G3 Genes|Genomes|Genetics* **5**: 2487–2495.

Nueda MJ, Tarazona S, Conesa A, 2014. Next maSigPro: updating maSigPro bioconductor package for RNA-seq time series. *Bioinformatics* **30**: 2598–2602.

O' Rourke SM, Herskowitz I, 1998. The Hog1 MAPK prevents cross talk between the HOG and pheromone response MAPK pathways in S*accharomyces cerevisiae*. *Genes and development* **12**: 2874–2886.

Pan X, Heitman J, 1999. Cyclic AMP-dependent protein kinase regulates pseudohyphal differentiation in Saccharomyces cerevisiae. *Molecular and cellular biology* **19**: 4874–87.

Penãlva MA, Arst HN, 2002. Regulation of gene expression by ambient pH in filamentous fungi and yeasts. *Microbiology and molecular biology reviews* **66**: 426–446.

Peñalva MA, Tilburn J, Bignell E, Arst HN, 2008. Ambient pH gene regulation in fungi: making connections. *Trends in microbiology* **16**: 291–300.

Pereira V, Royer JC, Hintz WE, Field D, Bowden C, Kokurewicz K, Hubbes M, Horgen PA, 2000. A gene associated with filamentous growth in *Ophiostoma novo-ulmi* has RNA-binding motifs and is similar to a yeast gene involved in mRNA splicing. *Current genetics* **37**: 94–103.

R Development Core Team, 2011. R Development Core Team.

Reichle RE, Alexander J V., 1965. Multiperforate septations, woronin bodies, and septal plugs in Fusarium. *Journal of Cell Biology* **24**: 498–496.

Richards WC, 1994. Nonsporulation in the Dutch elm disease fungus *Ophiostoma ulmi* : evidence for control by a single nuclear gene. *Revue canadienne de botanique* **72**: 461–467.

Richards WC, Takai S, Lin D, Hiratsuka Y, Asina S, 1982. An abnormal strain of *Ceratocystis ulmi* incapable of producing external symptoms of Dutch elm disease. *European Journal of Forest Pathology* **12**: 193–202.

Robertson LS, Fink GR, 1998. The three yeast A kinases have specific signaling functions in pseudohyphal growth. *Proceedings of the National Academy of Sciences of the United States of America* **95**: 13783–7.

Robinson MD, McCarthy DJ, Smyth GK, 2009. edgeR: A Bioconductor package for differential expression analysis of digital gene expression data. *Bioinformatics* **26**: 139–140.

Rui Jin, Craig J. Dobry, Phillip J. McCown and AK, 2008. Large-scale analysis of yeast filamentous growth by systematic gene disruption and overexpression. *Molecular biology of the cell* **19**: 284–296.

De Salas F, Martínez MJ, Barriuso J, 2015. Quorum sensing mechanisms mediated by farnesol in *Ophiostoma piceae* : its effect on the secretion of sterol esterase. *Applied and Environmental Microbiology* **81**: AEM.00079-15.

Sánchez-Martínez C, Pérez-Martín J, 2001. Dimorphism in fungal pathogens: *Candida albicans* and *Ustilago maydis*--similar inputs, different outputs. *Current opinion in microbiology* **4**: 214–21.

Schmieder R, Edwards R, 2011. Quality control and preprocessing of metagenomic datasets. *Bioinformatics* **27**: 863–864.

Selvig K, Alspaugh JA, 2011. pH response pathways in fungi: adapting to host-derived and environmental signals. *Mycobiology* **39**: 249–56.

Sherif S, Jones AMP, Shukla MR, Saxena PK, 2014. Establishment of invasive and non-invasive reporter systems to investigate American elm-*Ophiostoma novo-ulmi* interactions. *Fungal Genetics and Biology* **71**: 32–41.

Shively CA, Eckwahl MJ, Dobry CJ, Mellacheruvu D, Nesvizhskii A, Kumar A, 2013. Genetic networks inducing invasive growth in *Saccharomyces cerevisiae* identified through systematic genome-wide overexpression. *Genetics* **193**: 1297–310.

Sonneborn A, Bockmühl DP, Gerads M, Kurpanek K, Sanglard D, Ernst JF, 2000. Protein kinase A encoded by TPK2 regulates dimorphism of *Candida albicans*. *Molecular*

microbiology **35**: 386–96.

Soundararajan S, Jedd G, Li X, Ramos-pamplon M, Chua NH, Naqvi NI, 2004. Woronin body function in *Magnaporthe grisea* is essential for efficient pathogenesis and for survival during nitrogen starvation stress. *The Plant cell* **16**: 1564–1574.

Stringer MA, Timberlake WE, 1993. Cerato-ulmin, a toxin involved in Dutch elm disease, is a fungal hydrophobin. *The Plant cell* **5**: 145–6.

Supek F, Bošnjak M, Škunca N, Šmuc T, 2011. REVIGO summarizes and visualizes long lists of gene ontology terms. *PLoS ONE* **6**: e21800.

Tadesse Y, Bernier L, Hintz WE, Horgen P a., 2003. Real time RT-PCR quantification and Northern analysis of cerato-ulmin (*CU*) gene transcription in different strains of the phytopathogens *Ophiostoma ulmi* and *O. novo-ulmi*. *Molecular Genetics and Genomics* **269**: 789–796.

Takai S, Richards WC, Stevenson KJ, 1983. Evidence for the involvement of cerato-ulmin , the Ceratocystis ulmi toxin, in the development of Dutch elm disease. *Physiological plant pathology* **23**: 275–280.

Temple B, Horgen PA, Bernier L, Hintz WE, 1997. Cerato-ulmin, a hydrophobin secreted by the causal agents of Dutch elm disease, is a parasitic fitness factor. *Fungal genetics and biology* **22**: 39–53.

Tenney K, Hunt I, Sweigard J, Pounder JI, McClain C, Bowman EJ, Bowman BJ, 2000. *Hex*-1, a gene unique to filamentous fungi, encodes the major protein of the Woronin body and functions as a plug for septal pores. *Fungal genetics and biology : FG and B* **31**: 205–17.

Wang Y, 2009. CDKs and the yeast-hyphal decision. *Current Opinion in Microbiology* **12**: 644–649.

Wang C, Hu G, St. Leger RJ, 2005. Differential gene expression by *Metarhizium anisopliae* growing in root exudate and host (*Manduca sexta*) cuticle or hemolymph reveals mechanisms of physiological adaptation. *Fungal Genetics and Biology* **42**: 704–718.

Wang C, St. Leger RJ, 2007. The MAD1 adhesin of *Metarhizium anisopliae* links adhesion with blastospore production and virulence to insects, and the MAD2 adhesin enables attachment to plants. *Eukaryotic Cell* **6**: 808–816.

Warenda AJ, Konopka JB, 2003. Septin function in *Candida albicans* morphogenesis. *Molecular biology of the cell* **13**: 2732–2746.

Webber JF, Brasier CM, 1984. The transmission of Dutch elm disease: a study of the process involved. In: Anderson JM, Rayner ADM WD, ed. *Invertebrate-microbial interactions*. p. 271–306.

Wedge M-E, Naruzawa ES, Nigg M, Bernier L, 2016. Diversity in yeast – mycelium dimorphism response of the Dutch elm disease pathogens : the inoculum size effect. *Canadian Journal of Microbiology* **62**: 1–5.

Whiston E, Zhang Wise H, Sharpton TJ, Jui G, Cole GT, Taylor JW, 2012. Comparative transcriptomics of the saprobic and parasitic growth phases in *Coccidioides* spp. *PloS one* **7**: e41034.

Wickham H, 2009. *ggplot2: elegant graphics for data analysis.* New York.

Winnenburg R, Urban M, Beacham A, Baldwin TK, Holland S, Lindeberg M, Hansen H, Rawlings C, Hammond-Kosack KE, Köhler J, 2008. PHI-base update: Additions to the pathogen-host interaction database. *Nucleic Acids Research* **36**: 572–576.

Woronin M, 1964. Zur Entwicklungsgeschichte der *Ascobolus pulcherrimus* Cr. und einer Pezizen. *Abh. Senkend. Naturforsch.* **5**: 333–344.

Yang E, Chow W, Wang G, Woo PCY, Lau SKP, Yuen K, Lin X, Cai JJ, 2014. Signature gene expression reveals novel clues to the molecular mechanisms of dimorphic transition in *Penicillium marneffei*. *PLoS genetics* **10**: e1004662.

Young MD, Wakefield MJ, Smyth GK, Oshlack A, 2010. Gene ontology analysis for RNA-seq: accounting for selection bias. *Genome Biology* **11**: R14.

Table 4.1 General characteristics of the 18 RNAseq samples after trimming and filtration. No.: number.

Samples	Replicates	Time (h)	No. of reads[1]	No. of reads mapped	No. of bases	Exon coverage depth	No. of genes expressed[2]
MN1	1	0	11968893	6550928	790686427	54.0X	7413
MN2	1	2	12899265	7054621	881079467	60.2X	7436
MN3	1	4	12739833	7197167	897760976	61.3X	7465
MN4	1	6	13641971	7461971	930946766	63.6X	7515
MN5	1	10	8949640	4863675	604538988	41.3X	7487
MN6	1	27	9109003	4840961	558218816	38.1X	7543
MN7	2	0	7382503	3826743	454704414	31.0X	7256
MN8	2	2	9425687	4860220	594473189	40.6X	7420
MN9	2	4	9259734	5094283	630655472	43.1X	7418
MN10	2	6	9418078	5124364	614559004	42.0X	7468
MN11	2	10	11072018	6185630	751150263	51.3X	7551
MN12	2	27	7301344	3167396	371782642	25.4X	7531
MN13	3	0	11782413	6722999	812905343	55.5X	7401
MN14	3	2	8145563	4536653	567033310	38.7X	7306
MN15	3	4	11419771	6636608	827274989	56.5X	7408
MN16	3	6	10960584	6445652	797790606	54.5X	7550
MN17	3	10	12468947	7297888	900860683	61.5X	7570
MN18	3	27	7876023	4271786	504251284	34.4X	7580

1. All reads are 25-150 nt long.

2. At least one read after normalization in EdgeR

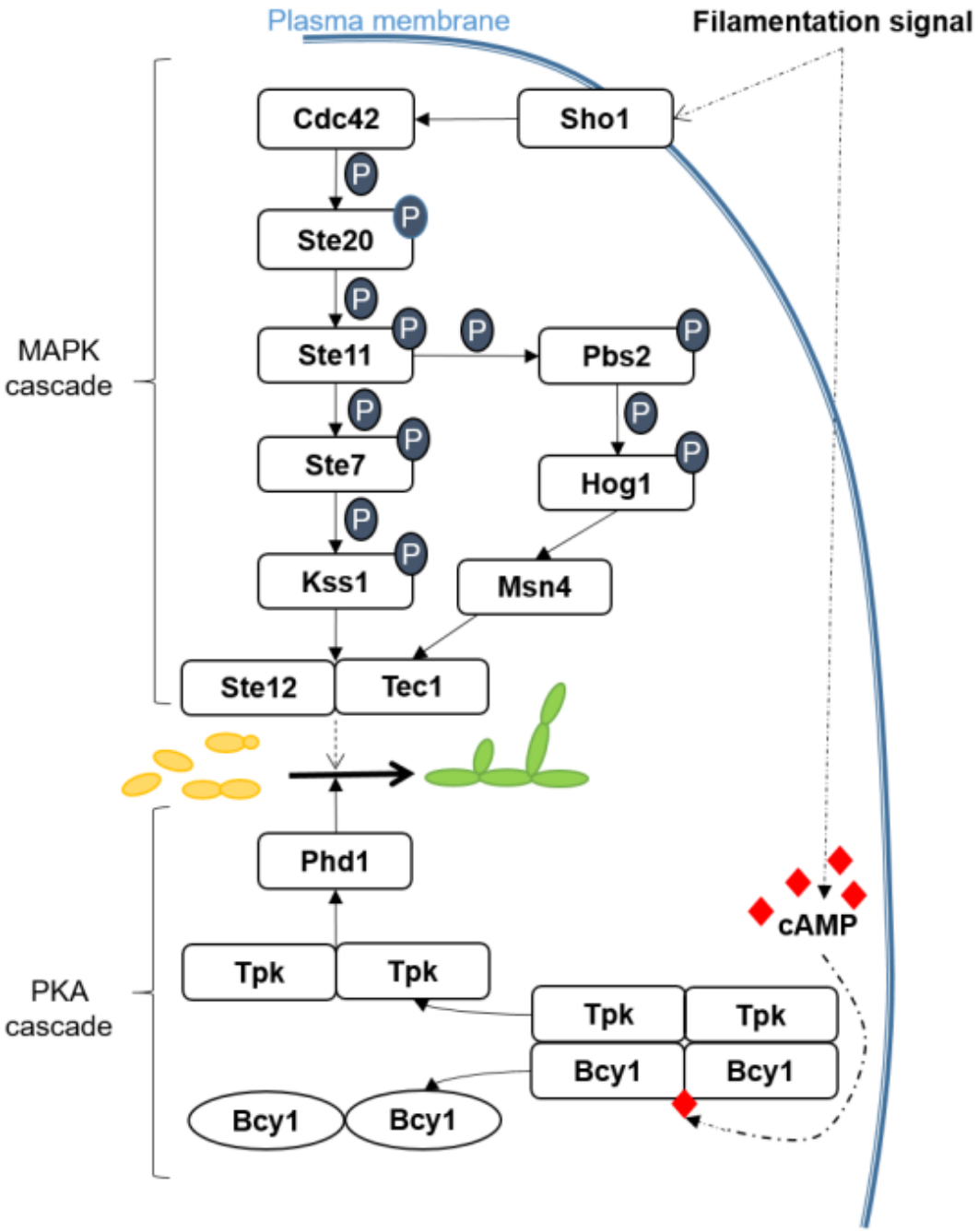

Figure 4.1 Simplified and non-exhaustive illustration of the *S. cerevisiae* proteins involved in the MAPK and cAMP-PKA cascades that regulate pseudohyphae formation. Dashed arrows indicate indirect regulation through other components that are not displayed here. P, phosphate (PO^{3-}).

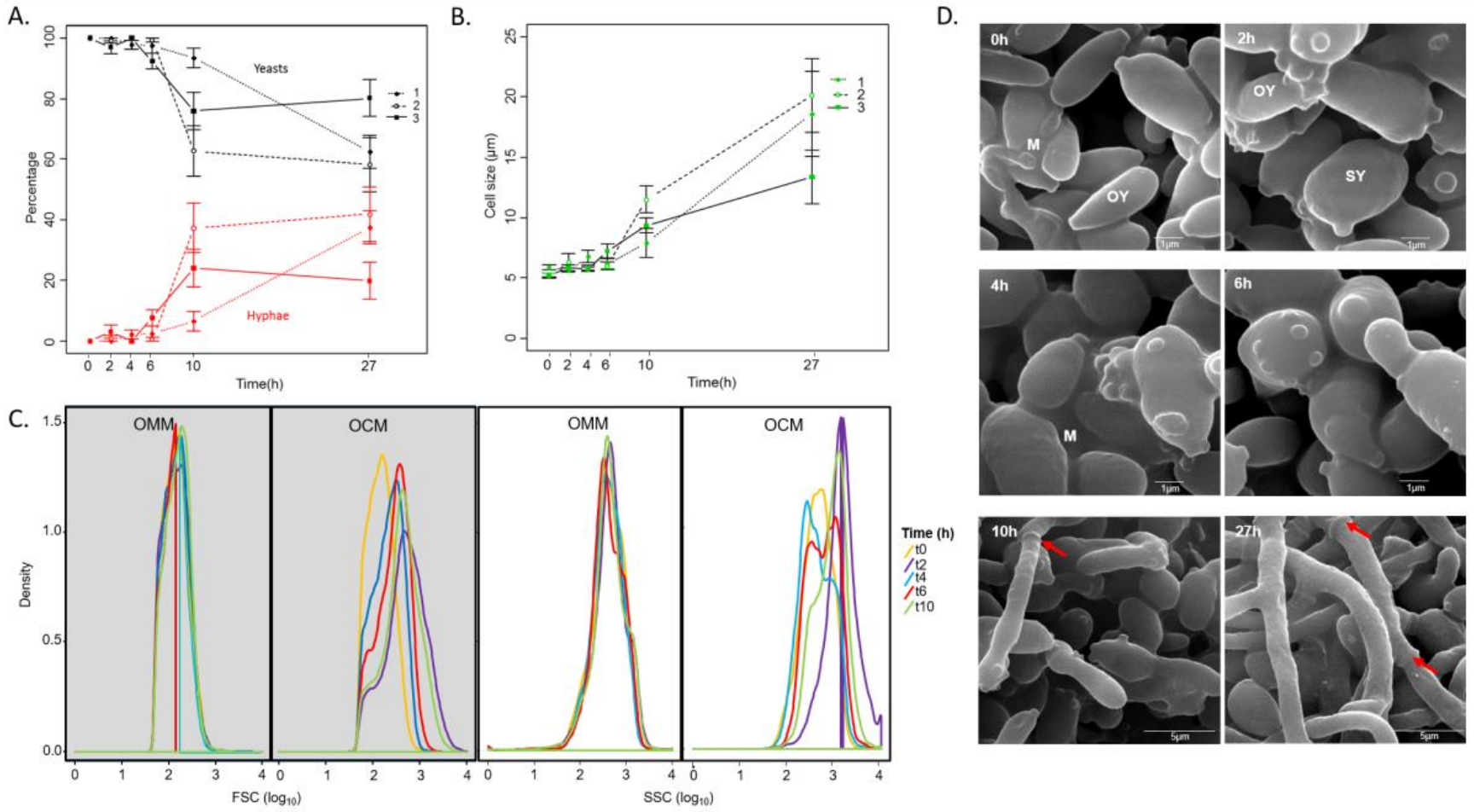

Figure 4.2 A. Percentage of yeast and mycelium in *Ophiostoma novo-ulmi* at 0, 2, 4, 6, 10 and 27 hours of incubation in conditions inducing the yeast-to-hypha transition. This was achieved by transferring yeast cells grown in shake liquid minimal medium to fresh liquid complete growth medium (OCM) without agitation. Values are means and standard deviations for three replicates. Black: yeast percentage; Red: Hyphae percentage. B. Cell size in µm at each of the 6 time points for the three replicates. C. Density of cell size (gray

panels) and density of cell granularity or internal complexity (white panels) at each of 5 time points measured by flow cytometry. FSC: Forward Scatter, cell size. SSC: Side Scatter, granularity. OMM: minimum medium under agitation, no transition. OCM: *Ophiostoma* complete medium in still conditions, switch from yeast to mycelium. D. Scanning-electron microscopy pictures taken at each time point. Scale is indicated on the pictures. OY: ovoid yeast cells; SY: spherical yeast cells; M: extracellular matrix. Red arrows indicate septa

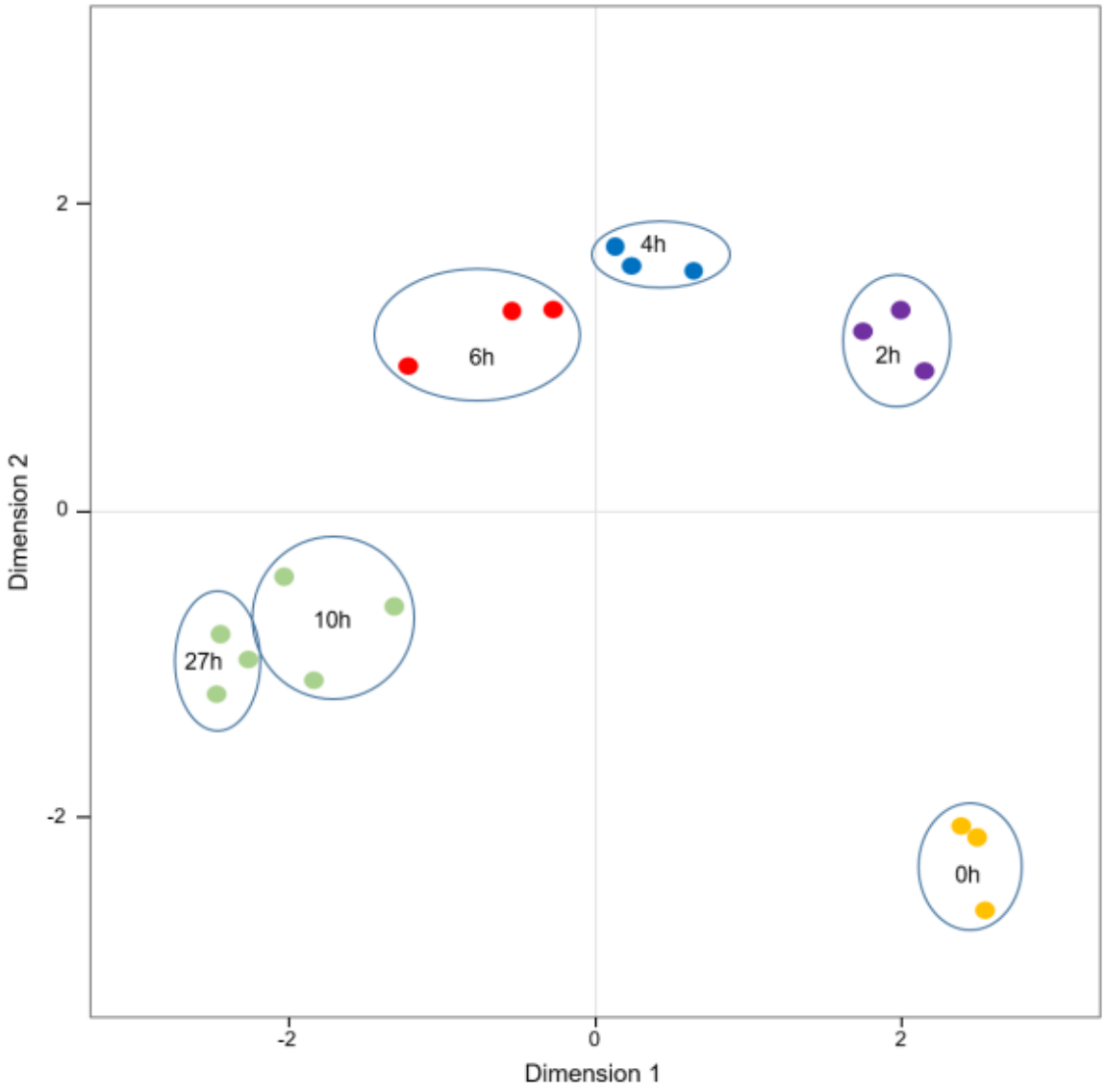

Figure 4.3 Multidimensional Scaling (MDS) plot of the 18 RNA samples sequenced during the yeast-to-hypha transition in *Ophiostoma novo-ulmi*. Dot colors: results of cluster analysis by *k*-means test. Dots from the same color represent values that are not significantly different according to the *k*-means test. Blue circle: contains the three replicates of each time point (0, 2, 4, 6, 10 and 27 hours after transfer to fresh complete medium).

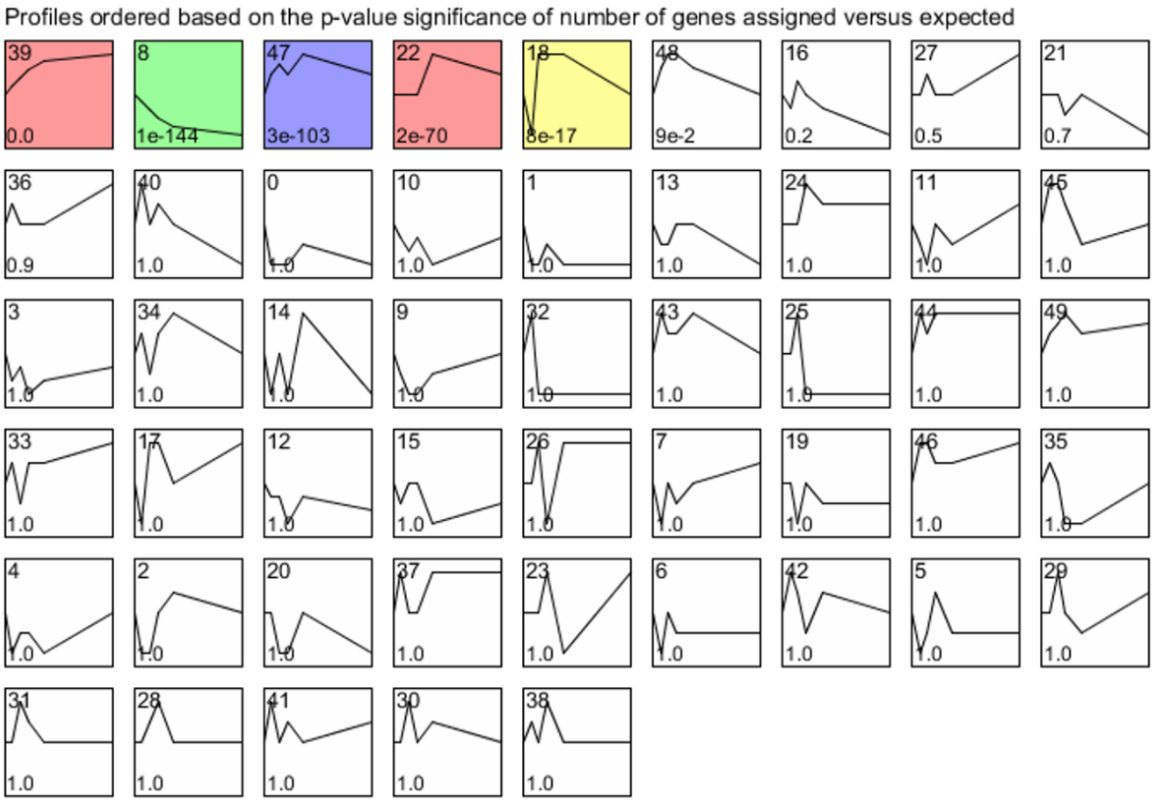

Figure 4.4 Expression profiles of genes during yeast-to-hypha transition in *Ophiostoma novo-ulmi* assessed using STEM on differentially expressed genes identified using *Next-maSigPro* package. Profiles are ordered based on the *P*-value significance of number of genes assigned versus expected. Numbers on the top right: profile ID; numbers on the bottom right: *P*-value significance of number of genes assigned versus expected. Colored profiles: *P*-value significant (corrected with FDR). Profiles with the same color are part of a unique cluster.

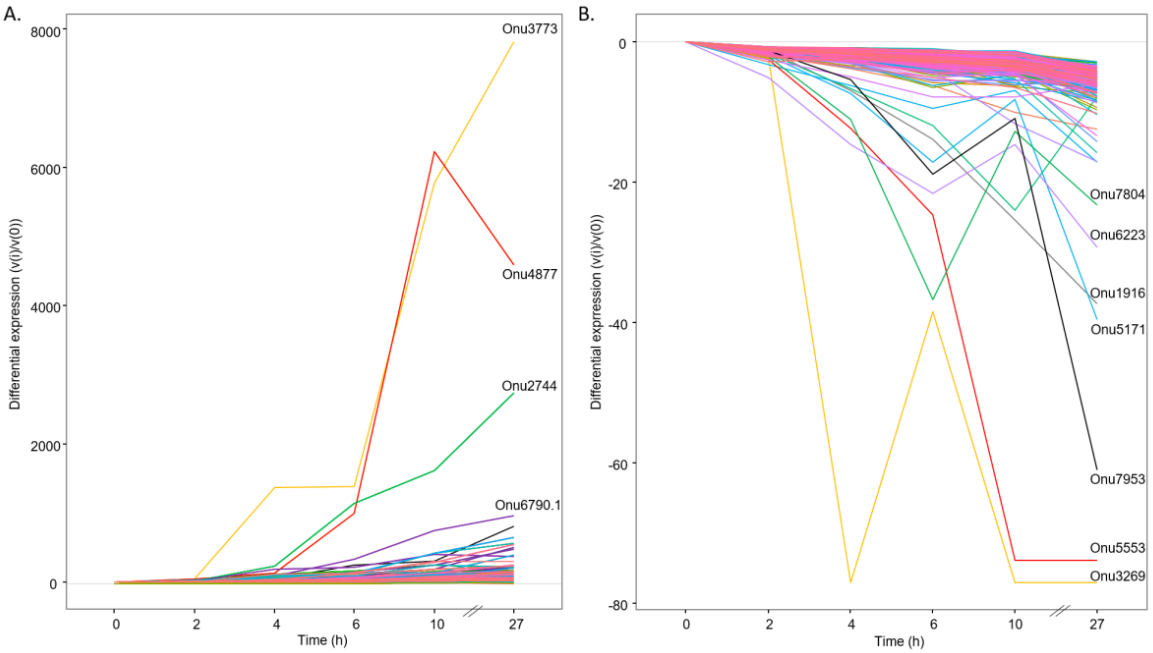

Figure 4.5 Differential gene expression along time points for genes in STEM profiles 39 (A) and 8 (B). Top genes for each profile are highlighted.

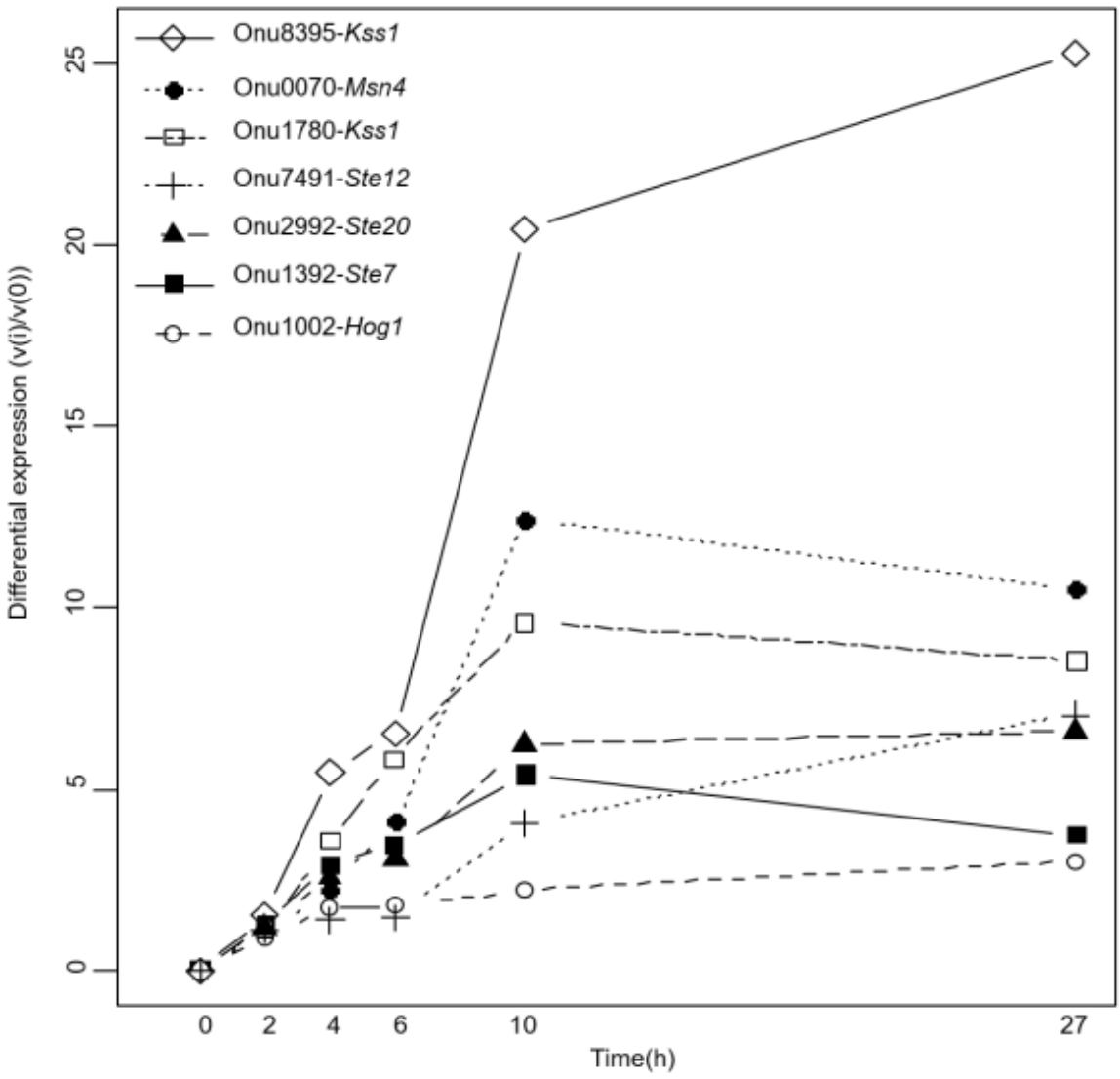

Figure 4.6 Differential gene expression for *Ophiostoma novo-ulmi* homologs to genes implicated in the MAPK cascade in *S. cerevisiae*. Differential gene expression is the difference in read count between the point of interest (i) and the start point of the experiment (0), calculated by STEM software (Ernst *et al.* 2005; Ernst and Bar-Joseph, 2006).

Tables S1-7 available at

https://bmcgenomics.biomedcentral.com/articles/10.1186/s12864-016-3251-8

Table S4.1 qRT-PCR primers for reference genes and tested genes.

Table S4.2 Results of BLASTp analysis of *Saccharomyces cerevisiae* dimorphism related proteins with *Ophiostoma novo-ulmi* genome. The last column indicates if the homologous proteins are orthologs (results of reciprocal best blast hits (RBH) using tblastx on exon sequences for each gene of the two species, e-value = 1x10^3 and word size = 5).

Table S4.3 Normalized read counts for the 7605 genes analyzed using EdgeR and maSigPro in R. 1-3: 0 h; 4-6: 2 h; 7-9: 4 h; 10-12: 6 h; 13-15: 10 h; 16-18: 27 h. DEGs : Differentially Expressed Genes detected using maSigPro, FDR $\leq$ 0.05. For each DEG, the number of the STEM profile associated is indicated. Nigg *et al.* 2015: genes overexpressed in Yeast or Mycelium growth phases in the study of Nigg and collaborators in 2015 (Nigg *et al.* 2015)

Table S4.4 Description of the 815 genes found in the STEM profile 39. Values are means of differential gene expressions for each time compared to 0 h.

Table S4.5 Enriched biological processes in the STEM profile 39 containing at least 4 DEGs genes after filtration using GO Trimming and REVIGO. GO term in bold are parent term retained as name for a regroupment.

Table S4.6 Description of the 256 genes found in the STEM profile 8. Values are means of differential gene expressions for each time compared to 0 h.

Table S4.7 Enriched biological processes in the STEM profile 8 containing at least 4 DEGs genes after filtration using GO Trimming and REVIGO. GO term in bold are parent term retained as name for a regroupment.

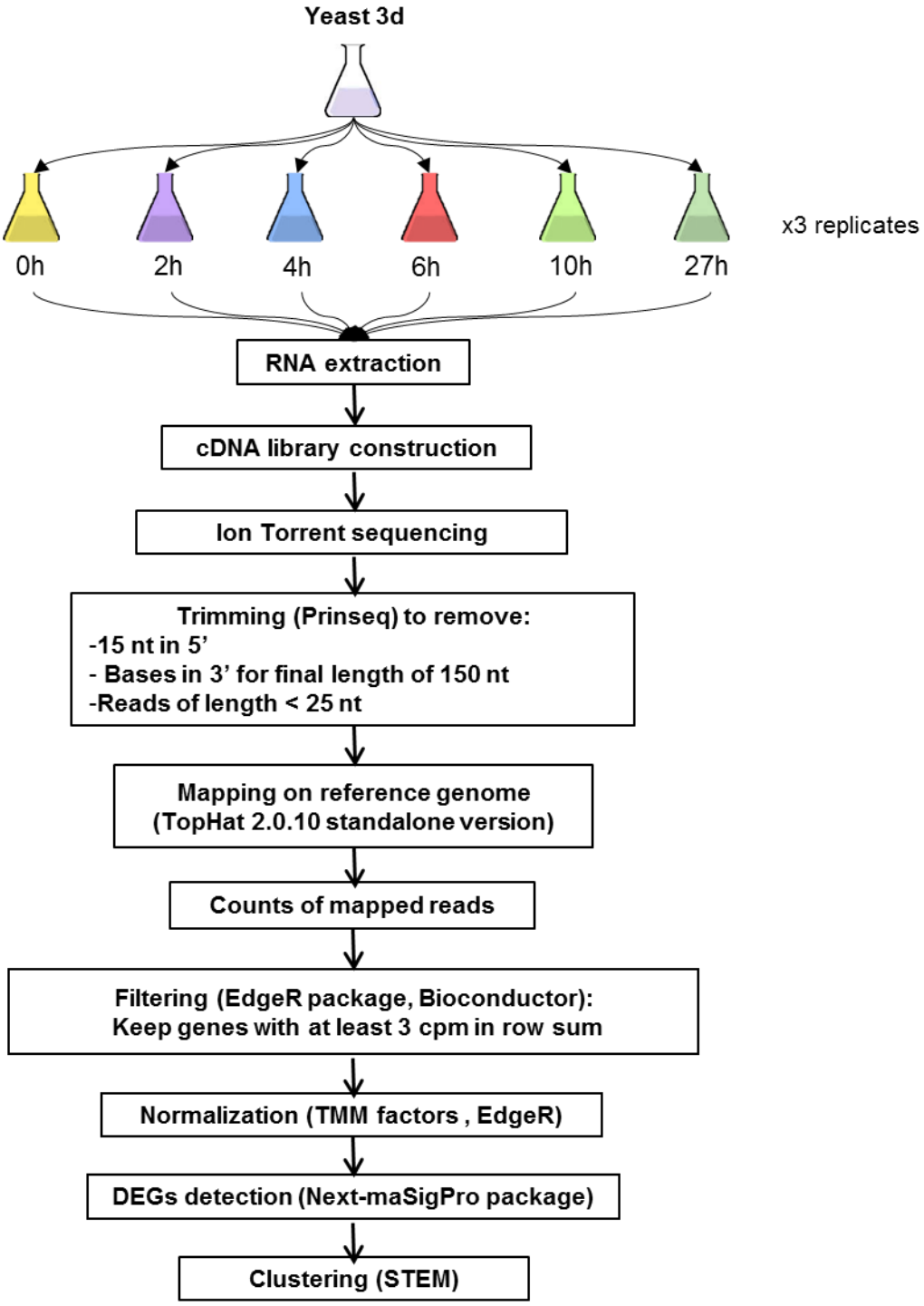

Figure S4.1 Workflow for RNAseq data production and analysis.

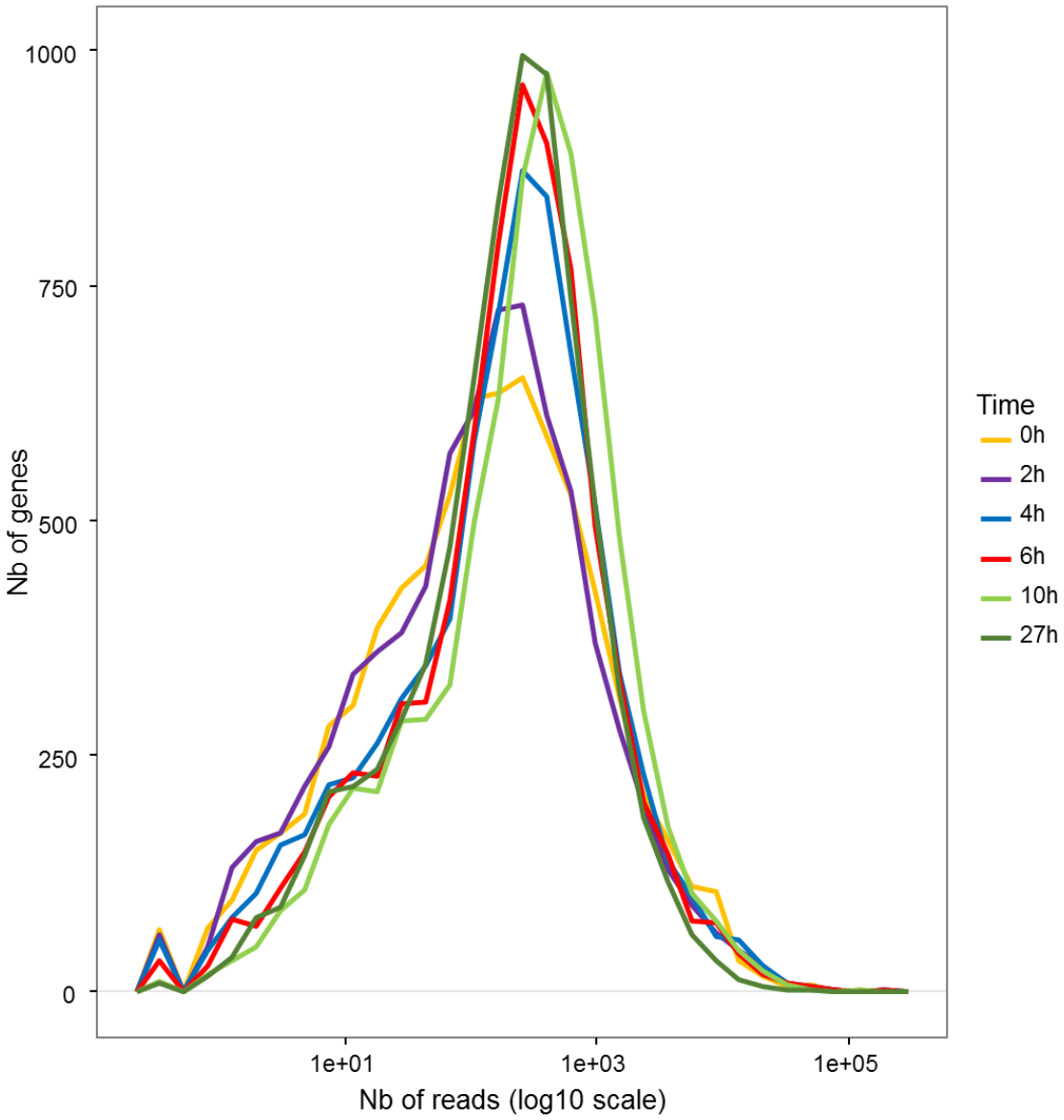

Figure S4.2 Distribution of the number of reads (log_{10} scale) per gene, per condition (mean of 3 replicates).

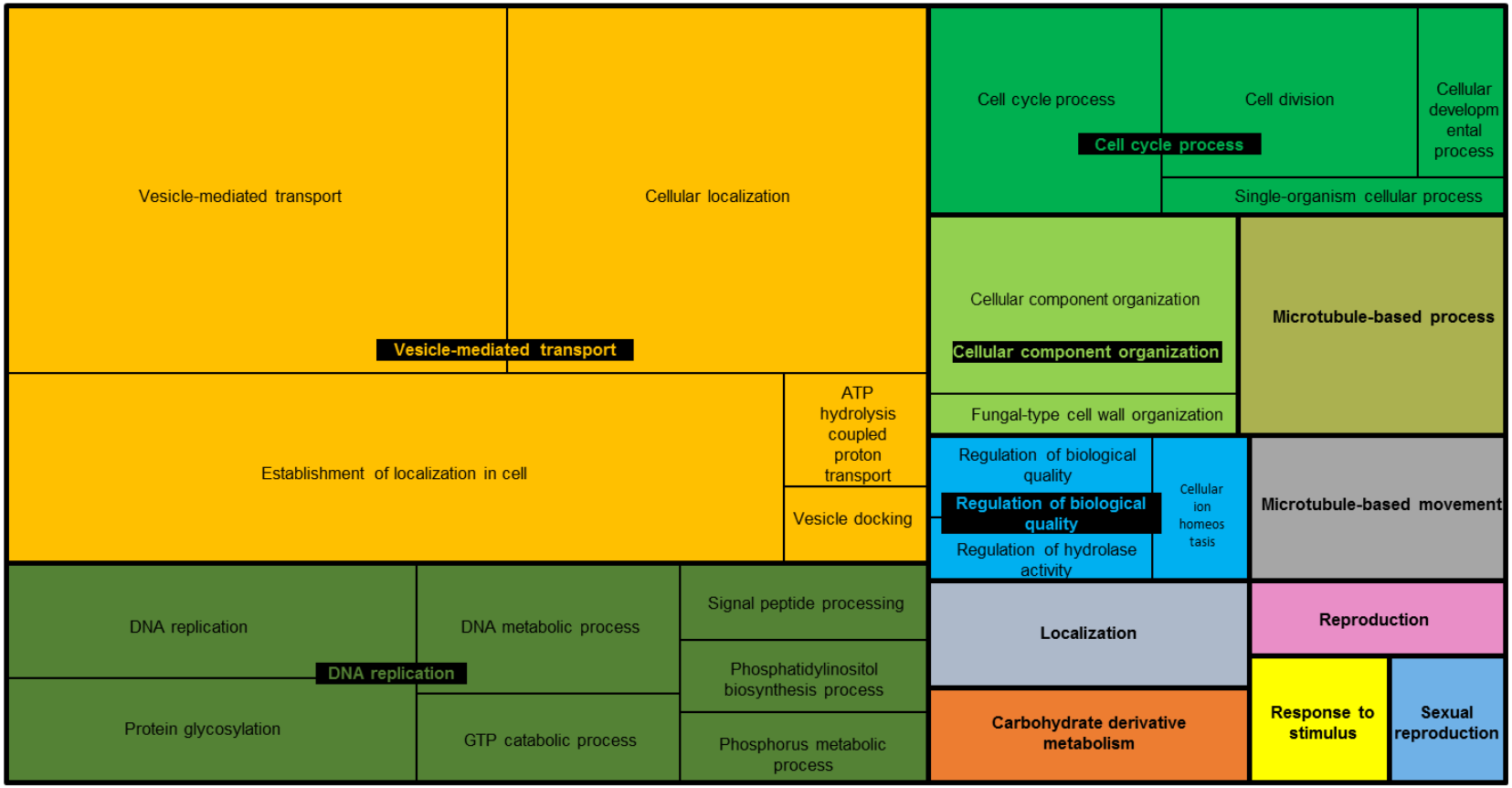

Figure S4.3 REVIGO Gene Ontology treemap for the 112 biological processes that were enriched in profile 39. The size of boxes represents the absolute P-value for enrichment of each GO term in the gene set of the profile ($\log_{10}$).

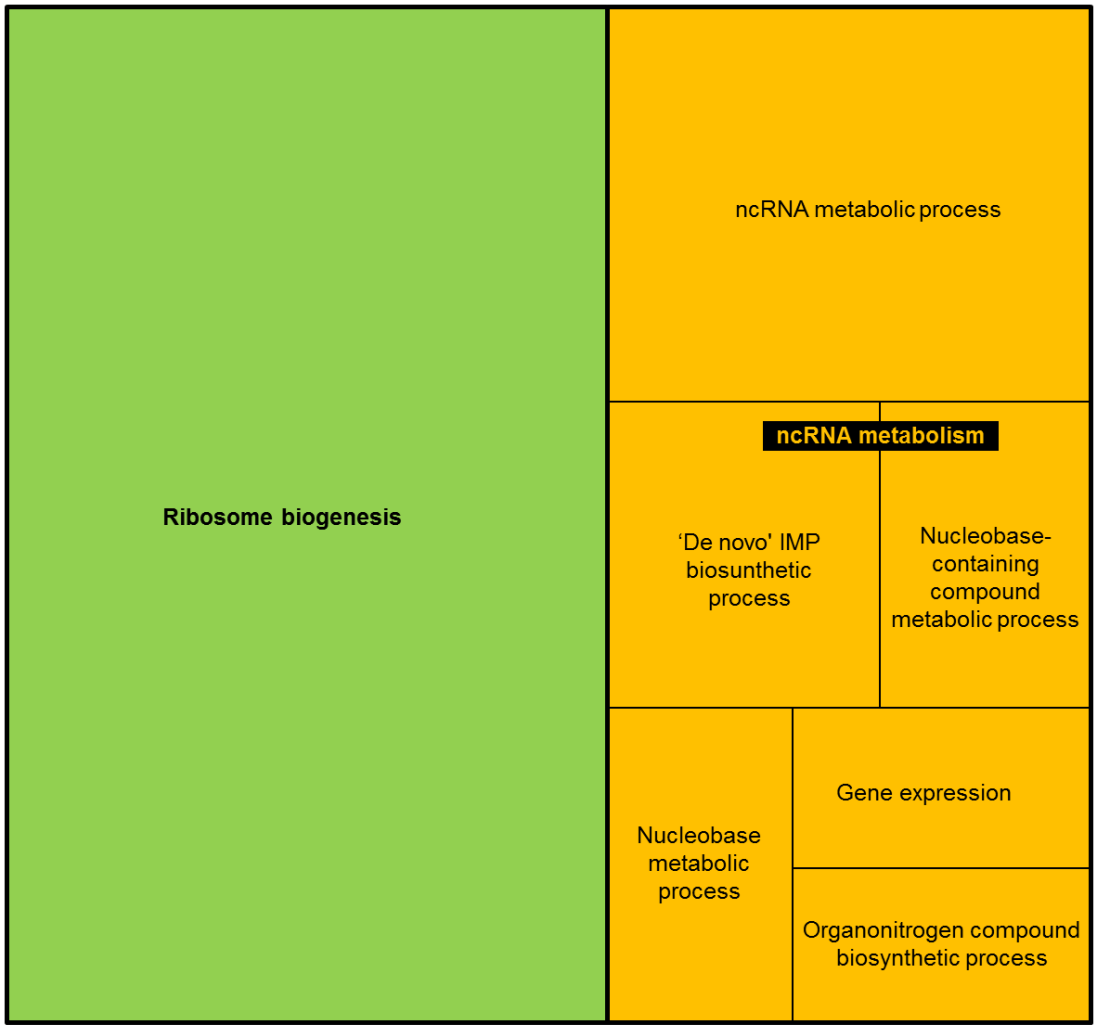

Figure S4.4 REVIGO Gene Ontology treemap for the 22 biological processes enriched in profile 8. The size of boxes represents the absolute P-value for enrichment of each GO term in the gene set of the profile (log_{10}).

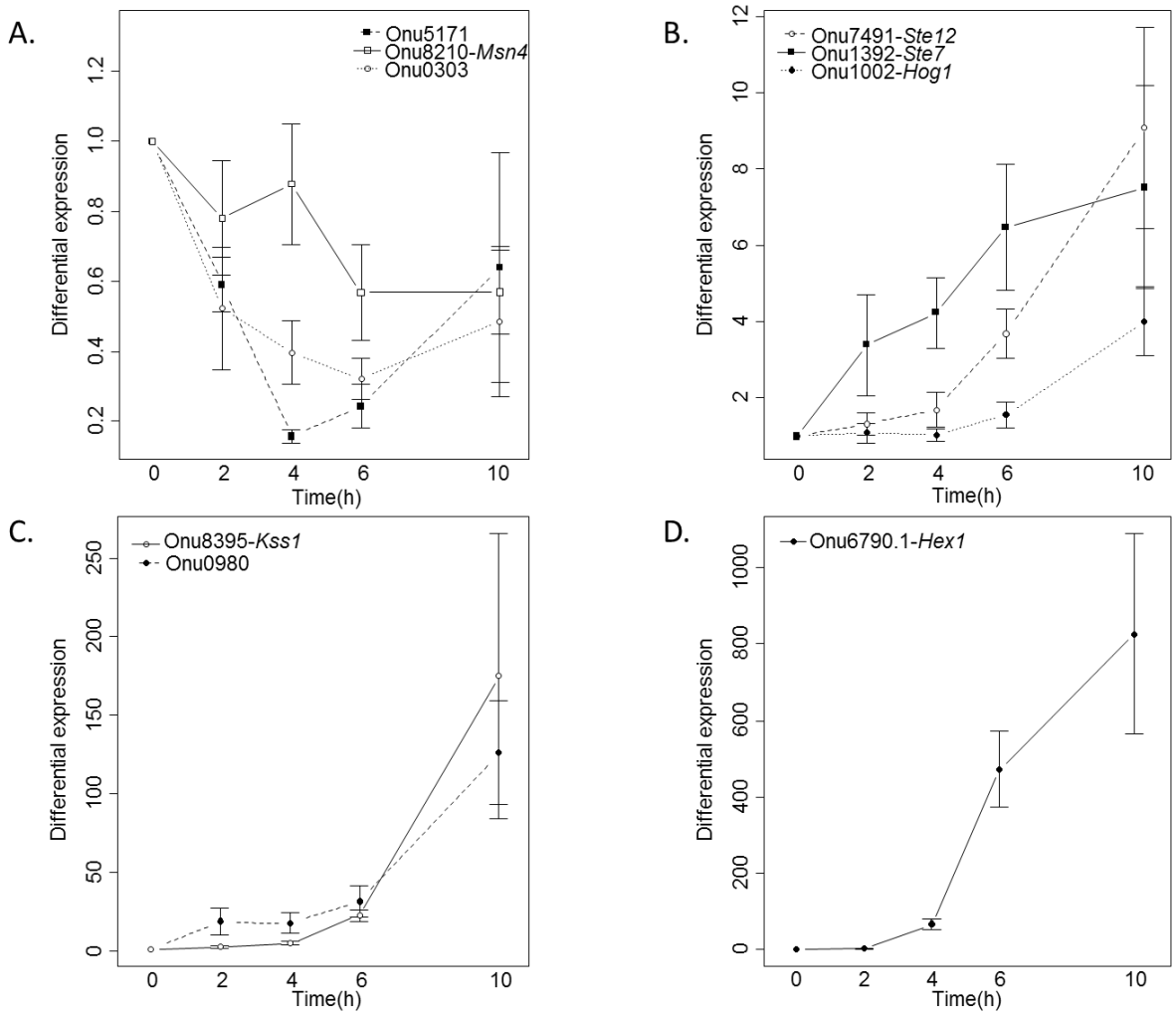

Figure S4.5 Quantitative Reverse Transcriptase-Polymerase Chain Reaction (qRT-PCR) results at 0, 2, 4, 6, and 10 hours following transfer to fresh complete growth medium (OCM) for A, downregulated genes; B, C and D, over-expressed genes. Differential expression: $2^{-\Delta\Delta Ct}$, fold increase in expression level compared to the start of the experiment (0 h). Standard deviations are calculated on three biological replicates for each gene. Three technical replicates per gene were run. Transcript levels were normalized with three control genes (Onu3626, Onu1683, Onu0623) that had the most stable expression and were used to calculate a reliable normalization factor according to *Normfinder* software (Andersen *et al.* 2004).

CHAPITRE 5 Conserved components of the yeast-to-hypha transition revealed through comparative transcriptomic analyses of orthologous genes in the ascomycete *Ophiostoma novo-ulmi* and the basidiomycete *Pseudozyma flocculosa*.

Nigg M.[a,b], Laur J.[c], Bélanger R.[a,c] and Bernier L.[a,b]

[a] Institut de Biologie Intégrative et des Systèmes (IBIS), Université Laval, Québec, G1V 0A6, Canada

[b] Centre d'Étude de la Forêt (CEF) and Département des sciences du bois et de la forêt, Université Laval, Québec, G1V 0A6, Canada

[c] Département de Phytologie, Université Laval, Québec, Québec, Canada G1V 0A6, Canada

Article en préparation pour soumission dans le journal *Fungal Biology*.

5.1 Résumé

Le dimorphisme existe chez plusieurs taxons à travers le règne fongique. Les mécanismes impliqués dans la transition levure-hyphe ont été étudiés de manière indépendante chez des espèces modèles mais très peu chez d'autres espèces malgré les avancées technologiques au niveau du séquençage à haut-débit. Dans l'étude présentée ici, nous avons mis en évidence des facteurs moléculaires régulant la transition morphologique qui sont conservés entre deux espèces éloignées phylogénétiquement : l'ascomycète phytopathogène *Ophiostoma novo-ulmi* et le basidiomycète *Pseudozyma flocculosa*, agent de biocontrôle du blanc proche des agents phytopathogènes appartenant aux Ustilaginales. Nous avons comparé des données de transcriptomiques obtenues dans les phases de germination et de filamentation chez *O. novo-ulmi* et *P. flocculosa* afin de vérifier si les processus biologiques impliqués dans la transition levure-hyphe étaient largement conservés. Parmi les 3824 gènes orthologues trouvés entre les espèces, nous avons identifié 695 gènes qui étaient différentiellement exprimés chez les deux organismes durant le changement dimorphique. Nous avons mis en évidence des gènes codant pour des kinases et des facteurs de transcriptions pour lesquels la régulation de l'expression génique est conservée au cours de la transition de la spore en germination à la croissance filamenteuse. Nous avons également révélé une répression majeure des processus associés à l'expression génique et à la synthèse protéique. De manière globale, la plupart des gènes identifiés sont impliqués dans des processus biologiques qui jouent des rôles essentiels dans le cycle cellulaire et le développement des hyphes. Ainsi, la comparaison des transcriptomes faite ici entre *O. novo-ulmi* et *P. flocculosa* a permis de mettre en évidence des facteurs qui semblent centraux pour la transition levure-hyphe chez des espèces phylogénétiquement distantes.

5.2 Abstract

Dimorphism exists in many taxa throughout the fungal kingdom. Important mechanisms of the yeast-to-hypha switch have been studied independently in model species but much less in others notwithstanding the opportunities high-throughput sequencing technologies provide. In the present study, we highlight conserved components regulated during the phase transition through the comparison of two unrelated fungi: the ascomycete plant pathogen *Ophiostoma novo-ulmi* and the basidiomycete *Pseudozyma flocculosa*, a biocontrol agent of powdery mildews related to plant pathogens within the Ustilaginales. To test whether the biological processes involved in the yeast-to-hypha transition were broadly conserved, we comprehensively analyzed *O. novo-ulmi* and *P. flocculosa* transcriptomic data of the germination and filamentation phases. Among the 3825 orthologous genes found between the two species, we identified 695 genes that were differentially expressed in both organisms during the dimorphic switch. We identified genes encoding kinases and transcription factors for which the regulation of expression is conserved during the switch from germinating spore to filamentous growth. We also observed a major downregulation of the gene expression and protein synthesis processes. Overall, most of the genes highlighted are associated with biological processes that play essential roles in the cell cycle and hyphal development. Hence, the comparison of *O. novo-ulmi* and *P. flocculosa* transcriptomes highlighted probable core components necessary for the yeast-to-hypha transition in phylogenetically distant species.

5.3 Introduction

Morphological plasticity favors adaptability to stressful environments. In this context, dimorphism has been extensively studied, especially in fungal pathogens in which it is often concurrent to sexual reproduction and associated with virulence.

Multiple biological processes are associated with the morphological switch that allows fungi to convert from yeast-like cells to filamentous growth, in a reversible manner (Romano, 1966). In a recent review, Nigg and Bernier (2017) highlighted several overlaps in gene expression regulation of the dimorphic transition in seven pathogenic species from very different taxonomic classes. For instance, carbohydrate metabolism associated with cell wall remodeling processes was found to be highly regulated since yeast and hyphal cell wall structures are composed of various polymers (Nigg and Bernier 2017; Domer *et al.* 1967; Chattaway *et al.* 1973). At a finer molecular scale, at least three interconnected molecular pathways, the Mitogen-Activated Protein Kinases (MAPK), cyclic Adenosine Monophosphate Protein (cAMP) and pH-response RIM cascades, have been described extensively in model species like *Saccharomyces cerevisiae*, *Candida albicans* and *Ustilago maydis* (reviewed in Sánchez-Martínez and Pérez-Martín 2001). Even though the main actors of these pathways are highly conserved among species, it has been shown that their specific involvement in the dimorphic switch can be different. In that context, a high level of cAMP induces the yeast-to-hypha switch in *C. albicans* (Pan and Heitman 1999), whereas the same process is repressed by cAMP in *U. maydis* (Gold *et al.* 1994; Mayorga and Gold 1999). Furthermore, as it has often been reviewed (Madhani and Fink 1998; Bölker 2001; Sánchez-Martínez and Pérez-Martín 2001), the specific crosstalk between the MAPK and cAMP pathways also leads to the fine regulation of the concomitant mating events. In a recent study, Nigg *et al.* (2015) compared yeast and mycelium transcriptomes of the Dutch elm disease fungus *Ophiostoma novo-ulmi* and human pathogens *C. albicans* and *Histoplasma capsulatum*. The authors found very little conservation in gene expression in yeast and mycelium growth phases between these three species (Nigg *et al.* 2015). Our understanding of the diversity of molecular processes that are involved in the dimorphic switch is limited to a small number of species. More investigations are needed to overcome this limitation and to cover a wider spectrum of the fungal kingdom.

In order to investigate the yeast-to-hypha switch, we present here a comparative transcriptomic analysis of this transition between two non-model species from very distant taxonomic classes: (1) the Sordariomycete *O. novo-ulmi* (Ascomycota), closely related to the human pathogen *Sporothrix schenckii* and (2) the leaf epiphyte *Pseudozyma flocculosa*, a biocontrol agent of powdery mildews with no known diploid phase, originally identified as *Sporothrix flocculosa* (Traquair *et al.* 1988) but later reclassified as a singular member of the Ustilaginales in the Basidiomycota (Begerow *et al.* 2000).

The two organisms present a somewhat similar morphological ability to switch from yeast-like cells to filamentous form (Figure 5.1). *In vitro* dimorphic transition in both species can be controlled by sources of nutrients or inoculum size (Kulkarni and Nickerson 1981; Hammami *et al.* 2008; Wedge *et al.* 2016) and essential elements of the cAMP and MAPK cascades are broadly conserved between the two genomes (Lefebvre *et al.* 2013; Comeau *et al.* 2015) and expressed (Nigg *et al.* 2015; Nigg and Bernier 2016). Hence, we hypothesized that *O. novo-ulmi* and *P. flocculosa* shared conserved genes and biological processes involved in the dimorphic trait. By comparing these two unrelated fungi, including one (*P. flocculosa*) for which the dimorphic transition is not associated with mating, we expected to reveal core components of the yeast-to-hypha switch. To this end, time-course transcriptomic data covering the critical phases of transition in *O. novo-ulmi* and *P. flocculosa* were compared with a particular emphasis on orthologous genes that were differentially regulated in the two species.

5.4 Materials and methods

5.4.1 *In vitro* culture assays

To achieve yeast-to-hypha transition in *O. novo-ulmi* subsp. *novo-ulmi* strain H327, yeast cells were grown for 27 h in triplicate in flasks of liquid complete medium as described in Nigg and Bernier (2016) after three days of preculture on an orbital shaker in liquid minimal medium (Bernier and Hubbes 1990). Optical microscopy (Olympus BX41) photographs of yeast cells and hyphal structures were taken at the beginning of the switch and 27 h after the induction, respectively. Scanning electron micrographs were obtained following the procedure described by Nigg and Bernier (2016). For the specific purpose of studying the yeast-to–hypha transition through transcriptomic analyses, the germination stage (G)

corresponded to cultures collected 6 h after the induction, and the filamentous growth (F) was harvested 27 h after induction of the yeast-to-hypha switch**.**

Pseudozyma flocculosa (DAOM 196992) was grown in triplicate in flasks following the methods and observations of Hammami *et al.* (2008). Cultures were harvested at four different times spanning different phases corresponding to germination (2h), filamentous growth (8h), flocculosin production under nutrient depletion (18h) and maturation of sporidia (30h). The phases corresponding to germination and filamentous growth were directly imaged using an Olympus SZ61 stereomicroscope (Olympus Tokyo, Tokyo, Japan) or collected for scanning electron microscopy (SEM) observation and transcriptomic analyses. For SEM observation, samples were immersed in 100% dry methanol, followed 100% dry ethanol. Finally, samples were mounted on aluminium stubs, coated with gold-palladium and imaged with a JEOL JSM6360LV Scanning Electron Microscope (JEOL, Tokyo, Japan) at 15 kV accelerating voltage.

5.4.2 RNA extraction, library construction and sequencing

Total RNA extractions and processing were done for *O. novo-ulmi* and *P. flocculosa* as described by Nigg and Bernier (2016) and Lefebvre at al. (2013), respectively. All of the primary sequencing data can be found in the NCBI under the study accession number SRP078831 for *O. novo-ulmi* and in the DDBJ Sequence Read Archive (DRA) under the accession number PSUB006820 for *P. flocculosa.*

5.4.3 Bioinformatic methods

Raw FastQ files from the *O. novo-ulmi* and *P. flocculosa* datasets were checked for contaminants and low quality bases before mapping on reference genomes as respectively described by Nigg and Bernier (2016) and Lefebvre *et al.* (2013).

Differential gene expression analyses were performed using the using the EdgeR algorithm implemented in CLC Genomics Workbench that utilizes the Exact Test developed by Robinson and Smyth (2008). The false discovery rate (FDR) threshold was set to ≤ 0.01 to judge the significance of the change in gene expression. Data were expressed by Reads Per Kilobase per Million mapped reads (RPKM) by calculating the mapped reads (total exon reads / (total mapped reads in millions) × exon length in kb) for each gene.

Orthologous genes were identified by reciprocal best blast hits (RBH) using tblastx (Altschul *et al.* 1990). Local databases were constructed from exon sequences of *O. novo-ulmi* (Forgetta *et al.* 2013) and *P. flocculosa* (Lefebvre *et al.* 2013). The databases were compared and the RBH analysis was conducted using the following parameters: e-value = $1x10^{-3}$ and word size = 5. Orthologous genes are renamed "OrthoG" followed by a number for increased readability.

Gene ontology (GO) term enrichment analyses were performed as described in Nigg and Bernier (2016) using the Goseq package in Bioconductor 3.0 (Young *et al.* 2010), GO Trimming (Jantzen *et al.* 2011) and REVIGO (Supek *et al.* 2011). We took the genes and GO annotation of *O. novo-ulmi* for GO enrichment analysis and confirmed that the GO annotation was highly identical for *P. flocculosa* (data not shown)

To evaluate the variability between biological replicates, a multidimensional scaling (MDS) analysis was conducted following the procedure described previously (Nigg *et al.* 2015). The MDS plot was produced using the R package ggplot2 (Wickham 2009).

5.5 Results

5.5.1 Visualization of gene expression

Based on the Reciprocal best Blast Hits (RBH) analysis, 3824 Orthologous Genes (OGs) were identified between *O. novo-ulmi* and *P. flocculosa* (Table S5.1; from 18.5 to 98.7% of identity, data not shown). The nuclear genome of *P. flocculosa* contains 6877 protein coding genes (Lefebvre *et al.* 2013), whereas that of *O. novo-ulmi* includes 8640 protein coding genes (Forgetta *et al.* 2013; Comeau *et al.* 2015). Thus, the OG set represented 44% and 56% of the genomes of *O. novo-ulmi* and *P. flocculosa*, respectively.

Differential expression analyses were conducted by two-by-two comparisons of the germination (G) and filamentation (F) phases that are part of the yeast-to-hypha transition. Of the 3824 OGs, only 695 were differentially expressed in both species between the G and F phases. Details of number of orthologous genes up- and downregulated in each species are summarized in Table 5.2. As shown in Figure 5.2, this relative small subset of Differentially Expressed Orthologous Genes (DEOGs) was still representative of the whole transcriptome dynamics. Indeed, MDS analyses showed that for the two species, similar profiles could be

observed when all expressed genes or when only the subset of 695 DEOGs were taken into account (see Figure 5.2A and Figure 5.2C for *O. novo-ulmi*, and Figure 5.2B and Figure 5.2D for *P. flocculosa*). In all cases, the transcriptional variation among biological replicates was low and samples clustered clearly according to the growth phase in the same positions, which were incidentally almost symmetrical between the two species.

In line with the latter observation, the general examination of the DEOG showed that 84% of the genes followed a similar expression pattern in the two species during the G-to-F transition (Table 5.2). A subset of 198 genes were significantly more expressed during filamentation (Fold-change ≥ 2; FDR p-value ≤ 0.01), compared to 386 genes during the germination phase.

5.5.2 Shared Differentially Expressed Orthologous Genes

Based on the gene ontology (GO) annotation of *O. novo-ulmi* genes, we first assessed the GO terms associated to the DEOGs that were downregulated or upregulated during the G-to-F transition in both species. In the portion of downregulated genes (*n*=386, Table 5.2), we mostly found terms related to biological processes such as gene expression, translation, post-transcriptional regulation of gene expression as well as ribosome biogenesis (Suppl. Table 2). By annotation screening, we found 117 DEOGs involved in ribosome biogenesis or ribosome metabolism (in green, columns L and M in Table S5.1). These genes were all downregulated in both species during the G-to-F transition.

Not surprisingly, in the portion of upregulated genes (*n*=198, Table 5.2), we found terms related to cell division (cell cycle, DNA replication and vacuolar transport). Consistent with the downregulation of genes playing roles in the gene expression process, we also highlighted an overrepresentation of genes involved in the negative regulation of gene expression (Table S5.3).

5.5.2.1 Details in categories

5.5.2.1.1 CAZymes

Among the orthologous genes encoding Carbohydrate Activated Enzymes (CAZymes), 16 genes were DEGs in *O. novo-ulmi* and *P. flocculosa* (Table 5.3, columns Q and R in Table S5.1), including 8 Glycoside Hydrolase- (GH) and 8 GlycosylTransferase (GT) encoding genes. The expression regulation was highly conserved among these genes. In fact, only three

genes encoding CAZymes showed contrasted transcriptional profiles (OrthoG2085, OrthoG3323 and OrthoG3738, Table S5.1). In *P. flocculosa*, these three genes were downregulated, whereas they were upregulated in *O. novo-ulmi.*

5.5.2.1.2 Transcription factors

We found 60 genes encoding transcription factors (TF) in *O. novo-ulmi* that have orthologous genes in *P. flocculosa* and 104 genes annotated as encoding TFs in *P. flocculosa* that have orthologous genes in *O. novo-ulmi*. Out of this set, only four genes were annotated as coding for TFs and DEOGs in both species (Table S5.1). In *P. flocculosa*, all the four DEOGs were downregulated in the G-to-F transition. By contrast, OrthoG813 and OrthoG2898 were upregulated in *O. novo-ulmi*. The second gene was annotated as coding for a homolog of the transcriptional corepressor SSN6.

5.5.2.1.3 Genes known to be involved in dimorphism in *S. cerevisiae*

Finally, we investigated the regulation of gene expression in *O. novo-ulmi* and *P. flocculosa* orthologs of some *S. cerevisiae* genes known to play a role in the yeast-to-pseudohypha transition and to be involved in the MAPK, cAMP-PKA and pH-response pathways (column N in Table S5.1). These genes had previously been studied in *O. novo-ulmi* (Nigg and Bernier 2016). Here, we found 13 orthologous genes common to *O. novo-ulmi, P. flocculosa* and *S. cerevisiae*. The only DEG in *O. novo-ulmi and P. flocculosa* was the ortholog of *Sho1* (Ortho3070). This gene was upregulated in *O. novo-ulmi* but downregulated in *P. flocculosa*. In *P. flocculosa*, we also found the ortholog of *Phd1* (OrthoG2030) which was downregulated. In *O. novo-ulmi*, orthologs of *Hog1*, *Ste11*, *Msn4* were upregulated during the G-to-F transition. Potential activation of the MAPK cascade in *O. novo-ulmi* has been already described by Nigg and Bernier (2016).

5.5.2.1.4 Kinases

In the set of differentially expressed genes, 14 orthologous genes were encoding kinases (Table 5.3, columns O and P in Table S5.1). Except for OrthoG2000 and OrthoG3646, the remaining 12 genes showed a conserved regulation of expression between *O. novo-ulmi* and *P. flocculosa*.

Among the eight genes encoding kinases that were upregulated during the G-to-F transition in both species, we found OrthoG441 (20 times upregulated in *O. novo-ulmi* and nine times upregulated in *P. flocculosa*). This gene codes for a serine/threonine kinase. Comparison by blastp in the NCBI database (www.ncbi.nlm.nih.gov) revealed homologies with the calcium-calmoduline kinase known as CaMK/CaMKL/GIN4.

We also found an ortholog of the gene *Cot1* (OrthoG1606) involved in filamentous growth in *Neurospora crassa* (Collinge and Trinci 1974; Steele and Trinci 1977; Collinge *et al.* 1978). COT1 interacts with kinases MAK1 and MAK2 (Pandey *et al.* 2004; Seiler *et al.* 2006; Maerz *et al.* 2008). Searches for homologies with the latter two proteins by blastp revealed that MAK1 shares 85% identity with the predicted Onu1780p sequence and MAK2 is a homolog of Onu8395p (96% of identity in predicted sequences) (data not shown). *Ophiostoma novo-ulmi* gene OnuG1780 is orthologous to *P. flocculosa* PFL1_06284 and corresponds to OrthoG3514, whereas gene OnuG8395 is orthologous to PFL1_05549 and corresponds to OrthoG3114. OrthoG3514 was not differentially expressed during the G-to-F transition in *O. novo-ulmi* nor in *P. flocculosa*. By contrast, OrthoG3114 was upregulated in both species during the transition.

Another gene, which was highly upregulated, is OrthoG3106 (four times in *O. novo-ulmi* and 16 times in *P. flocculosa*). This gene is annotated in *O. novo-ulmi* (OnuG6001) as coding for a Polo-Like Kinase (PLK). We found 47% predicted protein identity between PFL1_05533p and the PLK Cdc5 of *C. albicans*. Furthermore, we found OrthoG3491, which is encoding a potential aurora-related kinase (ARK). This orthologous gene was upregulated in both species (4.5 times in *P. flocculosa* and 3.2 times in *O. novo-ulmi*) during the G-to-F switch.

5.6 Discussion

The genes involved in the regulation of the yeast-to-hypha switch in fungi have been shown to be mostly conserved among fungal species like *S. cerevisiae, C. albicans* and *U. maydis*, although the mechanisms could diverge (Mitchell 1998; Lengeler *et al.* 2000; Sánchez-Martínez and Pérez-Martín 2001; Nemecek *et al.* 2006; Nadal *et al.* 2008; Shively *et al.* 2013). In order to investigate the conservation of the molecular processes involved in the morphological switch in less studied species, we present here a comparative transcriptomic analysis of this transition in *O. novo-ulmi*, an ascomycete and *P. flocculosa*, a basidiomycete.

We focused our attention on orthologous genes that were differentially regulated in the two species during this morphological change.

Genome-wide consideration of gene expression shows clear molecular distinctions between the growth stages taken in consideration in our study, confirming a major transcriptomic rewiring during the dimorphic switch common to the two species. A closer look at the patterns of gene expression shared between *O. novo-ulmi* and *P. flocculosa* suggests that the conservation of molecular regulation of the yeast-to-hypha switch mainly involves genes that are downregulated during the change between germinating yeast cell to filamentous growth. Actually, a large proportion of the genes that were downregulated in both species during the G-to-F transition are associated with ribosomal activity. This suggests that, for both species, the filamentation process is correlated with reduced ribosomal biogenesis and activity. This phenomenon may impact the transcription and translation machineries. By GO term enrichment on the portion of DEOGs that are downregulated during the G-to-F transition in both species, we highlighted overrepresentation of genes involved in biological processes such as translation, gene expression, post-transcriptional regulation of gene expression and protein metabolic process (see Table S5.2). Interestingly, the GO term enrichment analysis of the portion of DEOGs that were upregulated in both species points toward an induction of genes involved in the negative regulation of gene expression. This association supports the hypothesis of a downregulation of transcription and protein synthesis during the morphological switch in *O. novo-ulmi* and *P. flocculosa*. These results are in line with the transcriptomic variations observed during the whole yeast-to-hypha transition in *O. novo-ulmi* (Nigg and Bernier 2016). Interestingly, the opposite process was observed in *C. albicans* (Carlisle and Kadosh 2012) and *P. brasiliensis* (Nunes *et al.* 2005) where protein production was reduced in the mycelium to yeast transition. As recently proposed by Nigg and Bernier (2017), further quantifications of protein content in the unicellular phase, the mycelium phase and during the transition from the unicellular phase to filamentous growth are needed to confirm these observations.

Morphological changes induce large remodeling of the fungal cell wall (FCW). Glycoside hydrolases (GH), in particular, are known to degrade FCW by acting on the carbohydrate compounds, especially glucans, chitin, galactomannan and galactosaminogalactan. By

contrast, glycosyl-transferases (GT) are responsible for carbohydrate biosynthesis. In pathogenic fungi, the capacity of FCW reorganization differs depending on lifestyle. Hence, necrotrophic and biotrophic fungi do not require the same set of enzymes during host infection (Lyu et al 2015). There are 311 genes assigned to the CAZy family in *O. novo-ulmi* (Comeau *et al.* 2015) and 240 in *P. flocculosa* (Lefebvre *et al.* 2013). Even though *P. flocculosa* is not a plant pathogen, cell wall degrading enzymes, cellulases and xylanases were found in its genome in the same proportion as observed in pathogenic Ustilaginales (Lefebvre *et al.* 2013). Most of the orthologous CAZyme encoding genes that are DEGs were upregulated in both species, suggesting a conserved activation of CAZymes during the G-to-F switch. Accordingly, there appears to a conservation of expression regulation for some of the genes encoding GH and GT between *O. novo-ulmi* and *P. flocculosa,* in spite of their different lifestyles.

MAPK and cAMP pathways are known to be key molecular components involved in the dimorphic switch of model fungal species (Gold *et al.* 1994; Madhani and Fink 1997; Krüger *et al.* 1998; Lengeler *et al.* 2000; Martínez-Espinoza *et al.* 2004; Nadal *et al.* 2008; Hamel *et al.* 2012). Sho1 is an osmoreceptor acting upstream of the MAPK cascade involved in morphological changes in *S. cerevisiae* (Cullen and Sprague 2012). The MAPK pathway has been shown to be involved in the dimorphic transition in *U. maydis* where it is necessary to the mating process leading to the formation of the dikaryotic hyphae necessary for infection (Banuett and Herskowitz 1994). The downregulation of the gene orthologous to *Sho1* in *P. flocculosa* suggests a potential repression of the MAPK pathway. This may explain why, in *P. flocculosa,* mating does not or cannot occur (Lefebvre et al 2013), and morphological change is achieved without the need for switching from a monokaryotic to a dikaryotic structure (Hammami *et al.* 2008). This would bring further sense to the fact that, even though the actors of the conserved MAPK pathway, i.e *Ste20*, *Ste11*, *Hog1*, *Msn4* etc., are found expressed in *P. flocculosa*, none of them are DEGs during the G-to-F transition. By contrast, *Sho1*, *Ste11*, *Msn4* and *Hog1* are all DEGs in *O. novo-ulmi*, supporting a role for these genes in the filamentation process. These results not only highlight a potential divergence between *P. flocculosa* and *O. novo-ulmi* but also suggest an alternative pathway in *P. flocculosa* compared to the mechanisms proposed for the dimorphic switch in *U. maydis*. Acquisition

of this distinctive pathway in *P. flocculosa* needs to confirmed by specific analyses of the roles of the orthologous genes of the MAPK pathway in *P. flocculosa*.

The APSES transcriptional regulator PHD1 is known to be downstream of the cAMP cascade (Brown and Gow 1999; Pan and Heitman 1999). In *C. albicans*, filamentous growth is inhibited by deletion of the homolog of *Phd1*, *Efg1* (Lo *et al.* 1997). Overexpression of this gene in *S. cerevisiae* leads to increased induction of pseudo-hyphal growth in diploid strains (Gimeno and Fink 1994). In *A. nidulans*, the APSES StuA protein is required for conidiophore morphogenesis (Miller *et al.* 1992) and sexual reproductive cycle (Clutterbuck 1969). In *U. maydis*, disruption of the cAMP pathway in a haploid strain induces constitutive filamentous growth (Gold *et al.* 1994). The homologous gene of *StuA* in *U. maydis*, *Ust1*, is a critical regulator of morphogenesis and virulence. It is required for unicellular budding growth (García-Pedrajas *et al.* 2010). However, it is thought to act in parallel to the cAMP-PKA pathway instead of downstream as *Efg1* in *C. albicans* (Baeza-Montañez *et al.* 2015). The *P. flocculosa Phd1* orthologous gene is downregulated during the G-to-F transition. This result is consistent with the cAMP regulation in *U. maydis* where the repression of the cAMP-PKA pathway leads to yeast-to-hyphal transition (Gold *et al.* 1994). By contrast, this gene was not found to be differentially expressed in *O. novo-ulmi*. Nigg and Bernier (2016) showed a modulation of *Phd1* expression during the early stages of dimorphic changes, suggesting a regulatory role of *Phd1* in the morphological switch prior to germination. Those results were concomitant with the regulation by the cAMP-PKA of the dimorphic switch in the ascomycete *C. albicans*. In this study, we highlighted a potential conservation of the role of the cAMP-PKA pathway among basidiomycetes, or at least Ustilaginales, even though further investigations of the impact of cAMP levels on the filamentation process in *P. flocculosa* are needed to validate this hypothesis.

The protein SSN6 is known in *S. cerevisiae* and *C. albicans* to interact with the negative regulator TUP1 (Keleher *et al.* 1992; Hwang *et al.* 2003). In *C. albicans*, however, it has been shown that SSN6, on its own, plays an important role in the dimorphic switch and the regulation of filamentation. *Ssn6* expression level was found to decline during hyphal development (Hwang *et al.* 2003). Deletion of *Ssn6* in *C. albicans* induces increased filamentous growth in response to high temperature (37°C). However, overexpression of

Ssn6 leads also to enhanced filamentous growth and reduced virulence at 28°C. These results infer that SSN6 functions as a repressor as well as an activator of hyphal development (Hwang *et al.* 2003; Huang 2012). The functional homolog of SSN6 in *U. maydis*, SQL1, antagonizes the cAMP signaling during filamentation (Loubradou *et al.* 2001). The orthologous gene of *Ssn6* is upregulated in both *O. novo-ulmi* and *P. flocculosa*. Whereas this overexpression in *P. flocculosa* is consistent with a downregulation of the cAMP pathway and the antagonist role of Sql1 in *U. maydis*, SSN6 function in *O. novo-ulmi* is not as clear with respect to the repression of cAMP pathway since this molecular cascade seems to be activated during the yeast-to-mycelium switch in *O. novo-ulmi* (Muthukumar *et al.* 1985; Nigg and Bernier 2016).

Because of their central roles in growth, cell cycle control, cellular differentiation and development as well as response to stress, kinase-encoding genes beyond those related to the MAPK pathway were investigated. As a result, we identified four types of kinases potentially involved in the dimorphic switch of both *O. novo-ulmi* and *P. flocculosa*: the Nuclear Dbf2p-related (NDR) kinases, the calcium-calmoduline kinase GIN4, the Polo-like (PLK) kinases and the Aurora-like kinases.

The NDR kinases are known in many living species to influence processes such as morphological changes, cell differentiation and polar morphogenesis (Hergovich *et al.* 2006). In particular, NDR kinases have been studied in several filamentous fungi such as *N. crassa*, *Aspergillus nidulans*, *Cladiceps purpurea*, *Cryptoccocus neoformans*, *U. maydis*, *Colletotrichum trifolii* and, recently, *Colletotrichum higginsianum* (Dürrenberger and Kronstad 1999; Chen and Dickman 2002; Scheffer *et al.* 2005; Johns *et al.* 2006; Ziv *et al.* 2009; Schmidpeter *et al.* 2017). Two highly conserved protein networks are related to two different NDR kinases named the MORphogenesis related NDR kinase network (MOR) and the Septation Initiation Network (SIN) (Maerz *et al.* 2009; Maerz and Seiler 2010). The MOR network regulates polar tip extension and branching of hyphae and is articulated around a central NDR kinase, known as COT1 in *N. crassa*, which forms a complex with two redundant regulatory subunits (MOB2A and MOB2B) (Maerz *et al.* 2009).

In *N. crassa*, the temperature sensitive colonial mutant *cot1* is affected in hyphal extension, branching and septation (Steele and Trinci 1977; Collinge *et al.* 1978). The *U. maydis Cot1*

homolog, *ukc1*, has been found to be essential for pathogenesis and involved production of aerial filaments during mating, and hyphal morphology (Dürrenberger and Kronstad 1999). In *C. albicans*, the *Cot1* homolog, *Cbk1*, and its activator *Mob2* are required for hyphal formation and yeast-to-hypha transition under switch-promoting conditions (McNemar and Fonzi 2002; Song *et al.* 2008). Here, we pointed out an upregulation of the common homolog of *Cot1* in *O. novo-ulmi* and *P. flocculosa* during the filamentation process but searches for orthologies with *Mob-2A* of *N. crassa* in *O. novo-ulmi* and *P. flocculosa* revealed no common ortholog for this gene. In *N. crassa*, the COT1 pathway is linked with the two pathways dependent on the MAK1 and MAK2 MAP kinases (Maerz *et al.* 2008). *Ophiostoma novo-ulmi* and *P. flocculosa* share orthologous genes to *Mak1* and *Mak2*. No differential expression was found for the ortholog of *Mak1*, but *Mak2* orthologous gene is upregulated during the G-to-F transition. This study presents the first report of homologs of *Cot1* and *Mak2* in both species, results suggesting that they play a role in the morphological change.

In *C. albicans*, the GIN4 kinase negatively regulates pseudohyphal growth and the switch to hyphae. It also controls the septin ring organization (Wightman *et al.* 2004). In *Fusarium graminearum*, GIN4 kinase is involved in sexual development, hyphal growth, conidiogenesis, septation and virulence (Wang *et al.* 2011; Yu *et al.* 2017). In *Aspergillus nidulans*, GIN4 homolog is involved in asexual spore production and the negative regulation of the developmental switch form asexual to sexual reproduction (De Souza *et al.* 2013). Similarly, we identified an orthologous gene shared by *O. novo-ulmi* and *P. flocculosa* that bear sequence similarities with *Gin4*. This ortholog was highly upregulated during the G-to-F transition in both species, suggesting a potential role in asexual filamentation.

Like GIN4 kinase, the Polo-Like Kinase PlkA is known to play important roles in vegetative growth and sexual development in *A. nidulans* (Mogilevsky *et al.* 2012; De Souza *et al.* 2013). In *C. albicans*, the PLK Cdc5 is involved in the cell cycle and nuclear division. Repression of *Cdc5* expression induces the production of hyphal structures in yeast growth conditions (Bachewich *et al.* 2003). In *O. novo-ulmi* and *P. flocculosa*, the homolog of the PLK encoding gene is highly overexpressed in the filamentous stage versus the germination phase, which would indicate that the gene is also involved in hyphal production in both species.

Finally, Aurora-like kinases are essential in many fungal species such as *S. cerevisiae* or *C. albicans* as they are involved in the mitotic process and centrosome separation (Nigg 2001). Again, in *O. novo-ulmi* and *P. flocculosa*, we found one orthologous gene annotated as an Aurora-like kinase. Upregulation of this gene thus appears to be correlated with the activation of the cell cycle highlighted in the GO term enrichment analysis.

Overall, we identified homologs for several types of genes coding for kinases whose roles are linked to the dimorphic switch. PLKs, Aurora-like kinases and GIN4 kinase are all involved in cell division, cell cycle and hyphal growth. Our results thus suggest a great conservation of gene expression regulation of these genes between two fungi belonging to separate phyla.

In conclusion, the transcriptomic comparison of the transition from germinating yeast-like cells to filamentous growth in *O. novo-ulmi* and *P. flocculosa* suggest that the dimorphic behavior of these two unrelated fungi is linked to the downregulation of gene expression and protein synthesis, as well as to a set of conserved genes involved in key steps of the cell cycle, cell division and hyphal development (Figure 5.3). The potential divergence in the involvement of the MAPK and the cAMP pathways in the two species suggest that, even though the component of these signal cascades are present, their role in the morphological switch may vary. While transcriptomic regulations of the yeast-to-hypha transition in *O. novo-ulmi* are compatible with observations made in model ascomycete dimorphic fungi, patterns of expression in *P. flocculosa* were not systematically similar with known events in Ustilaginales. This observation may reflect the lack of mating capabilities in *P. flocculosa* or a higher divergence of molecular regulation in Basidiomycota than in Ascomycota. Regardless of the phylogenetic link, our results have highlighted a conservation of essential genes and core components of the cellular processes that are linked to the yeast-to-hypha switch.

5.7 Acknowledgements

This work was supported, on one hand, by the Natural Sciences and Engineering Research Council of Canada (NSERC, Discovery Grant 105519 to L. Bernier). On the other hand, this research was founded by grants from the NSERC, le Fonds de recherche du Québec - Nature et technologies (FRQNT) and the Canada Research Chairs Program to R. R. Bélanger

5.8 Bibliography

Altschul SF, Gish W, Miller W, Myers EW, Lipman DJ, 1990. Basic Local Alignment Search Tool. *Journal of Molecular Biology* **215**: 403–410.

Bachewich C, Thomas DY, Whiteway M, 2003. Depletion of a polo-like kinase in *Candida albicans* activates cyclase-dependent hyphal-like growth. *Mol Biol Cell* **14**: 2163–2180.

Baeza-Montañez L, Gold SE, Espeso EA, García-Pedrajas MD, 2015. Conserved and distinct functions of the "Stunted" (StuA)-homolog Ust1 during cell differentiation in the corn smut fungus *Ustilago maydis*. *Molecular Plant-Microbe Interactions* **28**: 86–102.

Banuett F, Herskowitz I, 1994. Identification of Fuz7, a *Ustilago maydis* MEK / MAPKK homolog required steps in the fungal life cycle. *Genes and Development* **8**: 1367–1378.

Begerow D, Bauer R, Boekhout T, 2000. Phylogenetic placements of ustilaginomycetous anamorphs as deduced from nuclear LSU rDNA sequences. *Mycological Research* **104**: 53–60.

Bernier L, Hubbes M, 1990. Mutations in *Ophiostoma ulmi* induced by N-methyl-N '-nitro-N-nitrosoguanidine. *Canadian Journal of Botany* **68**: 225–231.

Bölker M, 2001. *Ustilago maydis* - A valuable model system for the study of fungal dimorphism and virulence. *Microbiology* **147**: 1395–1401.

Brown AJP, Gow NAR, 1999. Regulatory networks controlling *Candida albicans* morphogenesis. *Trends in microbiology* **7**: 333–338.

Carlisle PL, Kadosh D, 2012. A genome-wide transcriptional analysis of morphology determination in *Candida albicans*. *Molecular biology of the cell* **24**: 246–60.

Chattaway FW, Bishop R, Holmes MR, Odds FC, Barlow a J, 1973. Enzyme activities associated with carbohydrate synthesis and breakdown in the yeast and mycelial forms of *Candida albicans*. *Journal of general microbiology* **75**: 97–109.

Chen C, Dickman MB, 2002. *Colletotrichum trifolii* TB3 kinase, a COT1 homolog, is light inducible and becomes localized in the nucleus during hyphal elongation. *Eukaryotic Cell* **1**: 626–633.

Clutterbuck AJ, 1969. A mutational analysis of conidial development in *Aspergillus nidulans*. *Genetics* **63**: 317–327.

Collinge AJ, Fletcher MH, Trinci APJ, 1978. Physiology and cytology of septation and branching in a temperature-sensitive colonial mutant (*cot* 1) of *Neurospora crassa*. *Transactions of the British Mycological Society* **71**: 107–120.

Collinge AJ, Trinci APJ, 1974. Hyphal tips of wild-type and spreading colonial mutants of *Neurospora crassa*. *Archives of Microbiology* **99**: 353–368.

Comeau AM, Dufour J, Bouvet GF, Jacobi V, Nigg M, Henrissat B, Laroche J, Levesque RC, Bernier L, 2015. Functional annotation of the *Ophiostoma novo-ulmi* genome: insights into the phytopathogenicity of the fungal agent of Dutch elm disease. *Genome biology and evolution* **7**: 410–430.

Cullen PJ, Sprague GF, 2012. The regulation of filamentous growth in yeast. *Genetics* **190**: 23–49.

Domer JE, Hamilton JG, Harkin JC, 1967. Comparative study of the cell walls of the yeastlike and mycelial phases of Histoplasma capsulatum. *Journal of Bacteriology* **94**: 466–474.

Dürrenberger F, Kronstad J, 1999. The *ukc1* gene encodes a protein kinase involved in morphogenesis, pathogenicity and pigment formation in *Ustilago maydis*. *Molecular and General Genetics* **261**: 281–289.

Forgetta V, Leveque G, Dias J, Grove D, Lyons R, Genik S, Wright C, Singh S, Peterson N, Zianni M, Kieleczawa J, Steen R, Perera A, Bintzler D, Adams S, Hintz W, Jacobi V, Bernier L, Levesque R, Dewar K, 2013. Sequencing of the Dutch elm disease fungus genome using the Roche/454 GS-FLX Titanium System in a comparison of multiple genomics core facilities. *Journal of biomolecular techniques* **24**: 39–49.

García-Pedrajas MD, Baeza-Montañez L, Gold SE, 2010. Regulation of *Ustilago maydis* dimorphism, sporulation, and pathogenic development by a transcription factor with a highly conserved APSES domain. *Molecular plant-microbe interactions : MPMI* **23**: 211–22.

Gimeno CJ, Fink GR, 1994. Induction of pseudohyphal growth by overexpression of *PHD1*, a *Saccharomyces cerevisiae* gene related to transcriptional regulators of fungal development. *Molecular and cellular biology* **14**: 2100–2112.

Gold S, Duncan G, Barrett K, Kronstad J, 1994. cAMP regulates morphogenesis in the fungal pathogen *Ustilago maydis*. *Genes and Development* **8**: 2805–2816.

Hamel L-P, Nicole M-C, Duplessis S, Ellis BE, 2012. Mitogen-activated protein kinase signaling in plant-interacting fungi: distinct messages from conserved messengers. *The Plant cell* **24**: 1327–51.

Hammami W, Labbé C, Chain F, Mimee B, Bélanger RR, 2008. Nutritional regulation and kinetics of flocculosin synthesis by *Pseudozyma flocculosa*. *Applied Microbiology and Biotechnology* **80**: 307–315.

Hergovich A, Stegert MR, Schmitz D, Hemmings BA, 2006. NDR kinases regulate essential cell processes from yeast to humans. *Nature reviews. Molecular cell biology* **7**: 253–64.

Huang G, 2012. Regulation of phenotypic transitions in the fungal pathogen *Candida albicans*. *Virulence* **3**: 251–261.

Hwang CS, Oh JH, Huh WK, Yim HS, Kang SO, 2003. Ssn6, an important factor of morphological conversion and virulence in *Candida albicans*. *Molecular Microbiology* **47**: 1029–1043.

Jantzen SG, Sutherland BJ, Minkley DR, Koop BF, 2011. GO Trimming: Systematically reducing redundancy in large Gene Ontology datasets. *BMC research notes* **4**: 267.

Johns SA, Leeder AC, Safaie M, Turner G, 2006. Depletion of *Aspergillus nidulans cotA* causes a severe polarity defect which is not suppressed by the nuclear migration mutation nudA2. *Molecular Genetics and Genomics* **275**: 593–604.

Keleher CA, Redd MJ, Schultz J, Carlson M, Johnson AD, 1992. Ssn6-Tup1 is a general repressor of transcription in yeast. *Cell* **68**: 709–719.

Krüger J, Loubradou G, Regenfelder E, Hartmann A, Kahmann R, 1998. Crosstalk between cAMP and phermone signalling pathways in *Ustilago maydis*. *Molecular and General Genetics* **260**: 193–198.

Kulkarni RK, Nickerson KW, 1981. Nutritional control of dimorphism in *Ceratocystis ulmi*. *Experimental Mycology* **5**: 148–154.

Lefebvre F, Joly DL, Labbé C, Teichmann B, Linning R, Belzile F, Bakkeren G, Bélanger RR, 2013. The transition from a phytopathogenic smut ancestor to an anamorphic biocontrol agent deciphered by comparative whole-genome analysis. *The Plant cell* **25**: 1946–59.

Lengeler KB, Davidson RC, D'Souza C, Harashima T, Shen WC, Wang P, Pan X, Waugh M, Heitman J, 2000. Signal transduction cascades regulating fungal development and virulence. *Microbiology and molecular biology reviews* **64**: 746–85.

Lo HJ, Köhler JR, Didomenico B, Loebenberg D, Cacciapuoti A, Fink GR, 1997. Nonfilamentous *C. albicans* mutants are avirulent. *Cell* **90**: 939–949.

Loubradou G, Brachmann A, Feldbrügge M, Kahmann R, 2001. A homologue of the transcriptional repressor Ssn6p antagonizes cAMP signalling in *Ustilago maydis*. *Molecular Microbiology* **40**: 719–730.

Madhani HD, Fink GR, 1997. Combinatorial control required for the specificity of yeast MAPK signaling. *Science* **275**: 1314–1317.

Madhani HD, Fink GR, 1998. The control of filamentous differentiation and virulence in fungi. *Trends in Cell Biology* **8**: 348–353.

Maerz S, Dettman A, Zic C, Liu Y, Valerius O, Yarden O, 2009. Two NDR kinase–MOB complexes function as distinct modules during septum formation and tip extension in *Neurospora crassa*. *Molecular M* **74**: 707–723.

Maerz S, Seiler S, 2010. Tales of RAM and MOR: NDR kinase signaling in fungal

morphogenesis. *Current Opinion in Microbiology* **13**: 663–671.

Maerz S, Ziv C, Vogt N, Helmstaedt K, Cohen N, Gorovits R, Yarden O, Seiler S, 2008. The nuclear Dbf2-related kinase COT1 and the mitogen-activated protein kinases MAK1 and MAK2 genetically interact to regulate filamentous growth, hyphal fusion and sexual development in *Neurospora crassa*. *Genetics* **179**: 1313–1325.

Martínez-Espinoza AD, Ruiz-Herrera J, León-Ramírez CG, Gold SE, 2004. MAP kinase and cAMP signaling pathways modulate the pH-induced yeast-to-mycelium dimorphic transition in the corn smut fungus *Ustilago maydis*. *Current microbiology* **49**: 274–81.

Mayorga ME, Gold SE, 1999. A MAP kinase encoded by the ubc3 gene of *Ustilago maydis* is required for filamentous growth and full virulence. *Molecular Microbiology* **34**: 485–497.

McNemar MD, Fonzi WA, 2002. Conserved serine/threonine kinase encoded by CBK1 regulates Expression of several hypha-associated transcripts and genes encoding cell wall proteins in *Candida albicans*. *Journal of Bacteriology* **184**: 2058–2061.

Miller KY, Wu JG, Miller BL, 1992. StuA is required for cell pattern-formation in *Aspergillus*. *Genes and Development* **6**: 1770–1782.

Mitchell AP, 1998. Dimorphism and virulence in *Candida albicans*. *Current opinion in microbiology* **1**: 687–92.

Mogilevsky K, Glory A, Bachewich C, 2012. The polo-like kinase PLKA in *Aspergillus nidulans* is not essential but plays important roles during vegetative growth and development. *Eukaryotic Cell* **11**: 194–205.

Muthukumar G, Kulkarni RK, Nickerson KW, 1985. Calmodulin levels in the yeast and mycelial phases of Ceratocystis ulmi. *Journal of bacteriology* **162**: 47–9.

Nadal M, García-Pedrajas MD, Gold SE, 2008. Dimorphism in fungal plant pathogens. *FEMS microbiology letters* **284**: 127–34.

Nemecek JC, Wüthrich M, Klein BS, 2006. Global control of dimorphism and virulence in fungi. *Science (New York, N.Y.)* **312**: 583–8.

Nigg EA, 2001. Mitotic kinases as regulators of cell division and its checkpoints. *Nature reviews. Molecular cell biology* **2**: 23–32.

Nigg M, Bernier L (2017) Large-scale genomic analyses of in vitro yeast-mycelium dimorphism in human, insect and plant pathogenic fungi: from ESTs to RNAseq experiments. *Fungal Biology Reviews*. Doi: 10.1016/j.fbr.2017.04.001

Nigg M, Bernier L, 2016. From yeast to hypha: defining transcriptomic signatures of the morphological switch in the dimorphic fungal pathogen *Ophiostoma novo-ulmi*. *BMC Genomics* **17**: 920.

Nigg M, Laroche J, Landry CR, Bernier L, 2015. RNAseq analysis highlights specific transcriptome signatures of yeast and mycelial growth phases in the Dutch elm disease fungus *Ophiostoma novo-ulmi*. *G3 Genes|Genomes|Genetics* **5**: 2487–2495.

Nunes LR, Costa de Oliveira R, Batista Leite D, Schmidt da Silva V, dos Reis Marques E, da Silva Fereira ME, Duarte Ribeiro DC, de Souza Bernardes LA, Goldman HMS, Puccia R, Travassos LR, Batista WL, Nóbrega MP, Nobrega, FG, Yang D-Y, De Bragança Pereira CA, Goldman, GH 2005. Transcriptome analysis of *Paracoccidioides brasiliensis* cells undergoing mycelium-to-yeast. *Eukaryotic cell* **4**: 2115–2128.

Pan X, Heitman J, 1999. Cyclic AMP-dependent protein kinase regulates pseudohyphal differentiation in *Saccharomyces cerevisiae*. *Molecular and cellular biology* **19**: 4874–87.

Pandey A, Roca MG, Read ND, Glass NL, 2004. Role of a Mitogen-Activated Protein Kinase pathway during conidial germination and hyphal fusion in *Neurospora crassa*. *Eukaryotic Cell* **3**: 348–358.

Sánchez-Martínez C, Pérez-Martín J, 2001. Dimorphism in fungal pathogens: *Candida albicans* and *Ustilago maydis*--similar inputs, different outputs. *Current opinion in microbiology* **4**: 214–21.

Scheffer J, Ziv C, Yarden O, Tudzynski P, 2005. The COT1 homologue CPCOT1 regulates polar growth and branching and is essential for pathogenicity in *Claviceps purpurea*. *Fungal Genetics and Biology* **42**: 107–118.

Schmidpeter J, Dahl M, Hofmann J, Koch C, 2017. ChMob2 binds to ChCbk1 and promotes virulence and conidiation of the fungal pathogen *Colletotrichum higginsianum*. *BMC Microbiology* **17**: 22.

Seiler S, Vogt N, Ziv C, Gorovits R, Yarden O, 2006. The STE20/germinal center kinase POD6 interacts with the NDR kinase COT1 and is involved in polar tip extension in *Neurospora crassa*. *Molecular biology of the cell* **17**: 4080–4092.

Shively CA, Eckwahl MJ, Dobry CJ, Mellacheruvu D, Nesvizhskii A, Kumar A, 2013. Genetic networks inducing invasive growth in *Saccharomyces cerevisiae* identified through systematic genome-wide overexpression. *Genetics* **193**: 1297–310.

Song Y, Cheon SA, Lee KE, Lee S-Y, Lee B-K, Oh D-B, Kang HA, Kim J-Y, 2008. Role of the RAM network in cell polarity and hyphal morphogenesis in *Candida albicans*. *Molecular biology of the cell* **19**: 5456–5477.

De Souza CP, Hashmi SB, Osmani AH, Andrews P, Ringelberg CS, Dunlap JC, Osmani SA, 2013. Functional analysis of the Aspergillus nidulans kinome. *PLoS ONE* **8**: e58008.

Steele GC, Trinci APJ, 1977. Effect of temperature and temperature shifts on growth and branching of a wild type and a temperature sensitive colonial mutant (*Cot* 1) of

Neurospora crassa. *Archives of Microbiology* **113**: 43–48.

Supek F, Bošnjak M, Škunca N, Šmuc T, 2011. REVIGO summarizes and visualizes long lists of gene ontology terms. *PLoS ONE* **6**: e21800. /10.

Traquair JA, Shaw LA, Jarvis WR, 1988. New species of *Stephanoascus* with *Sporothrix* anamorphs. *Canadian Journal of Botany* **66**: 926–933.

Wang C, Zhang S, Hou R, Zhao Z, Zheng Q, Xu Q, Zheng D, Wang G, Liu H, Gao X, Ma JW, Kistler HC, Kang Z, Xu JR, 2011. Functional analysis of the kinome of the wheat scab fungus *Fusarium graminearum*. *PLoS Pathogens* **7**: e1002460.

Wedge M-E, Naruzawa ES, Nigg M, Bernier L, 2016. Diversity in yeast – mycelium dimorphism response of the Dutch elm disease pathogens : the inoculum size effect. *Canadian Journal of Microbiology* **62**: 1–5.

Wickham H, 2009. *ggplot2: elegant graphics for data analysis.* New York.

Wightman R, Bates S, Amornrrattanapan P, Sudbery P, 2004. In *Candida albicans*, the Nim1 kinases Gin4 and Hsl1 negatively regulate pseudohypha formation and Gin4 also controls septin organization. *Journal of Cell Biology* **164**: 581–591.

Young MD, Wakefield MJ, Smyth GK, Oshlack A, 2010. Gene ontology analysis for RNA-seq: accounting for selection bias. *Genome biology* **11**: R14.

Yu D, Zhang S, Li X, Xu J-R, Schultzhaus Z, Jin Q, 2017. A Gin4-like protein kinase GIL1 involvement in hyphal growth, asexual development, and pathogenesis in *Fusarium graminearum*. *International Journal of Molecular Sciences* **18**: 424.

Ziv C, Kra-Oz G, Gorovits R, März S, Seiler S, Yarden O, 2009. Cell elongation and branching are regulated by differential phosphorylation states of the nuclear Dbf2-related kinase COT1 in *Neurospora crassa*. *Molecular Microbiology* **74**: 974–989.

Table 5.1 Number of differentially expressed orthologs (DEOGs) which are upregulated (up) or downregulated (down) in *O. novo-ulmi* and *P. flocculosa*.

2-by-2 comparisons	*O. novo-ulmi*			*P. flocculosa*		
	DEOGs up	DEOGs down	Total	DEOGs up	DEOGs down	Total
G[1] vs F[2]	515	638	1153	826	1150	1976

[1]Germination
[2]Filamentation

Table 5.2 Number of differentially expressed orthologs (DEOGs) in common which are upregulated (up) or downregulated (down) in either one or the two species.

2-by-2 comparisons	Common *O. novo-ulmi*/*P. flocculosa*					
	DEOGs up/up[3]	DEOGs down/down	Total	DEOGs up/down	DEOGs down/up	Total
G[1] vs F[2]	198	386	584	47	64	111

[1]Germination
[2]Filamentation
[3]Upregulated in *O. novo-ulmi*/ upregulated in *P. flocculosa*

Table 5.3 Summary of the common DEOGs in different categories

Categories	Nb DEOGs in *P. flocculosa*	Nb DEOGs in *O. novo-ulmi*	Nb DEOGs in common
Kinases	15	21	14
CAZymes	19	16	16
Transcription factors	7	6	4

Table S5.1 List of the orthologous genes between *Ophiostoma novo-ulmi* and *Pseudozyma flocculosa* with fold changes between the germination and the filamentation phases in both species. G: germination; F: filamentation.

Available in the excel file entitled "Martha-Nigg-33585-TableS5-1.xlsx" joined with the present document.

Table S5.2 List of the enriched GO terms in the portion of orthogous genes that are downregulated in *Ophiostoma novo-ulmi* and *Pseudozyma flocculosa* in the filamentation process (annotations are based on *O. novo-ulmi* genes)

Term ID	**Description**	***p*value**	**Number of *O. novo-ulmi* DEG in cat**	**Number of *O. novo-ulmi* genes in cat**
GO:0006412	Translation	1,1E-100	132	240
GO:0008150	Biological process	6,6E-07	299	4053
GO:0008152	Metabolic process	2,7E-12	259	3059
GO:0009987	Cellular process	1,4E-22	262	2700
GO:0022613	Ribonucleoprotein complex biogenesis	6,7E-26	40	85
GO:0032501	Multicellular organismal process	1,2E-04	23	154
GO:0032502	Developmental process	6,1E-04	24	182
GO:0044707	Single-multicellular organism process	1,2E-04	23	154
GO:0071840	Cellular component organization or biogenesis	2,9E-09	52	347
GO:0032259	Methylation	6,0E-04	12	63
GO:0009058	Biosynthetic process	7,8E-47	188	1095
GO:0044238	Primary metabolic process	1,3E-30	242	2140
GO:0006807	Nitrogen compound metabolic process	2,4E-06	118	1261
GO:0071704	Organic substance metabolic process	4,8E-26	240	2239
GO:0044767	Single-organism developmental process	5,6E-04	24	181
GO:0044237	Cellular metabolic process	8,0E-40	247	1987
GO:0043038	Amino acid activation	2,5E-10	16	37
GO:0043170	Macromolecule metabolic process	2,5E-25	184	1471
GO:0045333	Cellular respiration	2,5E-03	7	30
GO:1901135	Carbohydrate derivative metabolic process	1,1E-03	29	246
GO:0046483	Heterocycle metabolic process	3,6E-06	104	1077
GO:1901564	Organonitrogen compound metabolic	3,7E-14	77	497
GO:0043094	Cellular metabolic compound salvage	5,5E-06	7	13
GO:0044281	Small molecule metabolic process	1,4E-12	79	553
GO:1901360	Organic cyclic compound metabolic process	5,6E-06	106	1112
GO:0042430	Indole-containing compound metabolic process	1,4E-04	6	14

GO:0006725	Cellular aromatic compound metabolic process	3,9E-06	104	1079
GO:0006576	Cellular biogenic amine metabolic process	2,4E-04	7	21
GO:0009308	Amine metabolic process	3,1E-03	7	31
GO:0034660	NcRNA metabolic process	2,4E-22	43	118
GO:1901137	Carbohydrate derivative biosynthetic process	8,3E-04	15	93
GO:0072527	Pyrimidine-containing compound metabolic process	2,4E-04	7	21
GO:0009165	Nucleotide biosynthetic process	4,5E-07	17	65
GO:0010467	Gene expression	2,7E-54	169	799
GO:0070408	Carbamoyl phosphate metabolic	4,2E-03	2	2
GO:0010608	Posttranscriptional regulation of gene expression	3,1E-14	16	24
GO:0044249	Cellular biosynthetic process	2,2E-49	186	1035
GO:0019538	Protein metabolic process	3,3E-44	149	732

Table S5.3 List of the enriched GO terms in the portion of orthogous genes that are upregulated in *Ophiostoma novo-ulmi* and *Pseudozyma flocculosa* in the filamentation process (annotations are based on *O. novo-ulmi* genes)

Term ID	**Description**	***p*value**	**Number of *O. novo-ulmi* DEG in cat**	**Number of *O. novo-ulmi* genes in cat**
GO:0006260	DNA replication	8,8E-07	11	57
GO:0016192	Vesicle-mediated transport	9,7E-04	10	101
GO:0007049	Cell cycle	4,2E-04	10	91
GO:0070085	Glycosylation	8,3E-05	6	25
GO:1901135	Carbohydrate derivative metabolic process	3,4E-03	16	246
GO:0030261	Chromosome condensation	8,8E-03	2	5
GO:0005975	Carbohydrate metabolic process	6,4E-03	16	263
GO:0022402	Cell cycle process	3,2E-03	7	64
GO:0051301	Cell division	1,5E-03	7	56
GO:0007034	Vacuolar transport	3,9E-03	3	11
GO:0043412	Macromolecule modification	7,0E-05	23	313
GO:0006464	Cellular protein modification process	9,9E-06	23	277
GO:0019538	Protein metabolic process	1,2E-03	37	732
GO:0045892	Negative regulation of transcription, DNA-templated	5,4E-05	4	8
GO:0009100	Glycoprotein metabolic process	2,8E-05	6	21
GO:0042158	Lipoprotein biosynthetic process	6,5E-03	3	13
GO:0042157	Lipoprotein metabolic process	6,5E-03	3	13
GO:1901137	Carbohydrate derivative biosynthetic process	5,0E-04	10	93
GO:0040029	Regulation of gene expression,	9,1E-04	3	7
GO:0006465	Signal peptide processing	5,4E-03	2	4
GO:0006259	DNA metabolic process	6,9E-07	20	185

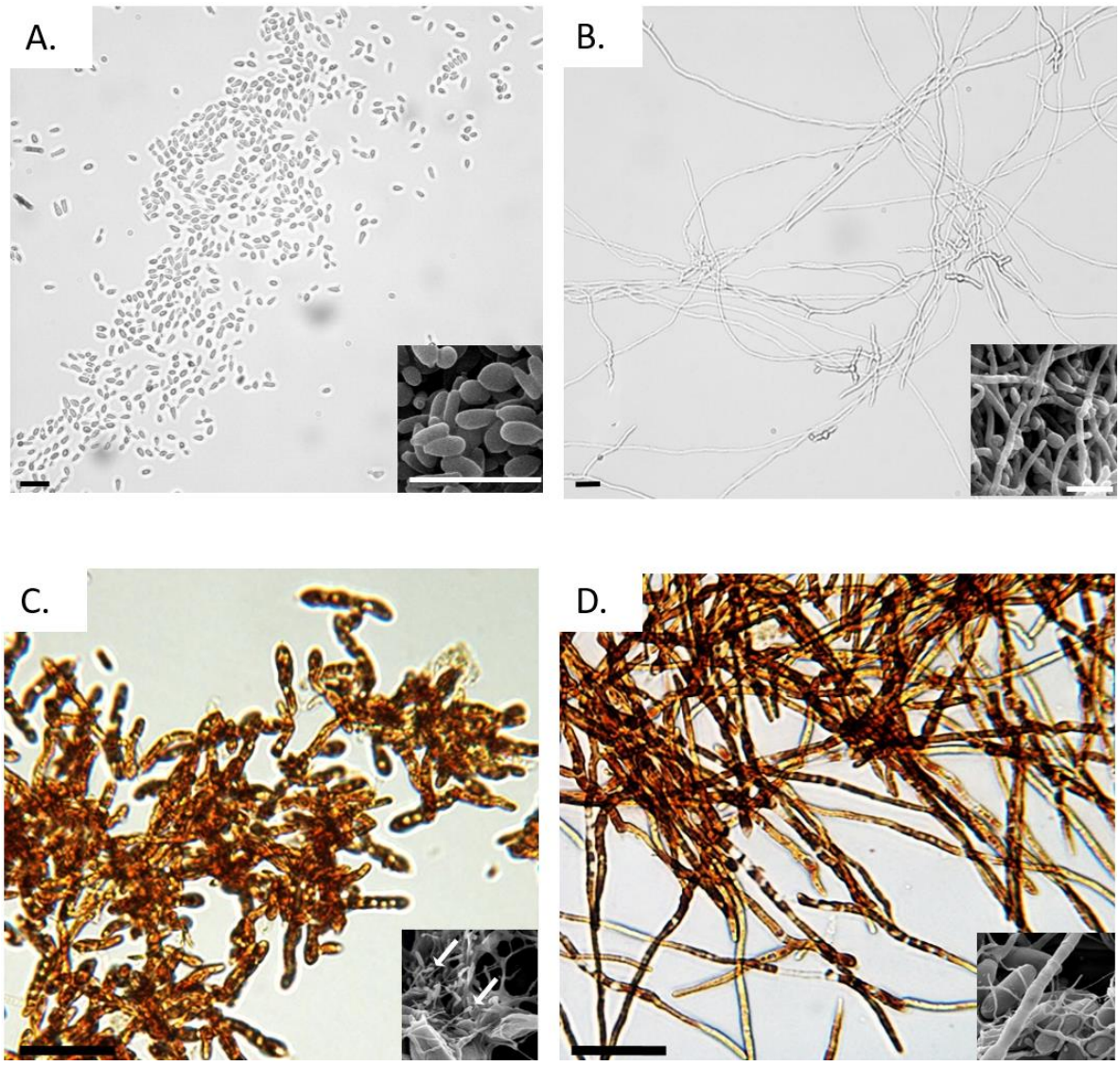

Figure 5.1 Microscopic observations of yeast and mycelia of *Ophiostoma novo-ulmi* (A, B) and *Pseudozyma flocculosa* (C, D). *O. novo-ulmi* (A, B) *s*hake flask liquid cultures were observed in optical microscopy (large images) and in Scanning Electronic Microscopy (SEM; thumbnails). *P. flocculosa* (C, D)) *s*hake flask liquid cultures were observed in optical microscopy (large images). SEM images are typical observations of the corresponding morphological phases *in planta* (thumbnails). Scale bar = 10 µm. Arrows highlight sporidia.

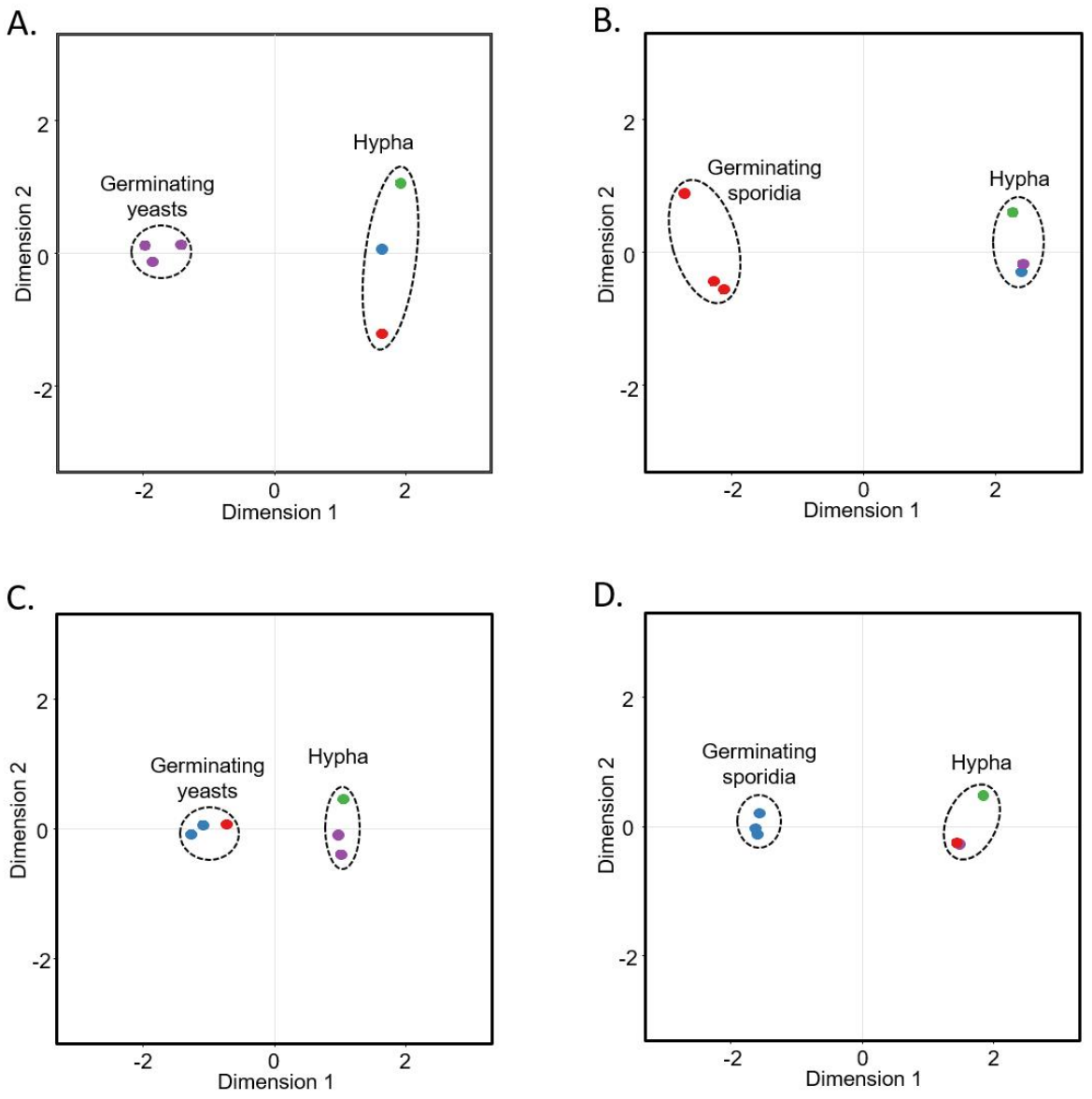

Figure 5.2 Multidimensional Scaling (MDS) analysis for *Ophiostoma novo-ulmi* (A and C) and *Pseudozyma flocculosa* (B and D) RNA-seq libraries. (A) Overall transcriptomic variation between *O. novo-ulmi* RNA-seq libraries (6475 expressed genes). (B) Overall transcriptomic variation between *P. flocculosa* RNA-seq libraries (7339 expressed genes). (C) and (D) represent the molecular variability in the set of differentially expressed orthologous genes (DEOGs, *n*=695) in each species. (C) Transcriptomic variation within the DEOGs in *O. novo-ulmi* RNA-seq libraries. (D) Transcriptomic variation within the DEOGs in *P. flocculosa* RNA-seq libraries. Dotted lines contain the three replicates of each growth phase. Same color dots represent values that are not significantly different according to cluster analysis (*k*-means).

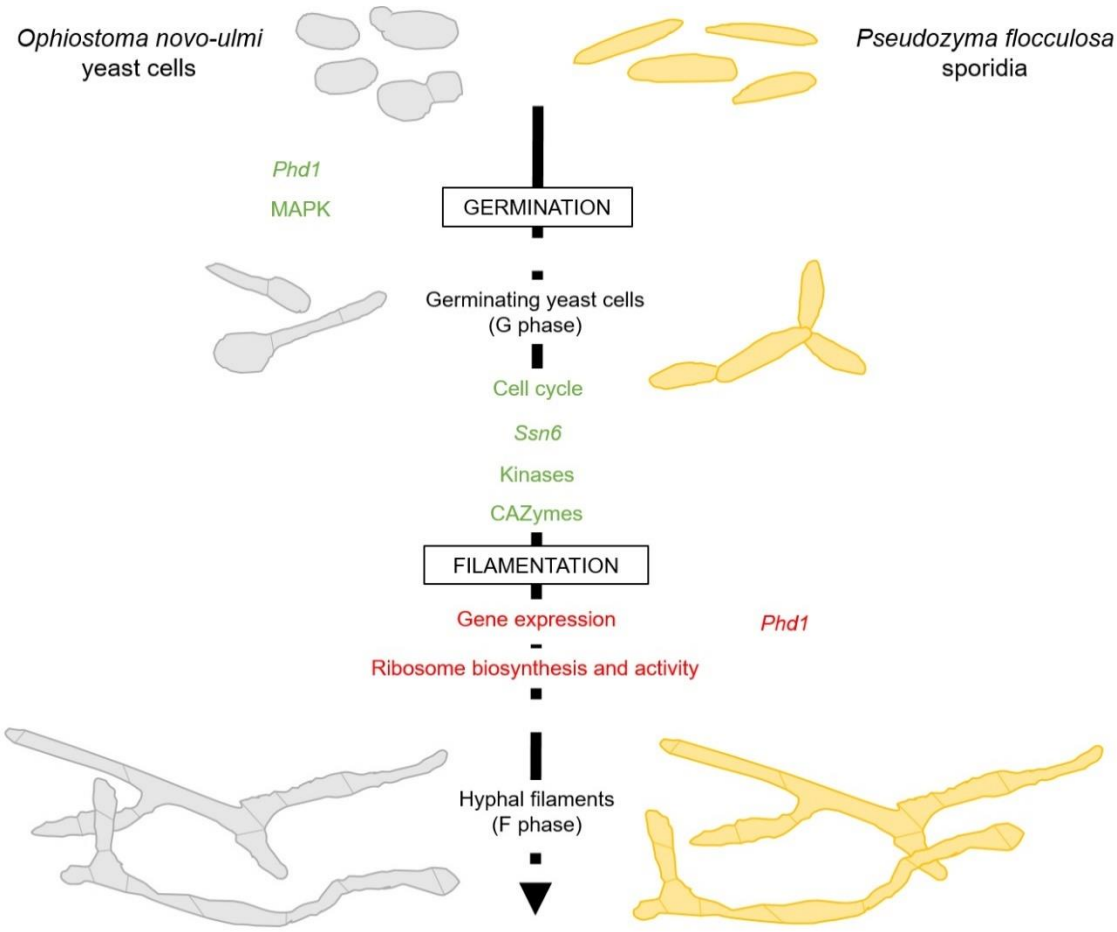

Figure 5.3 Schematic representation of the molecular factors (genes and biological processes) involved in the dimorphic swtich in *Ophiostoma novo-ulmi* (grey) and *Pseudozyma flocculosa* (orange). Factors in green are upregulated during the switch, those in red are downregulated during the switch. Factors along the central arrow are common to both species. Growth phases are indicated in black along the central arrow.

CHAPITRE 6 Conclusions générales

Chez les champignons pathogènes, le dimorphisme fongique levure-mycélium est une caractéristique morphologique qui est souvent associée à la virulence. Ainsi, une approche classique pour la compréhension des maladies associées aux champignons dimorphiques constitue en l'étude des facteurs morphologiques et moléculaires qui sont liés au pouvoir pathogène de ces espèces. Avec la popularisation des analyses de séquençage, l'accès aux données « omiques », i.e. à l'échelle des génomes entiers, est grandement facilité. Dans cette thèse, nous nous sommes intéressée en particulier au cas d'*Ophiostoma novo-ulmi*, l'agent pathogène responsable de la MHO.

L'objectif de notre étude était d'étudier les facteurs moléculaires qui permettent de contrôler la transition levure-mycélium chez *O. novo-ulmi*. Le but était de déterminer les voies moléculaires conservées/uniques présentes chez ce champignon. Pour ce faire, nous avons choisi d'utiliser l'approche par analyse transcriptomique à large échelle en RNAseq pour visualiser le profil complet de l'expression des gènes dans les différentes phases de croissance du champignon et explorer chacune d'entre elles de manière plus approfondie que tout ce qui a été réalisé sur le sujet jusqu'alors. En effet, avant ce travail, les connaissances en matière de gènes impliqués dans le dimorphisme se résumaient à des études ciblées sur un gène en particulier (Richards 1994; Pereira *et al.* 2000). L'approche génomique offre une vue d'ensemble de la régulation de l'expression génique associée au phénomène étudié.

6.1 Analyses transcriptomiques chez les champignons pathogènes dimorphiques

Afin de nous positionner quant à la pertinence de la production de telles données chez une espèce fongique considérée comme non-modèle, il nous a semblé important d'évaluer l'étendue des connaissances sur la régulation de l'expression génique dans le contexte de changements de morphologies dans le règne des champignons. Dans le chapitre 2, nous avons identifié 26 espèces de champignons pathogènes des animaux, des insectes ou des plantes qui présentent des caractéristiques dimorphiques. De ces 26, nous n'en avons trouvé que six, en plus d'*O. novo-ulmi*, pour lesquels des analyses transcriptomiques à large échelle ont porté sur la description des mécanismes impliqués dans le changement de morphologie entre levure et mycélium (transition levure-mycélium ou vice-versa). Ce faible nombre d'espèces

étudiées nous a motivée à entreprendre des analyses comparatives afin d'apprécier le degré de conservation au niveau de l'expression génique entre espèces appartenant à des familles éloignées phylogénétiquement. En recensant et comparant toutes les expériences de transcriptomique réalisées par le biais d'ESTs, puces à ADN (microarray) ou encore de RNAseq, nous avons été en mesure de mettre en évidence plusieurs processus biologiques qui semblent être conservés entre différentes espèces et qui pourraient avoir été l'objet de convergence évolutive dans des branches éloignées de l'arbre phylogénétique fongique. Ainsi, nous avons constaté la nécessité d'étendre les analyses à un nombre plus élevé d'espèces afin de disposer d'un portrait transcriptomique représentatif de la diversité fongique et de généraliser l'implication des processus biologiques mis en évidence.

6.2 Comparaison des transcriptomes des phases levuriforme et mycélienne chez *O. novo-ulmi*

Dans le chapitre 3, nous nous sommes concentrée sur le cas d'*O. novo-ulmi* et intéressée à la description des différences moléculaires entre les phases de croissance levuriforme et mycélienne. Pour la première fois chez cette espèce, nous avons utilisé la technique de RNAseq pour étudier, à l'échelle du génome entier, les profils d'expression génique qui sont associés à chacune des phases de croissance. Nous avons comparé les transcriptomes de levures obtenues *in vitro* en culture liquide et de mycélium cultivé en milieu liquide et solide. Cette expérience nous a permis de mettre en évidence certains processus biologiques qui semblent être propres à une des deux formes et de dresser les portraits transcriptomiques associés à chacune des conditions testées. Nos résultats montrent une distinction moléculaire claire entre les profils de chacune de deux phases. Nous avons notamment identifié une implication contrastée des CAZymes, une activation préférentielle des catalases en phase levuriforme ainsi qu'un potentiel rôle des MAPKs en phase mycélienne. Dans une perspective de compréhension de la conservation de la régulation du phénomène dimorphique entre des familles d'espèces éloignées, nous avons ensuite comparé les profils transcriptomiques des gènes orthologues entre *O. novo-ulmi* et deux espèces modèles dimorphiques, *Candida albicans* et *Histoplasma capsulatum*, toutes deux pathogènes des animaux. Nous avons utilisé des données existantes de RNAseq produites chez ces deux espèces (Bruno *et al.* 2010; Edwards *et al.* 2013). Cette approche comparative était innovante et notre étude a démontré une faible conservation au niveau de la régulation transcriptomique

entre les deux phases de croissance chez ces trois espèces. Ainsi, malgré les similitudes mises en évidence dans le chapitre 2 par les comparaisons globales des résultats des analyses transcriptomiques effectuées par le biais d'ESTs, puces à ADN ou RNAseq, l'étude fine effectuée à l'échelle des gènes orthologues souligne à nouveau l'importance de diversifier les analyses chez les espèces modèles émergentes qui sont phylogénétiquement distantes des espèces étudiées traditionnellement et confirme le besoin de définir les mécanismes de régulation qui prévalent chez *O. novo-ulmi*.

6.3 Patrons d'expression génique au cours de la transition levure-mycélium chez *O. novo-ulmi*

Après avoir établi les différences moléculaires entre les phases de croissance levuriforme et mycélienne, nous nous sommes penchée, dans le chapitre 4, sur les patrons d'expression génique au cours de la transition levure-mycélium chez *O. novo-ulmi*. Pour ce faire, nous avons défini une série temporelle au cours de laquelle nous étions en mesure de suivre visuellement le changement de morphologie, d'une part en microscopie optique et à flux d'électrons, et d'autre part en cytométrie en flux. Cette combinaison de techniques nous a permis de déterminer une période de temps de 27 h à l'intérieur de laquelle nous observions la formation d'hyphes à partir de cultures de levures. La cytométrie en flux offre une résolution plus fine que la microscopie pour suivre les modifications cellulaires qui interviennent lors du passage de la phase levuriforme à mycélienne. L'utilisation de la cytométrie en flux est une innovation chez *O. novo-ulmi* et nous a permis d'observer des changements cellulaires dans des délais très brefs après la perception du stimulus favorisant la transition. L'analyse en RNAseq de cette même série temporelle a appuyé les observations visuelles en révélant de nombreux gènes qui sont différentiellement exprimés au cours de la transition levure-mycélium selon des profils temporels distincts. Entre autres, les gènes codant pour des CAZymes semblent préférentiellement activés au cours de la transition levure-mycélium, ce qui est cohérent avec un processus actif de transformation de la paroi cellulaire et de changement de morphologie. Dans un souci de mise en relation de nos découvertes avec les connaissances développées chez d'autres espèces dimorphiques, nous avons ici choisi de vérifier le niveau d'expression de certains gènes que nous avons identifiés comme homologues de gènes appartenant à la voie MAPK, AMPc et RIM chez *Saccharomyces cerevisiae*. Ces trois voies moléculaires sont connues pour être impliquées

dans le dimorphisme et régulées durant la transition levure-pseudohyphe chez *S. cerevisiae* ainsi que la transition levure-hyphe chez des champignons pathogènes tels que *C. albicans* ou *U. maydis* (Banuett and Herskowitz 1994; Madhani and Fink 1997; Pan and Heitman 1999; Lengeler *et al.* 2000; Sánchez-Martínez and Pérez-Martín 2001; Martínez-Espinoza *et al.* 2004; Selvig and Alspaugh 2011; Cullen and Sprague 2012; Hamel *et al.* 2012; Shively *et al.* 2013). Chez *O. novo-ulmi*, la plupart des gènes potentiellement liés à la voie des MAPKs sont surexprimés au cours de la transition. Ces résultats concordent avec l'identification de MAPKs dans les gènes surexprimés en phase mycélienne dans le chapitre 3 et suggèrent une convergence de la régulation de l'expression génique et de la régulation du sentier moléculaire impliquant les MAPKs.

6.4 Comparaison de l'expression génique durant la filamentation chez *O. novo-ulmi* et *P. flocculosa*

L'aptitude à changer de morphologie est présente dans des branches très éloignées de l'arbre phylogénique fongique, comme nous l'avons montré dans le chapitre 2. Ce constat a motivé notre comparaison de la régulation de l'expression génique entre les phases de germination et de filamentation chez le champignon ascomycète *O. novo-ulmi* et l'espèce basidiomycète *P. flocculosa*. Ces deux espèces non-modèles présentent des styles de vie très différents mais sont toutes deux dimorphiques. Dans ce dernier chapitre, nous avons étudié en particulier les modulations transcriptomiques au niveau des gènes orthologues entre les deux espèces. Nous nous sommes concentrée sur les gènes qui étaient différentiellement exprimés entre les phases de germination et de filamentation pour apprécier le niveau de conservation entre *O. novo-ulmi* et *P. flocculosa*. Malgré une distance phylogénétique certaine, nous avons trouvé 695 gènes pour lesquels la régulation de l'expression semblait conservée dans le passage de la phase de germination des spores asexuées à la croissance filamenteuse. En particulier, nous avons identifié plusieurs gènes codant pour des protéines kinases qui pourraient jouer des rôles similaires chez les deux espèces. Aussi, un résultat majeur de notre analyse est la répression des gènes régulant la biosynthèse et l'activité des ribosomes ainsi que l'expression génique. Ce phénomène, commun aux deux espèces, suggère une diminution de la transcription et de la traduction au cours de la transition vers la filamentation.

Dans l'ensemble, les processus associés aux gènes mis en évidence portent sur des fonctions essentielles du développement fongique tel que le cycle et la division cellulaires ou des mécanismes nécessaires à la croissance filamenteuse comme la mise en place des septa. Étant donné la grande distance phylogénétique entre *O. novo-ulmi* et *P. flocculosa*, ce constat était attendu. Cette étude a donc pris de mettre en évidence un certain nombre de gènes dont le rôle dans la transition dimorphique est potentiellement conservé entre basidiomycètes et ascomycètes et qui pourraient constituer la « base minimale » génique commune nécessaire à la production d'hyphes à partir de spores haploïdes asexuées.

6.5 Perspectives

A la suite de ce doctorat, il est clair que l'analyse fonctionnelle des facteurs moléculaires mis en évidence dans les trois chapitres expérimentaux (chapitres 3, 4 et 5) est nécessaire afin de valider leur implication dans le phénomène de changement de morphologie. Les gènes qui s'avèreront jouer un rôle certain dans le dimorphisme pourront être considérés comme des cibles pour l'obtention de souches mutantes ayant perdu la capacité de passer des phases levuriforme à mycélienne ou vice-versa. Afin de conclure sur l'hypothèse de départ selon laquelle la transition levure-mycélium chez *O. novo-ulmi* est un facteur essentiel à son pouvoir pathogène, il serait d'un grand intérêt de tester le niveau de virulence de telles souches. Cependant, la réalisation de telles expériences est jusqu'alors limitée par l'inefficacité des méthodes classiques de mutation génique ciblée chez *O. novo-ulmi*. Dans un chapitre parallèle à la thèse présentée ici, nous avons tenté de mettre au point un protocole de mutation en utilisant le système innovateur de CRISPR-Cas9 selon la méthode mise en place chez les *Aspergilli* (Nødvig *et al.* 2015) (voir Annexe 1). Cependant, ce projet présente de nombreux défis qui restent à surmonter et est encore en développement.

Une autre perspective de ce projet est le suivi de la transition et de l'expression génique chez *O. novo-ulmi* dans un contexte d'interaction avec l'arbre hôte. Ce projet nécessite une optimisation du protocole d'inoculation fongique car l'extraction d'ARN messager fongique à partir d'échantillons végétaux est limitée par la concentration fongique au sein des arbres. Cependant, un projet d'analyse de l'expression fongique au sein d'arbres issus de variétés présentant des niveaux de résistance contrastés à la maladie hollandaise de l'orme est en cours (Sherif *et al.* données non publiées). De manière complémentaire avec l'expérience de

mutations ciblées proposée précédemment, ce projet (auquel nous collaborons) permettra potentiellement de mettre en lien dimorphisme et virulence dans le cas où certains facteurs identifiés dans le contexte de dimorphisme se retrouveraient également exprimés au sein de l'hôte.

Les deux avenues proposées ici ont toutes deux pour but de mieux comprendre les facteurs qui font d'*O. novo-ulmi* un agent pathogène qui reste menaçant malgré les efforts portés sur la lutte contre la MHO. L'identification de facteurs liés à la pathogénicité est de grande importance afin de mieux combattre la maladie et d'envisager des traitements plus efficaces et plus ciblés que ceux développés actuellement.

6.6 Bibliographie

Banuett F, Herskowitz I, 1994. Identification of Fuz7, a *Ustilago maydis* MEK / MAPKK homolog required steps in the fungal life cycle. *Genes and Development* **8**: 1367–1378.

Bruno VM, Wang Z, Marjani SL, Euskirchen GM, Martin J, Sherlock G, Snyder M, 2010. Comprehensive annotation of the transcriptome of the human fungal pathogen *Candida albicans* using RNA-seq. *Genome Research* **20**: 1451–1458.

Cullen PJ, Sprague GF, 2012. The regulation of filamentous growth in yeast. *Genetics* **190**: 23–49.

Edwards JA, Chen C, Kemski MM, Hu J, Mitchell TK, Rappleye CA, 2013. *Histoplasma* yeast and mycelial transcriptomes reveal pathogenic-phase and lineage-specific gene expression profiles. *BMC genomics* **14**: 695.

Hamel L-P, Nicole M-C, Duplessis S, Ellis BE, 2012. Mitogen-activated protein kinase signaling in plant-interacting fungi: distinct messages from conserved messengers. *The Plant cell* **24**: 1327–51.

Lengeler KB, Davidson RC, D'Souza C, Harashima T, Shen WC, Wang P, Pan X, Waugh M, Heitman J, 2000. Signal transduction cascades regulating fungal development and virulence. *Microbiology and molecular biology reviews* **64**: 746–85.

Madhani HD, Fink GR, 1997. Combinatorial control required for the specificity of yeast MAPK signaling. *Science* **275**: 1314–1317.

Martínez-Espinoza AD, Ruiz-Herrera J, León-Ramírez CG, Gold SE, 2004. MAP kinase and cAMP signaling pathways modulate the pH-induced yeast-to-mycelium dimorphic transition in the corn smut fungus *Ustilago maydis*. *Current microbiology* **49**: 274–81.

Nødvig CS, Nielsen JB, Kogle ME, Mortensen UH, 2015. A CRISPR-Cas9 system for genetic engineering of filamentous fungi. *PLoS ONE* **10**: 1–18.

Pan X, Heitman J, 1999. Cyclic AMP-dependent protein kinase regulates pseudohyphal differentiation in *Saccharomyces cerevisiae*. *Molecular and cellular biology* **19**: 4874–87.

Pereira V, Royer JC, Hintz WE, Field D, Bowden C, Kokurewicz K, Hubbes M, Horgen PA, 2000. A gene associated with filamentous growth in *Ophiostoma novo-ulmi* has RNA-binding motifs and is similar to a yeast gene involved in mRNA splicing. *Current genetics* **37**: 94–103.

Richards WC, 1994. Nonsporulation in the Dutch elm disease fungus *Ophiostoma ulmi* : evidence for control by a single nuclear gene. *Revue canadienne de botanique* **72**: 461–467.

Sánchez-Martínez C, Pérez-Martín J, 2001. Dimorphism in fungal pathogens: *Candida albicans* and *Ustilago maydis*--similar inputs, different outputs. *Current opinion in microbiology* **4**: 214–21.

Selvig K, Alspaugh JA, 2011. pH response pathways in fungi: adapting to host-derived and environmental signals. *Mycobiology* **39**: 249–56.

Shively CA, Eckwahl MJ, Dobry CJ, Mellacheruvu D, Nesvizhskii A, Kumar A, 2013.Genetic networks inducing invasive growth in *Saccharomyces cerevisiae* identified through systematic genome-wide overexpression. *Genetics* **193**: 1297–310.

ANNEXE A La mutation génique chez *Ophiostoma novo-ulmi* en utilisant la méthode CRISPR-Cas9 : une technique en développement.

A.1 Introduction

À ce jour, plusieurs méthodes de mutagénèse ont été testées chez *Ophiostoma novo-ulmi*, n'offrant malheureusement que peu résultats concluants pour une mutation ciblée malgré le criblage de banques de nombreux transformants (Bowden *et al.* 1994; Pereira *et al.* 2000; Plourde *et al.* 2008; Temple *et al.* 2009).

Récemment, Carneiro *et al.* (2013) ont développé un système d'ARN interférence (RNAi) utilisant des plasmides contenant des cassettes d'expression portant un promoteur endogène, le promoteur *AlcA*. Ce promoteur est régulé par les conditions carbonées dans lesquelles se trouve le champignon. En cas de carence, il est induit par le produit du gène *AlcR* qui régule le processus de fermentation, et donc, la libération de carbone à partir d'une source alcoolique (éthanol). Le promoteur est, en revanche, réprimé en présence de glucose par une action négative du gène *CreA*. Ainsi, l'utilisation de ce promoteur *AlcA* dans la technique de RNAi permet de contrôler l'expression des gènes cibles en modifiant la source de carbone dans le milieu de culture fongique (Carneiro *et al.* 2013). Cependant, un des désavantages de cette technique est qu'elle induit principalement des mutations « knock-down », soit une réduction de l'expression des gènes cibles et non une extinction complète.

Une autre technique de mutation qui semble améliorer le ciblage de gènes, et qui permettrait cette fois l'obtention de mutations de délétions, consiste en l'inactivation du système de recombinaison non-homologue (NHEJ, Non-Homologous End-Joining) (Krappmann, 2007). Ce dernier est impliqué dans la réparation des cassures de l'ADN double brin. Il induit la liaison de deux extrémités d'ADN cassées de manière peu spécifique, entrainant ainsi des délétions, translocations ou mutations dans le génome. Lors de manipulation génétique et mutation par insertion de plasmide, la recombinaison non-homologue est responsable des intégrations ectopiques des fragments d'ADN transformés. Chez la plupart des champignons, la NHEJ est favorisée par rapport à la recombinaison homologue (HR) qui, elle, permet une réparation fidèle des cassures double brin et une intégration ciblée des fragments d'ADN transformés par interaction entre séquences homologues. En effet, la fréquence de HR, bien que dépendante de l'espèce à laquelle on s'intéresse, dépasse rarement 30 % des cas de réparations des cassures doubles brins de l'ADN. En inactivant la NHEJ, les intégrations ectopiques sont éliminées et la précision de la mutation est augmentée (Krappmann, 2007; Meyer, 2008). Bien que cette technique ait montré de bons résultats chez des champignons modèles comme *Neurospora crassa* (Ninomiya *et al.* 2004) et *Aspergillus nidulans* (Nayak *et al.* 2006), l'application chez *Ophiostoma novo-ulmi* offre des résultats limités (Naruzawa, 2015 ; Naruzawa *et al.* données non publiées) et encore difficiles à reproduire (L. Bernier et P. Tanguay, communication personnelle).

Le développement récent de la technique de mutation basée sur des motifs d'ADN répétés (« Clustered Regularly Interspaced Short Palindromic Repeat », CRISPR) reconnus par l'enzyme d'origine bactérienne Cas (Jinek *et al.* 2012) présente une nouvelle perspective

pour la mutation génique ciblée. Cette technique a montré de nombreux résultats encourageants et positifs chez une multitude d'espèces vivantes, que ce soit chez les animaux (Hruscha *et al.* 2013; Ni *et al.* 2014; Platt *et al.* 2014; Xue *et al.* 2014; Zhou *et al.* 2015), les plantes (Belhaj *et al.* 2015; Jiang *et al.* 2013; Zhang *et al.* 2014), les insectes (Yu *et al.* 2013) ou les humains dans le contexte de l'édition génique et le traitement des maladies (Tebas *et al.* 2014). Chez les champignons filamenteux, un grand nombre d'espèces ont répondu favorablement aux essais de mutation génique via CRISPR-Cas, telles que plusieurs *Aspergilli* (Fuller *et al.* 2015; Katayama *et al.* 2016; Nødvig *et al.* 2015), *Magnaporthe grisae* (Arazoe *et al.* 2015), *Candida albicans* (Vyas *et al.* 2015), *Neurospora crassa* (Matsu-ura *et al.* 2015), *Trichorderma reesei* (Liu *et al.* 2015), *Penicillium chrysogenum* (Pohl *et al.* 2016) et *Ustilago maydis* (Schuster *et al.* 2016).

En se basant sur ces succès, nous proposons de tester la technique de mutation via CRISPR-Cas chez *O. novo-ulmi* en utilisant la méthode optimisée chez les *Aspergilli* par Nødvig et collaborateurs (2015) puisqu'elle présente l'avantage d'avoir été développée de manière à être transférable chez des espèces différentes. Nous proposons de cibler le gène *PyrG* qui, lorsque muté, rend les souches auxotrophes pour l'uridine et l'uracile (REF).

A.2 Matériels et méthodes

A.2.1 Souches et conditions de croissance

La souche H327 d'*Ophiostoma novo-ulmi* sp. *novo-ulmi* est cultivée pendant 2 j sous forme levure en milieu liquide minimum (OMM) (Bernier and Hubbes 1990) complémenté avec de la proline sous agitation (150 rpm) et à 22°C.

A.2.2 Obtention de cellules compétentes pour la transformation

Les cellules compétentes d'*O. novo-ulmi* sont obtenues à partir des cultures âgées de 2 j ($2x10^9$ cellules/ml) selon le protocole utilisant du tampon Tris-EDTA (TE) avec de l'acétate de lithium (LiAc) (Gietz *et al.* 1995) optimisé par Naruzawa et collaborateurs (non publié).

La transformation des cellules compétentes est réalisée comme suit : 10^7 cellules compétentes sont incubées avec 300µl de TE-LiAc contenant 50% de PEG. Les cellules sont mélangées à 50 µg d'ADN de sperme de saumon pré-bouilli et 5 µl du plasmide à insérer (0.5-1 µg). Les cellules sont ensuite incubées pendant 30 min à température ambiante puis 20min à 37°C. Le mélange est centrifugé 45 sec à 13000g et les cellules sont resuspendues dans du milieu OMM liquide complémenté avec de l'extrait de levure (YE) (5 g/L) et 0.6% de sucrose. Les cellules compétentes transformées sont gardées à 4°C pendant une nuit ou 4 h à température ambiante. Finalement, les cellules sont à nouveau centrifugées rapidement et resuspendues dans 300 µl d'eau stérile. 100 µl de cellules sont ajoutés à 10 ml de milieu liquide complet (OCM) (Bernier and Hubbes, 1990) mou (0.7% agar) avec le marqueur de sélection (hygromycine) complémenté avec de l'uracile (ura) (1.12 g/L) et de l'uridine (uri) (2.44 g/L) et le tout est répandu sur des boites de pétri contenant 10 ml de milieu solide OCM contenant le marqueur de sélection complémenté avec ura et uri (Plourde *et al.* 2008). Les boites sont incubées 7 j à température ambiante et à l'obscurité. Les colonies identifiées comme de potentiels transformants sont transférées sur boites de pétri de OMM et OMM complémenté

avec YE, ura et uri. Les transformants sont aussi sélectionnés par repiquage sur milieu contenant de l'acide 5- fluoroorotic (5-FOA, 3 mg/mL).

A.2.3 Extraction d'ADN génomique d'*O. novo-ulmi*

A partir de culture sur boite de pétri Malt Extract Agar (MEA, Oxoid) de la souche H327 (3 j), le mycélium est récolté et lyophilisé pendant 24 h. Le protocole suivi pour l'extraction d'ADN est décrit par Zolan et Pukkila (1986).

A.2.4 Produits PCR, plasmides et ARN guide

Tous les produits PCR sont amplifiés et purifiés comme décrit par Nødvig et collaborateurs (2015). Toutes les amorces utilisées dans cette étude sont listées dans le tableau A.1.
Les réactions de PCR sont composées comme suit : 0.5 µl enzyme PfuX7 (REF Nørholm 2010) ou Phusion U Hot Start DNA Polymerase (ThermoFisher), 10 µl de tampon 5x Phusion HF Reaction Buffer (New Englands Biolabs, USA), 5 µl de dNTPs (2µM), 1.5 µl DMSO 100%, 1 µl $MgCl_2$, 2 µl d'amorces « forward » (F) et « reverse » (R) (10mM), 1 µl d'ADN génomique ou de plasmide. Le volume final est ajusté à 40 µl avec de l'eau stérile.

Les plasmides optimisés pour *O. novo-ulmi* sont construits selon Nødvig et collaborateurs (2015). Tous les plasmides utilisés pour la transformation contiennent les séquences suivantes : l'origine de réplication bactérienne (Ori) et le gène de résistance à l'ampicilline (Amp) pour la transformation bactérienne ; l'élément de réplication autonome dans *Aspergillus* (AMA1) permettant au plasmide de se maintenir dans la cellule transformée sans être intégrer dans le génome; le gène *Cas9* de *Streptococcus pyogenes* (codons optimisés pour *Aspergillus*) sous le contrôle du promoteur et terminateur du facteur d'élongation de la transcription (Tef1) d'*O. novo-ulmi* (pMN1); le gène de résistance à l'hygromycine (marqueur fongique) pour la transformation fongique sous le contrôle du promoteur du gène *TrpC* d'*A. nidulans*; une cassette de restriction PacI/Nt.BbvCI pour le clonage de produits PCR (séquences d'ARN guide) par l'enzyme USER™.

Les séquences d'ARN guide (sgRNA) contiennent toutes : le promoteur du gène *GpA* d'*A. nidulans* (pFC334) ou d'*O. novo-ulmi* (pFCgRNA); le protospacer (20 pb issues du gène cible pour la mutation); le squelette de l'ARN guide (Nødvig *et al.* 2015); le ribozyme du virus delta de l'hépatite (HDV); le ribozyme à tête de marteau (hammerhead ribozyme, HH); le terminateur du gène *TrpC* d'*O. novo-ulmi.*

A.2.5 Clonage de type USER™

Les plasmides utilisés pour la transformation contiennent des sites de coupures *Pac1*/*Nt.BbvCI* et sont linéarisés par une double digestion avec les enzymes *PacI* (une nuit à 37°C) et *Nt.BbvCI* (2 h à 37°C).

Le clonage est ensuite réalisé selon Nødvig et collaborateurs (2015) avec 10 µl de fragments PCR à insérer (maximum quatre fragments), 1 µl de plasmide linéarisé et 0.5 µl d'enzyme USER™. Le mélange est incubé 35 min à 37°C et 25 min à température ambiante, puis gardé sur glace jusqu'à la transformation bactérienne.

La totalité de la réaction de clonage est utilisée pour la transformation de 50 µl de cellules compétentes d'*E. coli* DH5-α. Les cellules sont ensuite incubées 5 min sur glace, 1 min à 42°C et à nouveau 5 min sur glace. Elles sont ensuite étalées sur des boites de pétri contenant du milieu Luria Broth (LB) et de l'ampicilline (100 µg/ml) et les boites sont incubées toute la nuit à 37°C.

Les colonies ayant poussé le lendemain (2-3) sont transférées dans 4 ml de milieu LB+ampicilline liquide pour une deuxième nuit à 37°C sous agitation. Les plasmides sont ensuite purifiés avec le kit GenElute Miniprep (Sigma-Aldrich).

Après la purification, un échantillon des plasmides obtenus est digéré par l'enzyme de restriction qui convient pour vérifier l'insertion correction de l'ARN guide.

A.3 Résultats et discussion

A.3.1 Production de plasmides optimisés pour *O. novo-ulmi* par clonage USER

A partir d'ADN génomique d'*O. novo-ulmi*, nous avons amplifié et purifié les promoteurs des gènes *Tef* 1 et *Gpd* et les terminateurs de *Tef1* et *TrpC* (Figure A.1). Les amorces F utilisées pour amplifier les promoteurs et R utilisées pour amplifier les terminateurs contiennent un site complémentaire à la coupure induite par l'enzyme de restriction Pac1 permettre la ligature dans le plasmide cible.

A partir du plasmide développé par Nødvig et collaborateurs (2015) pFC332, nous avons amplifié et purifié le gène *Cas9* divisé en deux fragments (Cas9_1 et Cas9_2) (Figure A.1).

A partir du plasmide développé par Nødvig et collaborateurs (2015) pFC334, nous avons amplifié et purifié la séquence codant pour l'ARN guide (sgRNA) incluant le ribozyme HH, le squelette de l'ARN guide (gRNA), la séquence du protospacer (proto), et le ribozyme HDV (Figure A1.1).

Le plasmide pMN1 est obtenu par ligature des fragments Ptef1Onu, Cas9_1, Cas9_2 et Ttef1Onu et clonage USER dans le plasmide pAMA1-hph (Nødvig *et al.* 2015) (Figure A.2).

Le plasmide pMN2 est obtenu par ligature des fragments PgpdOnu, gRNA et TtrpCOnu et clonage USER dans le plasmide pMN1 (Figure A.3).

A partir du plasmide pMN2, nous pouvons modifier les séquences de protospacers en utilisant des amorces construites spécifiquement pour les gènes ciblés, selon le protocole de Nødvig et collaborateurs (2015). Ainsi, nous avons amplifié et purifié six séquences d'ARN guide spécifique à trois protospacers définis dans le gène *PyrG* (Tableau A.2) avec les amorces PyrG PS_1, 2 et 3 F et R (Tableau A.1, Figure A.4). Les deux fragments complémentaires de chacun de protospacers sont ensuite ligaturés et clonés dans le plasmide pMN1.

A.3.2 Transformation chez *O. novo-ulmi*

Les cellules compétentes de la souche H327 d'*O. novo-ulmi* sont transformées avec les trois plasmides pMN2 contenant chacun un protospacer ciblant le gène *PyrG*. Après 7 jours d'incubation sur milieu sélectif, 19 colonies provenant des transformations avec les trois différents plasmides ont été repiqués sur des boites de pétri contenant du milieu OMM et du milieu OMM+YE+ura+uri (voir schéma Figure A.5). Après 4 jours d'incubation, les colonies n'ayant poussé que sur milieu OMM+YE+ura+uri (n=10) sont à nouveau repiquées, d'abord sur milieu OMM contenant du 5-FOA puis sur OMM et OMM+YE+ura+uri pour une seconde purification. Aucune colonie ne résiste au 5-FOA, et toutes les 10 colonies poussent sur OMM, indiquant l'absence de mutants. De plus, les 10 colonies sélectionnées car elles ne n'avaient pas poussé sur OMM ont finalement commencé à croître, malgré stockage des boites à 4°C. Ce résultat peut s'expliquer selon plusieurs hypothèses : 1. au moment du premier repiquage, les colonies étaient non homogènes et contenaient un mélange de cellules transformées et cellules sauvages ; 2. le gène *PyrG* chez *O. novo-ulmi* ne suffit pas à la résistance au 5-FOA et /ou n'induit pas l'auxotrophie à l'uridine et l'uracil; la taille de l'inoculum lors du premier repiquage n'était pas homogène et les colonies qui n'ont pas poussé étaient celles avec une taille d'inoculum plus faible, ce qui expliquerait pourquoi les colonies ont mis plus de temps à être visibles sur OMM.

A.4 Perspectives

Afin d'optimiser l'activité de l'enzyme Cas9, il faudrait optimiser les codons pour assurer que le potentiel de transcription et la traduction de Cas9 chez *O. novo-ulmi* soit à son maximum. De plus, afin de tester la traduction de Cas9, il serait intéressant de transformer *O. novo-ulmi* avec une séquence codant pour Cas9 couplée à un marqueur de fluorescence comme GFP, YFP ou RFP. Ainsi, il sera aisé de visualiser la localisation de la protéine dans les cellules. L'expression de *Cas9* pourrait aussi être suivie en qRT-PCR.

A.5 Bibliographie

Hruscha, A., Krawitz, P., Rechenberg, A., Heinrich, V., Hecht, J., Haass, C., *et al.* (2013). Efficient CRISPR/Cas9 genome editing with low off-target effects in zebrafish. *Development* 140, 4982–4987. doi:10.1242/dev.099085.

Arazoe, T., Miyoshi, K., Yamato, T., Ogawa, T., Ohsato, S., Arie, T., *et al.* (2015). Tailor-made CRISPR/Cas system for highly efficient targeted gene replacement in the rice blast fungus. *Biotechnol. Bioeng.* 112, 2543–2549. doi:10.1002/bit.25662.

Belhaj, K., Chaparro-Garcia, A., Kamoun, S., Patron, N. J., and Nekrasov, V. (2015). Editing plant genomes with CRISPR/Cas9. *Curr. Opin. Biotechnol.* 32, 76–84. doi:10.1016/j.copbio.2014.11.007.

Bernier, L., and Hubbes, M. (1990). Mutations in *Ophiostoma ulmi* induced by N-methyl-N '-nitro-N-nitrosoguanidine. *Can. J. Bot.* 68, 225–231.

Bowden, C. G., Hintz, W. E., Jeng, R., Hubbes, M., and Horgen, P. A. (1994). Isolation and characterization of the cerato-ulmin toxin of the Dutch elm disease pathogen, *Ophiostoma ulmi*. *Curr. Genet.* 75, 323–329.

Carneiro, J. S., de la Bastide, P. Y., and Hintz, W. E. (2013). Regulated gene silencing in the fungal pathogen *Ophiostoma novo-ulmi*. *Physiol. Mol. Plant Pathol.* 82, 28–34. doi:10.1016/j.pmpp.2013.01.001.

Fuller, K. K., Chen, S., Loros, J. J., and Dunlap, C. (2015). Development of the CRISPR / Cas9 system for targeted gene disruption in *Aspergillus fumigatus*. *Eukaryot. Cell* 14, 1073–1080.

Gietz, D., Schiestl, R. H., and Willems, A. R. (1995). Studies on the transformation of intact yeast cells by the LiAc/SS-DNA/PEG procedure. *Yeast* 11, 355–360.

Jiang, W., Zhou, H., Bi, H., Fromm, M., Yang, B., and Weeks, D. P. (2013). Demonstration of CRISPR/Cas9/sgRNA-mediated targeted gene modification in *Arabidopsis*, tobacco, sorghum and rice. *Nucleic Acids Res.* 41, 1–12..

Jinek, M., Chylinski, K., Fonfara, I., Hauer, M., Doudna, J. A., and Charpentier, E. (2012). A programmable dual-RNA – Guided DNA endonuclease in adaptive bacterial immunity. *Science (80-.).* 337, 816–822.

Katayama, T., Tanaka, Y., Okabe, T., Nakamura, H., Fujii, W., Kitamoto, K., *et al.* (2016). Development of a genome editing technique using the CRISPR/Cas9 system in the industrial filamentous fungus *Aspergillus oryzae*. *Biotechnol. Lett.* 38, 637–642.

Krappmann, S. (2007). Gene targeting in filamentous fungi: the benefits of impaired repair. *Fungal Biol. Rev.* 21, 25–29.

Liu, R., Chen, L., Jiang, Y., Zhou, Z., and Zou, G. (2015). Efficient genome editing in filamentous fungus *Trichoderma reesei* using the CRISPR/Cas9 system. *Cell Discov.* 1, 15007.

Matsu-ura, T., Baek, M., Kwon, J., and Hong, C. (2015). Efficient gene editing in *Neurospora crassa* with CRISPR technology. *Fungal Biol. Biotechnol.* 2, 4. doi:10.1186/s40694-015-0015-1.

Meyer, V. (2008). Genetic engineering of filamentous fungi--progress, obstacles and future trends. *Biotechnol. Adv.* 26, 177–85. doi:10.1016/j.biotechadv.2007.12.001.

Naruzawa, E. S. (2015). Bases moléculaires du dimorphisme levure-mycélium chez le champignon phytopathogène *Ophiostoma novo-ulmi*.

Nayak, T., Szewczyk, E., Oakley, C. E., Osmani, A., Ukil, L., Murray, S. L., *et al.* (2006). A versatile and efficient gene-targeting system for *Aspergillus nidulans*. *Genetics* 172, 1557–66.

Ni, W., Qiao, J., Hu, S., Zhao, X., Regouski, M., Yang, M., *et al.* (2014). Efficient gene knockout in goats using CRISPR/Cas9 system. *PLoS One* 9, 1–7.

Ninomiya, Y., Suzuki, K., Ichii, C., and Inoue, H. (2004). Highly efficient gene replacements

in *Neurospora* strains deficient for nonhomologous end-joining. *PNAS* 101, 12248–53.

Nødvig, C. S., Nielsen, J. B., Kogle, M. E., and Mortensen, U. H. (2015). A CRISPR-Cas9 system for genetic engineering of filamentous fungi. *PLoS One* 10, 1–18.

Pereira, V., Royer, J. C., Hintz, W. E., Field, D., Bowden, C., Kokurewicz, K., *et al.* (2000). A gene associated with filamentous growth in *Ophiostoma novo-ulmi* has RNA-binding motifs and is similar to a yeast gene involved in mRNA splicing. *Curr. Genet.* 37, 94–103.

Platt, R. J., Chen, S., Zhou, Y., Yim, M. J., Swiech, L., Kempton, H. R., *et al.* (2014). CRISPR-Cas9 knockin mice for genome editing and cancer modeling. *Cell* 159, 440–455.

Plourde, K. V, Jacobi, V., and Bernier, L. (2008). NOTE / NOTE Use of insertional mutagenesis to tag putative parasitic fitness genes in the Dutch elm disease fungus Ophiostoma novo-ulmi subsp . *novo-ulmi*. *Can. J. Microbiol.* 54, 797–802.

Pohl, C., Kiel, J. A. K. W., Driessen, A. J. M., Bovenberg, R. A. L., and Nygård, Y. (2016). CRISPR/Cas9 based genome editing of *Penicillium chrysogenum*. *ACS Synth. Biol.* 5, 754–764.

Schuster, M., Schweizer, G., Reissmann, S., and Kahmann, R. (2016). Genome editing in *Ustilago maydis* using the CRISPR-Cas system. *Fungal Genet. Biol.* 89, 3–9.

Tebas, P., Stein, D., Ww, T., Frank, I., Sq, W., Lee, G., *et al.* (2014). Gene editing of CCR5 in autologous CD4 T cells of persons infected with HIV. *N. Engl. J. Med.* 370, 901–910.

Temple, B., Bernier, L., and Hintz, W. E. (2009). Characterisation of the polygalacturonase gene of the dutch elm disease pathogen *Ophiostoma novo-ulmi*. *New Zeal. J. For. Sci.* 39, 29–37.

Vyas, V., Barrasa, M., and Fink, G. (2015). A *Candida albicans* CRISPR system permits genetic engineering of essential genes and gene families. *Sci. Adv.*, e1500248.

Xue, W., Chen, S., Yin, H., Tammela, T., Papagiannakopoulos, T., Joshi, N. S., *et al.* (2014). CRISPR-mediated direct mutation of cancer genes in the mouse liver. *Nature* 514, 380–4.

Yu, Z., Ren, M., Wang, Z., Zhang, B., Rong, Y. S., Jiao, R., *et al.* (2013). Highly efficient genome modifications mediated by CRISPR/Cas9 in *Drosophila*. *Genetics* 195, 289–291.

Zhang, H., Zhang, J., Wei, P., Zhang, B., Gou, F., Feng, Z., *et al.* (2014). The CRISPR/Cas9 system produces specific and homozygous targeted gene editing in rice in one generation. *Plant Biotechnol. J.* 12, 797–807.

Zhou, X., Xin, J., Fan, N., Zou, Q., Huang, J., Ouyang, Z., *et al.* (2015). Generation of CRISPR/Cas9-mediated gene-targeted pigs via somatic cell nuclear transfer. *Cell. Mol. Life Sci.* 72, 1175–1184.

Tableau A.1 Liste des amorces utilisées pour l'étude CRISPR-Cas9 et la création de plasmide optimisé pour *Ophiostoma novo-ulmi*.

Noms des amorces	Séquences	Identifiants
Cassette « PacI-Pef1Onu-Cas9-NLS-Tef1Onu-PacI » pour construction de pMN1		
Pef1Onu_Pac1_regen_F	GGGTTTAAUTAAGTCCTCAGC CAAGACACCAAACAAGAGGCC	MN15
Pef1Onu_Pac1_up_F	GGGTTTAAUCAAGACACCAAACAAGAGGCC	MN1
Pef1Onu_Cas9_dwn_R	AT TTTGACGGU TGTGAGATTGTTTTGTGTTTTG	MN2
Cas9_Pef1_up_F	ACCGTCAAAAU GGACAAGAAGTATAGCATCGGG	MN3
Cas9_int_R CSN307[1]	AGGGAAU CGTCGTGAATAAGCTG	CSN307
Cas9_int_F CSN308[1]	ATTCCCU GACGTTCAAGGAGGACATCCAGA	CSN308
Cas9_NLS_R CSN309[1]	ACCTTGCGCUTCTTCTTGGGAGGGTCGCCCCCCAGTTGACTAA	CSN309
Tef1Onu_Nls_F	AGCGCAAGGUCTGAATTATTTCTTCTTAACCCGAAG	MN4
Tef1Onu_PacI_down_R	GGTCTTAAUACGGCAGCTTACTTCGTGGC	MN5
Tef1Onu_Nls_F_2	AGCGCAAGGUCTGAATTATTTCTTCTTAACCCGAAGTATATCTAC	MN14
Tef1Onu_PacI_down_R_2	GGTCTTAAUCCGACATCCGAGCCTTGTG	MN6
Cassette sgRNA expression : « PacI-PgpdOnu-NNNNNN-HH-Protospacer-HDV-TtrpC-PacI » pour construction de pMN2		
PgpdOnu_PacI_up_F	GGGTTTAAUAGACGAGAGAGCTTGCCGG	MN8
PgpdOnu_proto_dwn_R	AGGGCGGAUTTGACTGAGAGGTTAGTTTTGGACG	MN9
TtrpCOnu_HDV_up_F	ACGCACGCGUATTATTATTTGGCTTGTTTC	MN10
TtrpCOnu_PacI_dwn_R	GGTCTTAAUTGGAAAACATATGGTGCTG	MN11

gRNA_F	ATCCGCCCUGATGAGTCCGTGAGGAC	MN12
gRNA_R	ACGCGTGCGUCCCATTCGCCATGCCGAA	MN13
Cassette PyrG gRNA		
PyrG_PS_1 R_custom	AGCTTACUCGTTTCGTCCTCACGGACTCATCAGG CGCGATTTGACTGAGAGGTTAGTTT	
PyrG_PS_2 R_custom	AGCTTACUCGTTTCGTCCTCACGGACTCATCAGG GTACCTTTGACTGAGAGGTTAGTTT	
PyrG_PS_3 R_custom	AGCTTACUCGTTTCGTCCTCACGGACTCATCAGG AGGAGTTTGACTGAGAGGTTAGTTT	
PyrG_PS_1 F	AGTAAGCUCGTCG CGCGAGCGTGTGCACTAC GGTTTTAGAGCTAGAAATAGCAAGTTAAA	
PyrG_PS_2 F	AGTAAGCUCGTCG GTACCGGCGACAACGATG GGTTTTAGAGCTAGAAATAGCAAGTTAAA	
PyrG_PS_3 F	AGTAAGCUCGTCG AGGAGGCGCCCCTGGACC GGTTTTAGAGCTAGAAATAGCAAGTTAAA	

[1] Amorces construites par Nødvig et collaborateurs (2015)

Tableau A.2 Séquences des trois protospacers (PS) utilisés pour cibler le gène PyrG chez *Ophiostoma novo-ulmi*

Nom	Position dans le gène (nt)	Séquence du protospacer
PyrG_PS 1	450-469	GCGCGAGCGTGTGCACTACG
PyrG_PS 2	859-878	GGTACCGGCGACAACGATGG
PyrG_PS 3	943-962	GAGGAGGCGCCCCTGGACCG

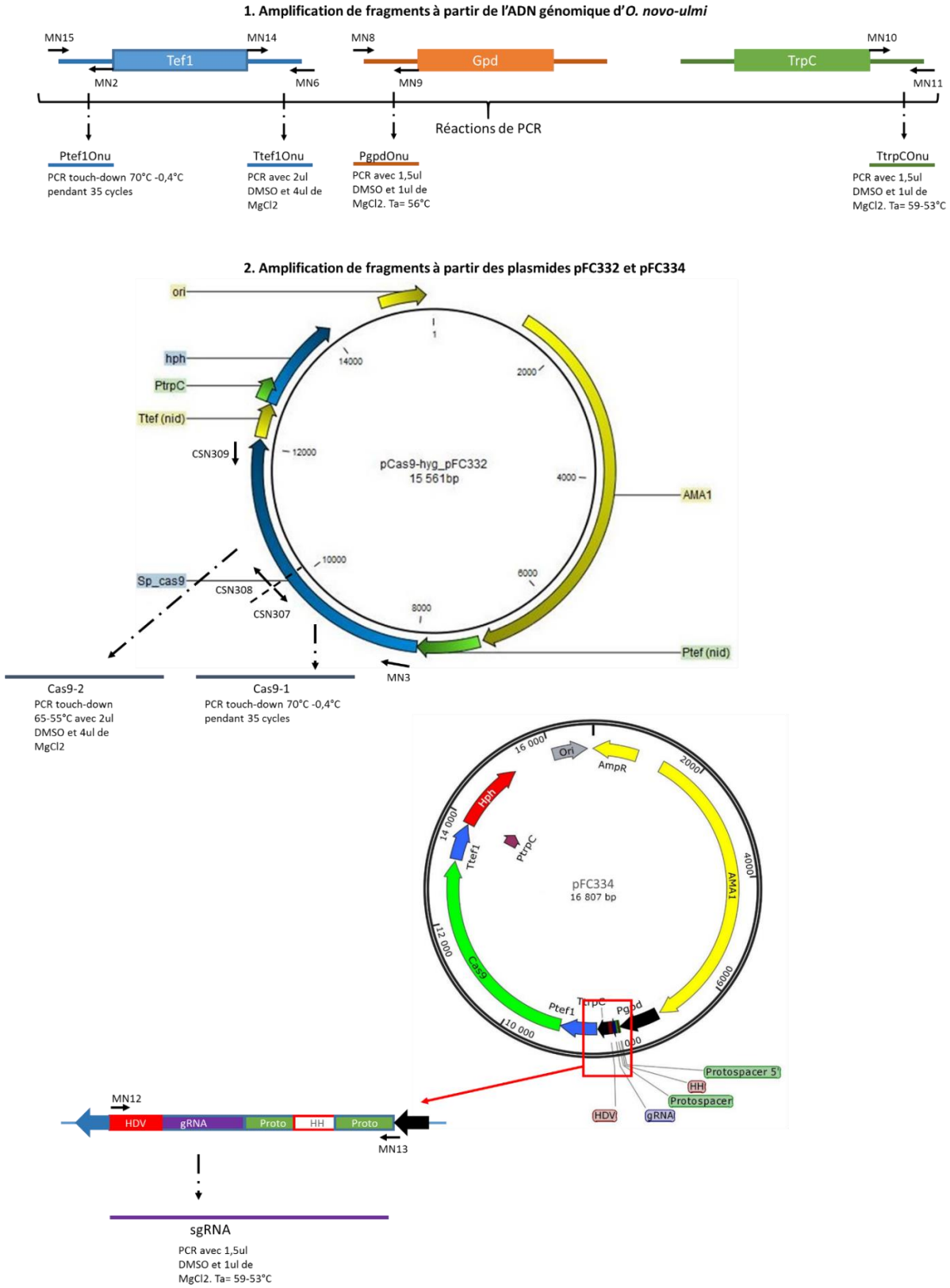

Figure A.1 Résumé des produits PCR obtenus pour la création des plasmides pMN1 et pMN2.

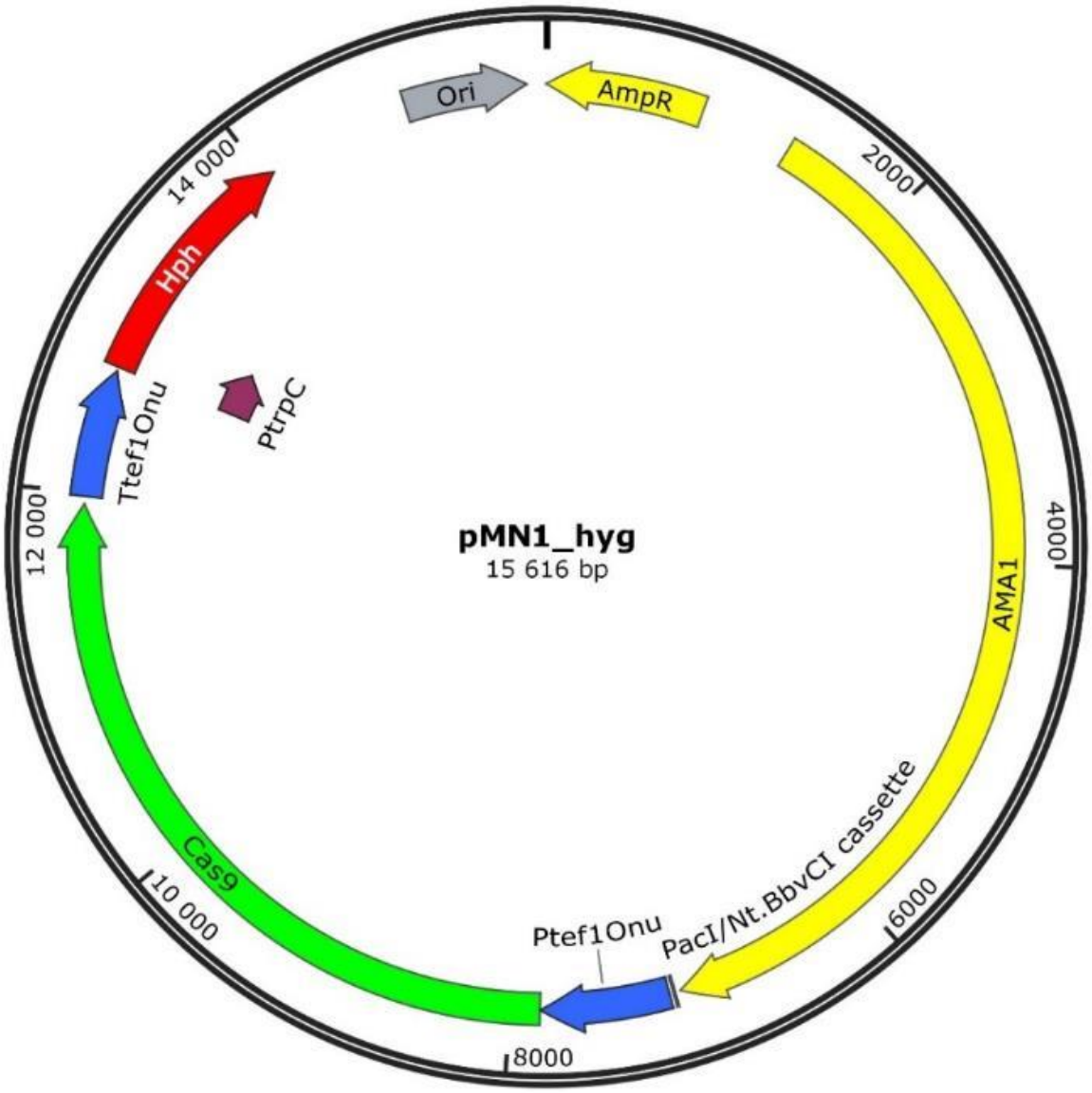

Figure A.2 Plasmide pMN1 pour transformation avec CRISPR-Cas9 chez *Ophiostoma novo-ulmi.*

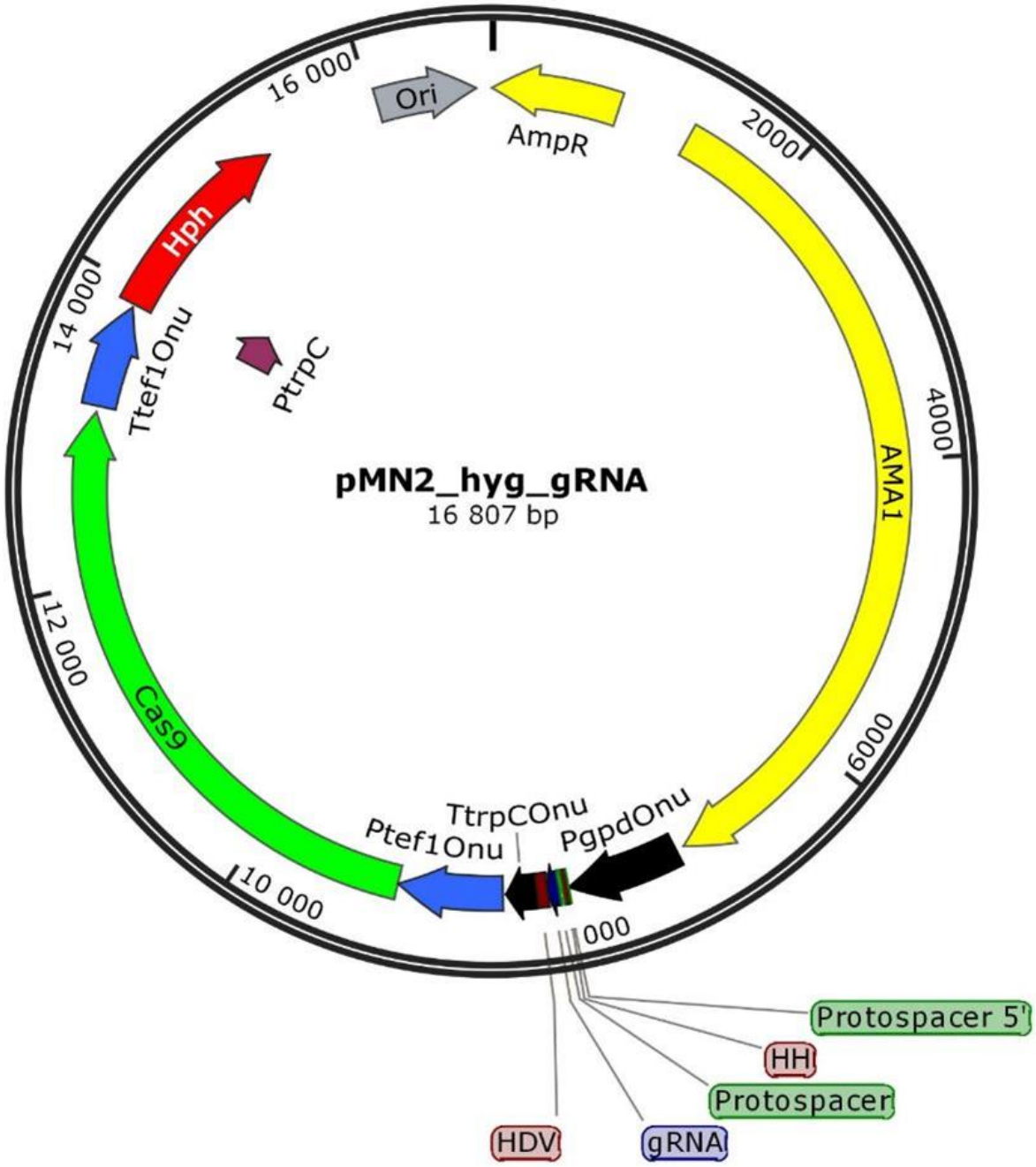

Figure A.3 Plasmide pMN2 pour transformation avec CRISPR-Cas9 chez *Ophiostoma novo-ulmi.*

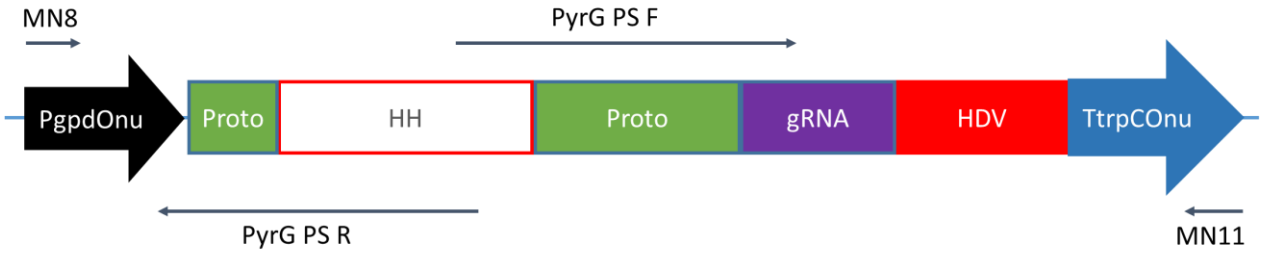

Figure A.4 Amplification de l'ARN guide en deux fragments complémentaires par des amorces permettant de modifier le protospacer.

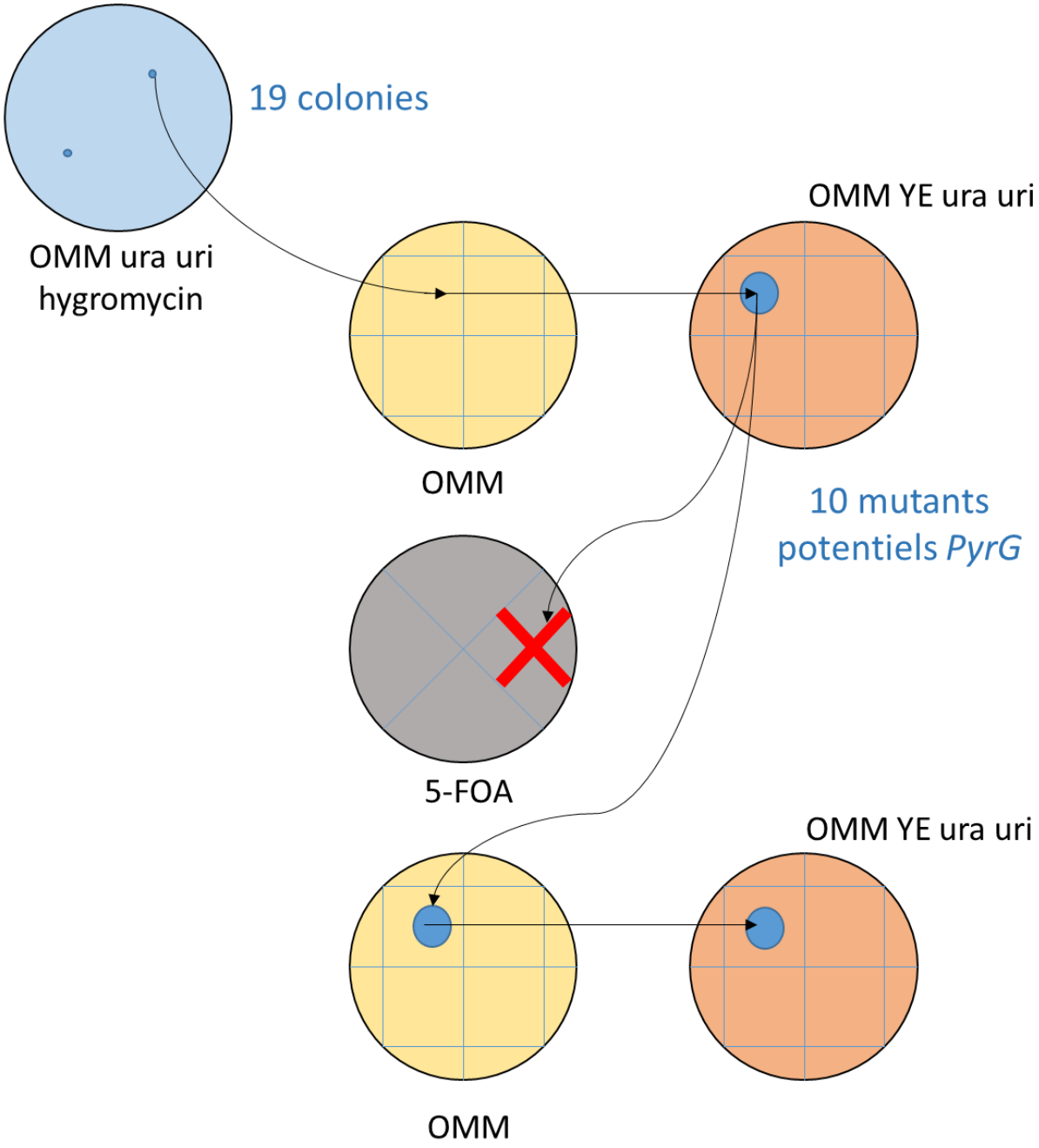

Figure A.5 Schéma du procédé de sélection des transformants inactivés au niveau du gène PyrG chez *Ophiostoma novo-ulmi*. Les grands ronds représentent des boites de pétri. Les petits ronds bleus représentent les colonies qui poussent sur les boites.